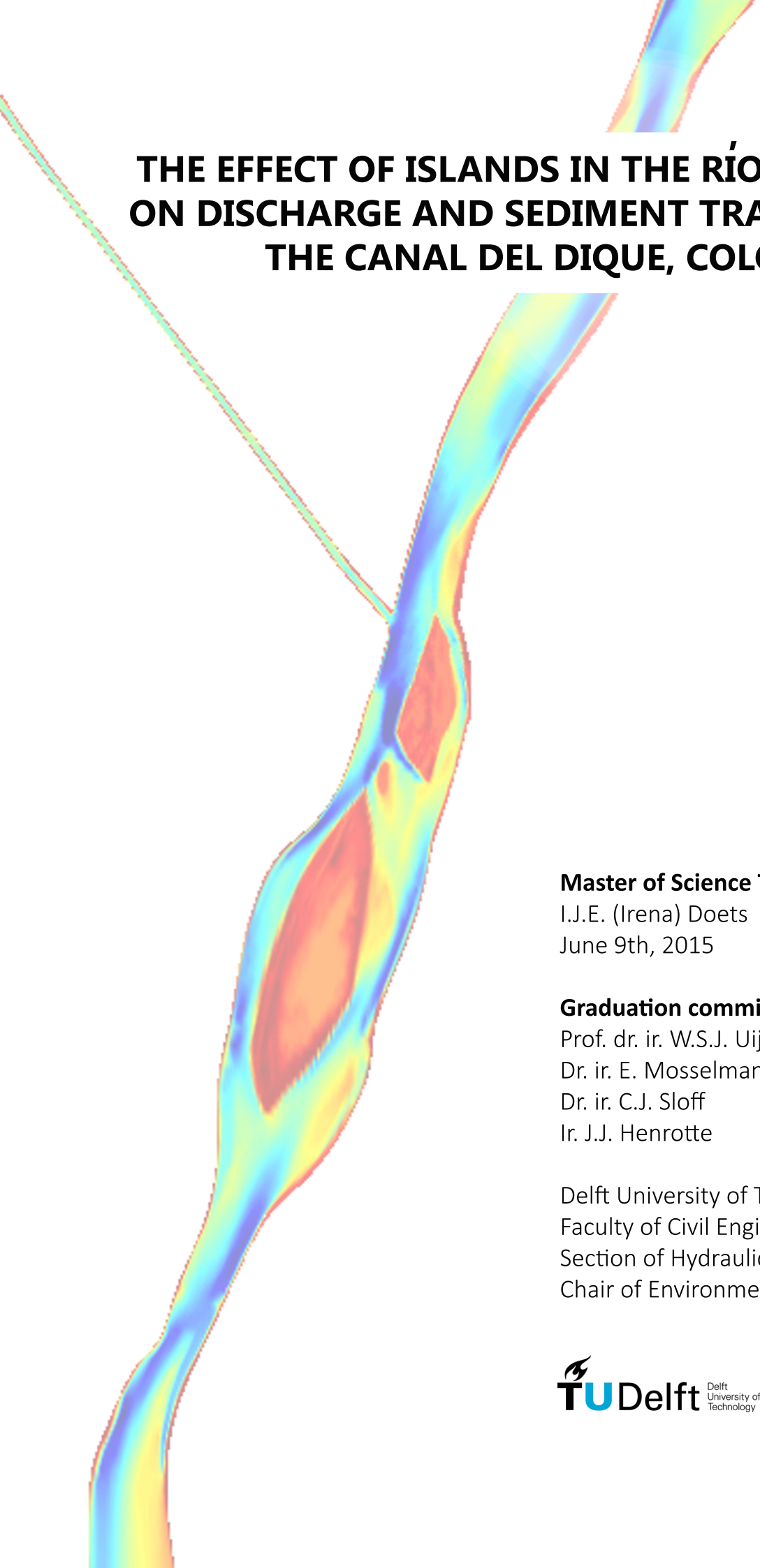

THE EFFECT OF ISLANDS IN THE RÍO MAGDALENA ON DISCHARGE AND SEDIMENT TRANSPORT INTO THE CANAL DEL DIQUE, COLOMBIA

Master of Science Thesis report

I.J.E. (Irena) Doets

June 9th, 2015

Graduation committee

Prof. dr. ir. W.S.J. Uijttewaal
Dr. ir. E. Mosselman
Dr. ir. C.J. Sloff
Ir. J.J. Henrotte

Delft University of Technology
Faculty of Civil Engineering and Geosciences
Section of Hydraulic Engineering
Chair of Environmental Fluid Mechanics

TU Delft Delft University of Technology

Royal HaskoningDHV
Enhancing Society Together

'Small streams make big rivers'

Ovidius

PREFACE

This thesis report is the final step in fulfilling the Master of Science degree in Hydraulic Engineering at Delft University of Technology, faculty of Civil Engineering and Geosciences. It marks the end of six enjoyable study years in Delft from which ten intensive months of conducting this research at Royal HaskoningDHV in Rotterdam.

Water has always inspired me. As a sailor I spent many days on and around the water. Besides, being a Dutch citizen and living beneath sea level I soon discovered the necessity of finding solutions in order to protect people from the harms of too much water. In addition, the challenge of finding sustainable solutions always interested me. During my study I developed interest in the, sometimes abstract, world of fluid mechanics and of coastal- and river engineering.

During my research on the bifurcation of the Río Magdalena and Canal del Dique, it was not only the movement of *water* that gained my interest, but also the movement of the *fluvial islands*. I hope this research contributes to a better understanding of the way islands in the Río Magdalena affect the amount of water and sediment entering the Canal del Dique in order to find solutions for the negative impact of fine sediment on the environment. I am thankful for being part of this interesting and challenging project of the environmental restoration of the Canal del Dique carried out by Royal HaskoningDHV and the freedom I have been given to choose the subject which fits with my interests. This graduation thesis period was a big learning process, with some bumps on the road, but in the end I came out better, stronger and wiser.

First, I would like to thank my daily supervisor ir. Johan Henrotte for his helping hand, the many talks we had and his critical notes. Furthermore, I would like to thank the other committee members: dr. ir. Erik Mosselman, for his willingness to help, his inspirational knowledge of river engineering and encouragement for submitting an abstract for the Rivers Coastal and Estuarine Morphology congress in Iquitos Peru, August 2015; dr. ir. Kees Sloff for his help in modelling and the interest in my research; and finally, I would like to thank prof. dr. ir. Wim Uijttewaal for accepting me as one of his graduation students and his critical comments during the committee meetings.

I would like to thank Royal HaskoningDHV and especially the department 'Hydraulics and Morphology' for giving me the opportunity of this special research as part of the ongoing project Canal del Dique. I had a great time at the office in Rotterdam and sometimes Amersfoort where I could meet so many inspiring people. Also, I would like to thank the fellow students for the coffee breaks, the support and their friendship.

Finally, I would like to thank all the friends I made during my whole study period, who made this journey a pleasant ride, especially my flatmates, for listening to me during the research process and giving me a warm home. I would like to thank my family, ma famille, mammie and my brothers for their warm heart and faith in me. But most of all, I would like to thank my parents for giving me the possibility to study and to love water by sailing, for their support and their everlasting love.

This journey has come to an end. But I'm sure this end will be the start of a wonderful new beginning with more water, sediment and Dutch hydraulic engineering.

Irena Doets,

The Hague, 2015

ABSTRACT

Controlling the distribution of water and sediment at river bifurcations is one of the main challenges in river engineering and management. This distribution affects the stability of river bifurcations as well as the distribution of flooding risk, navigability and environmental conditions. The governing factors are the hydrodynamics of the two branches downstream as well as the spatial distribution of sediment transport in the area of the bifurcation. Fluvial islands at the bifurcation may affect both. First, they may change the distribution of discharges over the downstream branches by creating marked water level differences in the area of the bifurcation. Second, they introduce a pattern of bed slopes and secondary flows that may change the ratio of sediment transported into the left branch and sediment transported into the right branch. This study focusses on the fluvial islands in the Río Magdalena on the discharge and sediment distribution into the Canal del Dique, Colombia.

Research objectives and methodology

The main objective of this research is to gain insight into the effect of size, position and shape of islands in the Río Magdalena on discharge and sediment distribution into the Canal del Dique. Where the high load of fine sediments has adverse environmental effects on the coastal area downstream of the Canal del Dique. Insight in the hydrodynamics and morphodynamics is obtained by carrying out model exercises with the use of Sobek-RE and Delft3D-FLOW on respectively a one-dimensional and two-dimensional scale. The distribution of fine sediment is assumed to depend on the distribution of discharges and is related to environmental problems. Whereas, the distribution of coarse sediment depends on local factors and is mostly deposited in the sediment trap located at the entrance of the Canal del Dique. Optimal island configurations are thrived to obtain creating a reduction of discharge and the amount of fine and coarse sediment entering the Canal del Dique.

Results

A literature review resulted in an understanding of the physical processes influencing discharge and sediment distribution at a bifurcation and around fluvial islands. Discharge and sediment distribution depends on the characteristics of the downstream branches (geometry, hydraulic roughness, bed slope and bed-friction) and is strongly depended on local factors. Therefore, no unique relationship for the distribution of water and sediment at a bifurcation exists and the local conditions need to be defined for each bifurcation. Local factors influencing the distribution of *coarse* sediment are: the Bulle effect, gravitational pull along bed slopes, the approach conditions, flow separation and human interferences. Furthermore, backwater effects may occur when the equilibrium depth of the downstream branches is not reached at the point of bifurcation. In this area the relationship between discharge and water level is not uniquely defined.

A fluvial island can be seen as a combination of a confluence and bifurcation. The confluence causes larger erosion holes and sediment bumps in the area of the bifurcation. Fluvial islands are formed by several mechanisms as for example the cut-off from river banks at high flow events or the stabilization of bars due to a long period of low flow velocity. And are characterized by vegetation and the presence during and after high flows.

In the case of the Canal del Dique, two fluvial islands, 'Isla la Loca' and 'Isla Becerra', are located in the Río Magdalena just upstream of the entrance of the Canal del Dique, where sharp edges result in flow separation and asymmetrical approach conditions are observed.

In the one-dimensional hydrodynamic model the area of the bifurcation is schematized as a network of branches around two fluvial islands. This resulted in a complex system with numerous branches, bifurcations and confluences with the Canal del Dique as offtaking branch. The distribution of water over the downstream branches is found to depend on the distribution of flows around the islands. For instance, if the discharge along the right side of the islands is widened or deepened, the discharge decreases in the offtake (located on the left side) and increases in the downstream main branch. A large discharge along the right side results in a convex shape of the water surface profile (M2-type of backwater curve) in the right branches and a concave shape (M1-type) in the left branches. As the water level at the confluence of the downstream island is equal, the M1 curve then implies a relatively low water level at the entrance of the offtake resulting in a lower discharge in the offtake. The presence of two islands results in a higher discharge in the offtake than one large island.

A strong correlation between the offtake, the channel between the two islands and the connecting upstream branch on the right side (opposite of the offtake) is found. If the discharge in *one* of these branches increases, the discharge in *all* of the branches increases. Changing the length of the branches along the downstream located island 'Isla la Loca' only has minor impact on the distribution of water over the branches downstream.

The results of the two-dimensional hydrodynamic simulations showed that even when Isla la Loca is attached to the left bank, the flow finds its way to the offtake with 8% less discharge than in the original configuration. Furthermore, the simulations show that the shape of the islands does not impact the discharge distributions, but does have considerable effects on flow velocities and directions. Protrusions cause high flow velocities that erode the protrusions, whereas sharp bank-line angles cause flow separation that fill the areas of large eddies by deposition. As a result of these feedback mechanisms, different initial islands shapes evolve into similar end states of smooth streamlines along smooth island shapes. Amalgamating the two islands into a single large island makes the left branch dominant in conveying discharges due to favourable approach conditions. As a result, the upstream flow is drawn to the left.

Including sediment in the two-dimensional model gave insight in the distribution of sediment with different island configurations. The sediment distributions are initially equal to the discharge distributions. However, small initial variations in discharge distribution and flow velocities will be enhanced. Branches that were initially less dominant in conveying discharge lead to sedimentation in these branches, which in turn results in decreasing flow velocities resulting in even more sedimentation in the branches; a re-inforcing process. Furthermore, sedimentation is observed in shallow areas at the lee side of the islands and at sharp edges where flow separation occurs. Areas of increasing flow velocities result in erosion of the islands. These mechanisms result in different size, position and shape of the islands. Where the current island configurations in the Río Magdalena evolve into englargement of the islands in downstream direction due to sedimentation at the tail of the islands where flow separation is observed. As a result of flow separation at the tail of the upstream located island 'Isla Becerra' even a small island evolves in the channel between the two

islands. The presence of a small island is also seen in historical bathymetries of the Río Magdalena which tend to appear and disappear throughout history.

By locating Isla la Loca in such a way that it is attached to the left bank results in a maximum reduction of the amount of coarse sediment entering the Canal with a factor 2.5.

Conclusion

Overall, it can be concluded that size and position of fluvial islands at a bifurcation have appreciable effect on the discharge and sediment distribution along the islands and to the downstream branches. Whereas, the shape of the islands does not seem to impact the distribution of discharges. A maximum reduction of discharge and fine sediment of 8% and coarse sediment with a factor 2.5 in the Canal del Dique is found when Isla la Loca is attached to the left river bank just upstream of the entrance of the Canal.

TABLE OF CONTENTS

LIST OF FIGURES

LIST OF TABLES

NOMENCLATURE

Symbol	Name	Unit
A	Cross-sectional area	m^2
B	Width	m
C	Chézy coefficient	$m^{1/2}/s$
c	Concentration of suspended sediment	kg/m^3
$\mathbf{c_a}$	Concentration at a reference level measured at level 'a' from the bed	kg/m^3
$\mathbf{c_f}$	Friction coefficient	$m^{1/2}/s$
$\bar{c}$	Depth averaged sediment concentration	kg/m^3
e	equilibrium sediment concentration	kg/m^3
D	Mean grain size diameter	m
$\mathbf{D_*}$	Dimensionless grain diameter	-
$\mathbf{D_{50}}$	Median grain size	m
D_{90}	Grain size for which 90% of the particles are smaller	m
F	Dimensionless shape factor	-
g	gravitational acceleration	m^2/s
h	Water depth	m
$\mathbf{h_c}$	critical water depth	m
$\mathbf{h_e}$	equilibrium water depth	m
i	water level slope	-
$\mathbf{i_b}$	Bed slope	-
k	Empirically determined parameter for nodal point relationship	-
m	Mass of body	kg
m	Degree of nonlinearity of sediment transport formula	-
n	Manning value *n* for bed friction	$s/m^{1/3}$
n	Exponent accounting for non-linearity	-
p	Porosity	-
Q	Discharge	m^3/s
Qs	Sediment transport	m^3/s
qs	Sediment transport per unit width	m^2/s
R	Hydraulic radius	m
s	Sediment transport	m^3/s
u	Flow velocity	m/s
uf	Flow velocity	m/s
$\mathbf{U_*}$	Bed shear velocity	m/s
wf	Fall velocity compared to moving water	m/s
ws	Fall velocity compared to stationary flow	m/s
z_b	Bed level	m
α'	Correction factor for non-uniformity of the flow	-
Δ	Difference operator	-
Δ	Relative density	-
$\boldsymbol{\varepsilon_h}$	horizontal mixing coefficient	m^2/s

ε_s	Mixing coefficient	m^2/s
ε_v	Vertical mixing coefficient	-
κ	Von Karman constant	-
λ_{BW}	Backwater adaptation length	m
ν	Viscosity	m^2/s
ρ	Density of water	kg/m^3
ρ_s	Density of the grains	kg/m^3
θ	Shields-parameter	-

Abbreviations	
CDD	Canal del Dique
MAGNA	Magna SIRGAS Bogotá (local coordinate system in study area)
RM	Río Magdalena

1 INTRODUCTION

Controlling the distribution of water and sediment at river bifurcations is one of the main challenges in river engineering and management. This distribution affects the stability of river bifurcations as well as the division of flooding risk, navigability and environmental conditions. Fluvial islands in the area of a bifurcation may affect both the discharge and sediment distribution. First, they may change the amount of water by creating marked water level differences in the area of the bifurcation. Second, they may change the amount of sediment transported into the left and right branch by introducing a pattern of bed slopes and secondary flows.

Examples of fluvial islands in the area of a bifurcation can be found in the Amazon in Brazil, the delta of Bangladesh and the Río Magdalena in Colombia (Figure 1.1). This study will focus on the bifurcation of the Canal del Dique and Río Magdalena where fluvial islands in the vicinity of the bifurcation have significantly changed in size, shape and position throughout history and therefore impact the distribution of water and sediment over the downstream reaches.

Figure 1.1 – From left to right: Amazon river in Brazil, delta of Bangladesh and Río Magdalena (Google Earth 2015; Esri 2015)

1.1 Background of the Canal del Dique

The Canal del Dique is a 120 kilometre long waterway, constructed in the XVI century, connecting the Río Magdalena with Cartagena at the Caribbean coast (Figure 1.2). The Canal has been developed by creating permanent connections between the Río Magdalena and a cascade of ciénagas (lakes or marshes) and caños (small rivers) connecting the Canal with the ciénagas. Due to the high amount of fine sediment from the Río Magdalena and lack of maintenance, sedimentation in the connections occurred, making the Canal accessible for navigation for only a short period of time of the year. Therefore, several major reconstructions, including cutting bends, widening and deepening were carried out in the 19th and 20th century, creating a large prismatic canal with only a few bends.

The reconstruction of the canal in the 1980s caused environmental deterioration of the adjacent system of lakes and the coastal area due the strongly increased water flow and sediment transport. During extreme flow in the Río Magdalena in 2010, dikes along the Canal were breached resulting in inundation of 35,000 ha of land and loss of 174 human lives (Consorcio Dique 2013). The Government of Colombia assigned Royal HaskoningDHV together with the partner Gómez Cajiao to design and implement the project providing an integral solution, optimized for the requirements of flooding safety, environment, agriculture and navigation. Part of this project consists of modelling the hydrodynamics and morphodynamics at the offtake from the Río Magdalena to the Canal del Dique at

Calamar in order to gain insight into the sediment load and discharge entering the Canal. This study will focus on this part of the project.

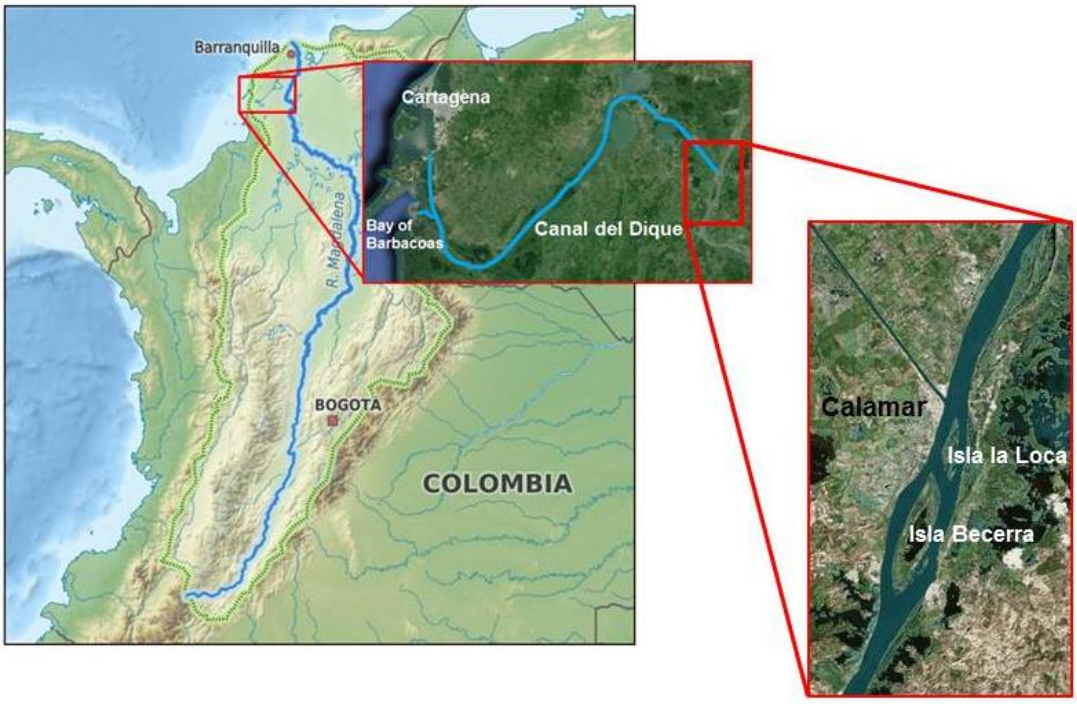

Figure 1.2 – Overview study area: offtake of the Canal del Dique from the Río Magdalena at Calamar in Colombia (modified from Karnstedt (2010), Google Earth (2015) and Esri (2015))

1.2 Problem description

At the offtake from the Río Magdalena to the Canal del Dique, two fluvial islands are located as shown in Figure 1.2. The most downstream located island has changed significantly in size, shape and position during history for which the local community named it 'Isla la Loca', meaning the crazy island. This morphologic change of the island may affect the distribution of water and sediment over the downstream branches. Recent measurements show an increase of discharge in the Río Magdalena at Calamar, located at the left side along Isla la Loca. It is thought that this might be caused by morphological changes, however the impact is not exactly known.

High amount of fine sediments from the Río Magdalena causes environmental problems downstream downstream of the Canal del Dique in the coastal area; in the Bay of Cartagena and the Bay of Barbacoas. Besides, a fair amount of coarse sediment is dredged in the sediment trap at the entrance of the Canal del Dique. In order to reduce the amount of fine sediment, which is determined by the amount of water entering the Canal and to reduce the amount of coarse sediment, which settles at the entrance of the Canal, it is of high importance to get a good understanding of the hydrodynamics and morphodynamics at the entrance of the Canal in order to reduce the sediment load in the Canal.

Although the stability of bifurcations is a well-known field of research in river engineering, the effect of fluvial islands in the area of a bifurcation has not been studied yet.

1.3 Objectives

The aim of this study is to gain insight into the effect of size, position and orientation of fluvial islands in the Río Magdalena on discharge and sediment transport into the Canal del Dique in Colombia. Although this study is based on one case it is thrived to obtain generic insights in order to use the obtained knowledge for other cases. Furthermore, it is of special interest to reduce the amount of discharge and accompanying fine sediment and the amount of coarse sediment into the Canal. Therefore, this study focusses on finding island configurations creating a maximum reduction of discharge and sediment into the Canal del Dique.

1.4 Research questions

With the previously identified problems and objectives as a basis, the main research question of this study is defined:

What is the effect of size, position and shape of fluvial islands in the Río Magdalena on discharge and sediment transport into the Canal del Dique in Colombia?

In order to find answers to the main research question sub-questions has been formulated:

1. What are the physical processes influencing discharge and sediment distribution at a bifurcation and around fluvial islands?
2. What is the influence of different size, position and shape of fluvial islands in the Río Magdalena on the amount of discharge distributed into the Canal del Dique and along the islands?
3. What is the influence of different size, position and shape of fluvial islands in the Río Magdalena on the amount of fine and coarse sediment distributed into the Canal del Dique and along the islands?
4. What island configurations create a reduction of discharge and sediment in the offtake from the Río Magdalena to the Canal del Dique and to what extent is it reduced?

1.5 Method

To achieve the objectives of the study several steps are undertaken. A literature study is carried out in order to understand the relevant physical processes influencing discharge and sediment distribution at a bifurcation. Consequently, the system of fluvial islands at a bifurcation is schematized into a one-dimensional network and hydrodynamic simulations are carried out with the modelling software 'Sobek-RE'. These simulations give insight into the effect of size and position of the islands on the discharge distributions. Subsequently, a two-dimensional, depth-averaged, model is made with the use of Delft3D-FLOW. First, only the hydrodynamics are taken into account. Thereafter, sediment transport and morphology are included and analysed. The two-dimensional simulations provide insight into the effect of angles between branches and sedimentation and erosion patterns. Finally, the insights obtained from the modelling exercises are used to find optimal island configurations causing reduction of discharge and sediment in the offtake from the Río Magdalena to the Canal del Dique. The steps in the research process are schematized in Figure 1.3.

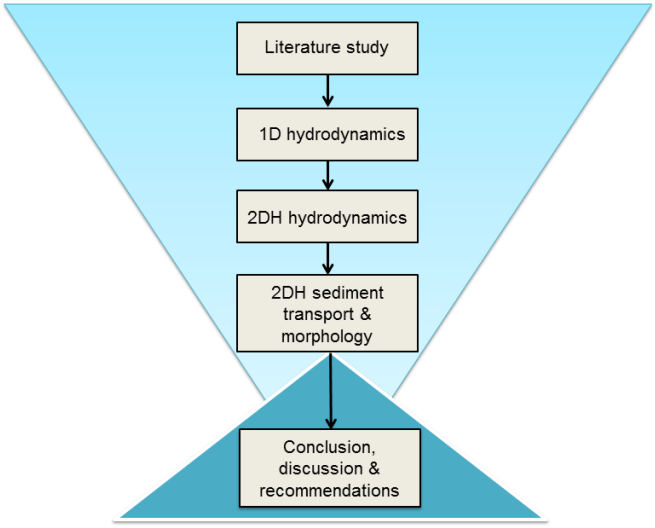

Figure 1.3 – Steps in the research process

1.6 Thesis outline

This thesis starts with the introduction of the research topic. A problem description is given to sketch the context of the current situation and point out the motivation of this research. Objectives and research questions are formulated. To guide readers through this research, the methodology and the structure of the report are described.

In Chapter 2, a theoretical background is given. The physical processes occurring at a bifurcation and around fluvial islands are described as well as the relevant hydrodynamic and morphodynamic equations. Also, more detailed information is given on the Canal del Dique system.

Chapter 3 describes the one-dimensional hydrodynamic model. A thorough analysis is carried out on the simulations regarding the effect of different size and position of fluvial islands on the discharge distribution.

Chapter 4 describes the two-dimensional (depth-averaged) hydrodynamic model. The way size, position and shape of the islands affect the discharge distribution along the branches and in the offtake is researched. Also, the optimal island configuration reducing the amount of discharge in the Canal del Dique is investigated.

Furthermore, Chapter 5 describes the two-dimensional morphodynamic model. The evolution of current and historical island configurations in the Río Magdalena is analysed and the impact on sediment transport rates of the coarse fractions. Besides, the impact of the most promising island configurations reducing the amount of water in the Canal del Dique, as found from the previous chapter, on the amount of coarse sediment entering the Canal is analysed.

Finally, this thesis report concludes with a discussion of the results and conclusions. Recommendations are given on using islands as a way to reduce the amount of sediment and discharge in the Canal del Dique as well as recommendations for further research.

2 THEORETICAL BACKGROUND

This chapter presents a literature study capturing first the relevant hydrodynamic and morphodynamic equation. Then, the hydrodynamic and morphodynamic processes at a bifurcation and fluvial island are described. Finally, the hydrodynamic and morphodynamic conditions at the bifurcation of the Canal del Dique and Río Magdalena are described.

2.1 Hydrodynamics

The movement of water is generally described by the conversation of mass and momentum, also known as respectively the continuity (Equation 2.1) and momentum equation (Equation 2.2). For one-dimensional (when averaging over the entire cross-section), unsteady flow this set of equations reads (see e.g. Jansen et al. 1979):

Continuity: $\frac{\delta A}{\delta t} + \frac{\delta Q}{\delta x} = 0$ (2.1)

Momentum: $\frac{\delta Q}{\delta t} + \alpha' \frac{\delta(\frac{Q^2}{A})}{\delta x} - gA\frac{\partial h}{\partial x} + gA\frac{\delta z_b}{\delta x} + gA\frac{\overline{U}|\overline{U}|}{C^2 h} = 0$ (2.2)

where,

A= cross-sectional area [m^2]
Q= discharge through the cross-section [m^3/s]
x= longitudinal co-ordinate [m]
t= time [s]
h= mean cross-sectional depth of flow [m]
z_b= mean cross-sectional bottom elevation relative to reference level [m]
g= gravitational acceleration [m/s^2]
C= Chézy-coefficient [$m^{1/2}/s$]
α'= correction coefficient for non-uniform flow in the entire cross-section [-]

These two equations are generally referred to as the St. Venant equations and form the foundation of hydrodynamics in rivers. The first equation is the conservation of mass, which states that there is a balance between the rate of increase of the volume over time, the first term, to the net inflow of water, the second term.

The second St. Venant equation, the momentum equation, is derived from Newton's second law of motion, stating that the sum of all the forces on an object is equal to the acceleration of the object. In this case the forces are the gravity in the direction of the flow and the friction. The first term in the momentum equation is the Eularian acceleration, while the second term is the convective acceleration describing the momentum crossing per unit time. The coefficient α' in this term accounts for the shape of the channel. The third term and fourth terms represent the pressure forces due to respectively a gradient in water depth and bed level. The fifth and last term is the force due to friction.

2.1.1 Backwater curves

For stationary flow in a prismatic channel the water levels along the river stretch can be derived from the linear backwater curve-equation. This equation is derived from the momentum equation by

eliminating the acceleration terms and applying the continuity equation for uniform, steady flow ($q = uh$) resulting in the linear backwater equation:

$$\frac{dh}{dx} = \frac{i_b - c_f Fr^2}{(1 - Fr^2)} \tag{2.3}$$

where,
$Fr = \frac{u}{\sqrt{gh}}$: the Froude number.
c_f= friction coëfficient

This equation can be rewritten as:

$$\frac{dh}{dx} = i_b \frac{h^3 - h_e^3}{h^3 - h_c^3} \tag{2.4}$$

where,
$h_c = \frac{u^2}{g} = \left(\frac{q^2}{g}\right)^{\frac{1}{3}}$: critical depth (Fr=1)
$h_e = \frac{u^2}{C^2 i_b} = \left(\frac{q^2}{C^2 i_b}\right)^{\frac{1}{3}}$: equilibrium (or normal) depth
which is also known as the formula of Bélanger and provides the basis for calculations of the surface profiles (backwater curves) in case of uniform, stationary flow.

For currents with low Froude numbers, which is common for lowland rivers, two possible surface profiles can be distinguished: the concave M1-type and convex M2- type, where 'M' indicates mild slope (Figure 2.1). In case the water depth at some point in the river, for example due to a confluence or bifurcation, is larger than the equilibrium depth ($h > h_e$) the surface profile upstream becomes convex shaped (M1-type). In contrast, when the water depth in the river is smaller than the equilibrium depth ($h < h_e$), the surface profile upstream becomes concave-shaped (M2-type).

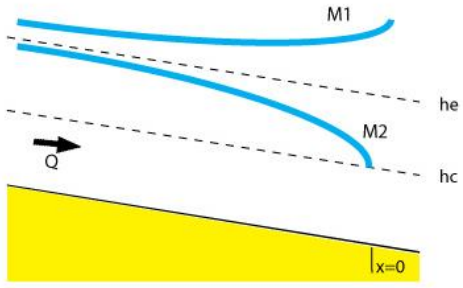

Figure 2.1 – Water level surface profiles for gradually varied flow (modified from Jansen *et al.* 1979)

The water level at a location upstream of the location at x= 0 can be calculated with:

$$h = h_e + (h_0 - h_e)\left(\frac{1}{2}\right)^{\frac{(x - x_0)}{L_{1/2}}} \tag{2.5}$$

where,

$L_{1/2} = \frac{0.24 h_e}{i_b}\left(\frac{h_0}{h_e}\right)^{\frac{4}{3}}$: the length over which half of the water level is reached from the downstream water level to the equilibrium depth.

In the area where the relation between discharge and water level is not uniquely defined, backwater effects occur.

In order to avoid backwater effects, meaning the area where the relation between discharge and water level is not uniquely defined, the downstream boundary should be located outside the backwater adaptation length. This is the length over which the effect of backwater is damped with 63%. The backwater adaptation length can be approximated with:

$$\lambda_{bw} = \frac{1}{3}\frac{h_e}{ib} \tag{2.6}$$

2.2 Morphodynamics

Morphodynamics is defined as the mutual adjustment of morphology and hydrodynamic processes involving sediment transport (Bosboom and Stive 2013). Morphodynamics play an important role in river dynamics and will be discussed in this section by first explaining sediment transport and the governing equations and consequently a description of morphology is given.

2.2.1 Sediment transport

Sediment transport is the movement of grains due to flow. If flow velocities are higher than a certain critical value, individual grain particles start moving along the bed. With higher flow velocities an increased amount of particles move at increasing speed. Sediment transport can be classified according to origin and mechanism as illustrated in Figure 2.2. Bed load (transport) is defined as the rolling, sliding and jumping of grains along the bed. Suspended load (transport) is defined as the transport of grains which stay in the water column for some time without touching the bed. Suspended load can be originated from bed material brought in suspension by turbulent velocity fluctuations as well as wash load brought into the flow from an area upstream. Wash load is usually very fine sediment, finer than the bed material. As this sediment results from erosion in the upstream catchment it therefore has no relation to the transport capacity of the stream.

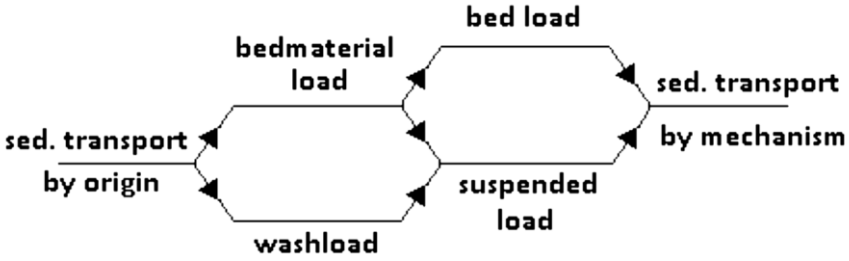

Figure 2.2 – Classification of sediment transport (Jansen, Bendegom et al. 1979)

The amount of sediment transport depends on the size, shape, density, fall velocity, chemical composition and the amount of pores. Shields described the mobility of the grains as the resultant of the gravity, drag and lift force and friction into the Shields parameter θ (see e.g. (de Vriend, Havinga et al. 2011):

$$\theta = \frac{u_*^2}{\Delta g D} \tag{2.7}$$

where,
$u_*^2 = \sqrt{\frac{\tau_b}{\rho}}$: shear velocity [m/s]
$\Delta = \frac{\rho_s - \rho}{\rho}$: relative density [-]
g= gravitational acceleration [m^2/s]
D= diameter grain [m]

This equation is closely related to the ratio of shear velocity divided by the fall velocity of the grains:

$$\frac{u_*^2}{w_s^2} \tag{2.8}$$

According to Shields, initiation of motion occurs after a critical value of the Shields-parameter which depends on the grain characteristics and the flow regime.

2.2.1.1 *Sediment transport formula*

Many empirical sediment transport equations exist, all with their specific application areas according to the conditions of laboratory flume experiment from which they are obtained. As measurement techniques become better, new formulas are drawn and old ones updated. However, all sediment transport formulas commonly define sediment transport as a function of gravity (g), fluid characteristics (ρ,ν), sediment characteristics (ρ_s, D) and parameters describing the influence of the flow (τ_b):

$$s = f(g, \rho, \nu, \rho_s, D, \tau_b) \tag{2.9}$$

In general, the transport formulas can be simplified to:

$$s = mu^n \tag{2.10}$$

where,
s= sediment transport [m^3/s]
m= parameter depending on the sediment characteristics and channel roughness [-]
n= exponent accounting for degree of nonlinearity of the relation between flow velocity and sediment transport rate [-]

The most frequently used sediment transport formulas will be described in the following sections.

The formula of Meyer-Peter and Müller

The sediment transport formula of Meyer-Peter-Müller (Meyer-Peter and Müller 1948) is a purely experimental formula relating to the bed load transport exclusively. The grain diameter in their experiments was larger than 0.4 mm. The formula is mainly applicable in situations where the fall velocity is larger than the shear velocity:

$$\frac{w_s}{u_*} > 1 \tag{2.11}$$

The formula concerns the volume transport of solid material per unit width and can be read as:

$$s_b = 8(\Delta g D^3)^{\frac{1}{2}}(\mu\vartheta - 0.047)^{\frac{3}{2}} \tag{2.12}$$

where,
D= mean diameter [m]

$\mu = \left(\frac{C}{C_{90}}\right)^{\frac{3}{2}}$: the ripple factor, which represents the influence of the bed form. Where, C_{90} is the Chezy-coefficient based the D_{90} grain size.

The formula of Engelund and Hansen

The formula of Engelund-Hansen (Engelund and Hansen 1967) is a semi-empirical transport formula concerning the total load. It combines the bed load and suspended load of the bed material (thus excluding wash load). The formula was originally derived for bed-load, but proves especially applicable for the total load of relatively fine material, where suspended load is large ($\frac{w_s}{u_*} < 1$). The formula is applicable for median grain size (D_{50}) ranges between 0.19 and 0.93 mm and can be written as:

$$s = \frac{0.05}{\sqrt{g}C^3\Delta^2 D_{50}} u^5 \tag{2.13}$$

The formula of Van Rijn

Another widely used formula is the formula of Van Rijn (1984) which makes a distinction between bed-load and suspended load transport. Due to the explicit distinction between bed-load and suspended load, the application area of this formula is large. The formula considering the transport of bed-load (excluding the pores) reads:

$$s_b = \varphi_b \sqrt{\Delta g D_{50}^3} \tag{2.14}$$

where:
φ_b= a parameter depending on the bed shear stress and the dimensionless parameter for the grain diameter ($D_* = D_{50}\left(\frac{\Delta g}{\nu^2}\right)$).

The transport of suspended load is defined as:

$$s_s = Fuhc_a \tag{2.15}$$

where:
u= depth averaged velocity [m/s]
h= water depth [m]
F= dimensionless shape factor [-]
c_a= sediment concentration at the reference level *a* measured from the bed at the edge of the bed boundary layer

2.2.2 Suspended sediment transport

The transport of suspended sediment particles is governed by turbulent mixing caused by an upward force due to turbulent mixing and the downward settling of sediment in the water column due to the larger specific density of the sediment compared to water. This sediment flux can be described as:

$$f_D = -\varepsilon_s \frac{\delta c}{\delta z} \tag{2.16}$$

where,
ε_s= mixing coefficient, analogous to the turbulent viscosity for transporting momentum in turbulent flow
c= concentration of the sediment particles in the water column

Settling of sediment particles in the water column occurs due to the larger density of the sediment particles compared to the density of water. However, the particles are also hindered by the water causing a slower adaption of the bed material which differs per flow regime. The vertical sediment flux corresponding to the settling can be written as:

$$f_s = -w_s c \tag{2.17}$$

with w_s= the settling velocity and c= concentration of the suspended sediment

In a steady, uniform flow, the vertical flux due to turbulent mixing is exactly compensated by the vertical flux due to settling. If a boundary condition is given, the concentration at a specific bed level can be calculated by:

$$c(z) = c(z_0)e^{-\frac{w_S(z-z_0)}{\varepsilon_S}} \tag{2.18}$$

In which $c(z_0)$ is the concentration at the bottom. The mixing coefficient can be calculated with:

$$\varepsilon_s = \kappa u_* h \frac{z}{h}(1 - \frac{z}{h}) \tag{2.19}$$

where, κ is the Von Karman constant and u_* the bed shear velocity.

Suspended sediment transport is not always in equilibrium. The vertical concentration can be filled up or emptied. To obtain a general formula, we need to consider the sediment balance of a small element (Figure 2.3).

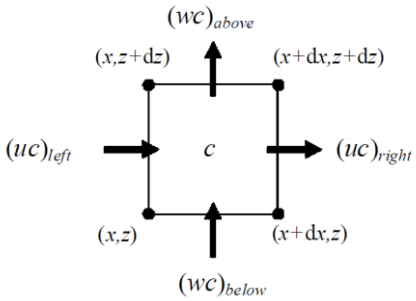

Figure 2.3 – Sediment balance (de Vriend, Havinga et al. 2011)

When balancing the net import of sediment into the element with the variation of the amount of sediment per unit of time in the element and using the continuity of water, the sediment concentration equation becomes:

$$\frac{\delta c}{\delta t} + u_f \frac{\delta c}{\delta x} + w_f \frac{\delta c}{\delta z} = w_s \frac{\delta c}{\delta z} + \frac{\delta}{\delta x}(\varepsilon_H \frac{\delta c}{\delta x}) + \frac{\delta}{\delta z}(\varepsilon_V \frac{\delta c}{\delta z}) \tag{2.20}$$

where:
c= concentration of suspended sediment [kg/m^3]
u_f= flow velocity [m/s]
w_f=fall velocity compared to moving water [m/s]
w_s=fall velocity compared to stationary flow [m/s]
ε_H= horizontal mixing-coefficient [m^2/s]
ε_V= vertical mixing-coefficient [m^2/s]

The first term in this equation describes the storage of sediment in the water column. The second and third term represent the suspended sediment transport due to horizontal and vertical water motion. The fourth term represents the falling of the grains. The last two terms are diffusion-terms, which express the gradual distribution of the suspended sediment in respectively horizontal and vertical direction.

For stationary, uniform flow and transport in x-direction: $\frac{\delta}{\delta t} = 0$, $\frac{\delta}{\delta x} = 0$ and $w_f = 0$. Therefore, the sediment concentration equation reduces to:

$$\frac{\delta}{\delta z}(w_s c + \varepsilon \frac{\delta c}{\delta z}) = 0 \tag{2.21}$$

As the net vertical flux at the water surface must be zero (no sediment can leave the water surface), this reduces to:

$$w_s c + \varepsilon \frac{\delta c}{\delta z} = 0 \tag{2.22}$$

As many mathematical models work in the depth-averaged mode a derivation for the depth-averaged suspended sediment concentration is obtained. A derivation taking into account vertical fluxes is formulated by Ribberink in 1983, which reads:

$$T_a \frac{\partial \bar{c}}{\partial t} + L_a \frac{\partial \bar{c}}{\partial x} = \bar{c_e} - \bar{c} \tag{2.23}$$

where:
$\bar{c}$= depth-averaged concentration
$T_a \propto \frac{h}{w_s}$: adaptation time needed for the sediment to settle to the bottom
$L_a \propto \frac{uh}{w_s}$: adaptation length which is equal to the distance the sediment particle travels while settling.
$\bar{c_e} = c(z_a)\exp(-\frac{w_s}{\varepsilon_z}(z - z_a))$: the equilibrium concentration

It can be said that when the depth-averaged concentration is smaller than the equilibrium concentration ($\bar{c} < \bar{c_e}$) erosion occurs, while when the contrary holds ($\bar{c} > \bar{c_e}$) suspended sediments are deposited to the bed.

2.2.3 Morphology

The movement of sediments from the bed causes changes in bed level, hence changes in morphology. By applying the continuity of mass in the bed at an infinitely small volume (Figure 2.4), the sediment balance for the bed can be determined, also known as the 'Exner principle' (Equation 2.24).

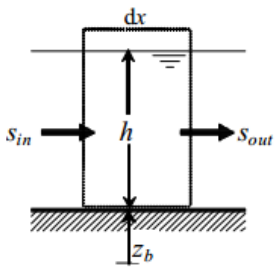

Figure 2.4 – Exner Principle (de Vriend, Havinga et al. 2011)

$$(1-p)\frac{\delta z_b}{\delta t} = -\frac{\delta s}{\delta x} \quad (2.24)$$

where,
p= porosity
z_b= bed level
s = sediment transport

This balance shows that changes in bed level, hence morphology, are caused by *gradients* in sediment transport.

2.3 Bifurcation dynamics

A river bifurcation occurs when one single stream is separated into two streams where water and sediment are divided into two branches, as schematized in Figure 2.5. This is a dynamic process, where the distribution of flow and sediment at the bifurcation leads to two stable bifurcates or closure of one of the branches. A bifurcation is not in equilibrium when one branch receives less sediment than its transport capacity, so that it erodes, and the other channel receives more sediment than its transport capacity, resulting in siltation of the branch. However, this may still lead to a stable end situation. An unstable bifurcation occurs when a small disturbance in one branch results in a larger increase in sediment supply than the increase in transport capacity.

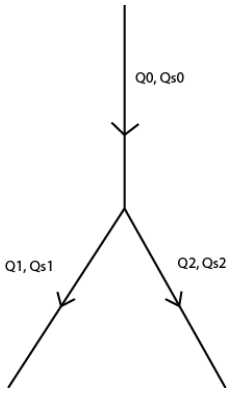

Figure 2.5 – Schematization of a bifurcation (Q= discharge, Q_s= sediment transport)

The distribution of water and sediment over the downstream branches depends on several local factors and therefore cannot simply be determined by the input of water and sediment and the characteristics of the downstream branches. Methods for defining the discharge and sediment distribution will be presented in this section as well as the local physical processes influencing the distributions.

2.3.1 Discharge distribution

The distribution of discharge at a bifurcation (Q_0 into Q_1 and Q_2 in Figure 2.5) is governed by the water level head from the downstream branches to the river basin and the conveyance of the branches. On a one-dimensional scale the discharge distribution can be determined by stating that the water level at the point of bifurcation should match (red arrow Figure 2.6). An example for the case of the Canal del Dique is carried out in Appendix B.

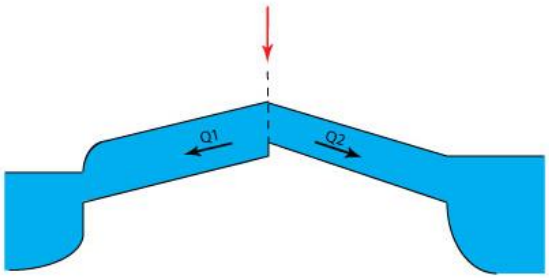

Figure 2.6 – Water level at downstream branches of a bifurcation, red arrow indicates point of bifurcation

When water levels are known, discharge in the branches can be calculated with the water balance equation ($Q = uBh$). When assuming stationary, uniform flow and applying Chézy ($u = C\sqrt{hi}$) the discharge in the branches can be calculated with:

$$Q = BhC\sqrt{hi} \tag{2.25}$$

where:
Q= discharge [m^3/s]
B= width [m]
C= Chézy coefficient [$m^{1/2}s^{-1}$]
h= water depth [m]
i= bed slope [-]

Furthermore, at the point of bifurcation or confluence, backwater effects can occur. This is caused by a difference between the equilibrium depth of the reach(es) upstream and the equilibrium depth of the reach(es) downstream (see section 2.1.1). If the equilibrium depth of the downstream branches is not reached at the point of bifurcation, the relationship between discharge and water level is not uniquely defined.

2.3.2 Sediment distribution

The distribution of sediment cannot solely be determined by stating that the water level at the point of bifurcation should match, the characteristics of the downstream branches and the conservation of mass and moment. Therefore, in one-dimensional models a nodal point relationship is necessary relating the sediment distribution with the discharge distribution. A well-known nodal point relationship from which the sediment *supply* in the bifurcates can be calculated is the empirical formula by Wang *et al.* (1995):

$$\frac{Q_{s1}}{Qs2} = \left(\frac{Q_1}{Q_2}\right)^k \left(\frac{B_1}{B_2}\right)^{k-1} \text{ (With k>0)} \tag{2.26}$$

where Q_{s1} and Q_{s2} are the sediment transports in the branches, B_1 and B_2 the width of the branches, Q_1 and Q_2 the discharges in the branches and k a parameter which can be determined empirically.

The (equilibrium) sediment transport *capacity* of the branches can be calculated with:

$$Q_{s,e} = B^{1-n/3} m Q^{n/3} C^{2n/3} i^{n/3} \tag{2.27}$$

where:

B= width of the river [m]
m= parameter which varies depending on sediment transport formula chosen [-]
n= exponent accounting for degree of nonlinearity of the relation between flow velocity and sediment transport rate [-]
Q= discharge [m^3/s]
C= Chézy coefficient [$m^{1/2}s^{-1}$]
i= bed slope [-]

This formula is derived from the sediment transport formula $q_s = mu^n$ with applying Chézy ($u = C\sqrt{Ri}$) and the continuity equation ($Q = Bhu$).

It can be said that when the increase of sediment supply (Q_s Equation 2.26) is weaker than the increase in transport capacity ($Q_{s,e}$ Equation 2.27) of a branch, erosion is enhanced leading to an unstable equilibrium and eventually closure of one branch. On the other hand, when the increase in sediment supply is stronger than the increase in transport capacity the erosion is counteracted, leading to a stable equilibrium and both branches stay open.

Wang *et al*. (1995) found from a phase-plane nonlinear stability analysis that the bifurcation is unstable for k< n/3 and for k> n/3 the bifurcation is said to be stable ('k' in Equation 2.26 and 'n' in Equation 2.27).

Only a small instability in the sediment supply compared to the sediment transport capacity in the branch can lead to an unstable bifurcation. When there is a slight abundant of sediment supply in one branch compared to its sediment transport capacity, a sedimentation shock wave is formed at the entrance of the branch. Therefore, at the entrance the branch becomes shallower, resulting in less discharge in the branches. This causes a positive feedback mechanism as the flow velocities decreases for which the sediment supply further decreases in this branch. As the discharge becomes smaller, vegetation can even develop on the silted branch which decreases the discharge capacity even further leading eventually to silting up of the branch. In contrary, the other branch will erode due to increasing discharge and flow velocity. A negative feedback mechanism occurs for example when the sediment in a silted branch causes such a bed slope that the sediment supply in the branch decreases.

Finally, in order to determine the sediment distribution occurring at a river bifurcation, one needs to know the local dominant transport mechanism. When most of the sediments consist of fine material (D_{50}< 63µm) suspended sediment transport is dominant and the sediment distribution will simply depend on the distribution of discharges (Slingerland and Smith 1998). However, when most of the sediment fractions are coarser, bed load transport dominates and the distribution of sediment depends on several local factors influencing the morphology at the bifurcation. These factors will be described in the following sections.

2.3.2.1 *Local factors*

Flow resistance

When the hydraulic roughness of one of the branches is higher, caused by different bed topography or a longer distance to the sea, the flow resistance in that branch is higher leading to more siltation of the branch.

Bulle effect

In 1926 a large flume experiment by Bulle led to the conclusion that the sediment transport near the bed is more curved than near the surface. The river and offtaking branch form a bend together in which spiral flow occurs, where the water at the surface is directed towards the main river and at the bed towards the offtake. As the sediment concentration at the bed is higher than at the water surface, more sediment is transported towards the inner bend and a sediment bulb forms. Therefore, more sediment is transported to the offtake than to the main river. A schematization of this effect is shown in Figure 2.7.

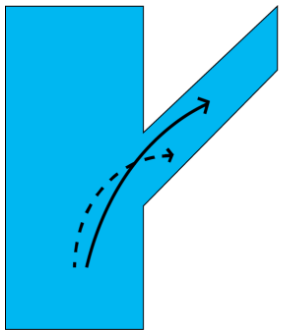

Figure 2.7 – Schematisation Bulle Effect

The amount of sediment transported towards the offtake depends on the angle of the offtake as shown in Figure 2.8. It can be seen that for an angle of 120 degrees, the amount of sediment transport is minimum in the offtake and maximum in the main channel.

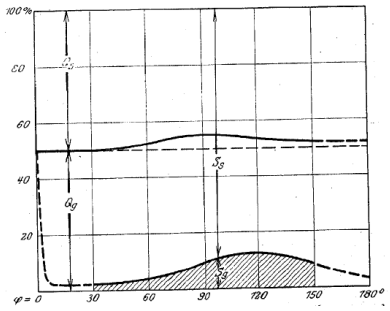

Figure 2.8 - Sediment and discharge distribution as a function of the offtake-angle at a total discharge of 5 L/s. Qg=discharge main channel, Qs= discharge side channel, Ss=sediment transport side channel, Sg= sediment transport main channel (Bulle, 1926)

Furthermore, the occurrence of the Bulle effect depends on the discharge distribution over the branches, the width to depth ratio and the local geometry of the dividing point.

Gravity pull

A transverse bed slope in the direction of one branch can favour the direction of the sediment transport by the gravity pull towards the deeper part, leading to higher sediment transport in one branch than the other. In Figure 2.9 this is shown for a transverse bed slope favoured towards the offtake. Such a transverse bed slope can be created by spiral flow or by the presence of a bend upstream, favouring one branch with more sediment and the other branch with more discharge (Kleinhans *et al*., 2008).

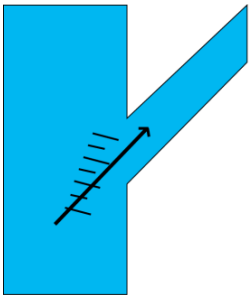

Figure 2.9 – Gravity pull along bed slopes

Flow separation

At sharp edges, the flow cannot follow the bank lines anymore. At a bifurcation the sharp edge results in flow separation, where a reattachment point can be seen where the flow is connected to the river bank again. Between the reattachment point and point of offtake an eddy is formed as shown in Figure 2.10. Due to turbulence at the edge of the eddy, sediment is transported into the eddy and gets trapped in the centre (like leaves when stirring in a cup of tea), where it is deposited. In addition, due to the presence of the eddy, the effective width of the offtake becomes smaller influencing the distribution of discharge.

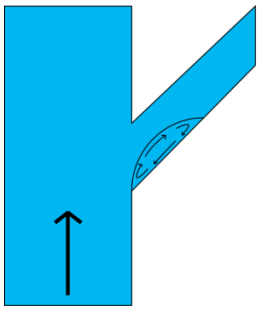

Figure 2.10 - Flow separation

Asymmetrical approach conditions

Large differences in the bed topography in transverse direction upstream of the bifurcation can influence the sediment distribution. If one side of the main channel is deeper, the flow velocities on that side are higher and more sediment is transported in this deeper part than the shallower side. This results in a higher sediment transport towards the bifurcate attached to the deeper part than the other branch. These asymmetrical approach conditions also result in grain sorting, as coarser sediments are only transported by higher flow velocities. Therefore, the deeper stretch contains more coarse sediment than the shallower stretch. A good example is found at the 'Pannerdensche Kop', where the river Rhine enters the Netherlands and separates into the river Waal (lower stretch in Figure 2.11) and the canal of Pannerden (upper stretch in Figure 2.11). The bifurcation angle at the Pannerdensche Kop is stabilized to zero, therefore only the upstream bathymetry causes differences in sediment distribution. Figure 2.11 shows that the bathymetry upstream of the bifurcation is very different in transverse flow direction, where the upper part is much deeper than the lower part and the median grainsize in the upper part is larger than the lower part.

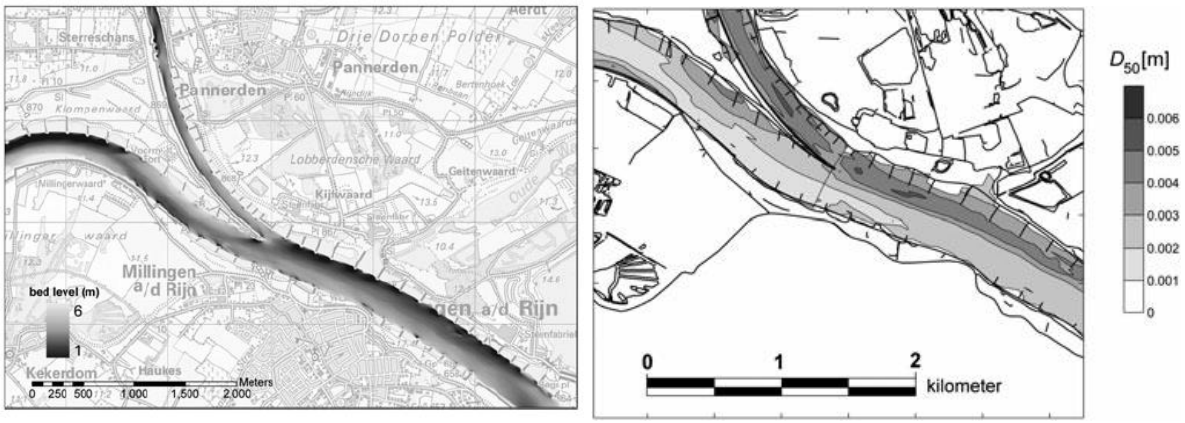

Figure 2.11 – Bed level topography (left) and average sediment composition of the top layer at the Pannerdensche Kop (right) (Sloff and Mosselman 2012)

Bend upstream

In river bends spiral flow occurs. Due to the curvature of a bend, the centripetal force excites a force to the water, directed towards the outer bend, resulting in a transverse water level gradient (Figure 2.12). This water level gradient in turn, causes a hydraulic pressure difference resulting in a force towards the inner bend ($F_p = \rho g \Delta h$). The pressure force is uniformly distributed over the vertical whereas the centripetal force is logarithmic distributed over the vertical due to the assumption of a logarithmic distribution of flow velocity over the vertical ($F_c = \frac{mu^2}{R}$). This results in a circular motion as shown in Figure 2.12, also known as spiral flow or helical flow. As the concentration of sediment near the bed is higher than near the surface, the sediment transport is higher towards the inner bend than the outer bend. This will eventually lead to a deeper outer bend and shallow inner bend. Therefore, when a bend is located just upstream of a bifurcation, the stretch located at the inner bend receives more sediment than the stretch at the outer bend (Kleinhans, Jagers et al. 2008).

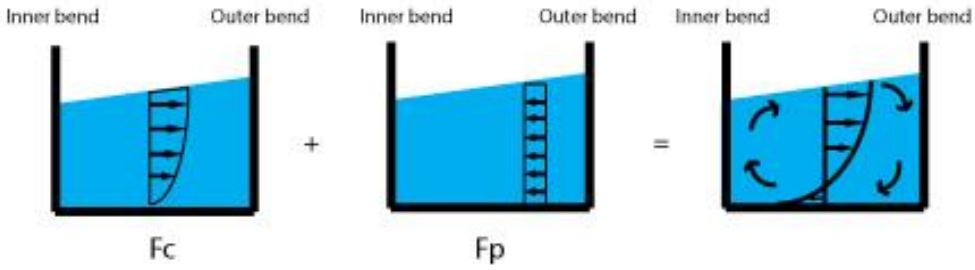

Figure 2.12 – Principal of secondary flow

Human interference

As stated before, a small perturbation can affect the stability of the bifurcation strongly. Therefore, human interferences such as groynes, levees, meander cut-offs and canals can impact the discharge and sediment distribution at the bifurcation.

2.4 Fluvial islands

Fluvial islands are present in nearly all major rivers and may change the fluid mechanics in rivers. A fluvial island as defined by Osterkamp (1998) is 'a land mass within a river channel that is separated from the floodplain by water on all sides, exhibits some stability and remains exposed during bankfull flows'. Fluvial islands are key ecosystems in a river where vegetation can grow and animals can rest.

An indicator of island stability is the existence of the island during and after high flows. Another indicator may be vegetation. However, this is not always true as it also depends on the sediment type, where too coarse sediment may not allow for the establishment of vegetation. A distinction between bars and islands can be made based on these parameters as bars have no vegetation and are submerged during high flows. Besides, bars exhibit higher instability over a shorter timescale, whereas islands may only be unstable for a timescale over centuries to millennia.

Fluvial islands can be considered as a combination of a bifurcation and a confluence (Figure 2.13). Therefore, a combination of effects corresponding to bifurcation and confluence occur for islands. Where, the shape of the bifurcation point influences the distribution of sediment transport, hence the equilibrium depth of the branches. The effect of discharge variation results in erosion of the left branch simultaneously with sedimentation right and vice versa. Downstream of the confluence erosion and sedimentation waves occur which are larger than in the corresponding case without island (de Vriend, *et al.* 2011). At the confluence contraction and curving of streamlines occurs accompanied by secondary flows and lateral transport. Depending on the geometry, this causes erosion holes and shallow areas.

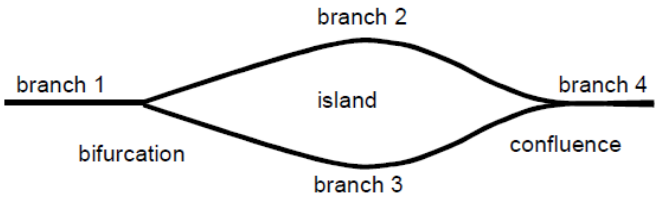

Figure 2.13 – Island as a combination of a bifurcation and confluence (de Vriend, Havinga et al. 2011)

Wyrick (2005) and Wyrick *et al.* (2011) defined several types of islands based on their formation, namely:

- Avulsion islands: are formed during high flow events where the river may excavate a shorter path, particularly at a bend.
- Gradual-erosion islands are formed in anabranching part of rivers (see e.g. classification of Nanson and Knighton (1996)). At converging flows erosion occurs, whereas at diverging flows deposition occurs. They are formed of coarse sediment flood deposits, upland erosion, bank failure or an abundant supply of bed sediments causing deposition of the coarse material and/or incision of the flanking channels.
- Lateral-shift islands are created by channel migration and meander cut-off or by the interactions at the confluence of multiple meandering streams. They are common features in braided and meandering rivers.

- Bar/riffle-stabilization islands are formed when a bar or riffle stabilizes due to vegetation or sediment coarsening which may occur during a long period of low flow.
- Structural- islands form almost exclusively in high gradient, bedrock channels. Structural-islands may emerge as the river preferentially erodes through bedrock fractures.
- Flood-deposit islands form during the rapid removal of sediment during a flood, mass movement, or general landscape instability. The difference between avulsion islands is that flood-deposit islands are formed by erosion of newly-deposited sediments, whereas avulsion islands are composed of older-deposited floodplain material. Flood-deposit islands are formed mostly along small streams which are altered during small time scale.
- Lee-deposition islands are formed downstream of a channel obstruction, where a local zone of shallow depth, reduced velocity, and accumulating sediment may develop and quickly become vegetated. This type is common in widened, braided channels of all sizes where steady sediment evacuation occurs.
- Mass-movement islands are formed due to deposited mass of non- natural river bed sediment within a channel. This type includes debris avalanches and bank failures. The material is generally too coarse or cohesive for the flow to erode and transport downstream, thus diverting the flow around it.

2.5 Bifurcation Canal del Dique – Río Magdalena

The Canal del Dique is connected to the Río Magdalena at Calamar at an angle of approximately 45 degrees, as shown in Figure 2.14 where the direction of the stream is from south to north. It is a man-made offtake of which the inlet is stabilized by bank protection and frequent dredging activities. A sediment trap is located just downstream of the inlet, where most of the large sediment fractions entering the Canal are deposited. The annual mean dredged volume from the sediment trap is around 500.00 m^3/s, however varies significantly per year (see Appendix A).

The Río Magdalena is a sediment laden river, with a predominantly suspended sediment load. Therefore, also in the Canal del Dique the transport in suspension is dominant consisting of mostly fine sediments (85% of the sediment fractions is smaller than 25 µm Appendix A). Most of the fine sediments do not settle in the Canal del Dique, but are deposited downstream in the Bay of Cartagena and Bay of Barbacoas (Figure 1.2).

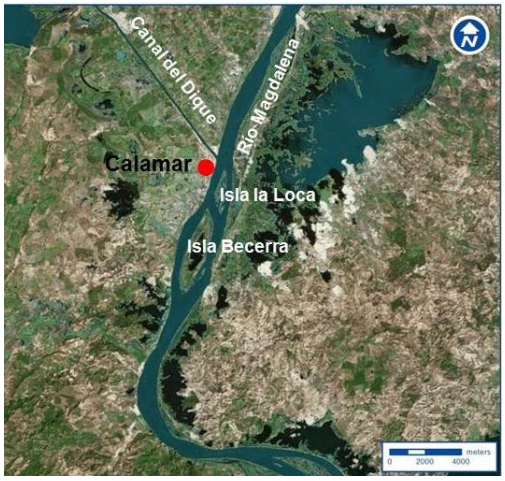

Figure 2.14 – Offtake Canal del Dique – Río Magdalena at Calamar in Colombia (modified from Esri (2015))

Two islands are located just upstream of the bifurcation (Figure 2.14): Isla Loca 'the crazy island', named after its highly morphodynamic character, and the more upstream located Isla Becerra which is larger and its location is more stable. Over the past 40 years Isla la Loca has migrated over 2000 metres in downstream direction and changed both in size and shape, as shown in Figure 2.15. Where, a trend can be observed of enlargement of the island in both downstream direction as to the right river bank. As the morphology of Isla Becerra seems to be more stable throughout history, the amount of water and sediment that is divided over the branches along this island is also stable and almost equally distributed. Whereas, the division of water and sediment along Isla la Loca has changed throughout history being more favourable in the left branch. Currently, the distribution of discharge along Isla la Loca is around 85 % along the left branch and 15 % along the right branch.

Furthermore, historical measurements show that approximately 5-10 % of the discharge from the Río Magdalena is distributed into the Canal del Dique (Section A.4 Appendix A).

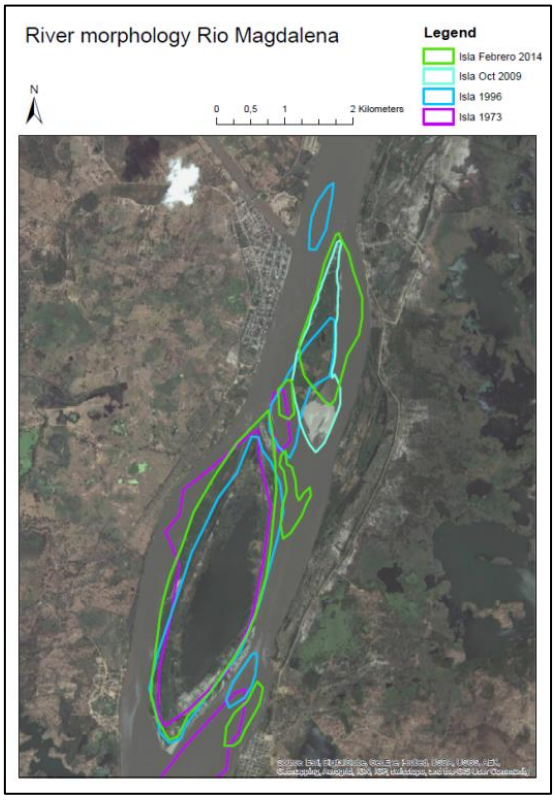

Figure 2.15 – Island contour lines at the Canal del Dique – Río Magdalena bifurcation from 1973 – 2014 (Consorcio Dique 2014)

Furthermore, analysing the historical morphological measurements it can be concluded that Isla la Loca in the Río Magdalena is formed out of the more stable Isla Becerra. Its formation is probably caused by the excavation of an area of sedimentation at the tail of Isla Becerra caused by flow separation during high flows. The origin of Isla Becerra is not known as no morphologic data are available which date back to the time when Isla Becerra was formed. However, it is likely that Isla Becerra was formed by stabilization of a bar due to vegetation during a long period of low flow. Furthermore, historical bathymetries show the presence of a small island between Isla la Loca and Isla Becerra and an island just downstream of the point of bifurcation in the Río Magdalena, which seem to appear and disappear over several years.

Recent measurements of Consorcio Dique in 2014, show that the measurements are exceeding the rating curve based on measurements from 1985-2004 by 10%. It is thought that this exceedance of the rating curve is due to morphological changes.

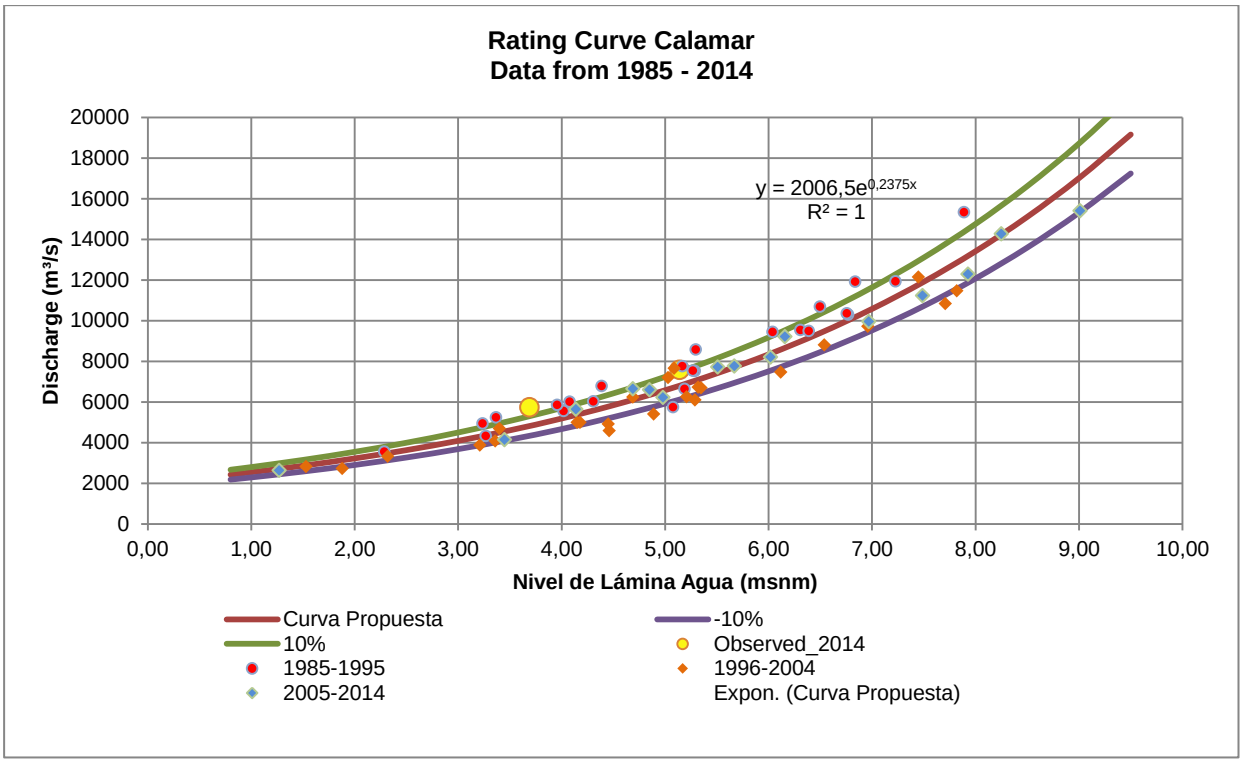

Figure 2.16 – Rating curve at Calamar in the Río Magdalena based on measurements from 1985-2014 as proposed by Consorcio Dique (2014)

Figure 2.17 is a sketch of the relevant physical processes occurring in the study area. Areas of sedimentation are marked yellow and areas where erosion is likely to occur red. The yellow arrows indicate the occurrence of lateral sediment transport. It can be seen that a bend is located just upstream of Isla Becerra, where spiral flow occurs, which will result in a larger outer bend than inner bend. This effect can result in a deeper stretch at the left side of Isla Becerra which will take more discharge to its account than the shallower branch. At the right tail of Isla Becerra the flow cannot fallow the banklines anymore due to a sharp edge, resulting in flow separation and an eddy where sedimentation is likely to occur. In contrary, at the left tail of Isla Becerra, a confluence of streams occurs where the streamlines are curved and contracted. In this area erosion it is assumable that erosion will occur. Furthermore, flow separation will occur at the left side at the entrance of the Canal del Dique, where sediment gets trapped in the eddy. Finally, flow separation at the tail of Isla la Loca will also result in sedimentation in this area.

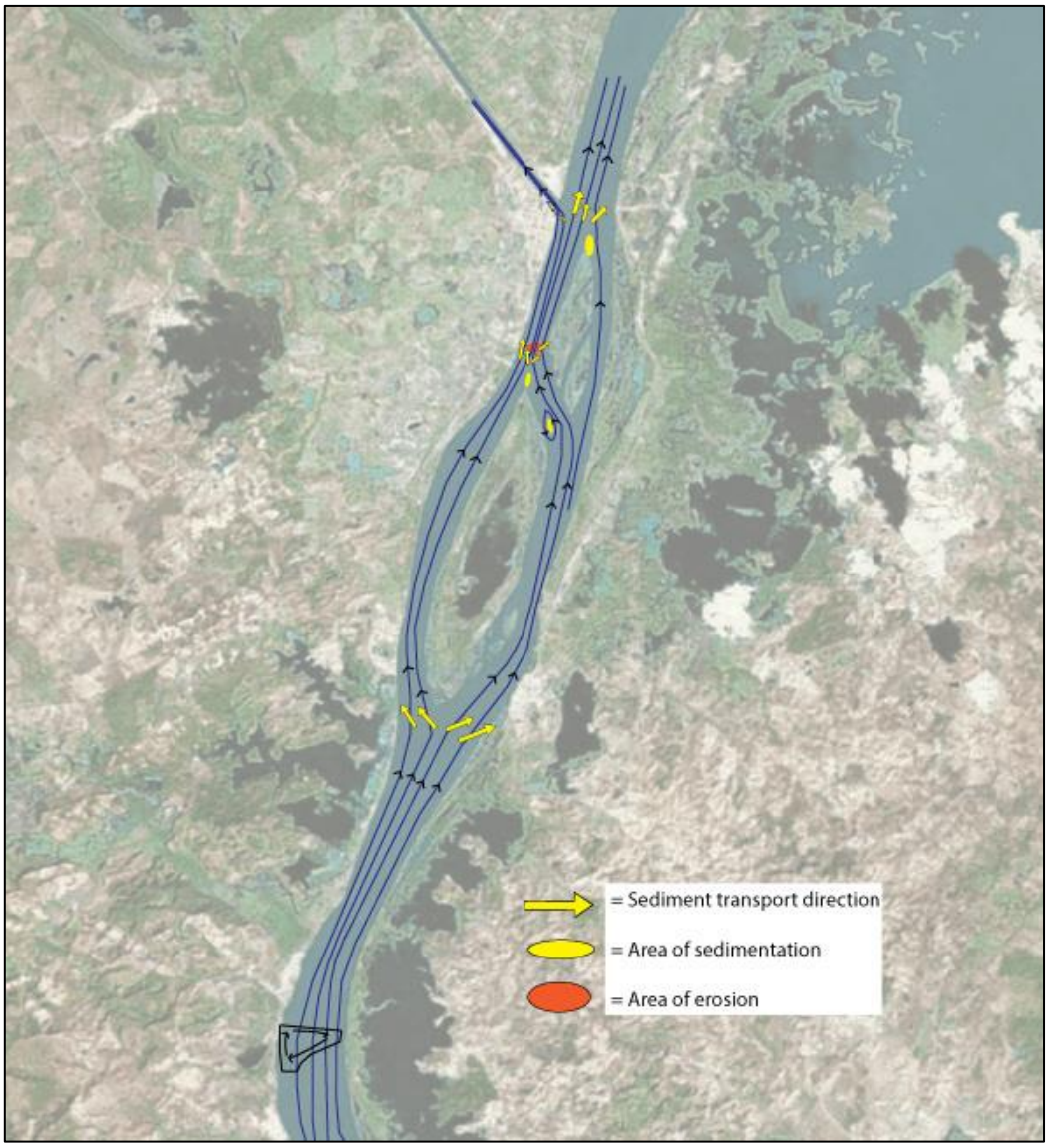

Figure 2.17 – Physical processes occurring in the area of the bifurcation of the Río Magdalena and Canal del Dique

Finally, a brief explanation of the discharges and sediments occurring in the Río Magdalena is given in this paragraph. A more detailed study can be found in Appendix A. The hydrograph of the Río Magdalena at Calamar shows two peak discharges throughout the year followed by periods of lower flow (Appendix A). The sediment load seems to follow the discharge, however, between the sediment *concentration* and the discharge in the Río Magdalena, no one-to-one relation can be made (Consorcio Dique 2014). During the wet season, annual high discharges in the Río Magdalena are around 10.000 m^3/s and in the dry season around 2.000 m^3/s.

During El Niño and la Niña years respectively extreme low and high discharges are observed, which occur every three years. During the 2010 flood, an extreme peak discharge of 18.250 m^3/s was measured corresponding to a return period of 100 years for the Río Magdalena at Calamar (Consorcio Dique, 2013). Despite the varying discharges and relatively high flow velocities (~ 1 m/s at the bifurcation point), navigability should be maintained the whole year around.

3 ONE-DIMENSIONAL HYDRODYNAMIC ANALYSIS

This chapter describes the set-up and model results of the hydrodynamic model simulations on a one-dimensional scale (averaged over the depth and width). The aim of this study as part of the entire research is to gain insight in the effect of size and position of fluvial islands at a bifurcation on the distribution of water along the islands and at the bifurcation in its most simple form. This study forms the basis for further research on a higher order scale for which recommendations are drawn at the end of this chapter.

3.1 Model set-up

3.1.1 Choice of model

As the system is complex with several confluences and bifurcations, manual calculations become quickly very complicated (shown in Appendix B). Therefore, the modelling software 'Sobek-RE' is used which allows for accurate one-dimensional calculations of hydrodynamic and morphodynamic processes (Deltares 2012). It is capable of handling one-dimensional problems in open channel networks and is able to calculate steady and unsteady water flow. 'RE' stands for rivers and estuaries, where in this case the 'River' module is chosen as tidal influences do not occur at the bifurcation. More detailed description of Sobek-RE is given in Appendix C.

3.1.2 Schematization

The area of the bifurcation is schematized as a network around two fluvial islands as shown in Figure 3.1. This results in a system with numerous branches, bifurcations and confluences, where dimensions of the study area from the bifurcation of the Canal del Dique and Río Magdalena are used. Boundary conditions were chosen such that backwater effects do not occur at the upstream start of the downstream branches (branch 12 and 13) by adapting the length of the downstream branches. More detailed calculations are described in Appendix B.

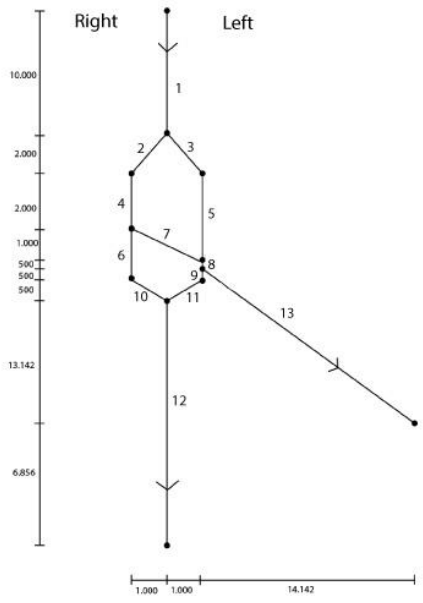

Figure 3.1 – Schematisation of the 1D model with dimensions in meter

The branches will be denoted in the following as:

- *Main channel upstream*: branch 1
- *Main channel downstream:* branch 12
- *Right branches along upstream island*: branch 2 and 4
- *Left branches along upstream island*: branch 3 and 5
- *Mid channel*: branch 7
- *Right branches along downstream island*: branch 6 and 10
- *Left branches along downstream island*: branch 9 and 11
- *Offtake:* branch 13

3.1.3 Method

The effect of the size and position of the islands on the discharge distributions along the islands and at the bifurcation is assessed by changing the width, length, depth and position of the branches along the islands. Where, the more downstream located island is chosen to change the most as the case in the Río Magdalena. Therefore, also the length, width and depth of the branches surrounding the most downstream located island are changed. Furthermore, the sensitivity of the physical characteristics of the offtake is investigated in order to gain insight in the influence of the characteristic of one of the branches to the system. The parameters which are investigated are:

Mid channel

- Width of the mid channel (size islands)
- Length of the mid channel (shape islands)

Bathymetry branches

- Ratio of the depth of the right branches to left branches
- Ratio of the depth of the right branches to the left branches along the downstream island

Position and size changes of the (downstream) island(s)

- Ratio of the width of the right branches to left branches
- Ratio of the width of the right branches along the downstream island to the width of the left branches along the downstream island
- Width of branch 8 and 9
- Length of branch 9
- Position of the offtake compared to the system by varying the start point of the branch on branch 8 and 9

Main physical characteristics offtake

- Width of the offtake
- Depth of the offtake
- Bed slope of the offtake
- Bed friction of the offtake

The values of the parameters as used in the reference case are shown in Table 3.1 as well as the range of variation of these parameters in order to investigate the bandwidth to the discharge distributions in the system. To have a starting point the values for the reference case correspond to the Canal del Dique case Canal del Dique are chosen.

Table 3.1 – Values parameters reference case and variation of simulations

Parameter	Value reference case	Variation range	Unit
Discharge boundary x=0	5000	[-]	m^3/s
Waterlevel boundary offtake (branch 13)	3	[-]	m
Waterlevel boundary mainchannel (branch 12)	3	[-]	m
Bed friction in the branches (Chézy)	50	Variation offtake: [10:300]	$m^{1/2}/s$
Bed slope in the branches	$1*10^{-4}$	Variation offtake: $[1*10^{-5}:1*10^{-3}]$	-
Width offtake (branch 13)	150	[20:10.000]	m
Average depth in the branches	4	[-]	m
Depth offtake (branch 13)	3	[2:28]	m
Width main channel (branch 1 and branch 12)	1000	[-]	m
Width mid channel (branch 7)	1000	[0:5000]	m
Length mid channel (branch 7)	2236	[2000:2500]	m
Width right branches (branch 2, 4, 6, 10)	500	[100:1000]	m
Width left branches (branch 3, 5, 8, 9, 11)	500	[100:1000]	m
Width branch 8 and 9	[200:5000]	500	m
Length branch 9	[100:1500]	500	m
Position of the offtake (from upstream boundary)	15	[15:15.9]	km

The value of the upstream discharge and downstream water level do not seem to affect the discharge distribution of the branches relative to the corresponding upstream discharge as shown in Figure C.1 and Figure C.2 (Appendix C). Therefore, only calculations are made with one steady discharge in order to reduce the computational effort. However, it has to be bared in mind that changing the upstream discharge or downstream water level does influence the (equilibrium) water levels in the branches. Furthermore, prismatic cross-sections are used to further simplify the model.

Finally, it has to be bared in mind that values of the variation range of the parameters may not be realistic, for example a width of the offtake of 5km does not seem to be realistic. However, the range is chosen to obtain physically possible maximum and minimum discharge and water levels occurring in the branches

3.2 Results

The most important results of the simulations are discussed in the following paragraphs. For a closer insight on the effects of each parameter separately the results are given in Appendix C.

3.2.1 Reference case

First, of all the reference case will be analysed in order to get an understanding of the system. Figure 3.2 shows the discharge in the branches and Figure 3.3 and Figure 3.4 the water surface profiles in the study area. It can be seen that the discharge in the right upstream branches (branch 2 and 4) is larger than the left upstream branches (branch 3 and 5) as the length of the right upstream branch is smaller for which the resistance in these branches is smaller and the discharge higher. Besides, the mid

channel extracts water from the right upstream branches, resulting in a lower water level at the end of the branch for which the water level head is larger in the right upstream branches and the discharge larger. Besides, it can be seen that the discharge in branch 8 is high due to the confluence of the mid channel and left upstream branch (branch 5). Furthermore, it can be seen that the discharge in the right downstream branch (branch 10) is smaller than the left downstream branch (branch 11) as the water level head is smaller in the right branch, due to the lower water level at the entrance of the branch caused by extraction of water by the mid channel. Finally, it can be seen that the discharge in the offtake is much smaller than the downstream main branch (branch 12) as the width is much smaller (150 m compared to 1000 m), resulting in a lower flow capacity.

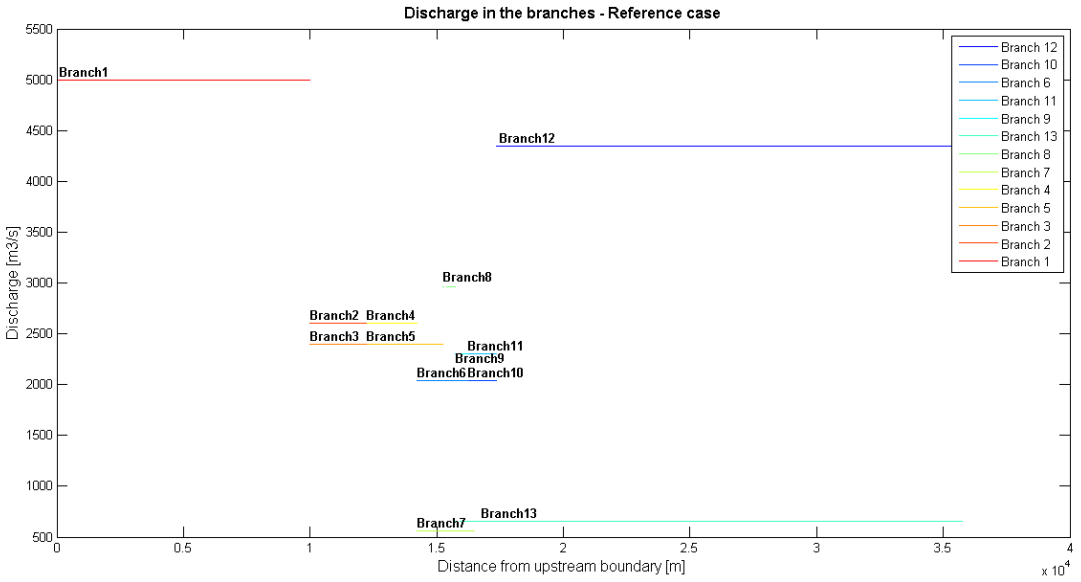

Figure 3.2 – Discharge in the branches in the reference case

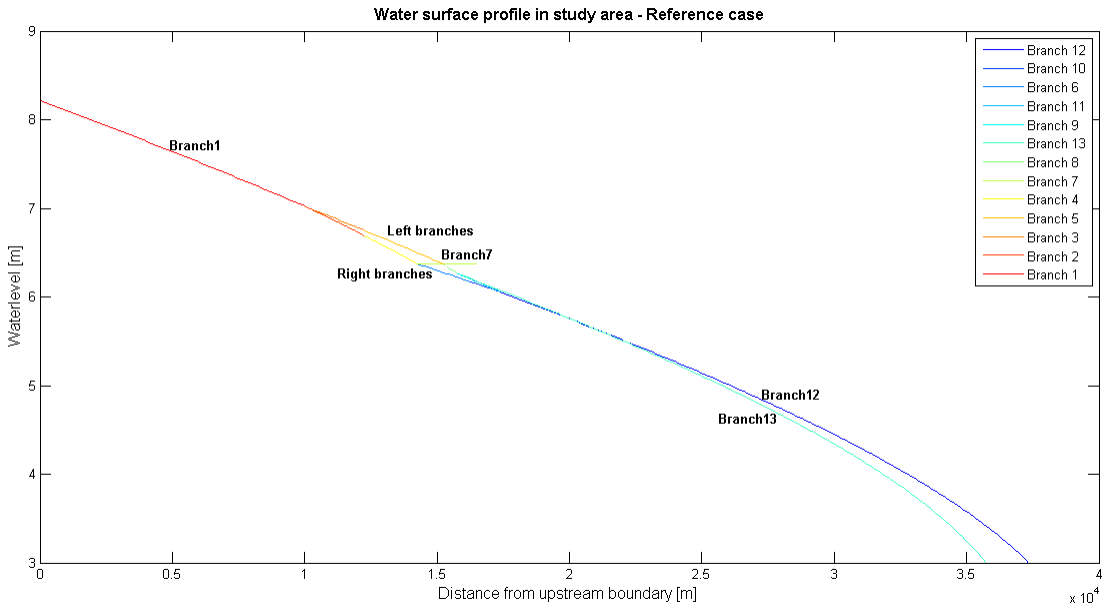

Figure 3.3 – Water surface profile reference case in the entire study area

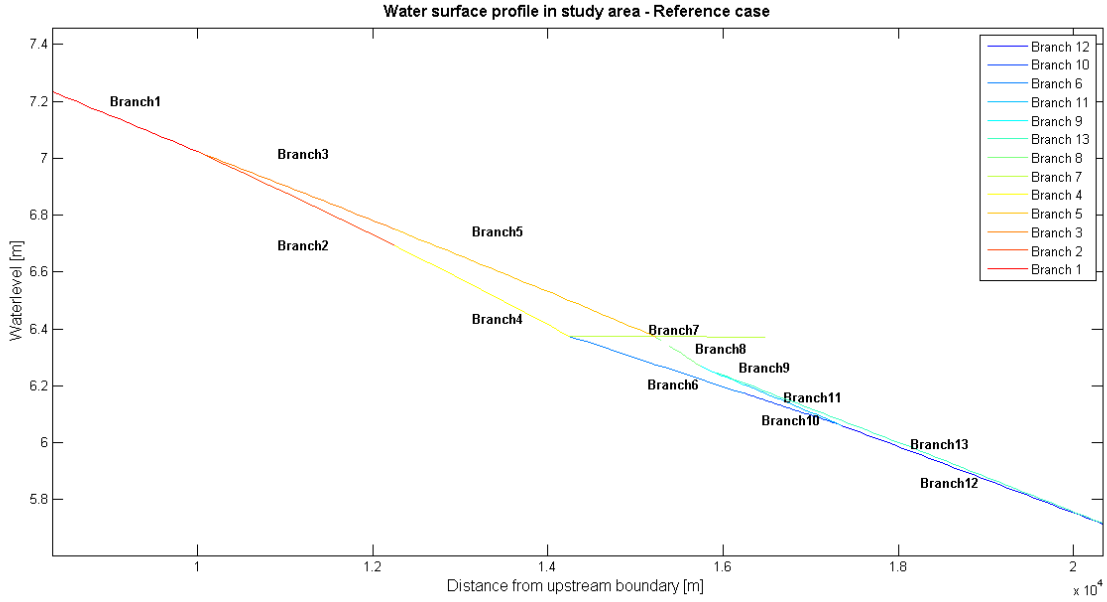

Figure 3.4 – Water surface profile in the reference case, zoomed in the area of interest

3.2.2 Effect of the width and length of the mid channel

The width and length of the mid channel depends on the size and position of the islands, e.g. when there is a large distance between the islands, the width of the mid channel could be considered large. Variation in length of the mid channel can be considered as changes in size of the islands. Different lengths of the mid channel are obtained by changing the position of the downstream end of the mid channel, while keeping one end of the mid channel at the same position as shown in Figure 3.5.

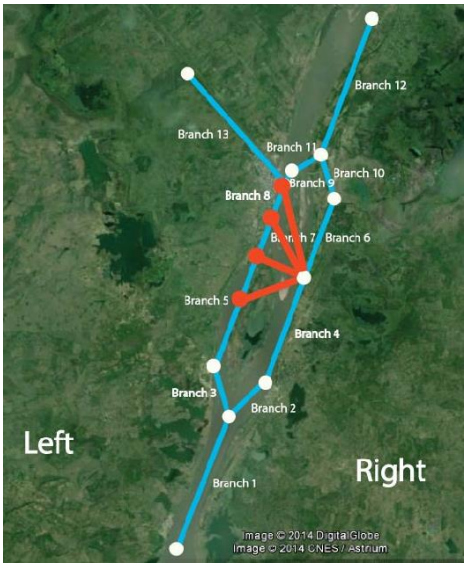

Figure 3.5 – Position changes of downstream end of the mid channel as varied in model simulations

Increasing the length or width of the mid channel results in a larger resistance to the flow in the mid channel. Therefore, the water level gradient in the mid channel decreases resulting in a higher water level at the end of the mid channel and therefore a higher water level at the entrance of the offtake (Figure 3.6). Besides, when the length of the mid channel increases such that the downstream end of

the branch is attached closer to the offtake, this results in a higher water level at the entrance of the offtake. A higher water level at the entrance of the offtake in turn results in a larger water level *head* in the offtake, as the downstream boundary is fixed; hence the discharge in the offtake is larger (Figure 3.8).

However, it can be seen that the water level differences in the offtake for changes in width and length of the mid channel are small, around 1 cm. Therefore, also the differences in discharge in the offtake are small, with a maximum variation of approximately 0.3 % relative to the upstream discharge, which is equal to a variation of 15 m^3/s of discharge in the offtake.

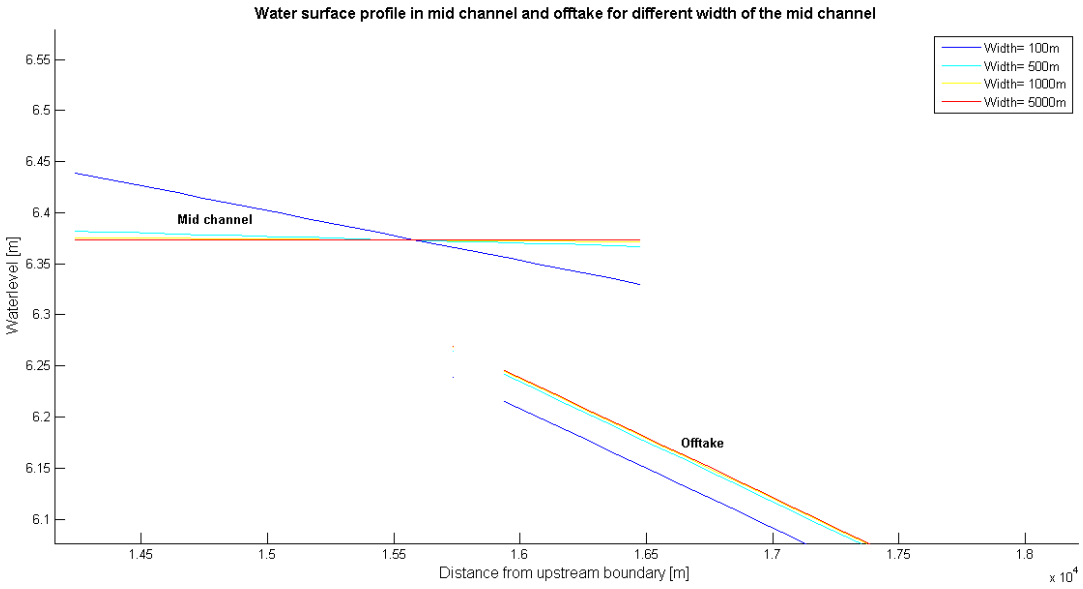

Figure 3.6 – Water level in mid channel and offtake for different width of the offtake

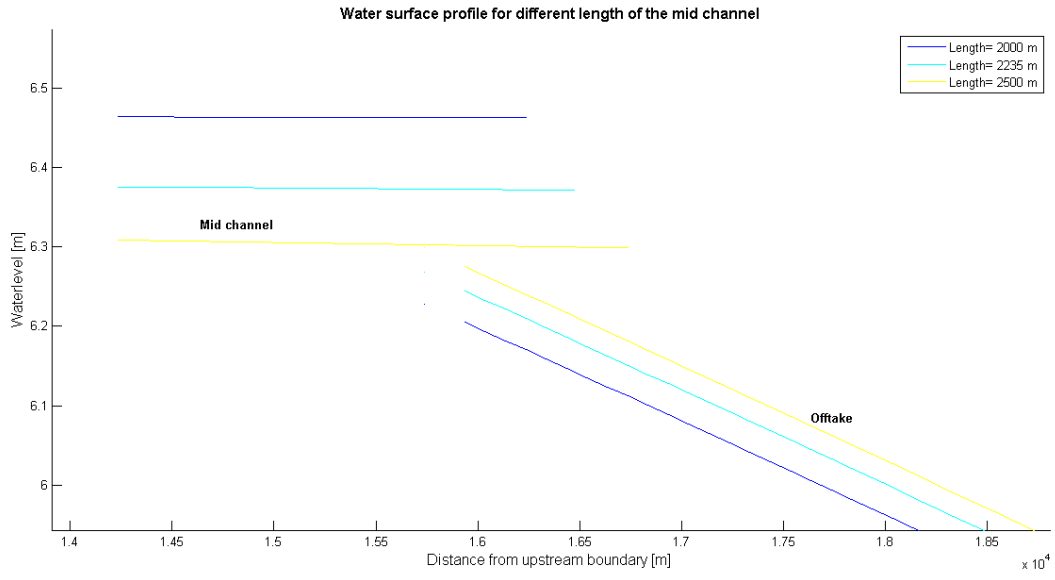

Figure 3.7 – Water level in mid channel and offtake for different length of the mid channel

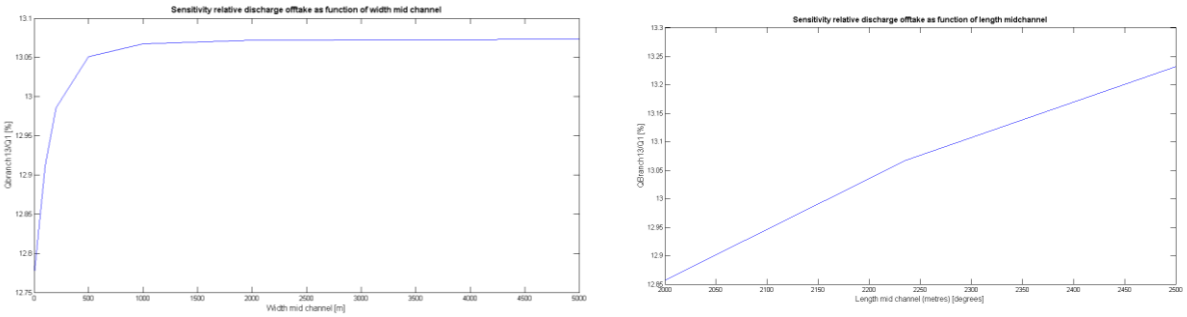

Figure 3.8 – Sensitivity of the width and length of the mid channel to the discharge in the offtake relative to the upstream discharge

When the length of the mid channel is changed, such that the length of the left upstream branch (branch 4) is smaller than the right upstream branch (branch 5), as shown in Figure 3.9, the water surface profile in the left branches becomes concave shaped (M1 type of backwater curve as explained in section 2.1.1), while in the right branches a convex shape (M2-type of backwater curve) is observed. As the water level at the downstream main branch and upstream of the islands is equal, this results in a lower water level at the entrance of the offtake, which implies a lower discharge in the offtake. The contrary holds in the reference case where the mid channel extracts water from the right branch upstream and discharges into the left branches, resulting in a lower water level at the point of extraction hence concave shape of the water surface profile in the right branches. The input of water from the mid channel to the left downstream branch results in a higher water level at the point of the mid channel resulting in a convex shape of the water surface profile in the left branches.

Besides, as the length of branch 5 becomes shorter, the resistance in this branch is smaller resulting in more discharge in the left upstream branch than the right upstream. Therefore, the dominant path of the flow becomes from the left upstream branch towards the right downstream branch (Figure 3.10 and Appendix C) while the contrary holds when the mid channel is located such that the length of branch 4 is larger than the length of branch 5.

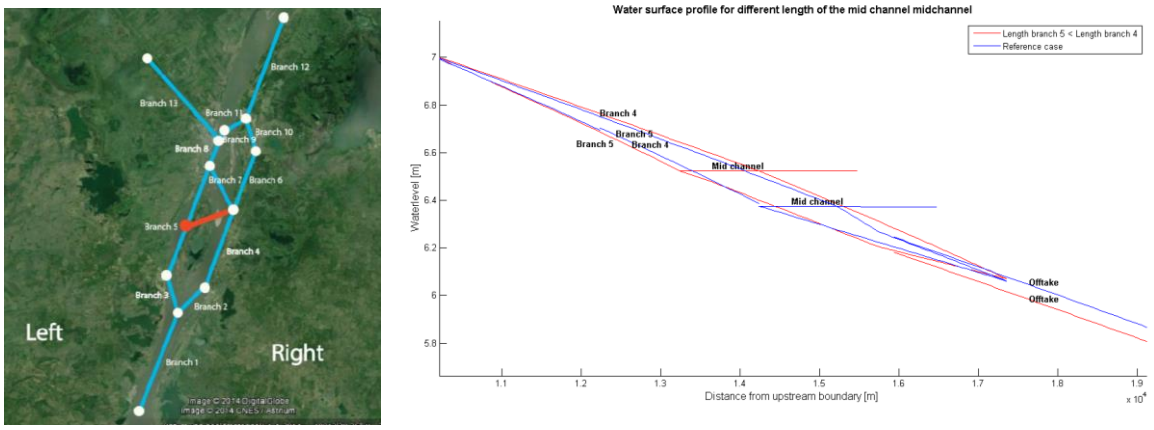

Figure 3.9 – Water level in the study area for a smaller length of branch 5 compared to branch 4 (red) and the reference case (blue)

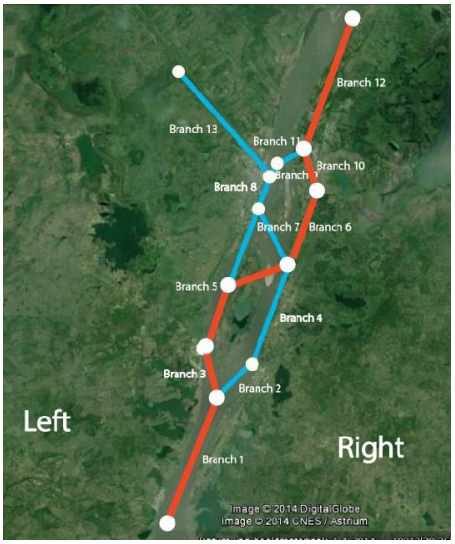

Figure 3.10 – Dominant path when the length of branch 5 is smaller than the length of branch 4

A strong correlation of the discharge is found between branch 7, 8 and 13 and opposite correlation with branch 10 and 11 (Figure 3.11) for changes in width of the mid channel. When the discharge in one of these branches increases, the discharge in all of the branches increases. As these branches are connected to each other, changes in characteristics of these branches influences the water level at the end and start of these branches, hence resulting in corresponding discharge changes in these branches.

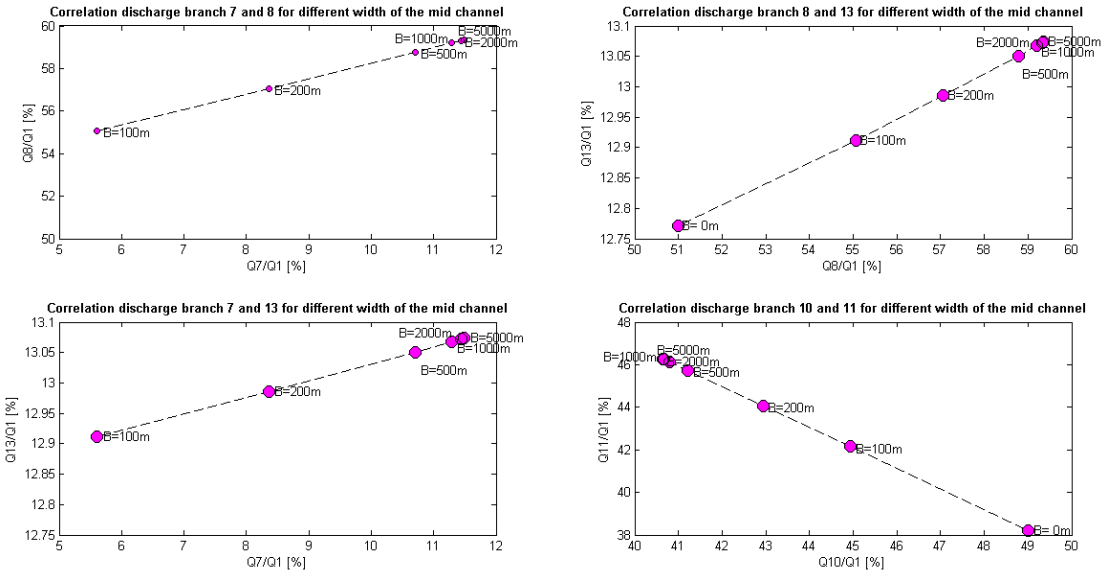

Figure 3.11 – Correlation branch 7, 8, 13, 10 and 10 for different width of the mid channel

In the case when there is no mid channel, i.e. when the width of the mid channel is zero, the distribution becomes more dominant along the left upstream branch (branch 5) and right downstream branch (branch 10) as shown in Figure 3.12. Having no mid channel can be seen as the presence of one big island instead of two islands. When there is a mid channel, the extraction of water from the mid channel along the right branches results in a concave shape (M1-type of backwater curve) of the

water surface along the right branches and a convex (M2-type) along the left branches (Figure 3.13). When there is no mid channel, the contrary holds. Therefore, the water level at the entrance of the offtake is lower when there is no mid channel, hence the discharge in the offtake is lower. Therefore, it can be said that the presence of a mid channel, i.e. two islands, results in a higher discharger in the offtake.

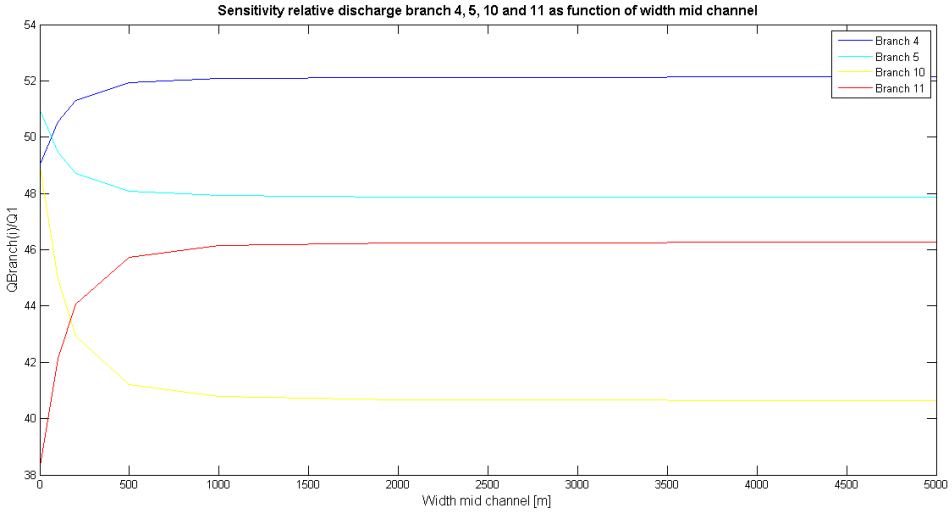

Figure 3.12 – Sensitivity width of the mid channel for discharge in the right and left branches

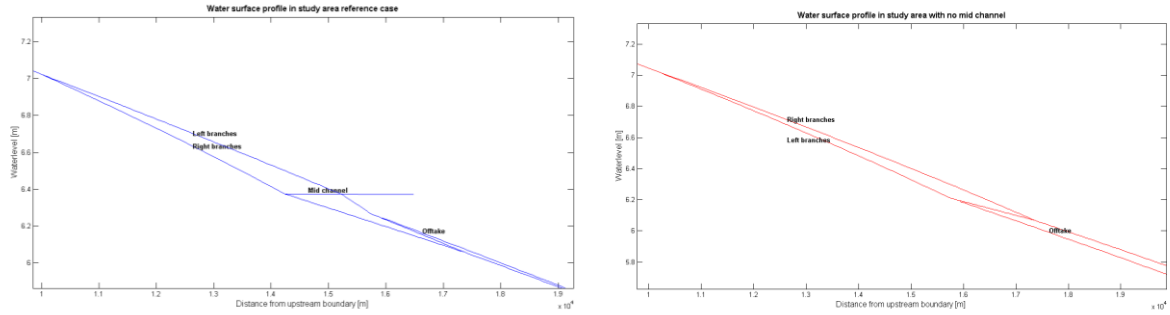

Figure 3.13 – Water level in area of interest in the reference case (left) and when there is no mid channel (right)

3.2.3 Effect of the width and depth of the branches along the islands

When the width and/or depth of the right branches (branch 2, 4, 6, 10) is increased compared to the left branches (branch 3, 5, 8, 9, 11) the discharge in the right branches increases as the flow area increases, while the discharge in the left branches decreases (Figure 3.14). When the width or depth of the right branches is larger than the left branches (ratio>1), the discharge in the right branches is larger than in the left branches. In contrary, when the width and depth of the right branches is *smaller* than the left branches (ratio<1), the discharge in the right branches is *smaller* compared to the left branches due to the smaller flow area. Besides, when increasing the width of the branches, the flow experiences more resistance than when increasing the depth of the flow causing the discharge in the branches to stabilize when applying large widths as shown in Figure 3.14. Depth ratios larger than 2 and smaller than 0.2 cannot be computed as the water level in the left and respectively right branches becomes so small that no flow will go through these branches anymore.

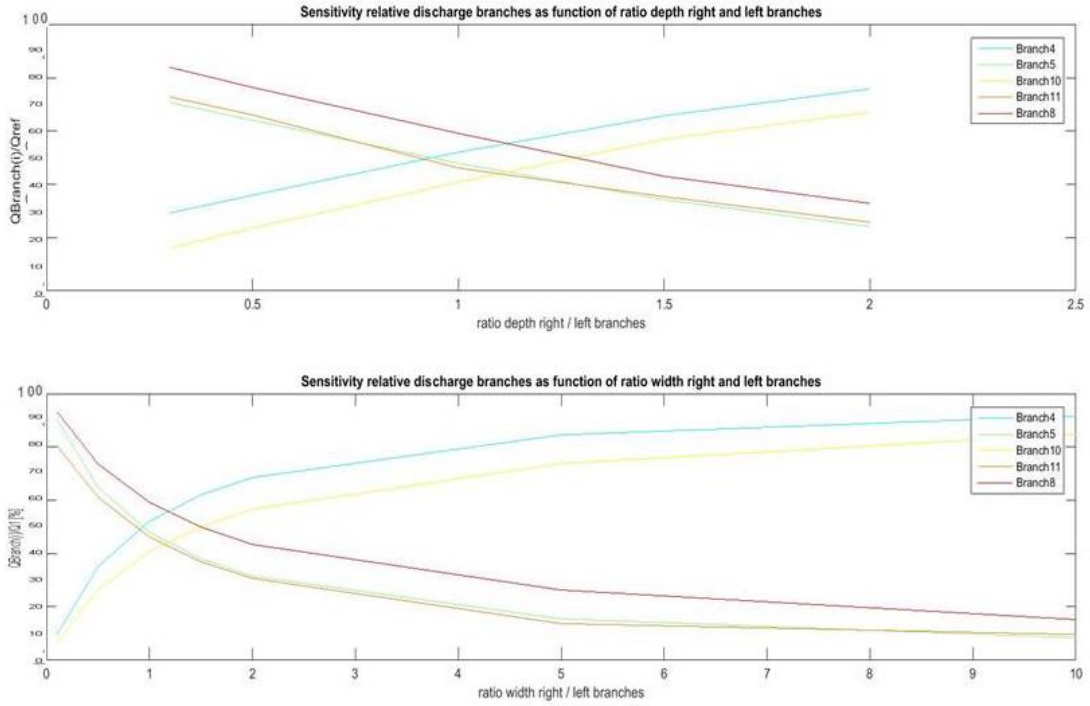

Figure 3.14 – Discharge left and right branches for different ratio of the width and depth of the right and left branches

The discharge in the offtake is determined by the water level at the entrance of the offtake, as also found in the previous section. When the width or depth of the left branches is larger than the right branches (ratio< 1), the water level along the left branches is more convex shaped (Figure 3.16 and Figure 3.17). Therefore, the water level at the entrance of the offtake is higher; hence the discharge increases in the offtake (Figure 3.15). It can be seen that the water surface profiles are more curved for the same depth ratios compared to the width ratios. Therefore, it can be seen that for equal changes in ratio of the width and depth, the differences in discharge al larger for depth rations. Furthermore, it can be seen that in the case the depth and width of the right and left branches are equal the discharge in the offtake is higher than in the case the depth in one side of the branches is deeper or wider than in the other side. This explains the peak in the discharge in the offtake at a ratio of 1 as shown in Figure 3.15.

With equal width of the right branches compared to the left branches, the water level in all the branches are larger, as the discharge becomes more equally distributed along both upstream branches. Therefore, the water level at the entrance of the offtake is larger, resulting in a larger water level head in the offtake and larger discharge. This explains the peak in Figure 3.15, which is most dominant for depth changes.

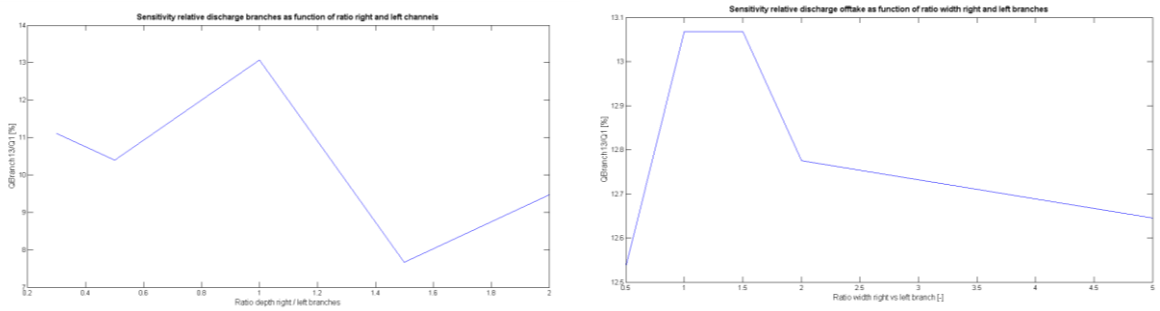

Figure 3.15 - Discharge in the offtake for different ratio of depth (left) and width (right) of right and left branches

Finally, it can be seen that increasing the depth of the right branches compared to the left branches with a factor 2 (for example from a ratio of 1 to 2), the discharge in the offtake decreases with 4% relative to the upstream discharge. This is equal to a decrease of discharge of around 30% relative to the reference discharge in the offtake. When comparing the same difference in ratio of the width, the discharge in the offtake decreases with only 0.3% relative to the upstream discharge. Therefore, it can be said that changes in depth have a larger influence than changes in width. This can be explained by the fact that with larger width, the resistance increases, as the flow experiencing friction from the bed on a larger area.

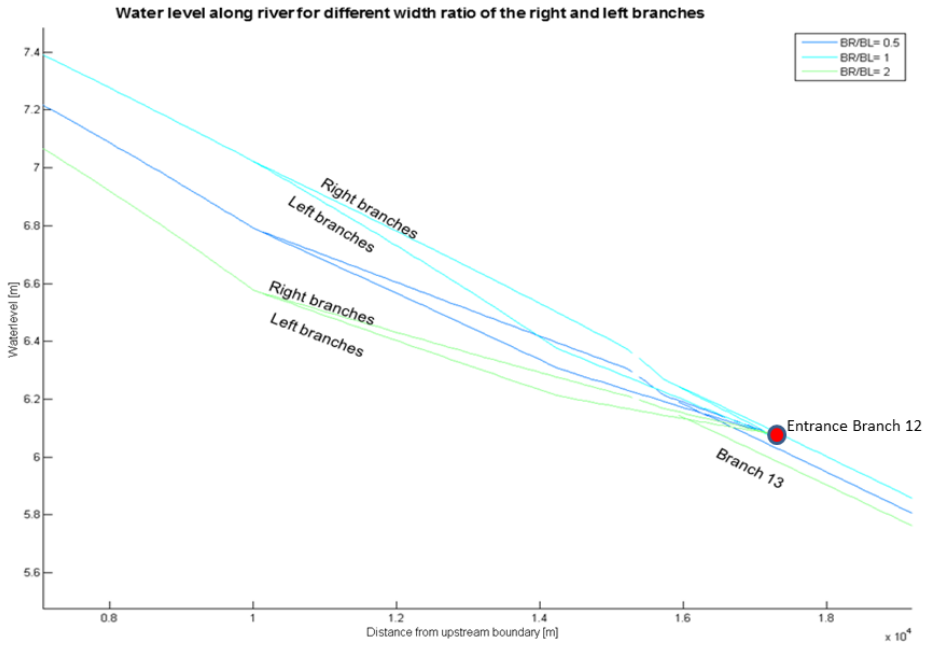

Figure 3.16 – Water level profile in branches along islands and in the offtake for different width of the right and left branches

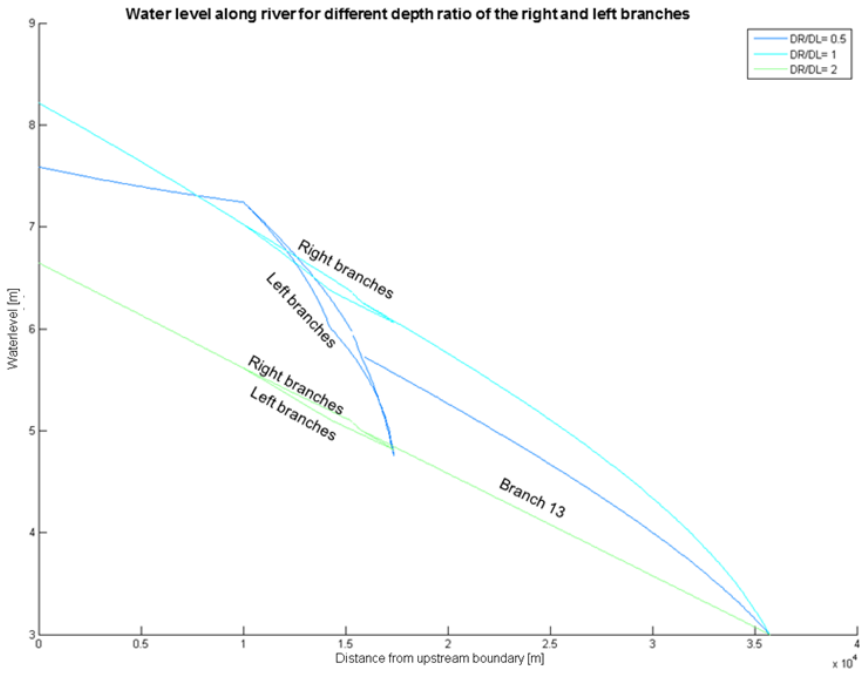

Figure 3.17 - Water level profile in branches along islands and in the offtake for different depth of the right and left branches

3.2.4 Effect of the width and length of the branches along the downstream island

In the case of the Canal del Dique, the most downstream located island is subject to higher morphologic activity than the more upstream located island. Therefore, the sensitivity of the width and length of the left branches of the downstream island (branch 8 and 9) to the discharge in all the branches is tested as shown in Figure 3.8 Changing the width and length of these branches is equal to a different position and size of the downstream island.

For increasing width of branch 8 and 9 the discharge increases in the these branches as well as the connecting mid channel (branch 7) and left downstream branch (branch 11) as shown in Figure 3.18. Due to the increased width of branch 8 and 9, the flow area increases resulting in a higher discharge. Furthermore, it can be seen that the water level gradient in these branches decreases due to a larger resistance to the flow (Figure 3.19), therefore the water level *head* in the connecting mid channel and left downstream branch is larger as the water level at the entrance of the downstream main branch and upstream of the mid channel is equal. This results in a larger discharge in the mid channel and left downstream branch (branch 11). The water level in branch 8 is lower for increasing width of this branch, this also results in a lower water level at the entrance of the offtake for increasing width of the left branches along the downstream island; hence the discharge in the offtake is smaller (Figure appendix). Furthermore, Figure 3.18 shows that the flow capacity of the branches is reached for a width of approximately 2500 meter of branch 8 and 9. Larger widths of these branches does not result in large water level differences and discharges in these branches.

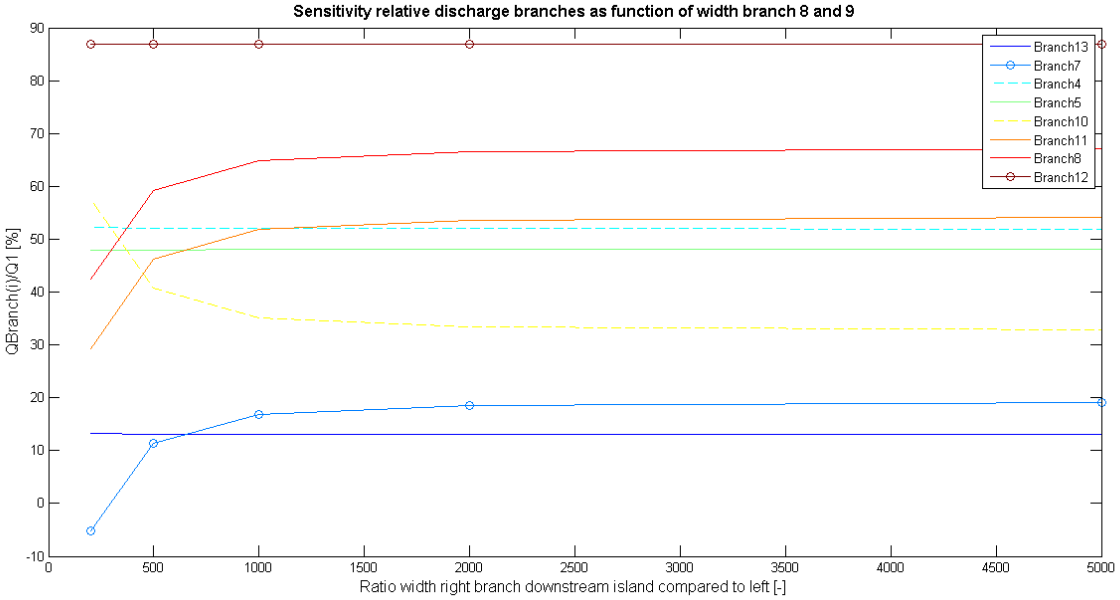

Figure 3.18 - Discharge in the branches for different width of the left downstream branches (branch 8 and 9)

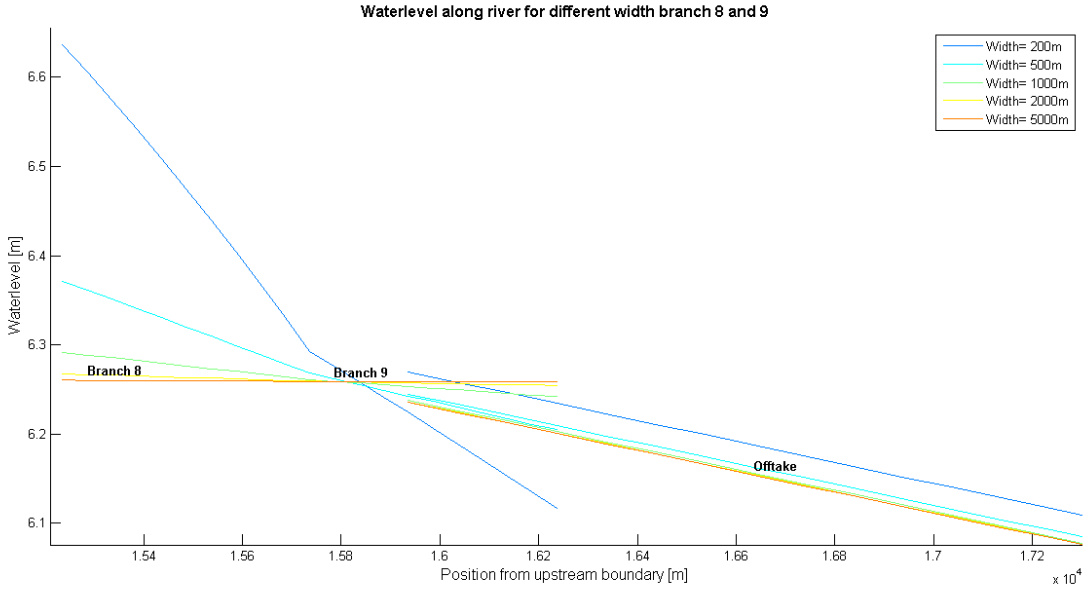

Figure 3.19 – Water level for different width branch 8 and 9

Varying the length of the branches along the downstream island (branch 10 and 11) within a range of 100 to 2200 meter does not impact the discharges in the branches significantly as seen in Figure 3.20 as this does not impact the water level differences in the branches to a large extent (Figure 3.21). The discharge in the offtake increases slightly with increasing length of branch 10 and 11 as the water level at the entrance of the offtake becomes slight higher (Figure 3.21). Due to the larger length of the downstream branches and a similar water level gradient in the branches, this results in a higher water level at the entrance of the offtake, hence larger discharge.

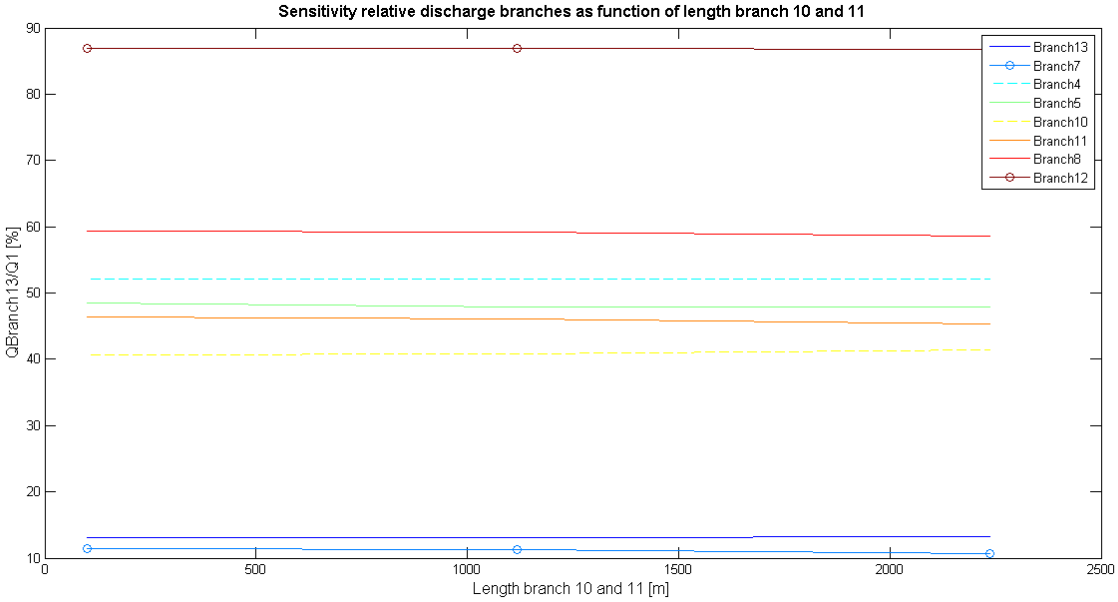

Figure 3.20 – Discharge in the branches as function of the length of branches along downstream island

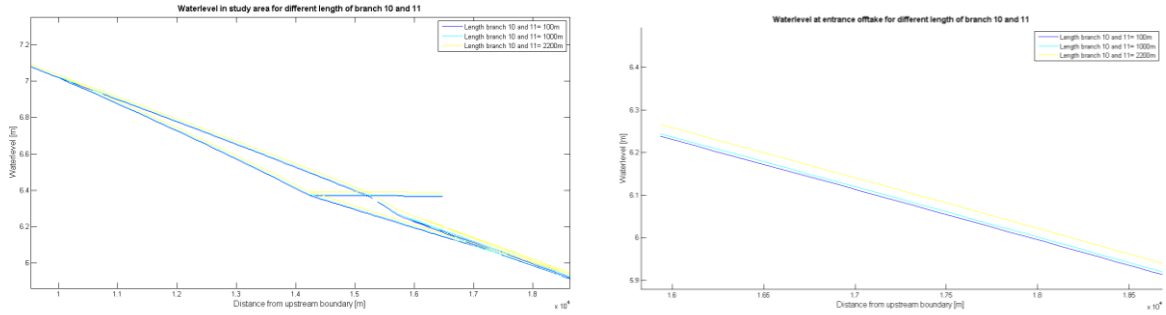

Figure 3.21 – Water level in the study area (left) and at the entrance of the offtake (right) for different length of branch 10 and 11

Overall, it can be said that increasing the width and length of the branch along the downstream island only has minor impact on the discharge distribution in the branches. The discharge in the offtake *decreases* for increasing width of the left downstream ranges and *increases* for increasing length of the downstream branches. Both cause a maximum range of 0.2% relative to the upstream discharge as can be seen from Figure 3.22

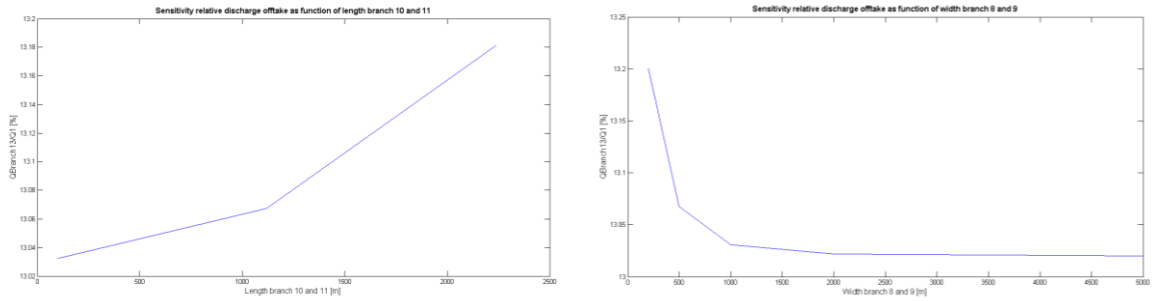

Figure 3.22 – Discharge in the offtake for different length and width of the branches along the downstream island

3.2.5 Sensitivity of the position of the offtake

In this section the sensitivity of the position of the offtake to the discharge in the branches is investigated. From Figure 3.23 it can be seen that a variation of offtake position in a range of 1000 metre, does not result in significant changes in discharge in the branches. Where, it can be seen that when the position of the offtake is located at a larger distance from the upstream boundary, the discharge in the offtake decreases slightly with 0.3% relative to the upstream discharge (Figure 3.24). Due to a smaller length of the main channel downstream of the offtake (branch 9 + 11 + 12) the water level at the beginning of the offtake is smaller hence the water level *head* in the offtake is smaller causing and the discharge in the offtake smaller. The discharge in branch 11 decreases as its length decreases. Again a correlation can be seen with branch 8 and 9 where the discharge decreases for a larger distance from the offtake to the upstream boundary (Figure 3.23).

However from Figure 3.23 it is visible that changing the position of the offtake in the applied range has only small effect on the discharge in the branches including a small the discharge in the offtake (order 0.5 % relative to upstream discharge).

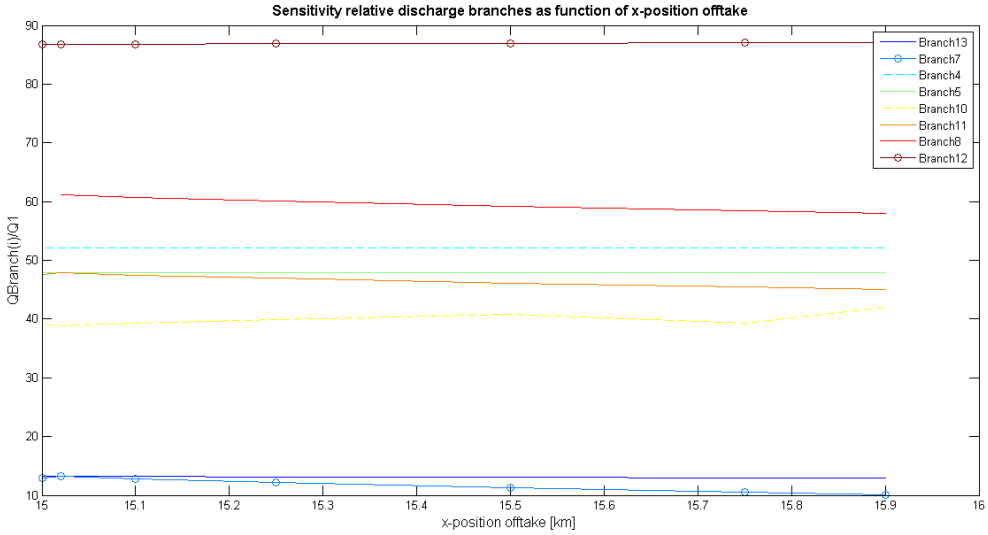

Figure 3.23 – Relative discharge branches as function of position offtake from upstream boundary

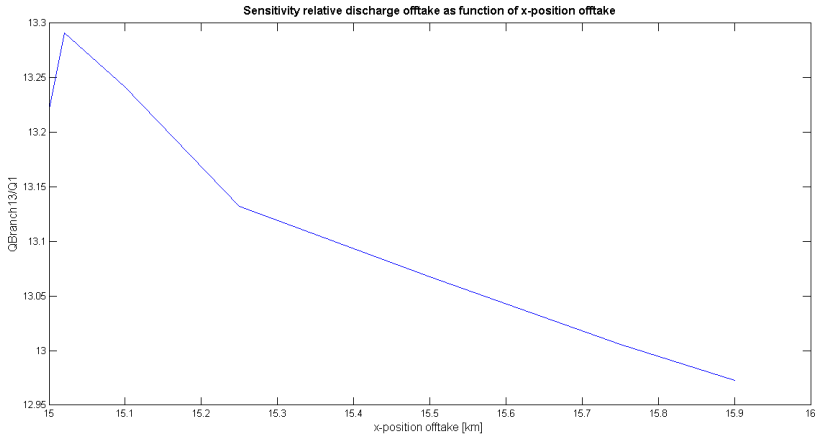

Figure 3.24 - Discharge in the offtake for different position of the offtake

3.2.6 Sensitivity of the main physical characteristics of the offtake

In order to gain insight in the sensitivity of the main physical characteristics of the offtake (width, depth, bed-friction and bed slope) on the discharge distribution along the islands and in the offtake, the characteristics are changed such that a band width of the discharge in the branches is found. Detailed figures are shown in Appendix C, the main findings are described in this section.

Changing the main physical parameters in the offtake results in a large variation of discharge in the offtake. Where, the discharge in the offtake varies within a range of 80% when applying different width and depth of the offtake (Figure 3.26). It has to be bared in mind that these values may not be realistic, for example a width of the offtake of 5000 metre is not realistic. Due to the larger width and depth of the offtake the flow area increases hence the discharge in the offtake increases. However, with increasing width and depth, the resistance to the flow increases resulting in a lower water level at the entrance of the offtake (Figure 3.25). This in turn, results in a larger water level head along the left upstream branch, where the offtake is connected to, and smaller water level head along the right branches (Figure 3.25). Therefore, more water is distributed in the left branches for increasing width and depth of the offtake and less in the right branches and downstream main branch (branch 12) (see Appendix C).

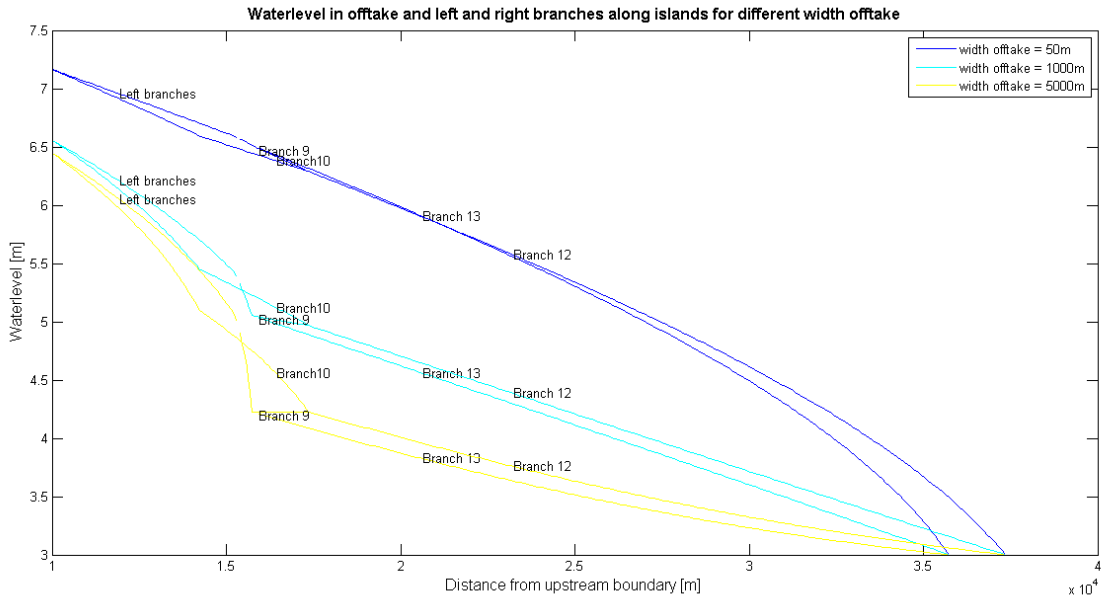

Figure 3.25 – Water surface profile in study area for different width of the offtake

When the width and depth of the offtake becomes so large that the water level at the entrance of the offtake becomes equal or lower than the water level at the entrance of the downstream main branch, this results in a horizontal or negative water level slope in branch 9 (Figure 3.25). Therefore, water is distributed from the right downstream branch (branch 10) into the left downstream branch (branch 11). This occurs in the case of a width of the offtake larger than 5000 m and a depth of the offtake larger than 20 m. It can be said, that from these optimum points the flow capacity of the offtake is reached.

For changes in bed slope and bed-friction the discharge in the offtake is bounded within a smaller range (40-20% relative to the upstream discharge) as shown in Figure 3.26. For very large values of the bed-friction and bed-slope the flow velocities in the offtake becomes so high that they cannot be computed anymore as the bed becomes very smooth and the gravity pull very large.

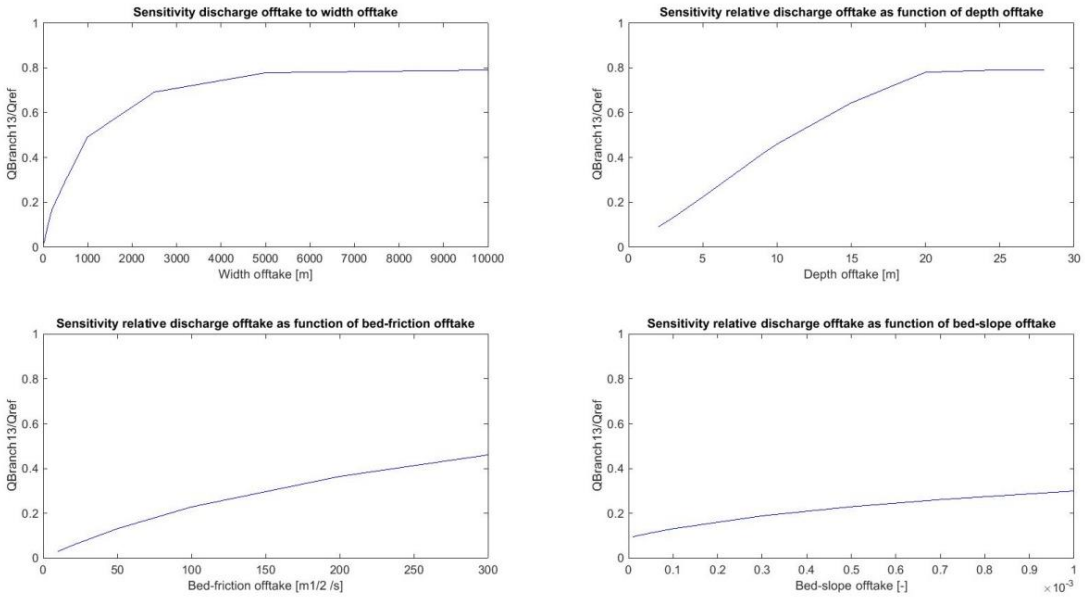

Figure 3.26 – Sensitivity physical parameters offtake on discharge in the offtake relative to the upstream discharge (Qref = Q upstream)

A strong correlation is found between branch 7, 8 and 13 for different physical characteristics of the offtake. This is illustrated in Figure 3.27 for the width of the offtake. As these branches are connected to each other a larger discharge in *one* of these branches results in a larger discharge in *all* of the branches as they influence the water level differences in the branches. By continuity, a larger discharge in these branches, results in a lower discharge in the left downstream branch (branch 11), which explains the opposite correlation as shown in the lower right graph in Figure 3.27. The curves in the correlation plots can be explained by the negative water level gradient in branch 10 and 9 for width of the offtake larger than 1000 metre as explained in the previous paragraph.

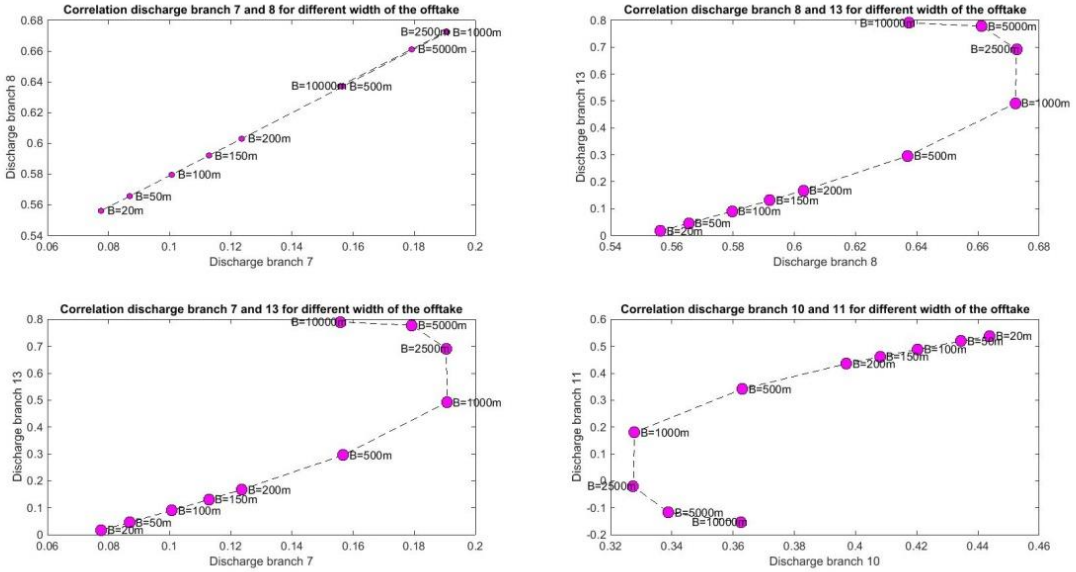

Figure 3.27 – Correlation branch 7, 8, 13 and correlation branch 10 and 11 for different width of the offtake

Furthermore, it is seen that the discharge and discharge distribution in the upstream branches remain almost equal for different width, depth, bed-friction and bed slope of the offtake as shown in Figure 3.28. Where, it can be seen that the discharge in the right upstream branch (branch 4) is slight higher than the discharge in the left upstream branch (branch 5) with a ratio of 52/48. This can be explained by the smaller length of the right branches around the upstream island than the left branches. Therefore, the resistance along the right side is smaller and the discharge large. Besides, due to the presence of the mid channel, water is extracted from the right upstream branch resulting in a lower water level at the end of branch 4 which in turn results in a larger water level head in the right upstream branch, hence larger discharge (Figure 3.25). As the mid channel is always present in the simulated cases, the discharge in the right upstream branches is always larger than the left upstream branches.

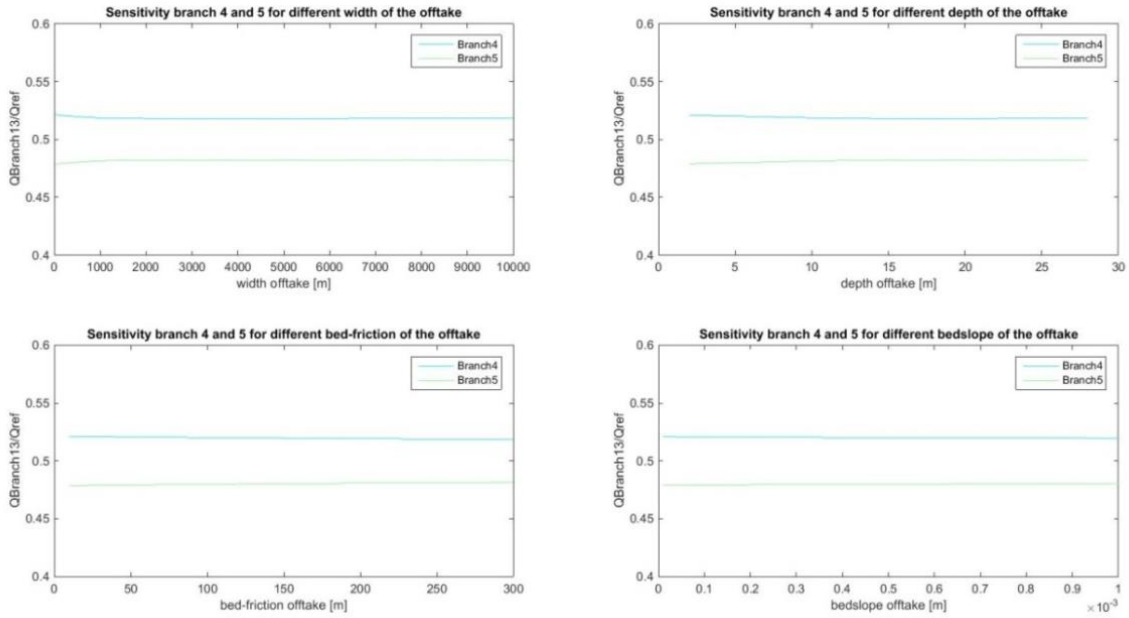

Figure 3.28 – Sensitivity physical parameters offtake on discharge in branch 4 and 5 relative to the upstream discharge (Qref)

Overall, a dominant path is observed from the right side along the upstream island to the left side along the downstream island and towards the downstream main branch (Figure 3.29). Where, the discharge along the upstream island is constant in most case, but is subject to more variation in the branches along the downstream island.

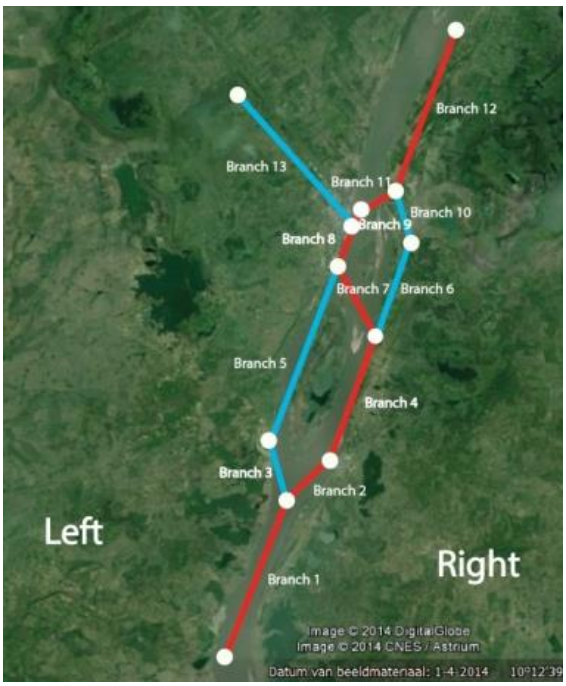

Figure 3.29 – Dominant path marked in red

3.3 Comparison results with Canal del Dique case

The results of the simulations are compared with the data-analysis obtained from the Canal del Dique case. First of all, it can be seen that 52% of the upstream discharge is distributed into the right upstream branch (branch 4 and 5) and approximately 48% into the left branch. This distribution is constant for different length and width of the downstream branches which confirms the constant distribution in time of the discharge along Isla Becerra in the Río Magdalena (Appendix A). Changes in this mostly constant distribution along the upstream island occur when the left upstream branch is shorter than the right upstream branch; when there is no mid channel or when the left branches are wider or deeper than the right branches.

The distribution of discharges along the downstream island is more variable as following from the one-dimensional analysis and confirmed by discharge measurements along Isla la Loca in the Río Magdalena. Values for which the discharge distribution becomes larger along the right branch (branch 10) than along the left branch (branch 11), as follows from the one-dimensional simulations are shown in Table 3.2.

Table 3.2 – Discharge distribution in right and left branch along downstream island (branch 10 and 11)

Parameter	Q right downstream branch > Q left downstream branch
Width mid channel	< 200 m
Length mid channel	>2100 m
Offtake position	Q left downstream > Q right downstream for x = 15-15.9 km from upstream boundary
Ratio width right/ left branches	Ratio> 1
Ratio depth right/ left branches	Ratio> 1
Length branch 10 and 11	> 1500 m
Width branch 8 and 9	< 400 m
Width offtake	>500 m
Depth offtake	>5 m
Bed-friction offtake	>115 $m^{1/2}/s$
Bed slope offtake	> 7e-4

Recent measurements show that the rating curve (Q-h relationship) at Calamar is exceeded by 10% compared to historical measurements in the Canal del Dique. This means that the discharge has increased along the left side of Isla la Loca. A trend is observed from Isla la Loca towards the right river bank, resulting in a larger width of the left branch along the island. From the one-dimensional analysis it is found that increasing the width of the left branch (branch 8 and 9) along Isla la Loca and decreasing the width along the right branch (branch 6 and 11) can indeed result in an increase in discharge of around 10% in the left branch. This is illustrated in Figure 3.30, where for example from a ratio of 1 to 0.5 of the right branches compared to the left branches the discharge in branch 8, where Calamar is located, results in an increase of the discharge of around 10%. Therefore, it can be assumed that changes in the rating curve are caused by morphological activity of Isla la Loca.

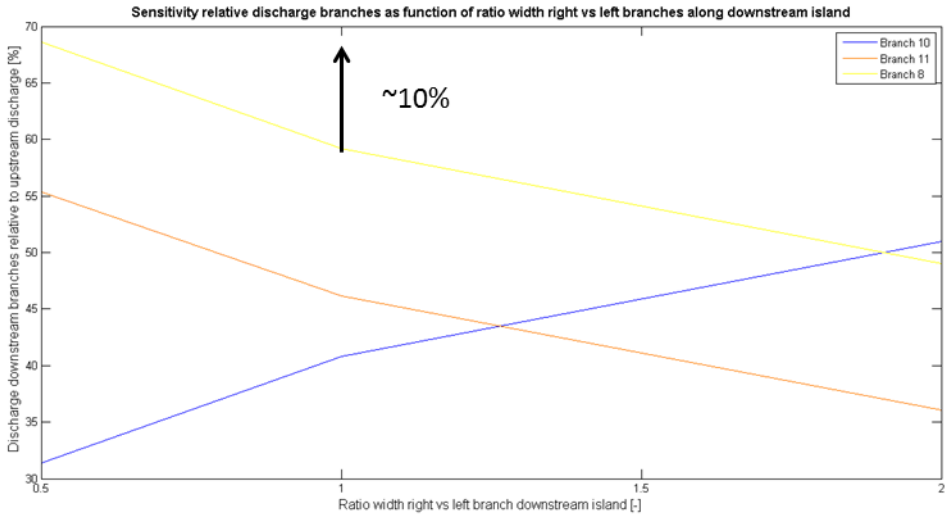

Figure 3.30 – Discharge in downstream branches relative to upstream discharge for different ratio of the width along the downstream island

3.4 Summary

The one-dimensional hydrodynamic analysis gave insight into the way length, width and depth of the branches influence the discharge distributions along the islands and over the downstream reaches.

The results showed that the water level at the entrance of the offtake is the governing factor for the amount of discharge in the offtake. Where a lower water level at the entrance of the offtake implies a larger discharge in the offtake as the water level head in the offtake is larger, because the downstream boundary is fixed. Furthermore, the discharge in the offtake is very sensitive to its physical characteristics (bed-slope, bed-friction, width and depth).

Mid channel

The presence of the mid channel is similar to the presence of two islands. When there are two islands the discharge in the offtake is larger compared to one island, as the mid channel results in input of water along the left branches resulting in a higher water level at the entrance of the offtake. Increasing the width and length of the mid channel results in a larger discharge in the mid channel, branch 8 and offtake.

Maximum variation of discharge in the offtake for changes in width and length of the mid channel is approximately 0.3 % relative to the upstream discharge.

Bathymetry branches

Bathymetrical differences of the right branches compared to the left branches along the islands results in a larger discharge in the deeper branches than the shallower branches. When the depth of the right branches is larger than the right branches, the water surface profile in the right branches has a more convex shape (M2-type) and the left branches a more concave shape (M1-type of backwater curve). This results in a lower water level at the entrance of the offtake, hence the discharge in the offtake is lower. When the ratio of the depth of the right branches compared to the left branches is changed from 1 to 2 this causes a decrease in discharge in the offtake of around 4% relative to the upstream discharge.

Position and size changes of the (downstream) island(s)
Changes in width of the right branches compared to the left branches imply different sizes of the islands. This results in similar effects as similar changes in depth. However, with increasing width, the resistance increases, for which the discharge in the branches have a limited flow capacity.

Changing the length of the downstream branches is similar to different size and position of the downstream island. It is found that changes in length of the branches does not result in significant changes of the discharge in the branches around the islands and in the downstream branches. For instance increasing the length of the downstream island from 100 to around 2200 metre results in an increase of discharge in the offtake of only 0.16% relative to the upstream discharge.

Main physical characteristics offtake
The physical characteristics of the offtake have a significant effect on the discharge in the offtake. Where a variation range from 60-80% is even observed when changing the width and depth in the offtake. However, this is for non-realistic large values. A strong correlation is found between the connecting branch 8, mid channel and right upstream branch. A larger discharge in *one* of these branches results in a larger discharge in *all* of these branches. Furthermore, it is seen that the discharge distributions along the upstream island remains equal for different characteristics of the offtake, while the distribution along the downstream island varies more.

Finally, it is seen that the discharge in branch 8 is often very large, in the order of 60-70% of the upstream discharge, and larger than the discharge in the upstream branches (branch 5 and 7). Therefore, it is to be expected that erosion in this area will occur as the flow velocities are high.

Although, some changes in discharge might seem to have a small impact on the discharge in the offtake it has to be bared in mind that this can still have a large impact on the environment downstream of the Canal del Dique. Furthermore, the given percentages are taken relative to the upstream discharge which is smaller than taking the percentage relative to the original value in the specific branch.

3.5 Recommendations

The analysis of the one-dimensional Sobek-model has given a lot of insight into the processes influencing the discharge distributions around the islands and in the offtake of the Canal del Dique from the Río Magdalena. However, further research should be carried out including higher order effects which cannot be computed with the one-dimensional model. Therefore, the following recommendations for further research on a more detailed, two-dimensional, scale are defined:

- Assess the sensitivity of the angle of the offtake and angle of the mid channel. As with the one-dimensional model, no effect of different approach angles of the branches are included.
- In this analysis no sediment has been taken into account, as sediment distributions are highly influenced by two-dimensional effects and the one-dimensional nodal point relationship used in Sobek is very empiric and changes per bifurcation type. Also morphological changes of the islands have to be investigated.
- In the 1D Sobek model, uniform depths and stationary flows are used. However, also the effect of bed level changes in the cross-section and non-stationary flow should be investigated.
- The effect of different shapes of the islands should be investigated as this cannot be assessed with a one-dimensional model.

4 TWO-DIMENSIONAL HYDRODYNAMIC ANALYSIS

This chapter presents the analysis of the two-dimensional hydrodynamic model simulations. The objective for this part of the research is first defined, where after the model set-up is described to a short extent. More information on the model set-up and results can be found in Appendix D. The conclusions of the results are presented in this chapter as well as recommendations for the research including sediments.

4.1 Objective

The aim of this study is to gain insight into the effect of different island configurations and the surrounding bed level changes on the discharge distribution at a bifurcation with fluvial islands on a two-dimensional, depth-averaged, scale accounting for turbulence and secondary flow. The results from the one-dimensional hydrodynamic analysis, as described in the previous chapter, form the basis of this study. From this previous analysis conclusions are obtained on the effect of size and orientation of the islands on the discharge distribution. This study will take into account the effect of angles of the branches. Therefore, the impact of the offtake angle on the discharge distributions should be investigated. Besides, the most promising island configurations causing reduction of discharge in the offtake, as obtained from the previous chapter, will be investigated further.

4.2 Model set-up

The study will be carried out by using the modelling software 'Delft3D-FLOW' which is able to calculate hydrodynamic and morphodynamic flows on a two- and three-dimensional scale. Planform, bed topography and flow data of the bifurcation of the Canal del Dique and Río Magdalena are used and allows for calibration and validation of the model. The discharges are calculated at cross-sections along both sides of the islands and in the downstream branches, corresponding to actual and historical water level and discharge measurement stations in the Río Magdalena and Canal del Dique (Figure 4.1). More detailed information on the model set-up and calibration can be found in Appendix D.

4.2.1 Model settings

A stationary flow is applied for all the simulations with a value in the order of the one-dimensional simulations, corresponding to a low discharge in the Río Magdalena. The model settings which are used for the different simulations are shown in Table 4.1 and follow from the calibration process as described in Appendix D. The calibration process showed good fit with water levels, discharge distributions and velocities along the islands. One layer in the vertical is used, corresponding to a depth-averaged flow.

Table 4.1 – Model settings as used in simulations following from the calibration

Parameter	Value	Unit
Discharge upstream	5737	m^3/s
Water level downstream Canal del Dique	3.28	m
Water level downstream Río Magdalena	3.03	m
Horizontal eddy viscosity	1	m^2/s
Bed-friction Río Magdalena (Manning *n*)	0.022	$s/m^{1/3}$
Bed-friction Canal del Dique (Manning)	0.016	$s/m^{1/3}$
Number of layers	1	-
Latitude	10	degrees
Time step	0.5	s
Bed roughness Río Magdalena	0.022 (Manning *n*)	$s/m^{1/3}$
Bed roughness Canal del Dique	0.016 (Manning *n*)	$s/m^{1/3}$

4.3 Results

The results of the computations regarding the two-dimensional hydrodynamic simulations are presented in the following sections. The model domain and the cross-sections where the discharges are measured (RM01 to RM06 and CDD01) are shown in Figure 4.1. The discharges are computed relative to the upstream discharge (at RM01). It should be noted that a decrease of discharge in a branch relative to the upstream discharge is smaller than the decrease of discharge compared to the original discharge in the specific branch, as the discharge in the branches downstream of the islands are smaller than the discharge at the upstream boundary. The upstream located island in the Río Magdalena is named 'Isla Becerra' and the downstream located island 'Isla la Loca'.

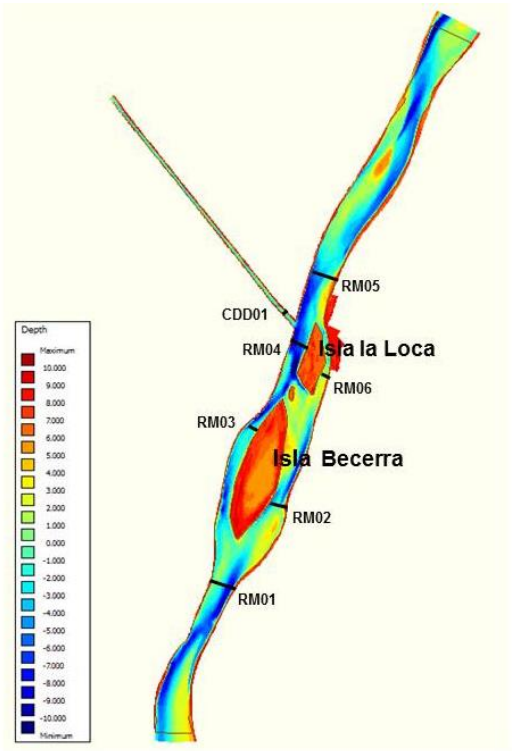

Figure 4.1 – Model domain and cross sections. Red is shallow area, blue is deep area

4.3.1 Impact of bathymetric changes on the hydrodynamics

The influence of bathymetric changes along the islands is investigated. From the one-dimensional hydrodynamic simulations it followed that changes in bathymetry along the islands have a relatively large impact on the discharge in the offtake (the variation range in discharge is 4% relative to the discharge upstream discharge which is equal to 30% relative to the original discharge in the offtake). As special interest of this study is to find possible island configurations causing a reduction of discharge in the offtake, the bathymetric changes resulting in a reduction of the discharge in the offtake are investigated further. A distinction is made between bathymetric changes along Isla la Loca only and along both islands. Besides, recent bathymetric measurements in the Río Magdalena show the presence of a small island between Isla Becerra and Isla la Loca and downstream of the offtake, which were not always present during history (Appendix A). Therefore, the influence of these small islands on the discharge in the Canal del Dique will be investigated.

4.3.1.1 *Bathymetric changes along both islands*

It is seen that when the depth in the branches along one side of the islands is decreased, the discharge in these branches decrease and increases in the branches along the other side of the islands. This also impacts the discharge distribution at the offtake as water levels at the entrance changes. These results confirm the results from the one-dimensional hydrodynamic simulations as seen in the previous chapter.

For example when decreasing the depth at the left side of the islands and increasing the depth along the right side, such that the depth in the right branches is four times larger than the depth in the left branches, the discharge increases in the right branches (RM02 and RM06) and decreases in the left branches (RM03 and RM04) compared to the case with the original bathymetry. Figure 4.2 illustrates the relative discharges in the cross-sections compared to the upstream discharge at RM01 during the simulation period.

Due to a lower water level at the entrance of the offtake (Figure 4.3) the discharge in the offtake is smaller. However, the decrease in discharge is small, with approximately 0.1% relative to the upstream discharge (Figure 4.2), which is equivalent to a decrease of 1% of the discharge relative to the original discharge in the offtake. This decrease in discharge in the offtake is smaller in comparison to the one-dimensional simulations. So, apparently the energy loss in the left branches is smaller when taking into account the two-dimensional scale.

Furthermore, it is found that when the bathymetric changes at the downstream end of Isla la Loca do not attach, resulting in large variations of depth on a small area, a drop in transverse water level gradient is seen at this location (Figure 4.4 and Figure 4.5). This drop in water level implies energy dissipation and results in less discharge in the downstream branch of the Río Magdalena and more in the Canal del Dique (Figure D. 60 Appendix D).

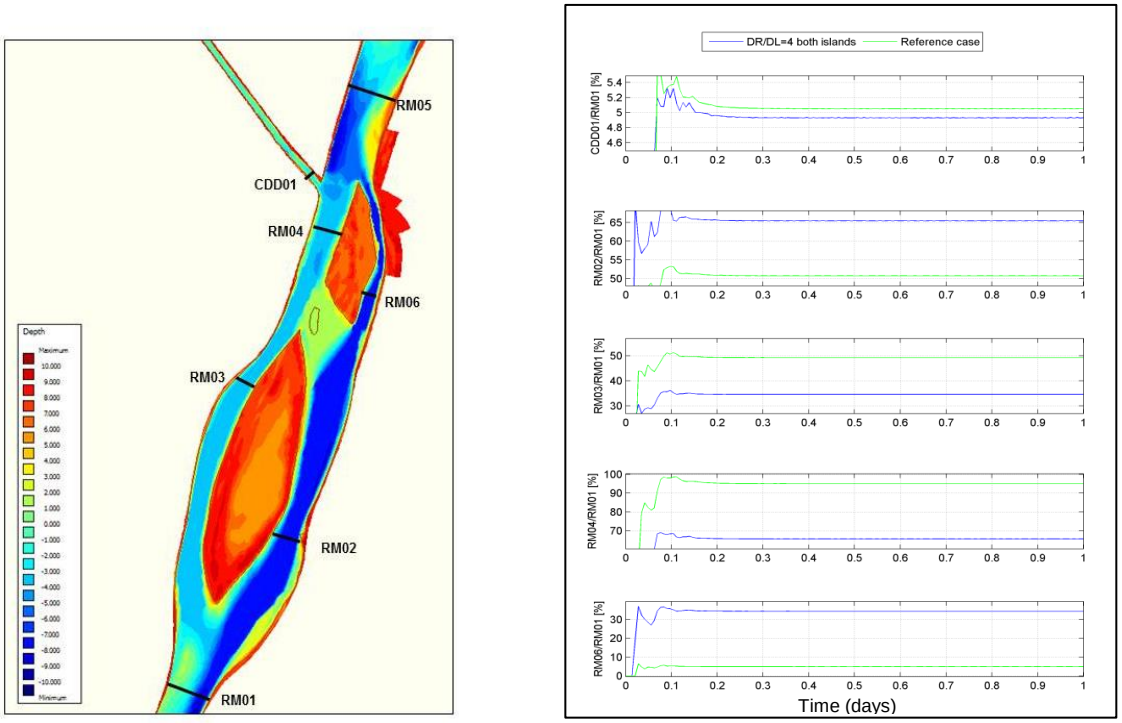

Figure 4.2 – Left: bathymetry with depth along right branches 4x deeper than left branches along islands; right relative discharge distribution for this ratio of depth (blue) compared to the reference case

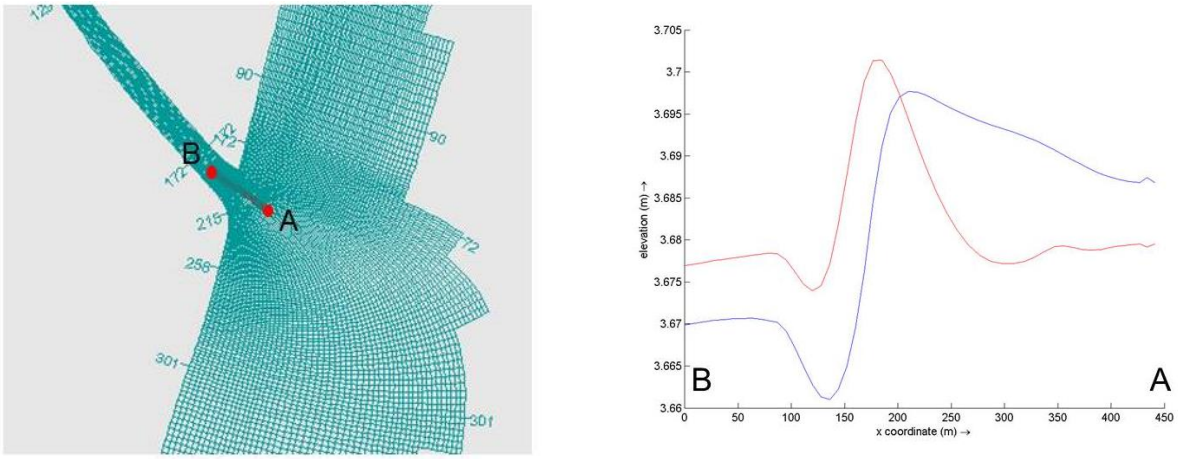

Figure 4.3 – Left: location of water level at the entrance of the offtake; right: water level at this location for original bathymetry (red) and ratio of depth right branches along the islands versus left = 4 (blue)

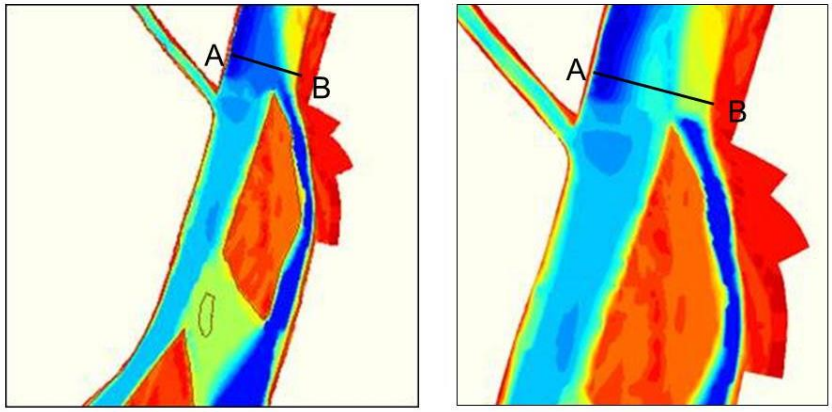

Figure 4.4- Bathymetric differences at downstream end of Isla la Loca

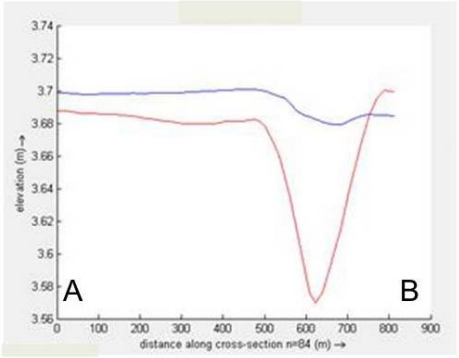

Figure 4.5 – Transverse water level gradient at locations of Figure 4.4, where the red line denotes the right figure with large bathymetric differences and the left figure denotes the blue line

4.3.1.2 *Bathymetric changes along Isla la Loca only*

Changes in depth along Isla la Loca only result in similar changes along the upstream island, however to a smaller extent as shown in Figure 4.6. The discharge in the offtake again, decreases with approximately 0.1% compared to the original bathymetry due to a lower water level at the entrance of the offtake. Large flow velocities can be observed in the area where differences in depth are large (Figure 4.7). Also, a larger eddy is seen at the left side at the entrance of the offtake which is not computed in the reference case as shown in Figure 4.8. So, for smaller changes in depth in the area of the bifurcation, the effect of flow separation is larger. However, this eddy does not seem to impact the discharge in the offtake to a large extent.

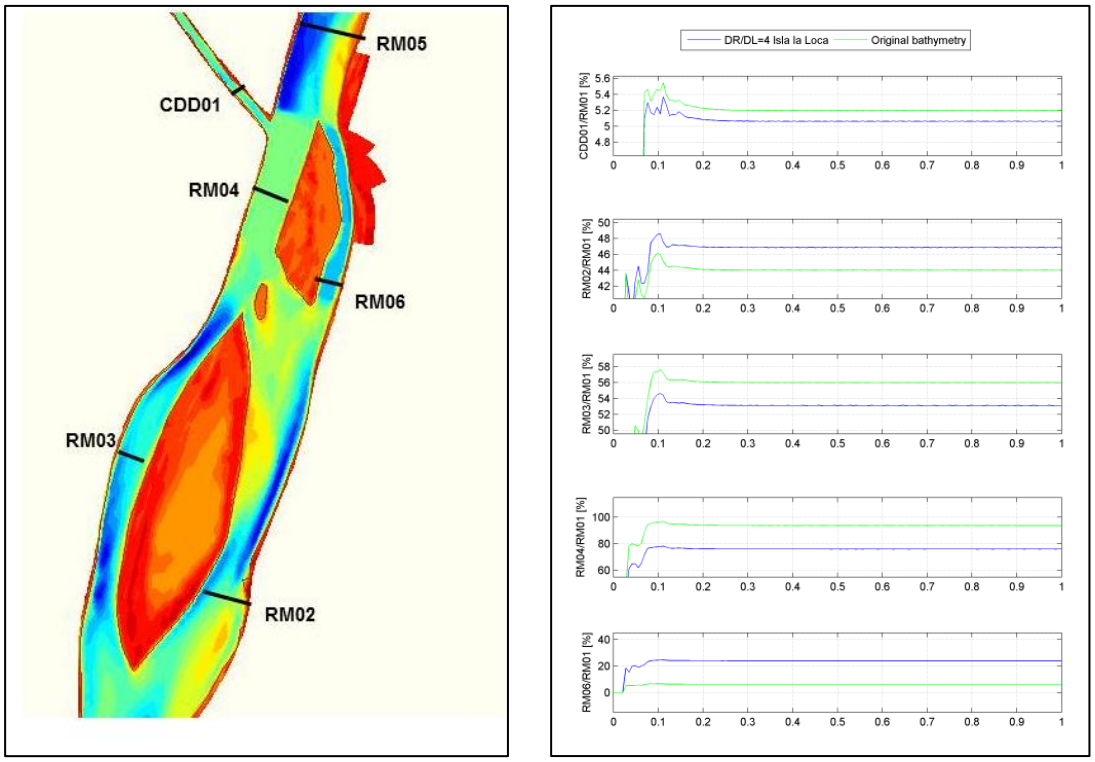

Figure 4.6 – Left: bathymetry with right side Isla la Loca 4x deeper than left side. Right: discharge distribution relative to upstream discharge for depth ratio of right branches vs left branches along Isla la Loca = 4 (blue) and original bathymetry (green)

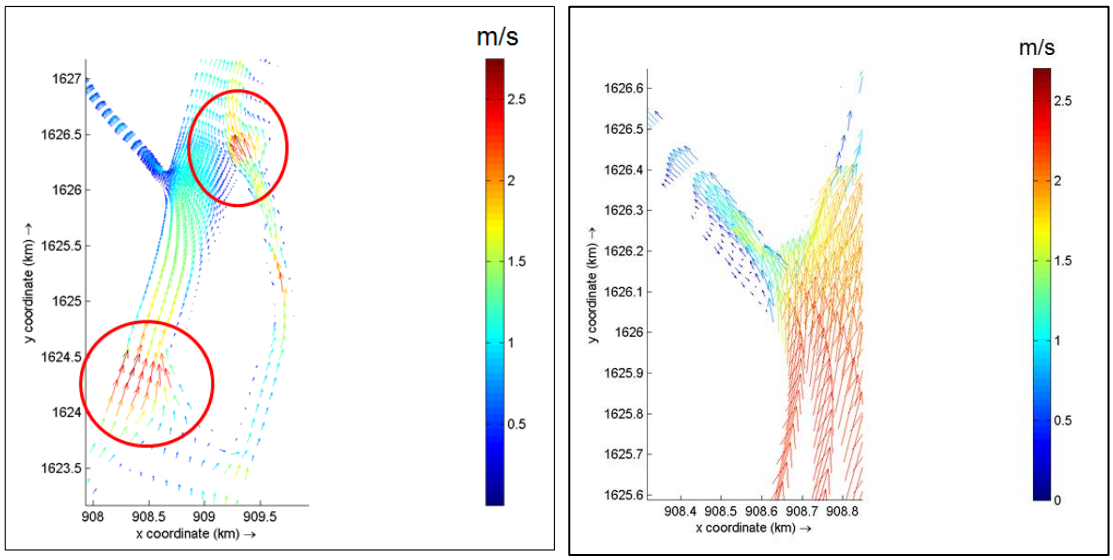

Figure 4.7 – Velocity magnitude and direction for depth at the left side of Isla la Loca decreased and right side increased

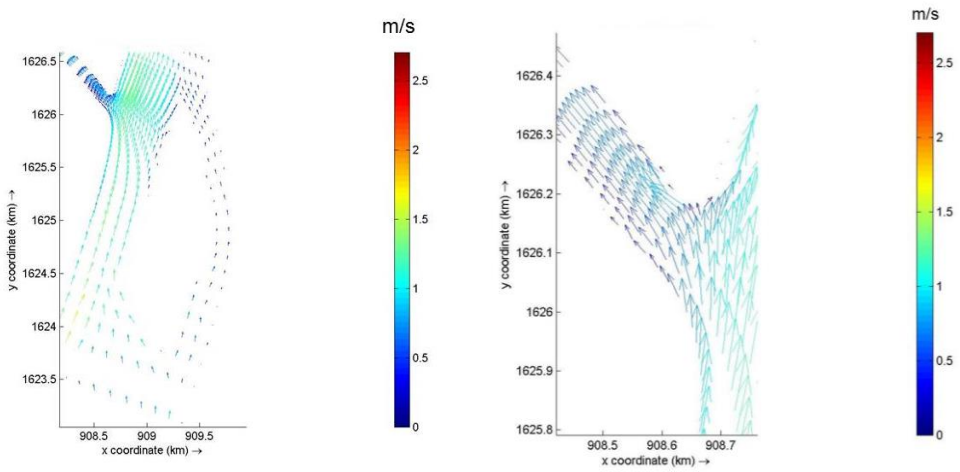

Figure 4.8– Velocity magnitude and direction for reference case

4.3.1.3 *Effect of small islands*

Recent bathymetric measurements of the Río Magdalena show the appearance of a small island between Isla la Loca and Isla Becerra and a small island downstream at the Río Magdalena as shown in Figure 4.9. These small islands were not always apparent during history (Appendix A). Therefore, the effect of the small islands on the discharge distributions is investigated.

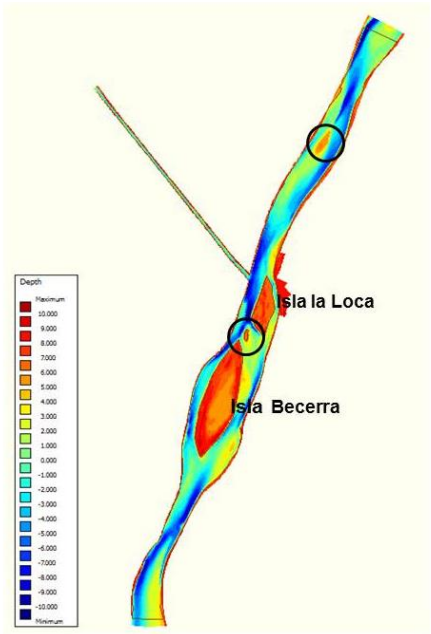

Figure 4.9 - Bathymetry as used for reference case with small islands marked with circles. Depth is positive downwards and relative to m.s.n.m. (local mean sea level)

Figure 4.10 shows the result of the discharges in the branches along the islands and at the bifurcation relative to the upstream discharge. This shows that in the case no small islands are present, the discharge distribution along the islands and in the offtake changes. Where it can be seen that the discharge in the right branch along Isla Becerra (RM02) increases with around 7% and the discharge in the branch at the left side of Isla la Loca (RM04) increases as well, however to a smaller extent. So, the dominant path becomes from the right side along Isla Becerra towards the left side along Isla la Loca.

Due to the presence of the small island, the streamlines are more curved and flow separation at the tail of Isla Becerra is observed (Figure 4.11). In the water level profiles it is seen that the presence of the small islands results in smoother water level gradient along the right side of the islands (Figure 4.13). The small island functions as a separation between the flow of the right and left side (Figure 4.12). The water level at the left side of Isla la Loca is therefore larger when there is a small island resulting in a higher water level at the entrance of the offtake, hence a lower discharge in the offtake. The decrease in discharge in the offtake is approximately 0.2% relative to the upstream discharge.

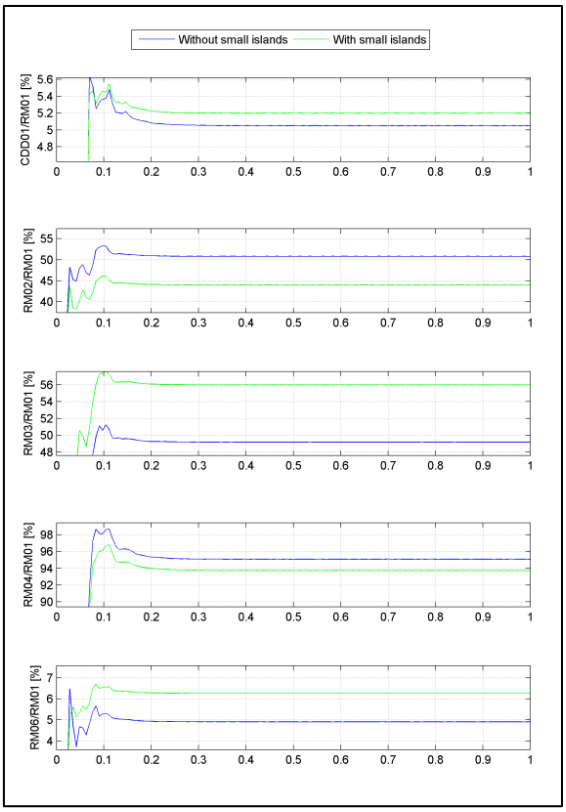

Figure 4.10 – Discharge distribution relative to upstream discharge without small islands between Isla la Loca and Isla Becerra (blue) and with small islands (green)

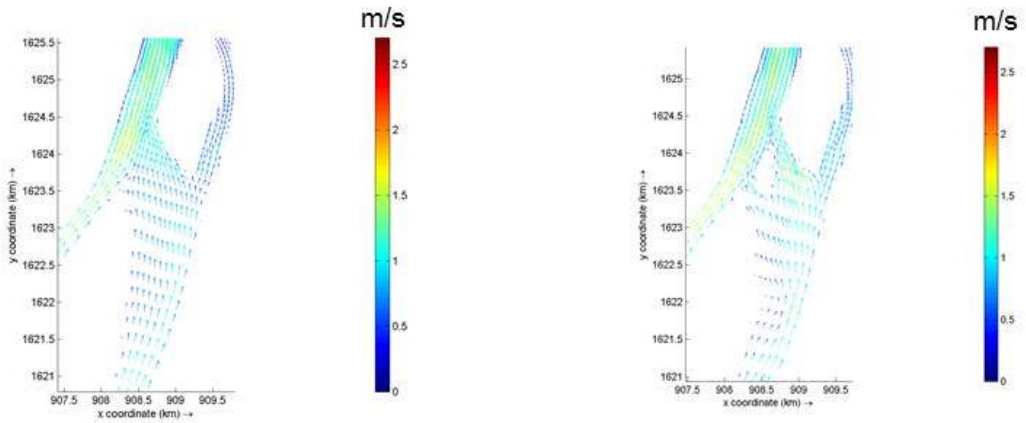

Figure 4.11 – Flow pattern and magnitude with (right) and without (left) a small island between Isla la Loca and Isla Becerra

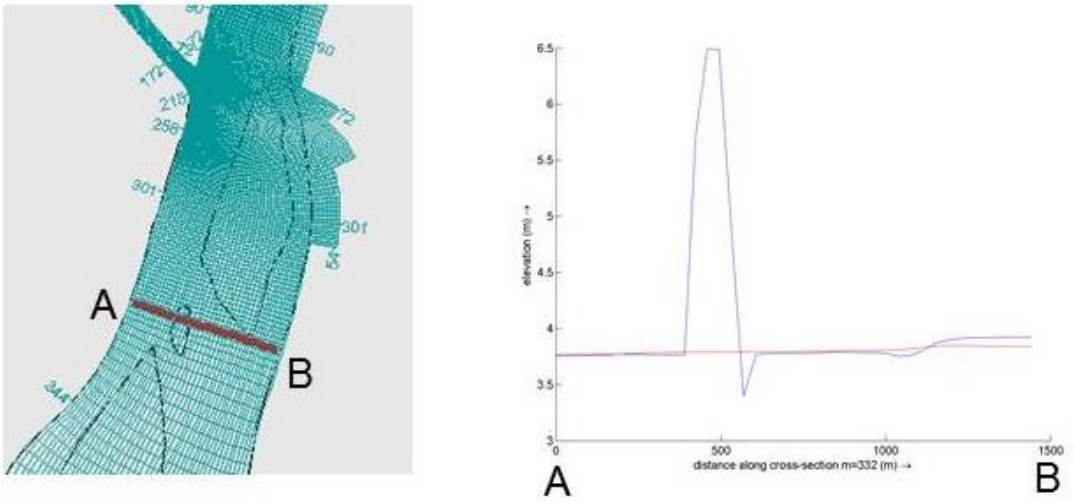

Figure 4.12 - Water level profile between islands with (blue) and without small island (red)

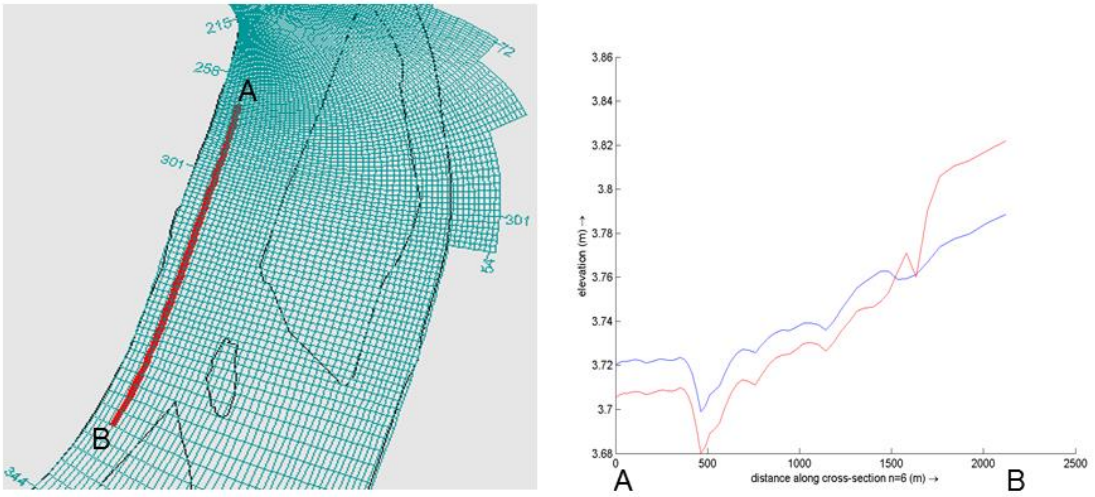

Figure 4.13 – Water level profile along left side with (blue) and without small island (red)

4.3.2 Impact of changes in position of the downstream located island

This section presents the results of the effect of position changes of the most downstream located island 'Isla la Loca' on the discharge distributions in the branches along the islands and in the offtake. The change in position of this island is particularly in our interest as from historical bathymetric measurements of the Río Magdalena it appears that the position of this island has changed significantly throughout history (Appendix A). Furthermore, also the combined effect of changes in depth along this island is investigated, as changes in position of fluvial islands often comes with changes in bathymetry. A distinction is made between position changes of Isla la Loca in direction perpendicular to the flow, the 'lateral movement', and in the direction of the flow, 'longitudinal movement' (Figure 4.14).

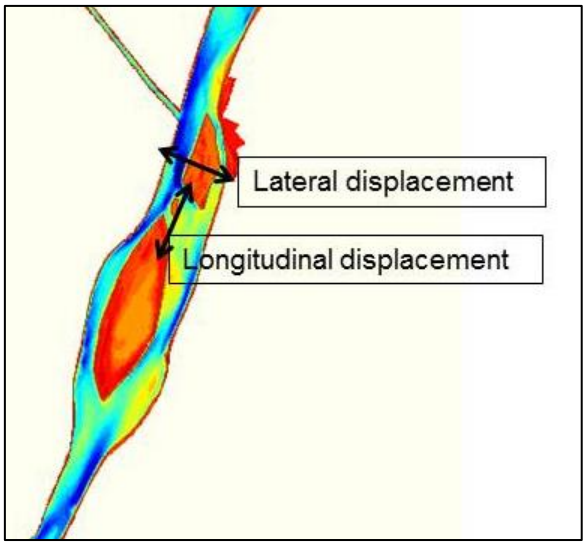

Figure 4.14 – Lateral and longitudinal movement Isla la Loca

4.3.2.1 *Impact of position change in lateral direction of Isla la Loca*

First, the lateral movement of the island is investigated. It is seen that when the island is located more towards the left side (Figure 4.15) the discharge in the left branch (RM04) decreases significantly, while the discharge in the right branch along Isla la Loca (RM06) increases significantly due to the respectively decreased and increased width of the branches. This also affects the discharge distribution along the upstream island, where the discharge in the right branch along the island increases and decreases along the left side, however the impact is smaller.

When Isla la Loca is located towards the left river bank, the discharge in the offtake decreases as the water level at the entrance of the offtake decreases (Figure 4.16). However, the water level difference is small, around 5 cm, resulting in a small decrease of discharge in the offtake of approximately 0.15% compared to the upstream discharge (Figure 4.15). Large velocities in the left branch and at the entrance of the offtake are observed due to contraction and curving of streamlines. Also, a large eddy is seen at the entrance of the offtake due to flow separation (Figure 4.17). However, these factors do not seem to have a large influence to the discharge in the offtake. When the island is located towards the right river bank, opposite effects occur as shown in Appendix D.

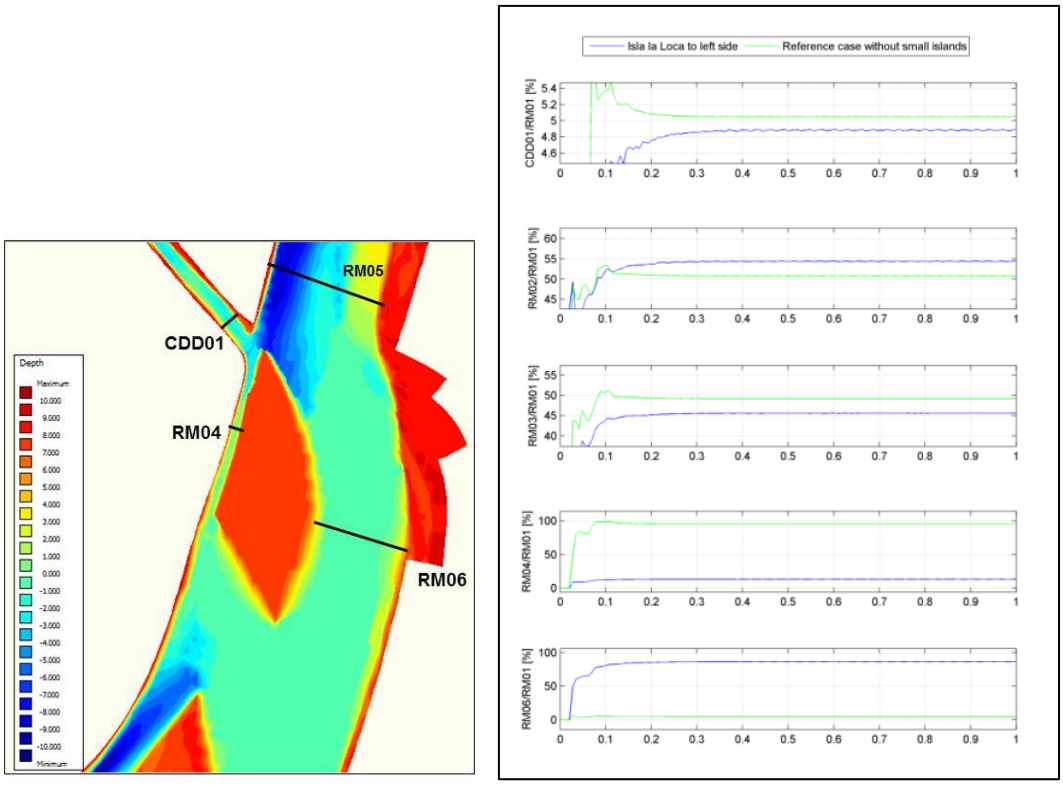

Figure 4.15 – Left: bathymetry for Isla la Loca placed more to the left side; right: relative discharge distribution for island positioned just in front of bifurcation (blue) and reference case (green)

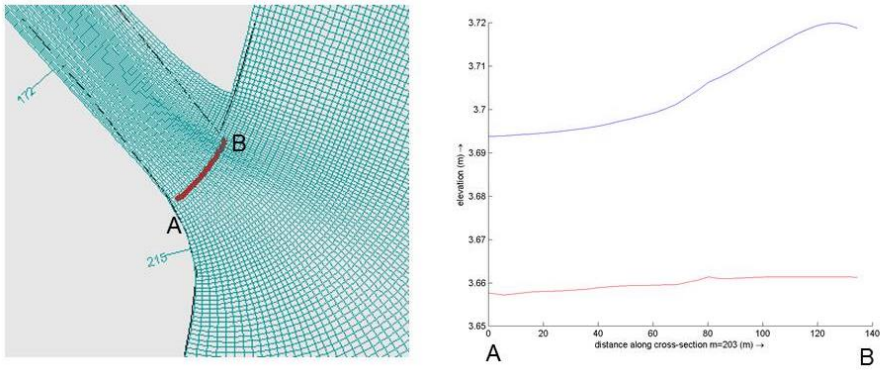

Figure 4.16 – Transverse water level gradient at the entrance of the offtake for position of Isla la Loca towards the left side (red) and original configuration (blue)

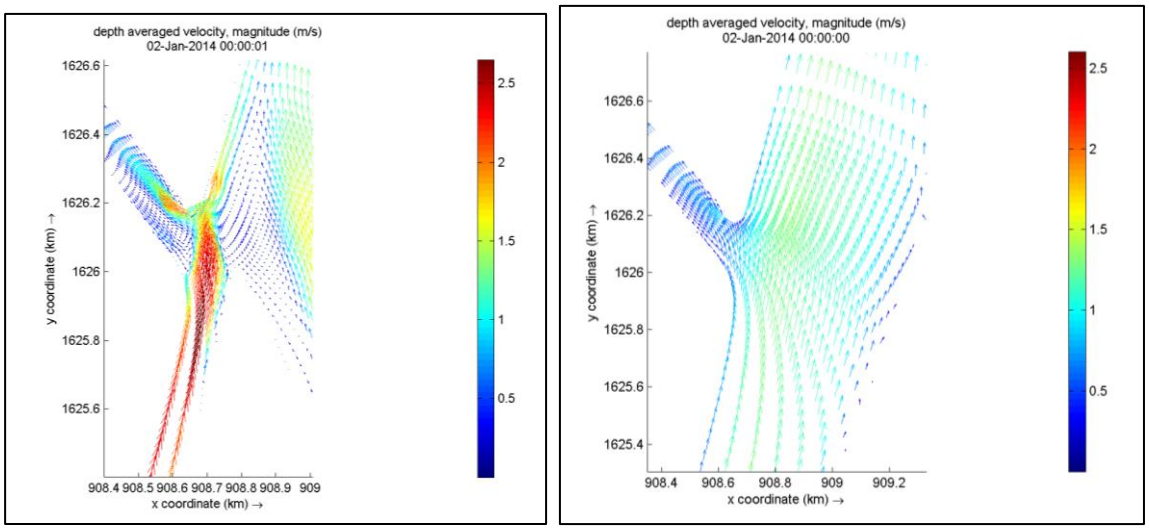

Figure 4.17 – Right: velocity at the entrance of the bifurcation with position Isla la Loca at left bank; left: velocity for original position Isla la Loca

Even when Isla la Loca is totally attached to the left river bank, the flow finds its way to the offtake (Figure 4.18), with a relative decrease of the discharge in the offtake compared to the upstream discharge of 0.4% (Figure 4.19), which is equal to a decrease relative to the original discharge in the offtake of 8%. So, again, curving of streamlines and flow separation resulting in respectively higher and lower flow velocities do not have a large influence on the discharge distributions.

Finally, it is seen that bathymetric changes along the branch of the islands and between the two downstream branches can further influence the discharge distribution (see Appendix D), where deeper reaches convey more discharge than shallower reaches.

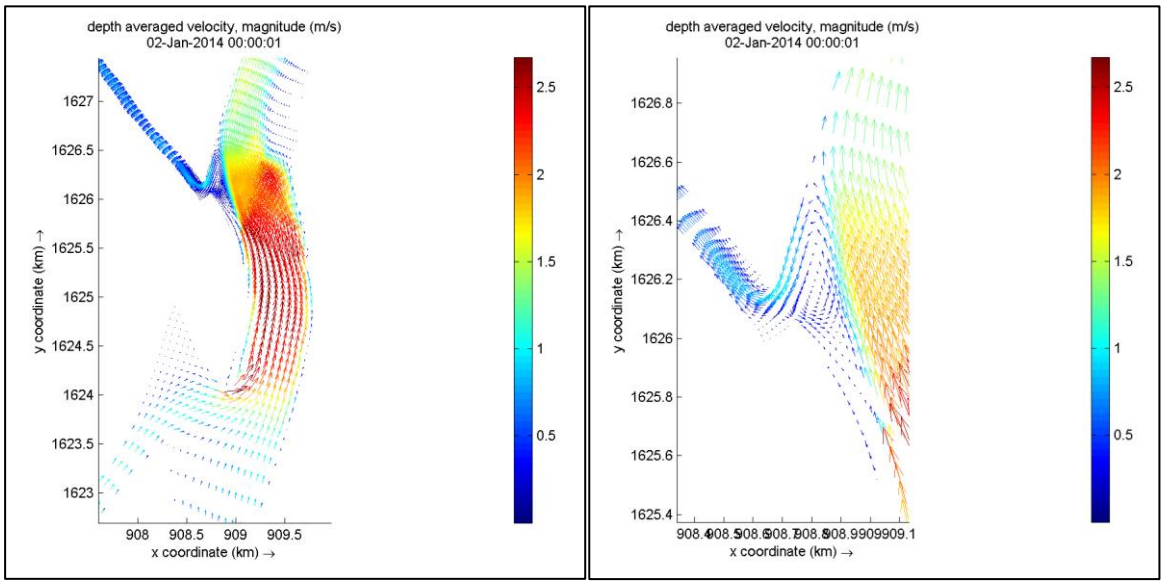

Figure 4.18 – Flow velocity direction and magnitude for Isla la Loca attached to left bank (left) and zoomed in on bifurcation area (right)

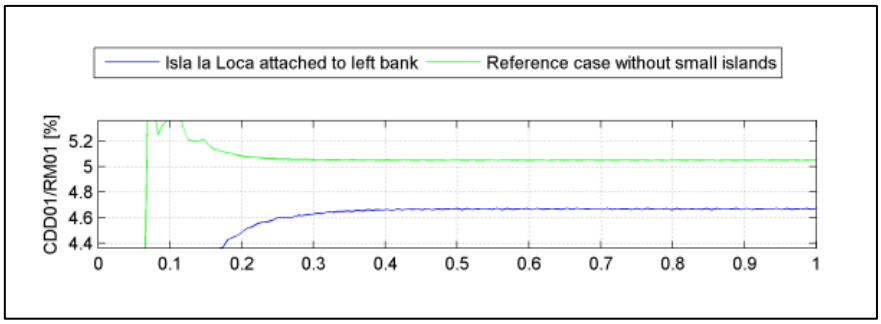

Figure 4.19 –Discharge in the offtake relative to upstream discharge for island attached to left bank and reference case without the small islands

4.3.2.2 *Impact of longitudinal movement of Isla la Loca on discharge distribution*

Next to changing the position of Isla la Loca in lateral direction, the direction of Isla la Loca is also varied in longitudinal direction (direction of the main flow). When the island is located more towards the upstream island the discharge distribution changes slightly (Figure 4.20). Where the discharge increases in the left branch along Isla Becerra (RM03) and right branch along Isla la Loca is seen (RM06). As the width of the mid channel is decreased, less water is extracted from the right branches, resulting in more discharge in the right side downstream of the mid channel along Isla la Loca. The opposite holds for the left branch along Isla la Loca, where the discharge decreases. As the input of water from the mid channel into the branch at the left side of Isla la Loca (RM04) is less, the water level is lower in this branch, resulting in a lower water level at the entrance of the offtake hence smaller discharge. Due to large curving of streamlines, the velocity is large at the left tip of Isla la Loca (Figure 4.21).

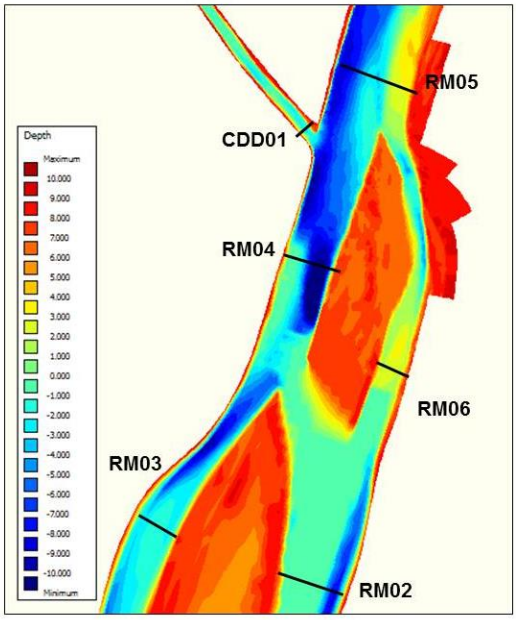

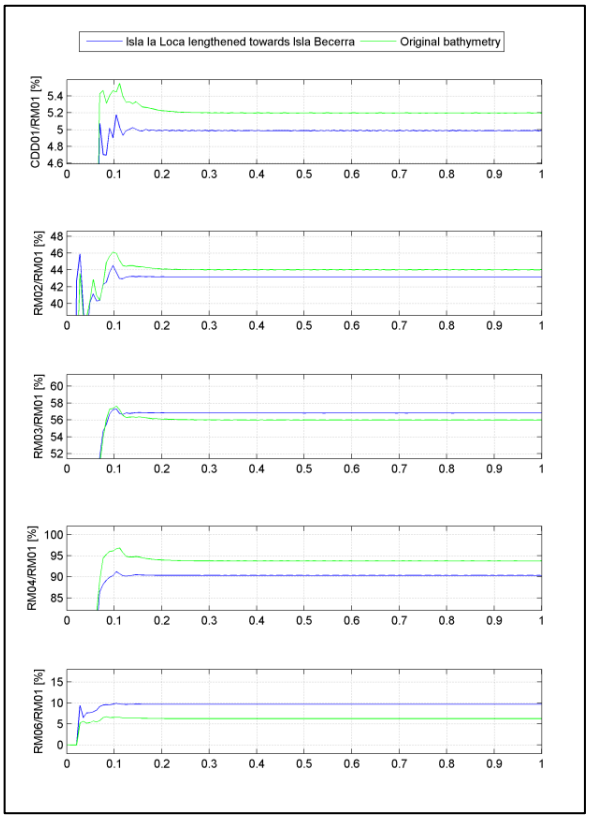

Figure 4.20 – Left: bathymetry for Isla la Loca lengthened towards Isla Becerra; right: relative discharge distribution for Isla la Loca lengthened towards Isla Becerra

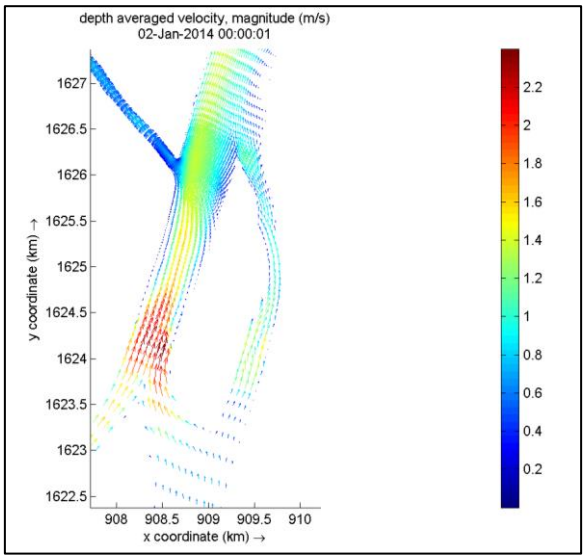

Figure 4.21 – Velocity for Isla la Loca located more towards Isla Becerra

When amalgamating the two islands into one large island the left branches become dominant in conveying discharges (Figure 4.22). As a result, the upstream flow is drawn to the left (Figure 4.23) and the flow velocities are higher in the left branches. The depth at the top of Isla Becerra is larger along the left side than the right side. This explains the favour of the flow towards the left side. Therefore, it can be said that the approach conditions influence the direction of the flow. The discharge in the offtake decreases with approximately 0.2% due to a larger water level gradient in the left branches, compared to the reference case, resulting in a lower water level at the entrance of the offtake.

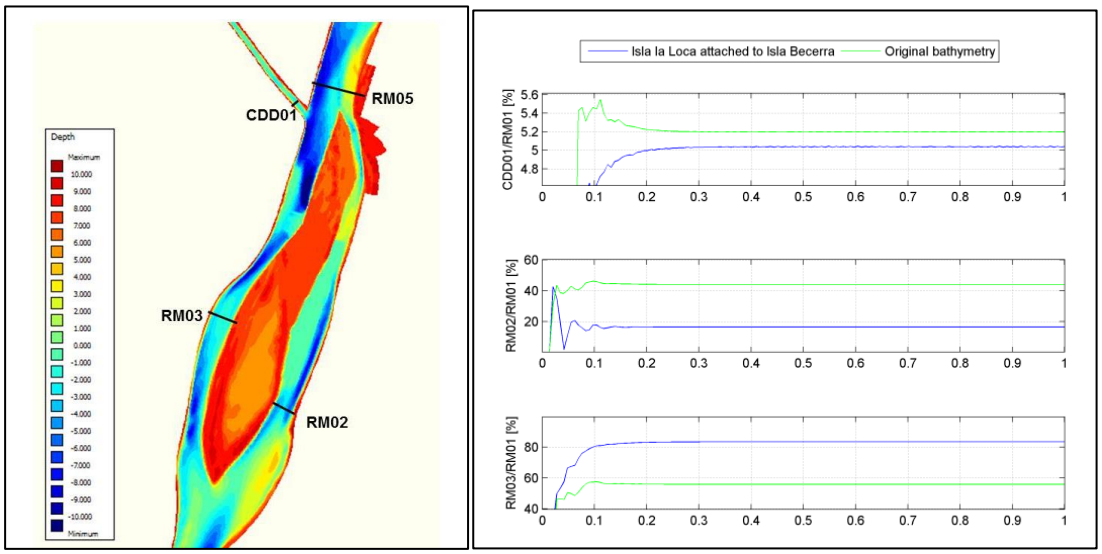

Figure 4.22 – Left: bathymetry with Isla la Loca attached to Isla Becerra; right: Discharge distribution relative to upstream discharge for Isla la Loca attached to Isla Becerra (blue) compared to reference case (green)

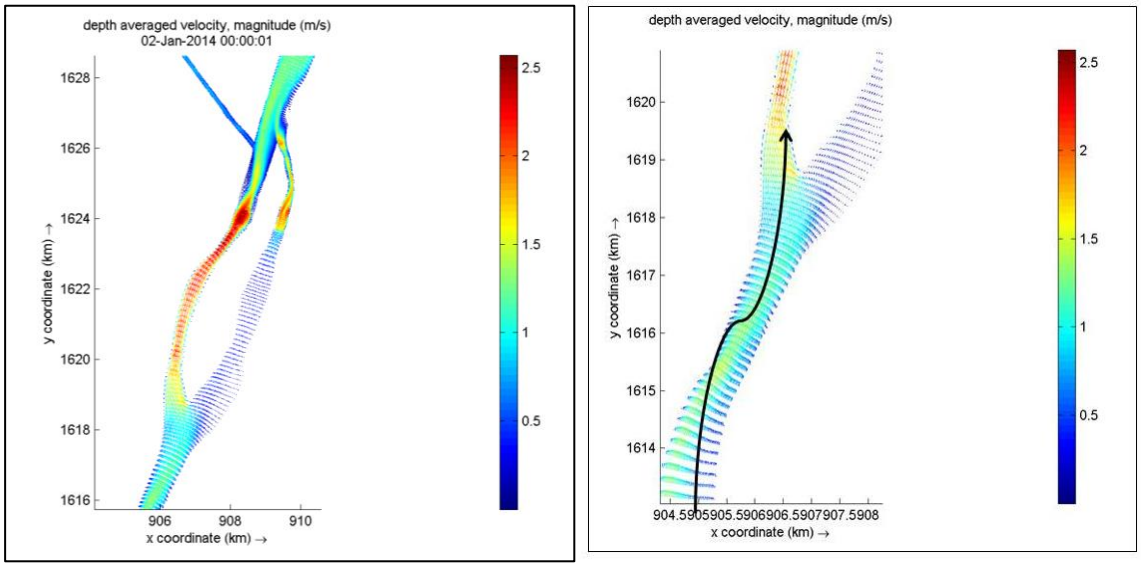

Figure 4.23 – Velocity pattern and magnitude for Isla la Loca attached to Isla Becerra

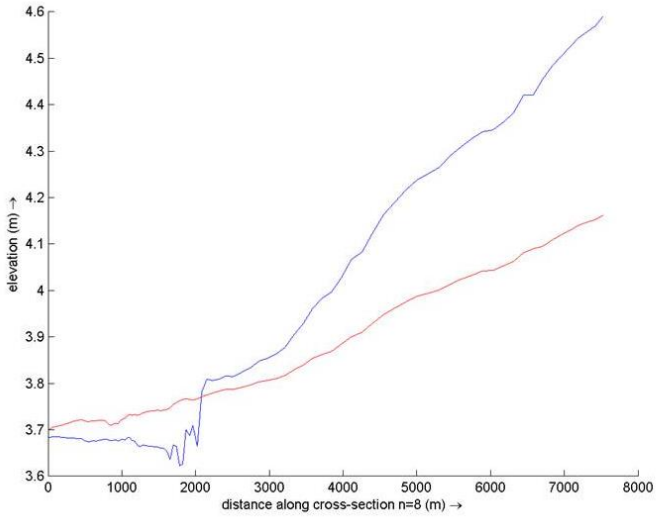

Figure 4.24 – Water surface profile in the left branches for one island (blue) and reference case with two islands (red)

4.3.3 Impact of the shape of the island on the discharge distributions

Finally, the influence of the shape of Isla la Loca on the discharge distribution is investigated. It is found that the shape of the islands does not have a significant influence on the distribution of discharges (see Appendix D). However, it does have considerable effects on the magnitude of the flow velocities and directions (Figure 4.25). Protrusions cause high flow velocities that may be expected to erode these protrusions. Whereas, sharp bank-line angles cause flow separation that may be expected to fill the areas of large eddies by deposition. As a result of these feedback mechanisms, different initial islands shapes can be expected to evolve to similar end states of smooth streamlines along smooth island shapes. More detailed information can be found in Appendix D.

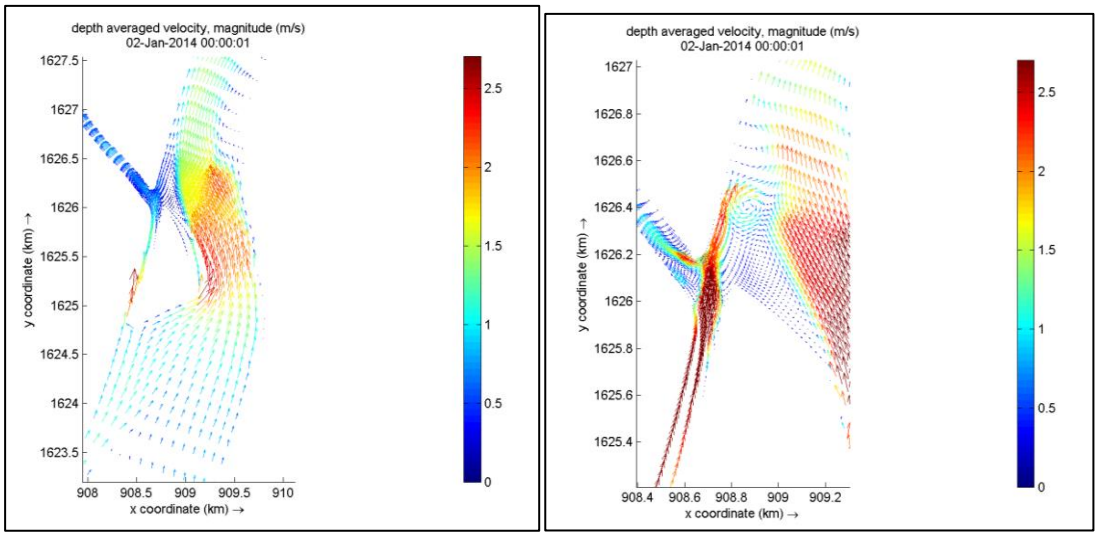

Figure 4.25 – Flow pattern and magnitude for island with protrusions (left) and with sharp bank line angles (right)

4.3.4 Impact of the angle of the offtake to the discharge distributions

The effect of changes of the offtake angle could not be investigated in the one-dimensional scale model, as flow separation curvature of streamlines due to different angles of approach cannot be computed with a one-dimensional model. Therefore, the impact of the offtake angle is investigated in this study. However, the results of this study show that the angle of the offtake does not influence the discharge distribution along the islands. The impact on the distribution of discharge to the downstream reaches is also very small: an increase of discharge of 0.02% relative to the upstream discharge is found when the angle of the offtake is increased from 45 to 90 degrees. This confirms the results of experiments by Bulle (Bulle 1926) where a similar increase in discharge in the offtake is seen for increasing angle of the offtake from 45 to 90 degrees (Figure 2.8).

4.3.5 The impact of islands compared to a bifurcation without islands

Finally, the effect of the presence of the islands on the discharge distribution compared to a bifurcation without fluvial islands is investigated. When there is no island located in front of the bifurcation or when there is only one island located more upstream (Isla Becerra in this case) of the bifurcation, the discharge distribution at the bifurcations changes very slightly. Where, an increase of discharge in the offtake of 0.2% relative to the upstream discharge is observed (Figure 4.26). Therefore, it can be said that the presence of fluvial islands at the bifurcation causes a reduction of discharge in the offtake due to water level impoundment caused by the islands.

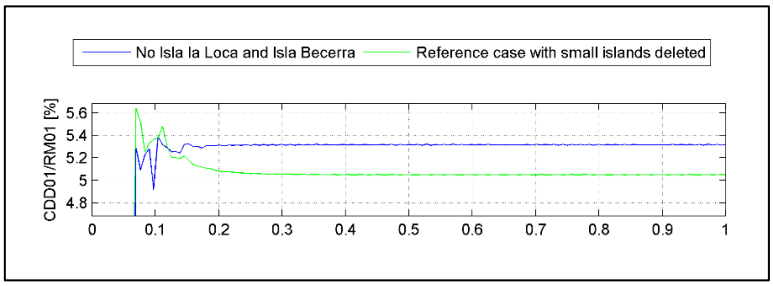

Figure 4.26 - Discharge in the offtake relative to upstream discharge without islands (blue) compared to case with two islands at a bifurcation (green)

4.4 Conclusion hydrodynamics

The aim of this study was to gain insight into the effect of different island configurations and the surrounding bed level changes on the discharge distribution at a bifurcation with fluvial islands accounting for two-dimensional flow effects due to different approach angles of the branches. Finally, the most promising island configurations causing reduction of discharge in the offtake, as obtained from the previous chapter, are further investigated. The conclusions on the analysis of the two-dimensional hydrodynamic simulations are presented in this section.

Bathymetric changes of the branches along islands

It is found that changes in bathymetry in the branches along the islands influence the discharge distribution along the islands. For instance, when deepening the depth along the right side of the islands, the discharge increases in those branches, while the discharge decreases in the branches along the left side of the islands. This implies a lower water level at the entrance of the offtake, hence the offtake is conveying less discharge.

When changing the bathymetry along the downstream island only, for instance deeper branches along the right side, more discharge is conveyed in this branch. Besides, this impacts the discharge distribution along the upstream island in a similar way, were the discharge in the right branch along the upstream island increases and decreases in the left branch. However, the impact on the upstream discharge distribution is smaller.

Finally, the impact of a small island between the two islands is investigated as seen in recent bathymetric measurements in the Río Magdalena. When the small islands are not present the left downstream branch is conveying more discharge as the water input from the mid channel is larger. When there is a small island, this results in a larger separation of the flow along the right and left branches of the islands. The discharge in the right upstream branches also increases, resulting in a dominant path from the right side along the upstream island to the left side along the upstream island when there is no small island.

Lateral displacement Isla la Loca

Changing the position of the most downstream located island ‘Isla la Loca’ to the left river bank causes a (large) increase in discharge in the right branch along this island and (large) decrease in discharge in the left branch. It also impacts the discharge along the upstream island, although the influence is much smaller, causing an increase in the right branch and decrease in the left branch. Also, the discharge in the offtake becomes lower as the water level at the entrance of the offtake decreases. This effect is even larger when the island is completely attached to the left bank just upstream of the offtake. This results in a maximum reduction of discharge of 8 % relative to the original discharge in the offtake. When the island is located to the left river bank, large eddies are observed at the tail of the island as a result of flow separation and large flow velocities due to the more curved streamlines. However, these factors do not seem to have significant influence on the discharge distributions.

Longitudinal displacement Isla la Loca

When the most downstream located island ‘Isla la Loca’ is lengthened towards Isla Becerra the discharge decreases in the left side of Isla la Loca as the flow input from the mid channel is smaller resulting in a smaller water level difference in this branch. The water level at the entrance of the offtake is smaller, resulting in a lower discharge in the offtake.

When the two islands are merged into a single large island, the branches along the left side become dominant in conveying discharges as a result of local bathymetric differences between the left and right branch at the top of Isla Becerra.

Shape islands
The shape of the islands does not seem to affect the discharge distribution much. However, it has considerable effects on the flow velocities and directions. Protrusions cause high flow velocities, whereas sharp bank-line angles cause flow separation.

Offtake angle
The angle of the offtake does not affect the discharge distribution along the islands. It does impact the discharge distribution along the downstream reaches, however to a very small extent. For example when the offtake angle is changed from an angle of approximately 45 degrees to an angle of 90 degrees the discharge in the offtake increases with 0.02% relative to the upstream discharge.

Measures decreasing the discharge in the offtake
A special interest of this study is to find possible island configurations which are able to decrease the discharge in the offtake. The island configurations causing a reduction of discharge in the offtake, as found from this hydrodynamic analysis, are summarized below. It has to be bared in mind that values are presented relative to the upstream discharge (5737 m^3/s), therefore the percentage of discharge reduction relative to the discharge in the offtake itself are larger.

- No small islands in between large islands: 0.2% relative to upstream discharge ≈ 4% relative to original discharge in offtake
- Depth right side Isla la Loca 2x left side: 0.2%
- Depth right side Isla Becerra 4x left side: 0.2%
- Isla la Loca towards left river bank: 0.2%
- Isla la Loca completely attached to left river bank: 0.4% ≈ 8% relative to original discharge in the offtake
- Isla la Loca located more towards or merged with Isla Becerra: 0.2%

So, it can be concluded that reduction in discharge in the offtake due to different island configurations are in the order of 0.2% relative to the upstream discharge which is an equivalent reduction of discharge of 4% relative to the discharge in the offtake with the original island configurations. The largest increase in discharge occurs when the downstream located island is totally attached to the left bank. This causes a relative decrease in discharge in the offtake of 0.4% which is equal to an absolute decrease in the offtake of approximately 8%.

Overall, it can be concluded that due to the presence of the islands the discharge in the offtake is lower than in the case of no fluvial islands. As the water is distributed over more branches this results in less water in the offtake. However, even though an island is located in front of the offtake the maximum relative decrease of discharge in the offtake is 8%.

5 SEDIMENT TRANSPORT AND MORPHOLOGY

In this chapter, the influence of the fluvial islands on the sediment transport and morphology are investigated with the use of the two-dimensional model as explained in the previous chapter. First, the objective of this part of the research is explained. Thereafter, the model set-up is described as well as the most import assumptions made in this model. Then, the results are described and conclusions are drawn.

5.1 Objective

The aim of this study is to gain insight in the sediment transport distribution of coarse sediments and the sedimentation and erosion patterns along the branches of the fluvial islands and at the downstream branches with different island configuration. In this way future island shape, orientation and position can be forecasted and historical island migration explained. The focus of this study is on the coarser sediment fractions as the distribution of fine sediment at a bifurcation mostly depends on the distribution of discharges (Slingerland and Smith 1998), while coarse sediment is influenced by local factors. Therefore, coarse sediments can change the position of size, shape and orientation by deposition and erosion.

In the Canal del Dique case it is of special interest to decrease the amount of coarse sediment entering the canal in order to decrease the amount of dredged sediments at the sediment trap located at the first kilometre of the canal. Therefore, the most promising island configurations causing reduction of discharge in the Canal, as found from the hydrodynamic simulations, are investigated in order to reduce the amount of coarse sediment entering the Canal.

5.2 Model set-up

The Delft3D hydrodynamic flow model as described in the previous chapter forms the basis of this study. Simulations will again be carried out on a two-dimensional (depth-averaged) scale. However, in this study morphodynamic simulations will be carried out by including non-cohesive sediment fractions and their characteristics. This allows us to investigate sediment transport rates and morphological changes. As morphological developments take place on a much larger time scale than flow changes a larger timescale should be applied in comparison to the hydrodynamic simulations. To speed up the simulation time a 'morphological time scale factor' can be applied. This factor multiplies the erosion and deposition fluxes from the bed to the flow and vice-versa at each computational time-step (Deltares 2014). In this study a 'MorFac-factor' of 12 is used with a simulation time of the hydrodynamics of 30 days, resulting in a morphodynamic simulation time of 360 days (almost one year).

5.2.1 Assumptions

- As mentioned in the previous section it is assumed that the distribution of fine sediments is equal to the discharge distribution. Therefore, the focus of this study will be on the **coarse sediment fractions** only.
- From the hydrodynamic calibration it was found that the bed-friction in the Río Magdalena increases with increasing discharge. However, in this study a **steady bed-friction in the Río Magdalena** will be applied when applying non-stationary flow input as Delft3D has no

possibility of applying a non-stationary bed-friction. A bed-friction corresponding to the mean flow in the Río Magdalena will be used.

- As there are no (recent) measurements available of grain size of the bed and bed load transport rates, it is hard to correctly calibrate the model. Therefore, the sensitivity of several parameters on the computed bed load transport and sedimentation and erosion patters should be tested. Besides, a few historical bathymetries are available which can be used for a rough validation of the computed sedimentation and erosion patterns. Also annually dredged volumes of the sediment trap are available. However, the annual variation seems to be large.
- Flow simulations will initially be made with a **stationary discharge of 7572 m^3/s**. This value is obtained from the second measurement campaign of Consorcio Dique in May 2014 and corresponds to the mean annual discharge rate of the Río Magdalena at Calamar (Restrepo and Kjerfve 2000).

5.2.2 Calibration

Calibration of the morphodynamics is carried out by varying the grain size and the sediment transport formulas. A calibration curve for the bed load transport of coarse sediment at Calamar in the Río Magdalena is available as well as mean annual dredged volumes from the sediment trap at the first kilometer in the Canal del Dique. However, as the dredged volumes vary significantly per year and the reliability of the measurements where the calibration curve is based on cannot be verified, the calibration process cannot be carried out to a large extent and should be treated with care. However, it gives an idea of the order of magnitude of the modelled transport rates with the values based on the calibration curve and annual transport rates. Due to the lack of (reliable) data, a sensitivity analysis is part of the calibration process in order to find model settings which give the most realistic results considering the sedimentation and erosion patterns. More detailed information on the calibration process can be found in Appendix E.

The order of magnitude of the computed sediment transport rates fits with the calibration values. Applying different grain sizes results in slight different sediment transport rates, while applying different sediment transport formula has significant impact. Besides, it is seen that applying the sediment transport formula of Van Rijn (1993) results in large erosive channels along the islands (Figure 5.1) which are not observed from bathymetric measurements in the Canal del Dique. The formula of Engelund-Hansen shows more reliable sedimentation and erosion patterns and is applicable for the used grain size of 200 µm. Also, from a measurement campaign of NEDECO in 1973 (NEDECO, 1973) it is found that this formula fits well with measurement results (see Appendix E). Therefore, this sediment transport formula will be used in the reference case.

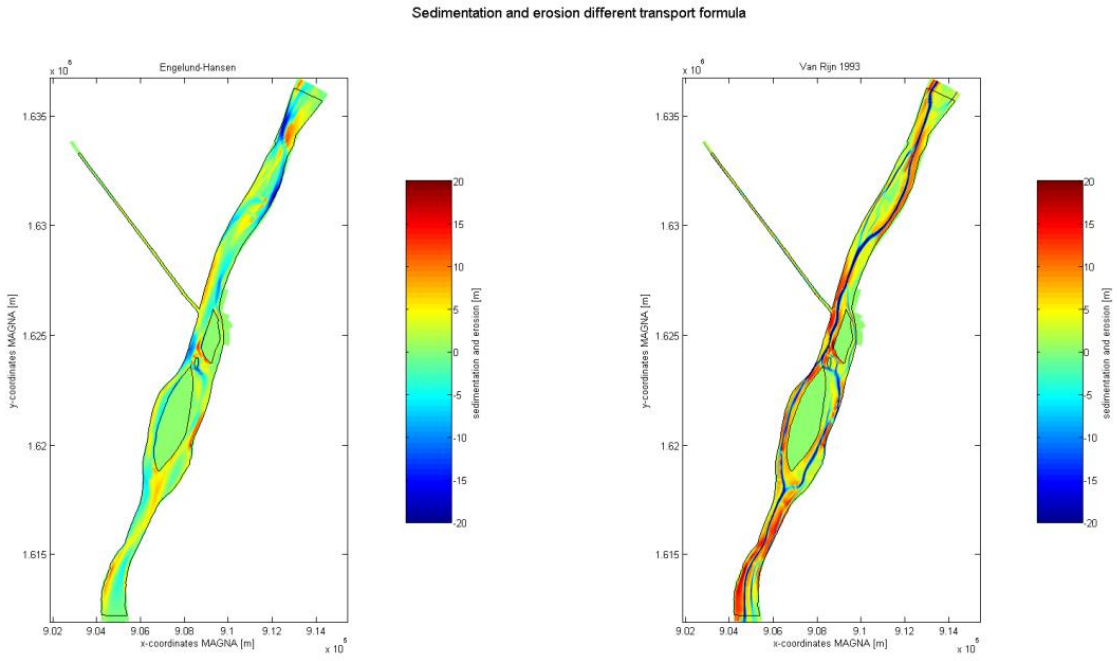

Figure 5.1 - Sedimentation and erosion pattern for sediment transport formula Engelund-Hansen and Van Rijn 1993

5.2.3 Model input reference case

The parameters resulting from the calibration process and the sensitivity analysis which are used for the reference case are shown in Table 5.1. Besides, it is accounted for secondary flow, as this has large impact on the distribution of sediment.

Table 5.1 – Model input reference case after calibration and sensitivity analysis

Parameters	Value	Unit
Grain size (D50)	200	µm
Specific density	2650	kg/m^3
Dry bed density	550	kg/m^3
Reference density for hindered settling	1600	kg/m^3
Initial sediment layer thickness at bed	50	m
Morphological scale factor	12	-
Sediment concentration at boundaries	Equilibrium sediment concentration	kg/m^3
Sediment transport formula	Engelund Hansen	-
Hydrodynamic upstream boundary condition	7572	m^3/s

5.3 Results

First of all, the sedimentation and erosion patterns of the reference case are analysed in order to gain insight in the evolution of the islands at the Río Magdalena – Canal del Dique bifurcation. The expectations as drawn in 2.5 are validated.

Furthermore, an analysis of the resulting sedimentation and erosion patterns of several island configurations and the influence on the distribution of coarse sediment is carried.

The cases which will be discussed are:

- Isla la Loca located to left river bank
- Isla la Loca totally attached to left bank
- Isla la Loca located towards Isla Becerra

Finally, the morphological evolutions of the islands are validated by initially imposing no small island between Isla la Loca and Isla Becerra.

5.3.1 Evolution islands in reference case

Figure 5.2 and Figure 5.3 show respectively the sedimentation and erosion pattern and bed level evolution during a simulation period of one year. This shows that sedimentation occurs mostly at the left tip of the downstream island, where flow velocities decreasing flow velocities occur due to flow separation at the lee side of the small island between the two large islands (Figure 5.4). Also, sedimentation occurs at the right tail of Isla Becerra where flow velocities are low due flow separation and a shallow area, finally resulting in enlargement of the island in downstream direction. This was also expected as shown in Figure 2.17. Besides, at the tip of Isla Becerra sedimentation is seen as a result of flow separation. Sedimentation can furthermore be seen at the entrance of the offtake, which is a transition zone between the deep main branch and shallower offtake resulting in decreasing flow velocities, hence sedimentation.

Considering the distribution of sediment, the bed load transport is dominant and increases in the left branches (RM04 and RM03 in Figure 5.5) as a result of higher initial flow velocities in the left branch. However, the distribution of discharge remains more constant, whereas it follows from the data-analysis (Appendix A) that the discharge distribution shows a larger variation of discharge along Isla la Loca. This difference can be ascribed by the fact that here only a simulation of one year is carried out with a stationary flow, while the variation in discharge at Isla la Loca in the Río Magdalena occurs over several years with a varying discharge over the year.

Furthermore, it can be seen that the bed load transport increases in the offtake and sedimentation occurs in the offtake. This confirms the sedimentation at the entrance of the Canal del Dique for which yearly dredging activities take place (Appendix A).

A sedimentation bump can be seen halfway of the simulation period in the left branch along Isla la Loca (RM04). This is a result from a sediment bump along the left bank of Isla la Loca as shown in Figure 5.3.

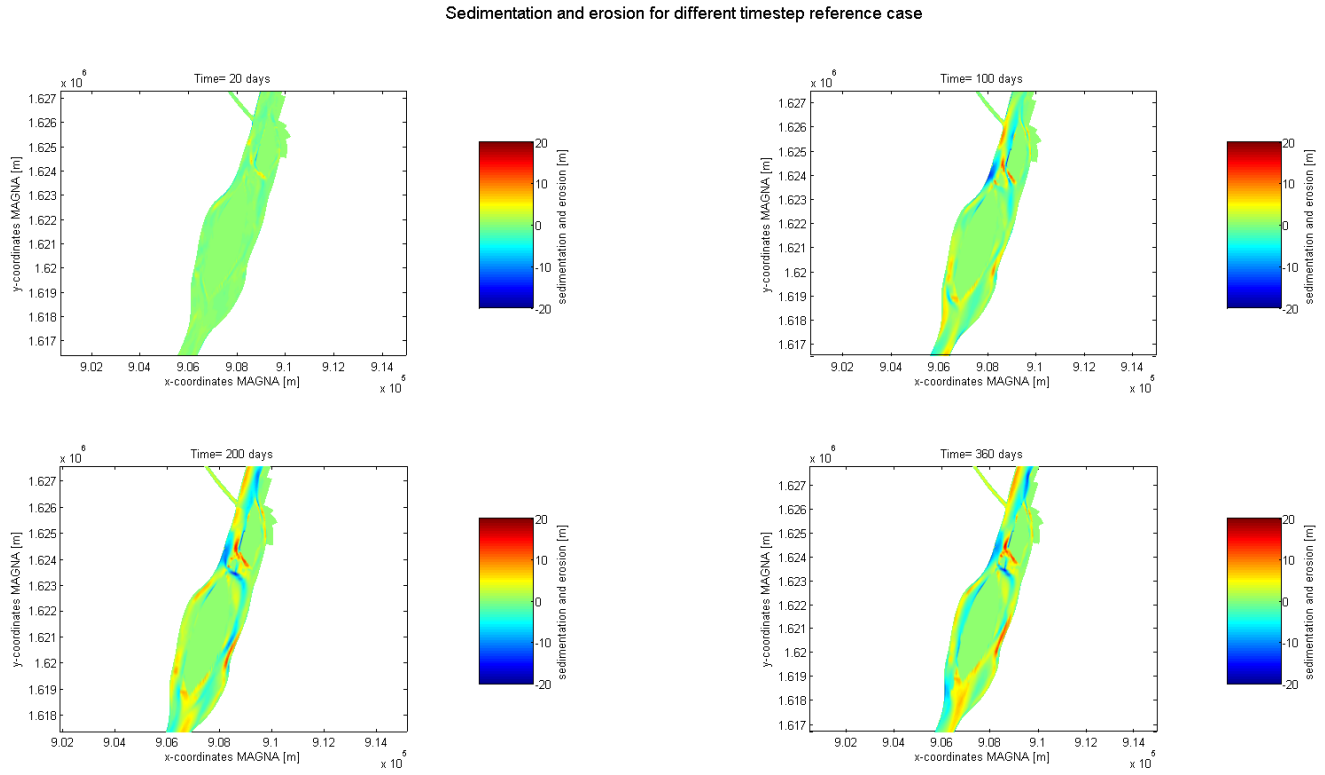

Figure 5.2 – Sedimentation and erosion pattern during simulation for reference case

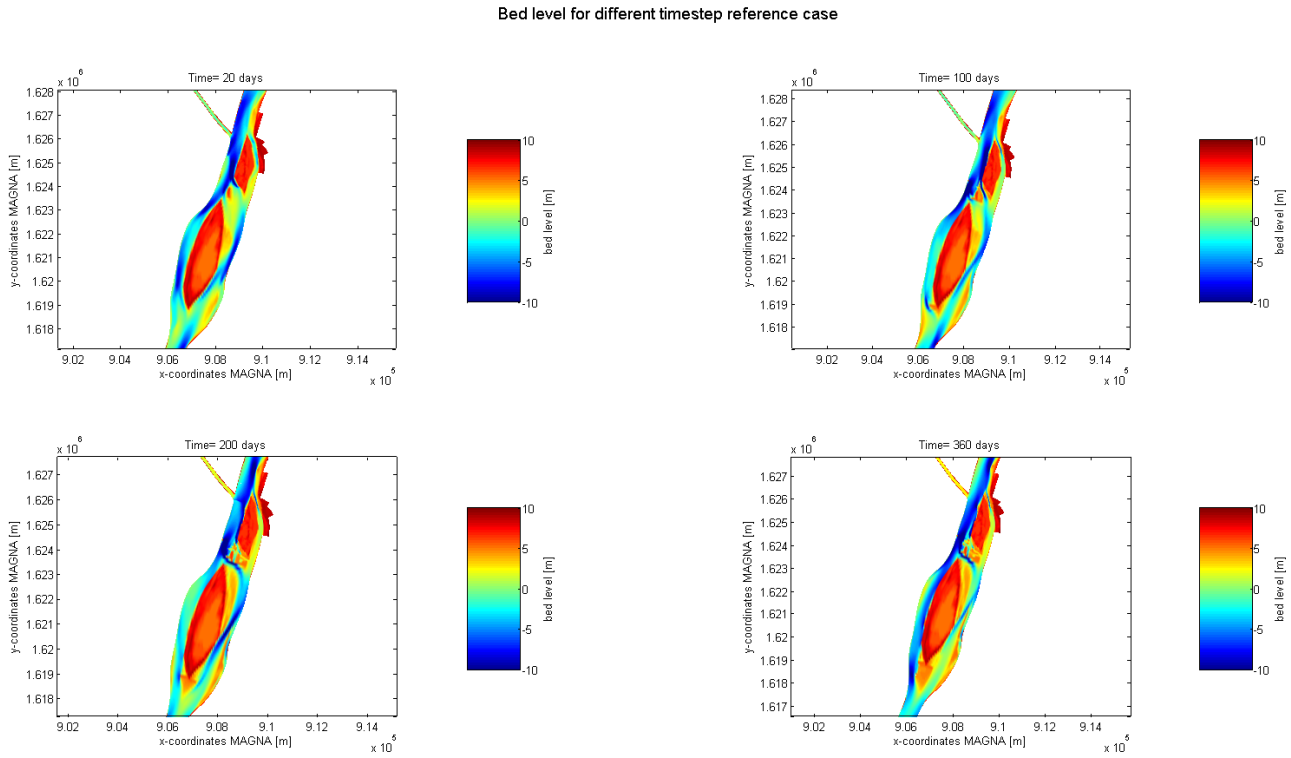

Figure 5.3 – Bed level evolution during simulation time for reference case

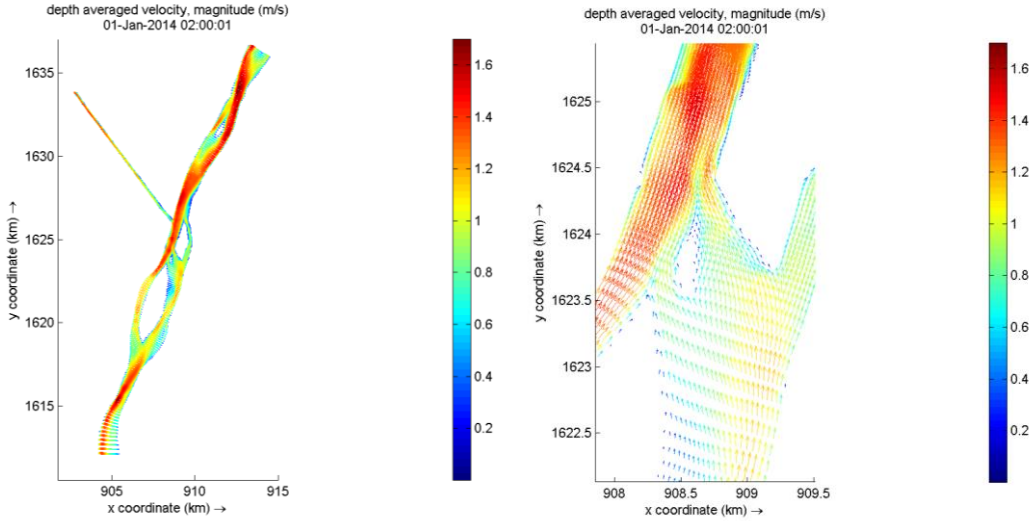

Figure 5.4 – Flow velocity at initial time step with reference case.

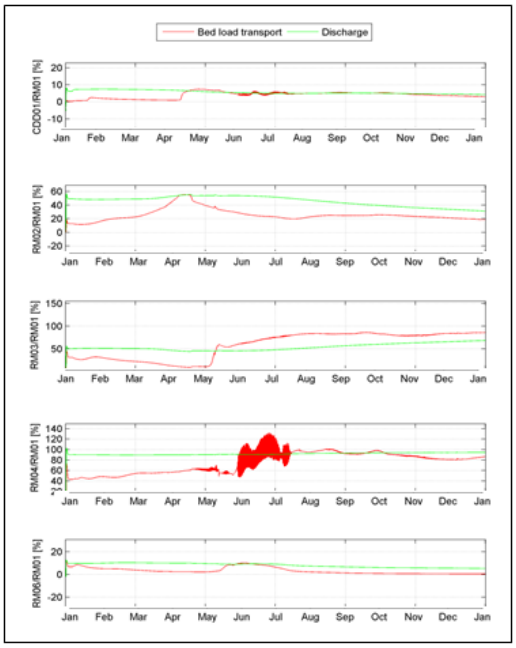

Figure 5.5 – Distribution bed load transport and discharge along islands and in the Canal del Dique

5.3.2 Impact of Isla la Loca located towards the left river bank

When Isla la Loca is located towards the left river bank it is found from the hydrodynamic simulations that this causes a decrease of discharge in the offtake. When including (coarse) sediments and accounting for morphological changes it can be seen from Figure 5.6 that erosion occurs at the right side of both islands, but especially along Isla la Loca, where flow velocities where initially high (Figure 5.7). Oppositely, sedimentation is observed at the left side of the islands which was less dominant in conveying discharges as following from the hydrodynamic computations (Figure 4.15). This results in a positive feedback mechanisms, where in areas of decreasing flow velocities sedimentation occurs, causing a lower depth hence even lower flow velocities. This is a reinforcing process and will

eventually lead to siltation of one branch and erosion of the other branch resulting in more smooth curving of streamlines and lower flow velocities (Figure 5.8).

Figure 5.9 shows the resulting depth in the study area after simulation of one year, where it can be seen that there is almost no water in the left branches. Finally, a large area of deposition of sediment just downstream of the bifurcation is observed which even becomes dry after a simulation period of one year. This is caused by the low flow velocity due to flow separation at the lee side of Isla la Loca Figure 5.7.

The resulting sediment and discharge distribution during the simulation period are shown in Figure 5.10. Where it can be seen that the discharge and sediment distribution indeed become dominant in the deeper right branches (RM02 and RM06) along the islands. However, it is seen that the final morphological equilibrium state is not yet reached along Isla Becerra after the simulation period of one year, where the bed load transport still increases along the right side and decreases along the left side of the islands.

Furthermore, it can be seen that the bed load transport decreases with a factor 2.5 at the entrance of the Canal (Figure 5.11) compared to the reference case with original position of Isla la Loca. Due to the decreased transport of bed load in the offtake, less sedimentation occurs in the canal and the bed level decreases.

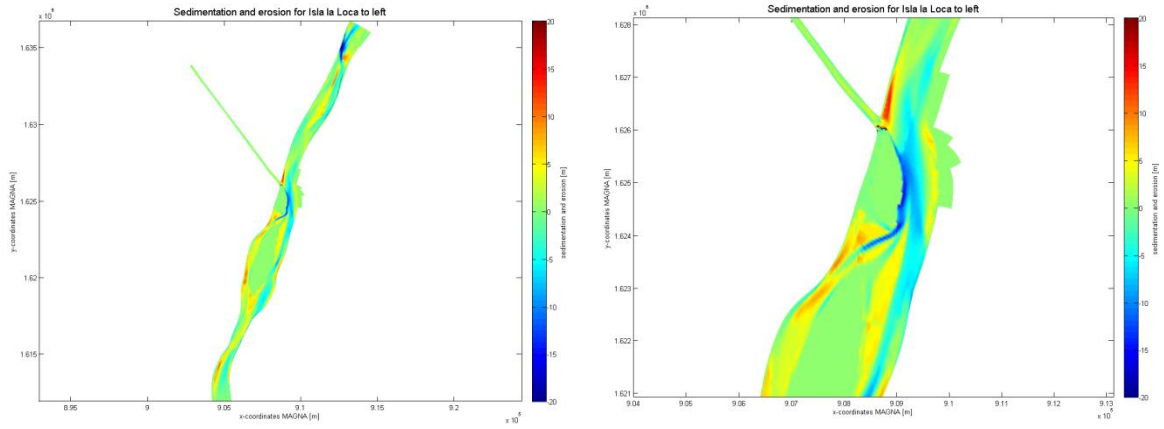

Figure 5.6 – Sedimentation and erosion pattern at final time step when Isla la Loca located more towards left bank

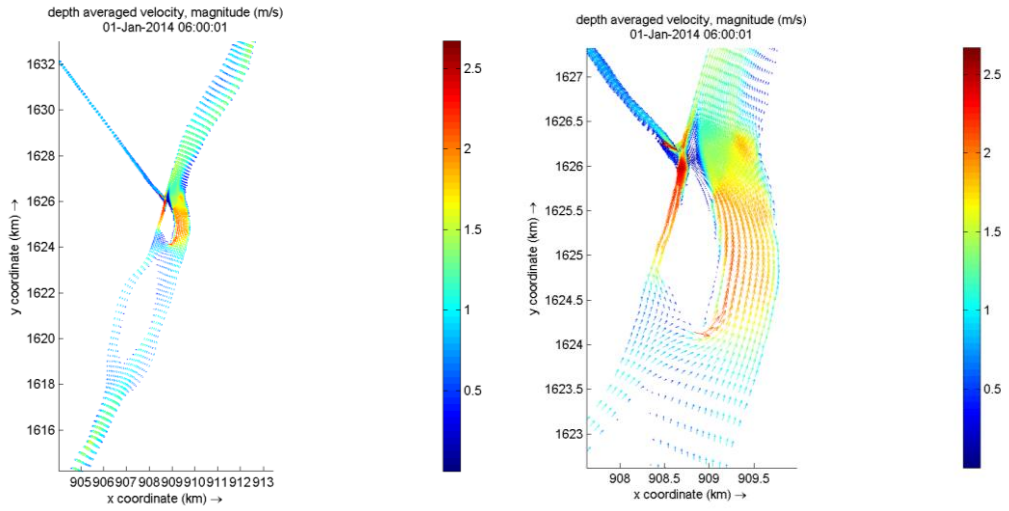

Figure 5.7 – Flow velocity at first time step when Isla la Loca positioned towards the left river bank

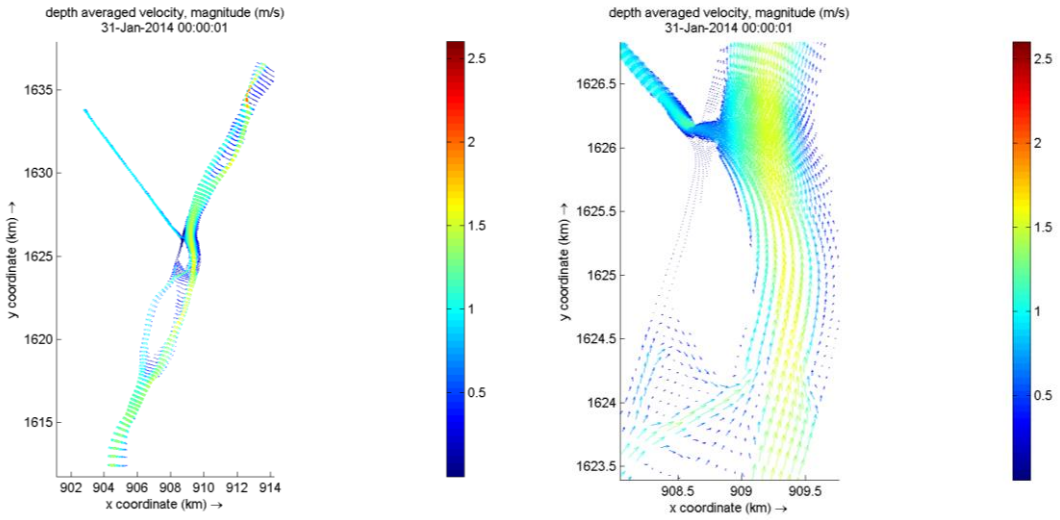

Figure 5.8 – Flow velocity magnitude and direction after one year of simulation time

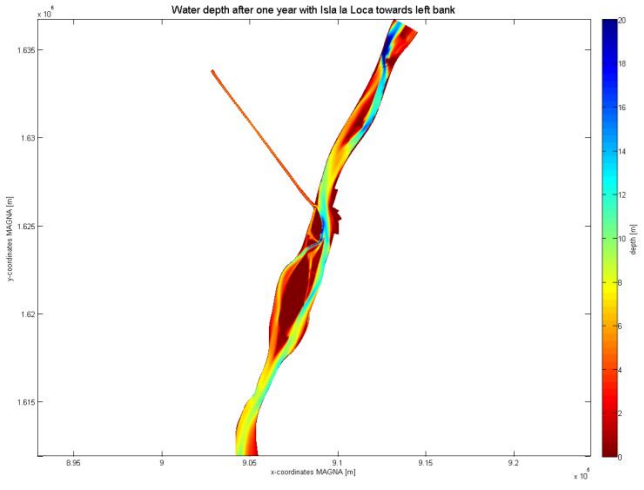

Figure 5.9 – Water depth after one year when Isla la Loca positioned towards the left river bank

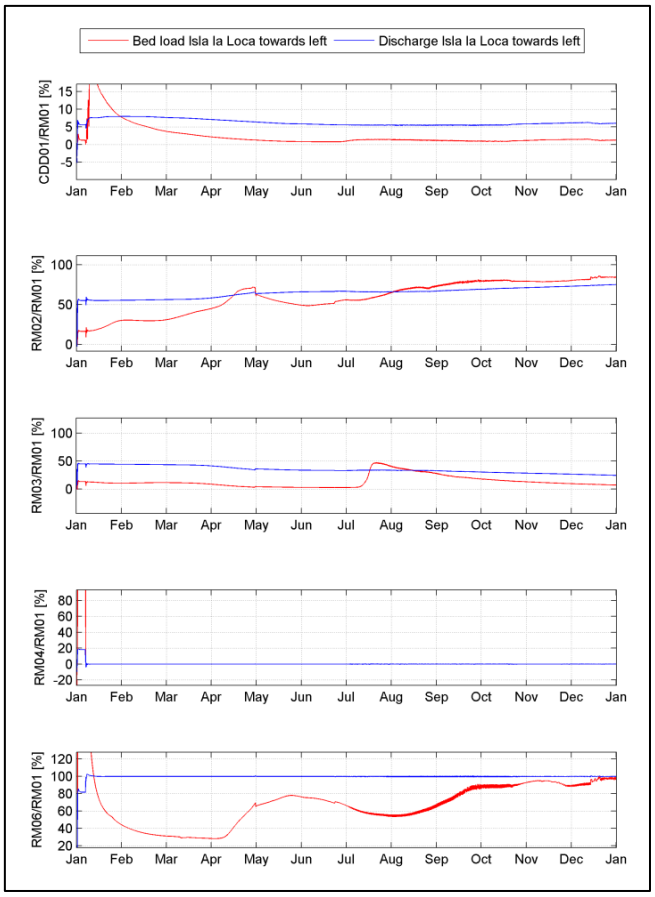

Figure 5.10 – Bed load and discharge distribution relative to upstream value for Isla la Loca located towards left river bank

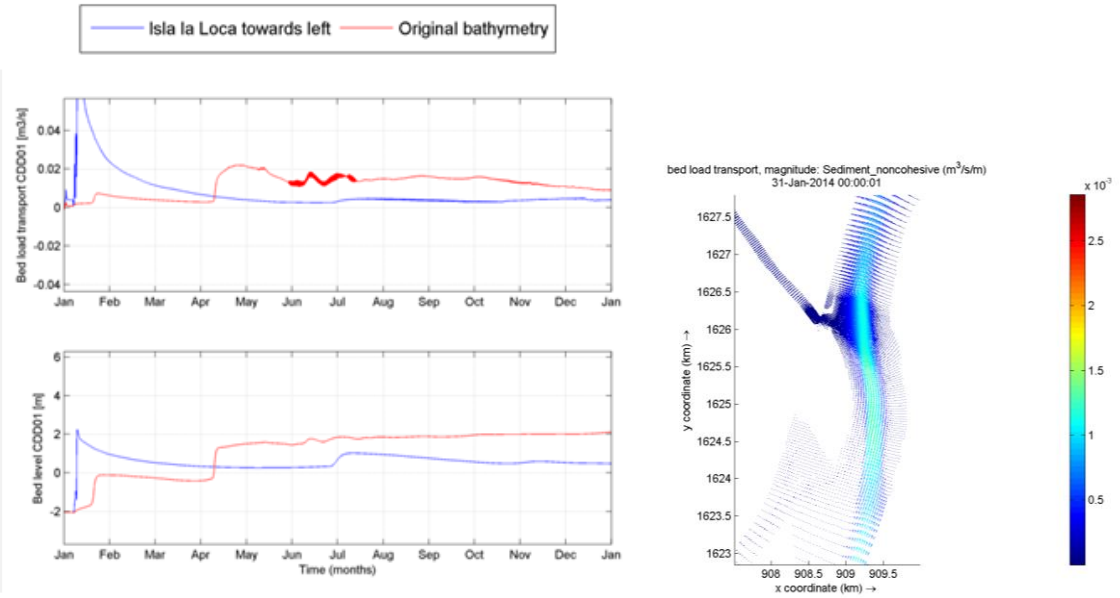

Figure 5.11 – Bed load transport in the offtake and bed level at the entrance of the canal when Isla la Loca positioned towards the left river bank compared to the original position. Right: bed load transport direction and magnitude

5.3.3 Impact of Isla la Loca attached to left river bank

When Isla la Loca is totally attached to the left river bank the same sedimentation and erosion pattern can be found at the end of the simulation period as found from the previous case where the island was located more towards the left side. Therefore, also the bed load transport rate and bed level at the entrance of the offtake is equal to the previous case (Figure 5.12). So, it can be concluded that when Isla la Loca is located towards the left river bank but not totally attached to it, the same equilibrium state is reached as in the case Isla la Loca is totally attached to the left bank.

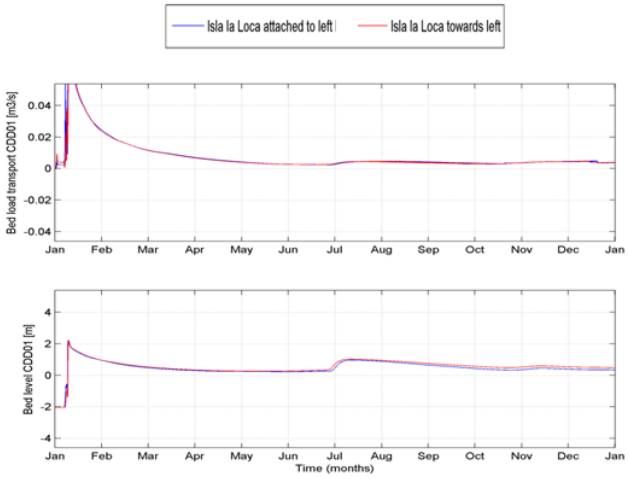

Figure 5.12 – Bed load transport in the offtake for Isla la Loca towards left side and totally attached to left

2.1.1 Impact of changing the position of Isla la Loca towards Isla Becerra

When the position of Isla la Loca is more towards the upstream located island 'Isla Becerra' sedimentation in the right branch along Isla Becerra and left branch along Isla la Loca occurs (Figure 5.13). As seen from the hydrodynamic simulations the left branch was dominant in conveying discharges (Figure 4.20) which is the starting point of the morphodynamic computation. Figure 5.14 shows that both the discharge and sediment transport distribution becomes more favourable towards the left branches (RM03 and RM04) after a simulation period of one year due to siltation of the right branches and erosion in the left branch causing respectively a smaller depth in the right branches and larger depth in the left branches (Figure 5.15). Therefore, it can be said that, again, a slight initial variation in discharge distribution and corresponding velocities is enhanced, a re-enforcing process.

Furthermore, erosion can be seen at the left tip of Isla la Loca caused by initially high flow velocities (Figure 5.16) due to the confluence of the right and left branch along Isla Becerra. However, just downstream of this area of high flow velocity sedimentation occurs, caused by large decreasing velocities due to a shallower area as seen in the initial bathymetry. At the final time step the magnitude of the flow is more uniform over the width of the channel, due to a smoother bed profile in the left branch caused by sedimentation in the deeper areas and erosion of the initial shallow areas.

In the area around the entrance of the offtake, which was initially a deep area, sedimentation is seen. Due to the extraction of discharge of the canal, less discharge and lower flow velocities occur just downstream of the bifurcation, resulting in deposition of sediment in the area.

Finally, it can be seen that the discharge in the offtake decreases during the simulation period, due to an initial lower flow velocity in the offtake, caused by a smaller depth of the offtake compared to the downstream main branch. This enhances sedimentation in the offtake and lower water depths causing less discharge in the offtake. However, the bed load transport *increases* in the offtake during the simulation period as the left branches (RM03 and RM04) along the islands become deeper and more dominant in conveying discharge causing higher flow velocities and a larger transport of sediment which also is distributed to the offtake. Compared to the morphological state at the end of the simulation period of the reference case, the bed load transport in the offtake is equal, however more sedimentation occurs in the offtake when the island is located more towards the upstream island (Figure 5.17).

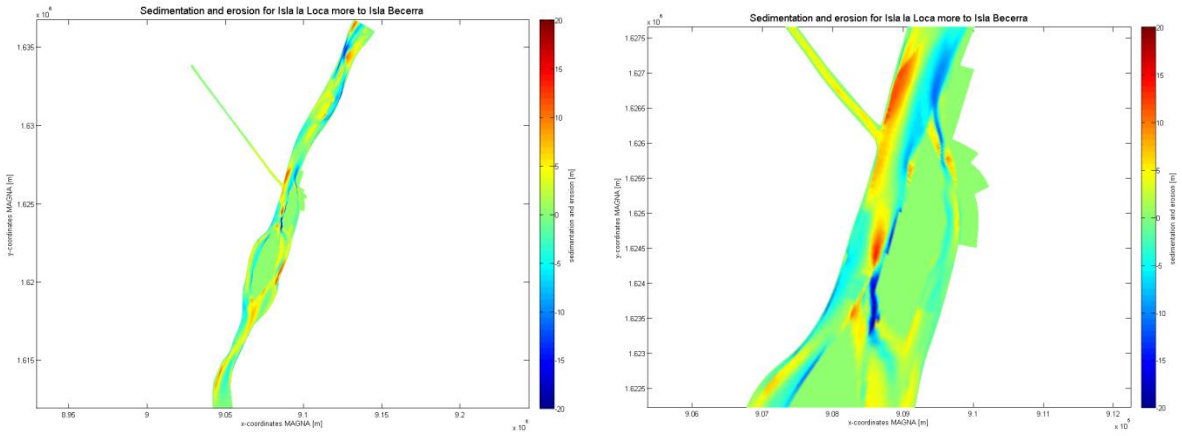

Figure 5.13 – Sedimentation and erosion at final time step for Isla la Loca placed more to Isla Becerra after simulation period of one year

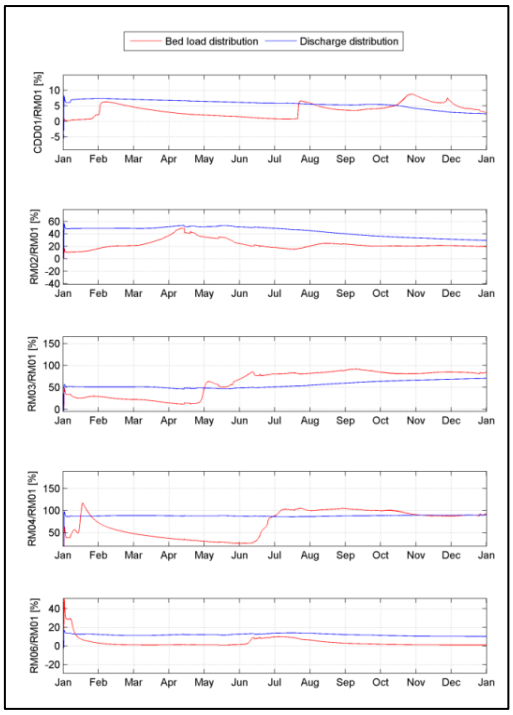

Figure 5.14 – Bed load and discharge distribution with Isla la Loca located towards Isla Becerra

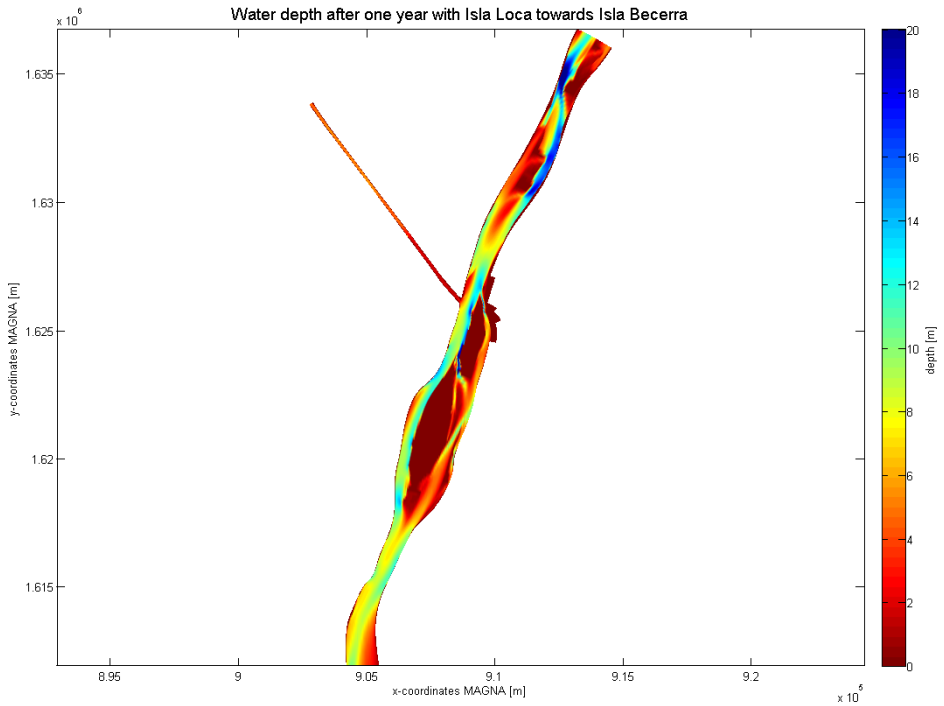

Figure 5.15 – Water depth after one year of simulation with Isla la Loca located towards Isla Becerra

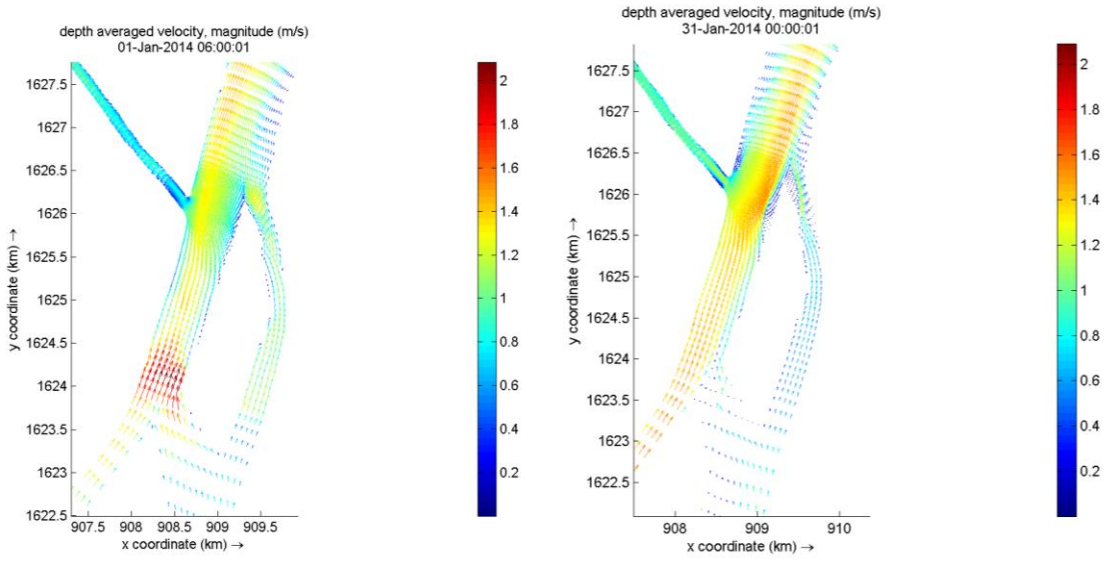

Figure 5.16 – Flow velocity at start (left) and end (right) of simulation in the area of the bifurcation

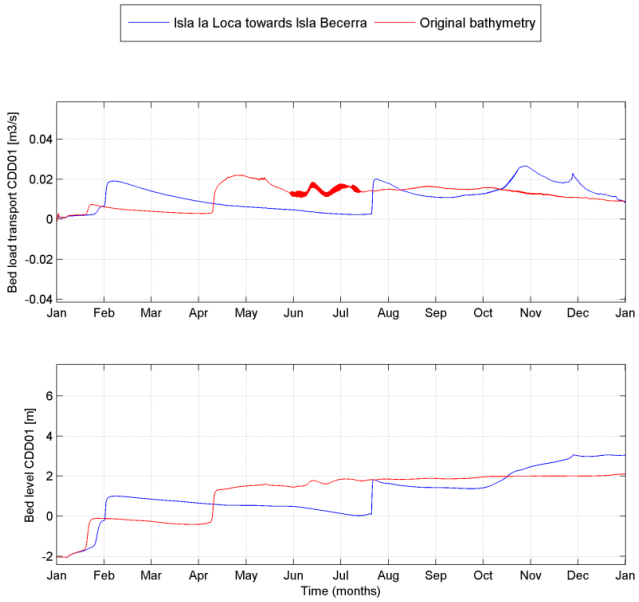

Figure 5.17 – Bed load transport in the offtake for Isla la Loca towards Isla Becerra compared to original bathymetry used in reference case

When Isla la Loca is merged with the upstream located Isla Becerra an almost equal sedimentation and erosion pattern is found along Isla Becerra compared to the previous case where there was still a branch between the two islands (Figure 5.18). However, more erosion is seen at the right tail of Isla la Loca. As in this case the discharge in the right side of Isla la Loca is larger as the mid channel does not extracts water from the right branches. Besides, it is seen that the bed load transport is initially larger along the left branches (RM03 and RM04 in Figure 5.19) when the islands are amalgamated, but decreases also faster causing a slight lower bed load transport along the left side at the end of the simulation period of one year.

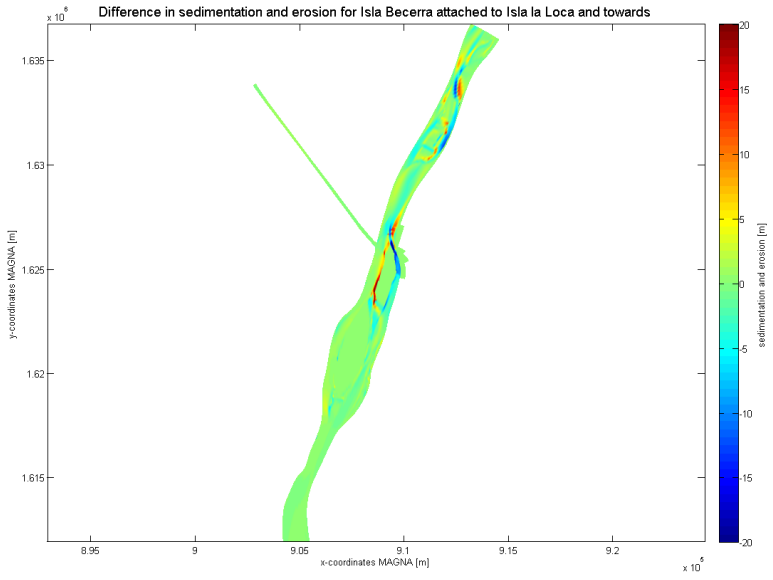

Figure 5.18 – Difference in sedimentation and erosion pattern for Isla la Loca amalgamated with Isla Becerra compared to Isla la Loca located more towards Isla Becerra but not attached at the end of the one-year simulation period

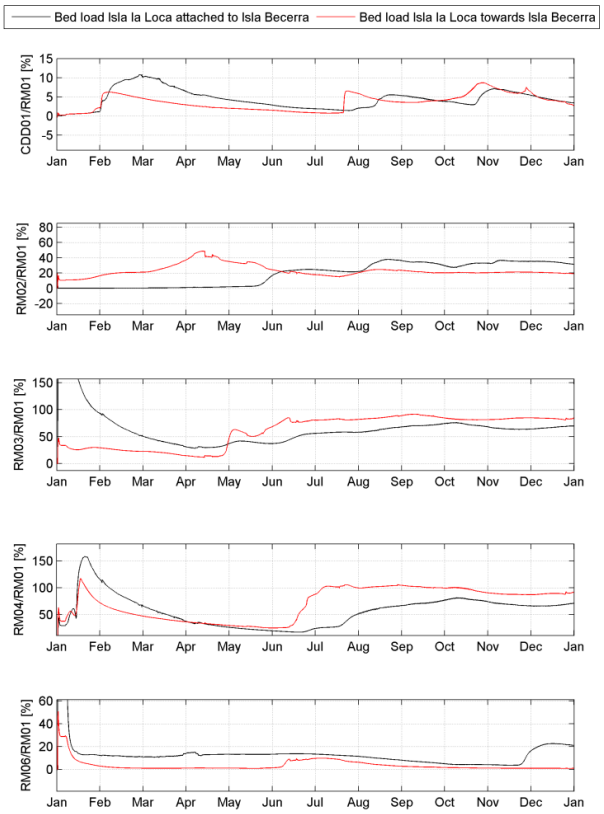

Figure 5.19 – Bed load distribution for Isla la Loca attached to Isla Becerra compared to Isla la Loca towards Isla Becerra

5.3.4 Validation bed level evolution reference case

From historical point of view, the small island in between the two large islands was not always present (Figure 5.20). Therefore, it is investigated what the evolution of the bed is when there is initially no small island. From Figure 5.21 it can be seen that indeed after a simulation period of one year with initially no small island, sedimentation occurs between the two large islands, resulting in a small island (Figure 5.22). However, the computed small island is located more to the right than is observed from historical bed level measurements as found in the Río Magdalena.

Besides, it is seen that sedimentation occurs in the right branches, where especially the depth along the right side of Isla la Loca becomes low. Also this trend is seen from historical measurements, where a trend of migration of Isla la Loca is seen towards the right river bank (Figure 5.23). Besides, Isla Becerra enlarges which is confirmed by historical measurements (Figure 5.24). Finally, model simulations show sedimentation around the entrance of the bifurcation in the Río Magdalena. In 1998 an island was seen at this location (Figure 5.24), whereas recent measurements show deepening of this area (Figure 5.23). Therefore, it is not sure if this simulated sedimentation trend is correct. Finally, it can be seen that the Canal del Dique experiences sedimentation, especially at the upper part of the Canal del Dique. Several sources confirm this sedimentation trend at the upper part, where also yearly dredging activities take place.

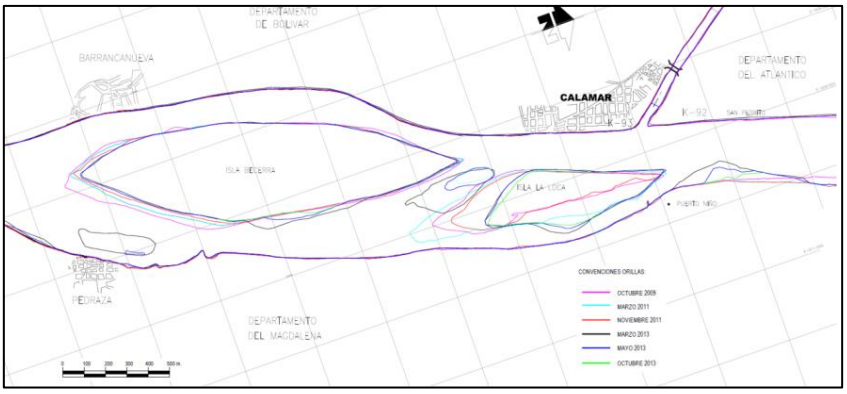

Figure 5.20 – Contour lines islands based on measurements from 2009-2013 (Cormagdalena and Universidad del Norte 2013)

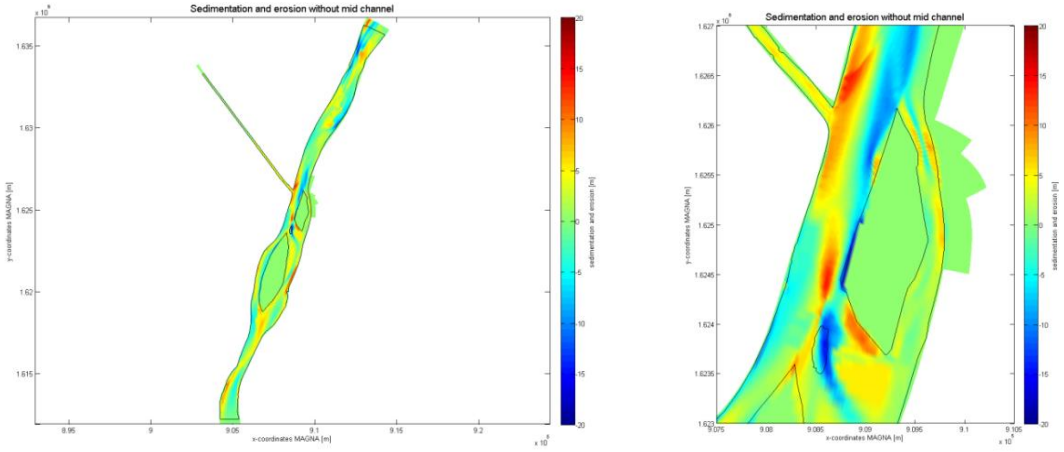

Figure 5.21 – Sedimentation and erosion pattern after one year with initially no small island between the two islands

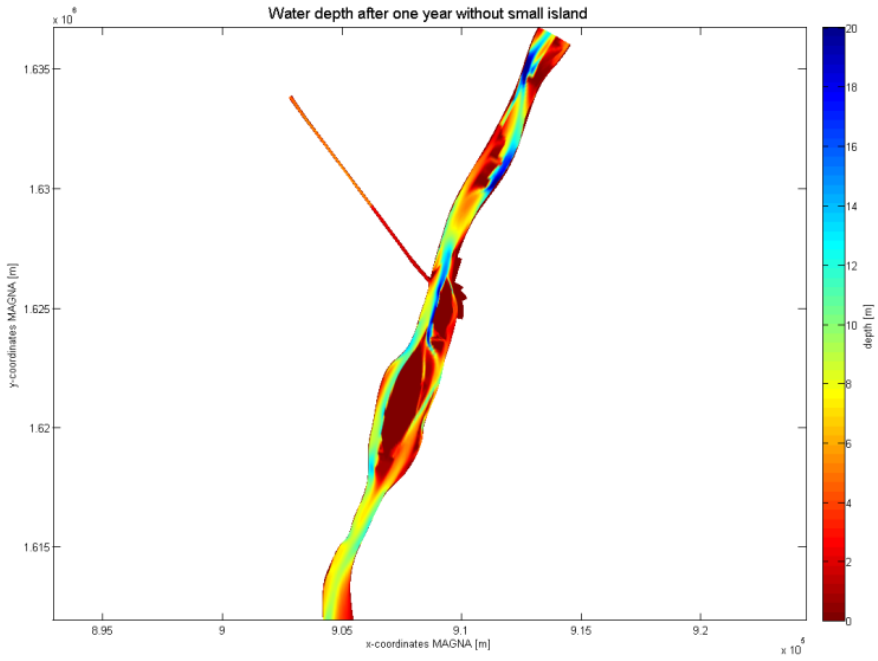

Figure 5.22 - Water depth after one year with initially no small island in between the large islands

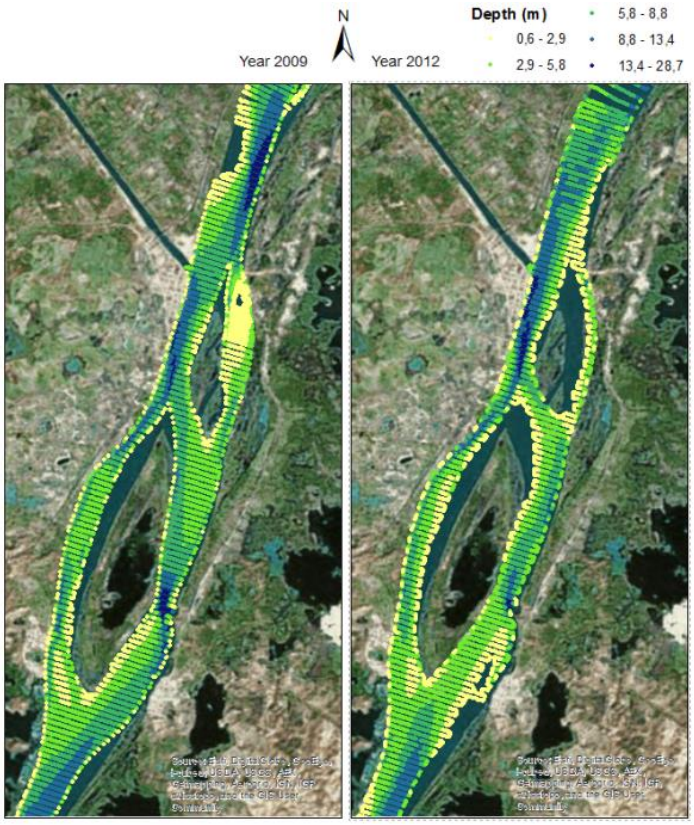

Figure 5.23 – Bathymetry comparison 2009 and 2012 (Consorcio Dique 2014)

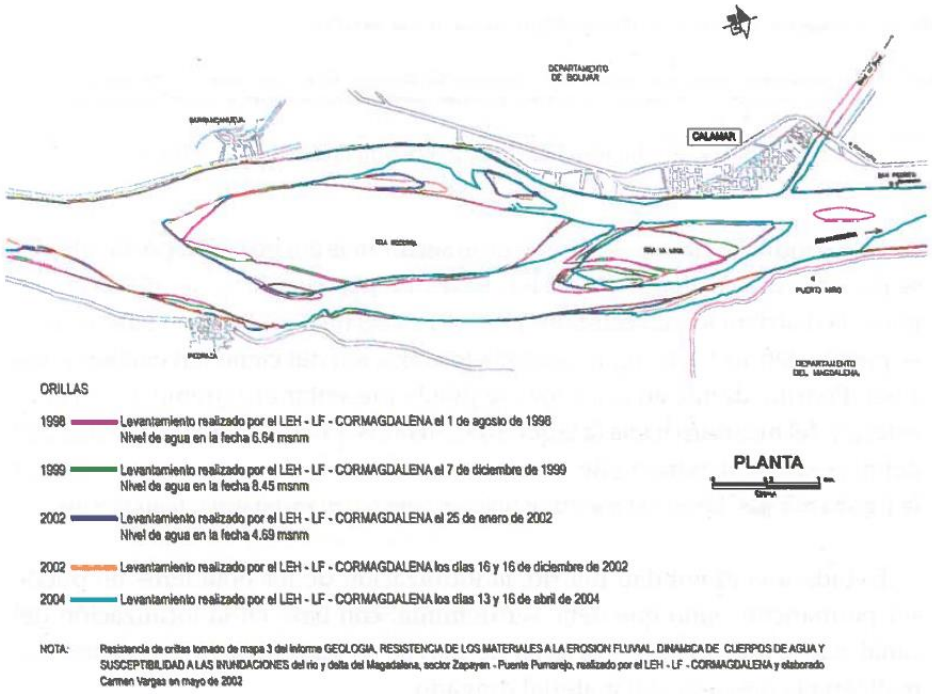

Figure 5.24 – Contour lines islands from 1998-2004 (Ortega, Escobar et al. 2008)

5.4 Conclusion

The aim of this study was to gain insight in the sediment transport distribution of coarse sediments and the corresponding sedimentation and erosion with different island configuration in order to predict future island shape, orientation and position and explain historical island evolution. Furthermore, the impact of island configurations, which cause a reduction of discharge in the offtake as found in the previous chapters, on the amount of *coarse* sediment entering the offtake is investigated.

Position Isla la Loca towards left river bank

It is found that when Isla la Loca is located towards the left river bank the amount of coarse sediment increases in the right branches along both islands during the simulation period of one year. As flow velocities are initially higher along the right side of Isla la Loca, due to a large width of the branch, this branch experiences erosion. Also, an initial large discharge is observed in the right branch along Isla Becerra, for which the amount of sediment transport is larger in this branch as well. It is found that this initial variation in discharge and sediment distribution along the islands will be enhanced, causing further erosion in the right branches and sedimentation in the left branches. Areas of decreasing flow velocities are subject to sedimentation which result in even lower flow velocities and further sedimentation. The opposite holds for initially deeper branches. Furthermore, the amount of sediment entering the Canal decreases with a factor 2.5 when Isla la Loca is located to the left river bank. Where sedimentation is observed at the entrance of the offtake.

Position of Isla la Loca attached to left river bank

The same distribution of sediment and equal sedimentation and erosion pattern are found when Isla la Loca is completely attached to the left river bank compared to when there is initially water along the left side of Isla la Loca. Therefore, it can be said that both island configurations will evolve into the same morphological equilibrium state.

Position of Isla la Loca towards Isla Becerra

When Isla la Loca is located more towards the upstream island Isla Becerra sedimentation can be seen in the right branches and erosion in the left branches. Initially, the left branches were slight favourable in conveying discharge compared to the left branches. This small difference causes, again, a positive feedback mechanism resulting in sedimentation (and eventually siltation) of the right branches. The increase in discharge and bed load transport in the left branches along the islands results furthermore in an increase of sediment towards the offtake. Moreover, due to decreasing flow velocities at the entrance of the offtake, sedimentation at the entrance of the offtake occurs causing a decrease in discharge in the offtake. Finally, erosion is seen at the left tip of Isla la Loca due to the confluence of streams causing high flow velocities in this area.

Evolution islands reference case

The evolution of the islands after one simulation year shows the enlargement of Isla Becerra, due to decreasing flow velocities at the right tail of the island, caused by flow separation and an initially shallow area. Also, sedimentation occurs at the left tip of Isla la Loca, due to decreasing flow velocities at the lee side of the small island in between the two large islands. Furthermore, it is seen that the left

side becomes dominant in conveying both water and sediment as the channels are deeper and flow velocities higher. Finally, a large amount of deposition of sediment is observed at the entrance of the offtake where flow velocities are decreasing due to the lower discharge in the offtake compared to the downstream branch in the Río Magdalena.

Validation historical island configurations Río Magdalena

Comparing the computed morphological changes of the islands to the historical morphological trends of Isla Becerra and Isla la Loca in the Río Magdalena shows several similarities. First of all, the evolution of a small island between the large islands, when initially this island was not present, is both computed and seen in reality. Although, the computation result in a location more to the right river bank, whereas in reality the island is located more in the middle of the river. Furthermore, a trend is seen of sedimentation of the right branch along Isla la Loca, resulting in migration of the island towards the right river bank, which is also computed by the model. Finally, simulations show sedimentation at the entrance of the offtake which confirm the amount of sediment being dredged in the first kilometre of the Canal del Dique. However, sedimentation is computed at the entrance of the offtake, whereas in reality deepening of this area is seen.

Efficiency of island configurations for reduction of the amount of sediment entering the offtake

Special interest in this study was to investigate the possibility of island configurations causing reduction of the amount of sediment entering the offtake, in order to reduce the amount of dredged sediment in the offtake. The most promising island configurations, causing a reduction of discharge in the offtake, were analysed. Where, it is found that when the position of Isla la Loca is changed to the left river bank, the amount of sediment entering the offtake reduces with a factor 2.5. This occurs both when the island is located towards the left river bank as in the case it is totally attached to the left bank. Furthermore, when Isla la Loca is located more towards Isla Becerra this results in a reduction of discharge in the offtake. However, it is found that this will eventually cause an *increase* of sediment entering the offtake as the left branches along the islands becomes favourable in conveying sediment due to favourable approach conditions towards the left branches; hence more sediment is transported to the offtake.

6 DISCUSSION

This chapter presents a critical reflection on the results found from this study. The limitations of the model simulations are outlined based on the assumptions made. It is discussed if morphological changes of the islands can explain the increase in discharge in the Río Magdalena at Calamar. Finally, the feasibility of fluvial islands as a design method for reducing sediment and discharge in the Canal del Dique is discussed.

Limitations of model assumptions and results

This study has given insight into the way different island configurations in the Río Magdalena impact the distribution of discharge and sediment into the Canal del Dique. However, several important assumptions were made in the model study, which have to be taken into account when interpreting the results.

First of all, the model domain of both the 1D and 2D model applied in this study is limited to the river banks of the Río Magdalena. As low discharges are applied, which do not result in overtopping of the banks along the Río Magdalena and Canal del Dique, this does not affect the model results. However, one has to be aware of the fact that floodplains of the Río Magdalena are inundated in reality with high discharges and breaching of the dikes occurred in the Canal del Dique during the high flow event of 2010. Therefore, when one is interested in extreme events the distribution of discharge and sediment into the Canal del Dique can be different from the results of this model study.

Besides, it is found in this study that applying higher discharges does not affect the distribution of discharges along the islands and in the Canal del Dique. The data-analysis showed that higher discharges upstream in the Río Magdalena result in slightly larger discharges in the right branches compared to the left branches.

Calibration of the two-dimensional hydrodynamic Delft3D model has been carried out resulting in a good fit of the model results compared to the measurements. However, due to a lack of data on the *coarse* sediment transport rates and bed level changes, the morphodynamic model could not be calibrated to a large extent. Therefore, the results of the morphodynamic study should be taken with care. Besides, the result of the sensitivity analysis showed that applying a different sediment transport formula resulted in very large differences in model results. Van Rijn computed very deep erosive channels, which are not seen in reality. This is a known shortcoming in Delft3D and the reason why Van Rijn is not recommended in river studies. Engelund-Hansen showed more realistic sedimentation and erosion patterns. However, varying other parameters such as the bed-friction could result in good model results for van Rijn as well. Due to lack of time an extensive calibration process has not been carried out.

Finally, the one-dimensional model was used as a first study to gain inside into the effects of different width and lengths of the branches along the islands on the discharge distributions. Dimensions of the Canal del Dique were used as a basis. However, as the objective of this part of the study was to gain more generic insights, exact dimensions and characteristics of the branches were not used. For example, a fixed Chézy-bed friction coefficient is used, whereas in the Río Magdalena a Manning-coefficient varying with different river discharges seems to be more reliable as followed from the two-

dimensional study. Therefore, the one-dimensional and two-dimensional model simulations cannot be compared one-to-one. However, the one-dimensional model appeared to be a good tool in order to gain insight into the effect of different positions and sizes of the islands without requiring large computation efforts. Although the two-dimensional model requires more computational effort, it gives a better understanding of the effect of different angles between the branches and horizontal water level gradients could be computed. Although these physical factors do not seem to influence the distribution of discharges, secondary flow structures do play a role when taking into account sediment which cannot be computed with a one-dimensional model.

Morphological changes islands as explanation for discharge reduction

Measurements in the Río Magdalena at Calamar from 2014 showed an increase of the rating curve of 10%, which can be explained by the increased depth and width of the left branch along Isla la Loca as confirmed by this study.

Side-notes islands as measure for reducing discharge in the Canal del Dique

In this study a closer look is taken at island configurations causing a reduction of discharge and sediment in the Canal del Dique in order to get a better understanding of the system. Besides, this study has been carried out in order to investigate a sustainable measure for reducing the negative impacts of fine sediments in the adjacent wetlands of the Canal del Dique and downstream in the Bay of Cartagena. From this point of view, it is found that locating Isla la Loca towards the left bank, by dredging sand on the right side of the island and depositing it to the left side, can cause a reduction of discharge (hence fine sediment) of 8% in the Canal del Dique and a reduction with a factor 2.5 of coarse sediment. Although these values seem to be low, it may have considerable effect on the deposited volumes of sediment downstream. However, when taking into account other factors, which play a role in the Canal del Dique such as navigation, such a measure is not feasible. Besides, islands are not able to *regulate* the amount of water and sediment entering the Canal. Therefore, in the Canal del Dique case they cannot be used as the sole solution for reducing sediment.

At other bifurcations where navigation plays a smaller role and coarse sediment is more dominant positioning an island more towards the offtake, by dredging one side and dumping the sediment on the other side, could result in a feasible and sustainable measure.

7 CONCLUSION & RECOMMENDATIONS

7.1 Conclusions

First of all, the answers to the sub-questions are given followed by the overall conclusion answering the main research question.

1. What are the physical processes influencing discharge and sediment distribution at a bifurcation and around fluvial islands?

The discharge and sediment distribution at a bifurcation depends on the characteristics of the downstream branches (e.g. geometry, hydraulic roughness, bed slope, bed-friction and water head) and is strongly dependent on local factors. Therefore, no unique relationship for the distribution of water and sediment at bifurcation exists and the local conditions need to be defined for each bifurcation. Local factors influencing the sediment distribution are: the Bulle effect depending on the angle of the offtake; the gravitational pull due to transverse bed slopes; the approach conditions by different transverse bathymetric conditions or a bend upstream; flow separation at sharp edges causing the formation of an eddy and human interferences affecting the stability of the bifurcation. Furthermore, backwater effects occur when the equilibrium depth of the downstream branches is not reached at the point of bifurcation. Also, it is important to determine the dominant transport mode as fine sediments are predominantly transported in suspension following the discharge distribution, whereas coarse sediment fractions are strongly affected by local factors and do not follow the discharge distribution one-to-one.

A fluvial island can be seen as a combination of a confluence and bifurcation. The confluence causes larger erosion holes and sediment bumps to occur in the area of the bifurcation than in the case of no island. Fluvial islands are formed by several mechanisms as for example the cut-off from river banks at high flow events or the stabilization of bars due to a long period of low flow velocity.

In the case of the Canal del Dique two fluvial islands are located in front of the bifurcation. Where Isla la Loca in the Río Magdalena is probably formed out of the more stable Isla Becerra, where sedimentation occurs at the tail due to flow separation which is probably cut-off during a high flow event. The origin of Isla Becerra is not known as no morphologic data are available which date back to the time when Isla Becerra was formed. However, it is likely that Isla Becerra was formed by stabilization of a bar due to vegetation during a long period of low flow. Upstream of the islands a bend is located, where spiral flow occurs resulting in a larger depth in the outer bend and left side of Isla Becerra than along the inner bend and right side of the island. This approach condition explains a slight larger discharge in the left side. Flow separation at sharp edges along the islands and the approach conditions are dominant local factors impacting the discharge and sediment distributions along the islands and in the downstream branches of the Canal del Dique and Río Magdalena.

2. What is the influence of different size, position and shape of fluvial islands in the Río Magdalena on the amount of discharge distributed into the Canal del Dique and along the islands?

From the one-dimensional simulations it can be concluded that the size of the islands, corresponding to different width of the branches along the islands, have a significant effect on the amount of discharge in the Canal del Dique as it impacts the water level at the entrance of the Canal. When for

example the width of the right branches along the islands is increased, the flow area increases and the discharge in these branches increase. In contrary, the discharge in the left branches decreases as the flow area decreases. A large discharge along the right side of the islands implies a more convex shaped backwater curve in the right branches and a concave shaped curve in the left branches. As the water level at the confluence of the downstream island is equal, the concave M1 curve then implies a relatively low water level at the entrance of the offtake, which can only be compatible with the water levels if its discharge is low. Conversely, a narrow left branch causes a low discharge in the left branches which implies a concave M1 curve hence the water level at the entrance of the offtake is lower causing a low discharge in the offtake.

The findings of this study show that the bathymetry of the branches along the islands influences the amount of water in the offtake. A similar effect occurs when increasing the depth of the branches compared to the width of the branches along the islands. The discharge distribution is bounded by the flow capacity and the resistance of the branches.

The results show that increasing the width of the branch between the two islands, which is equal to changing the size and position of the island, causes an increase in discharge in this branch as the flow area is increased. Moreover, a strong correlation is found between the connecting upstream and downstream branches. If the discharge in *one* of these branches increases, the discharge increases in *all* of the branches. As these branches are connected to each other impacting the water level gradients in the branches. When the mid channel is directly connected to the offtake an increase of discharge in these branches is observed.

Changing the length of the branches along the downstream island only has minor effect on the distribution of water over the branches at the bifurcation. Changing the length of the downstream branch with for example 1000 m causes only an increase of water level at the offtake of approximately 2 cm which does not result in a significantly larger water level head in the offtake, hence discharge in the offtake.

The two-dimensional simulations show similar effects of bathymetric changes of the right branches compared to the left branches along the islands on the distribution of discharges as the one-dimensional simulation. However, when large changes in depth occur on a small area, steep water level gradients are seen, resulting in energy dissipation and less discharge in this branch.

When the position of Isla la Loca is changed towards the left river bank a large eddy is seen at the entrance of the offtake. However, the flow still finds its way to the offtake. At the location of the eddy the water level is lower due to energy dissipation; however this reduction in water level is only in the order of 1 cm, which does not result in a larger reduction of discharge in the offtake when comparing the one-dimensional and two-dimensional simulations. Furthermore, it is found that the angle of the offtake does not impact the distribution of discharge over the downstream branches.

The shape of the island does not have significant influence on the discharge distributions, however does have considerable effects on flow velocities and directions. Protrusions cause high flow velocities that may be expected to erode these protrusions, whereas sharp bank-line angles cause flow separation that may be expected to fill the areas of large eddies by deposition.

3. What is the influence of different size, position and shape of fluvial islands in the Río Magdalena on the amount of fine and coarse sediment distributed into the Canal del Dique and along the islands?

The distribution of fine sediment at a bifurcation simply depends on the distribution of discharge (Slingerland & Smith 1998). Coarse sediment, on the other hand, settles in areas of decreasing flow velocities and erodes in areas of increasing flow velocities for which no one-to-one relationship between the flow and *coarse* sediment can be made as local factors play a role.

The results of the two-dimensional simulations with coarse sediment show that when Isla la Loca is located towards the left river bank, the distribution of sediment becomes dominant along the right branches, hence causing a reduction of sediment in the Canal del Dique and increase in the downstream reach of the Río Magdalena. The opposite holds when the location of the island is towards the right river bank. When the position of Isla la Loca is more towards Isla Becerra the left side becomes dominant in conveying sediment as the depth at the top of Isla Becerra is slightly larger along the left side resulting in a larger discharge and more sediment transported to this branch.

Furthermore, this study showed that small initial variations in discharge and sediment causing different flow velocities will be enhanced resulting in siltation in the branch where initially flow velocities were lower and erosion in the other branch. Areas of low flow velocity occur at locations of flow separation and in shallow areas for which it can be concluded that flow separation and the approach conditions at the islands at the Río Magdalena have a significant impact on the distribution of sediment in the Canal del Dique. Furthermore, in these areas of low flow velocity sedimentation occurs, resulting in the evolution of different size, position and shape of the islands. Even a small island is computed at the lee side of Isla Becerra where flow separation occurs. This small island is all seen in historical bathymetries from the Río Magdalena.

4. What island configurations create a reduction of discharge and sediment in the offtake from the Río Magdalena to the Canal del Dique and to what extent is it reduced?

The discharge in the offtake is governed by the water level at the entrance of the offtake and its physical characteristics. The presence of the islands results in a reduction of discharge in the offtake compared to no islands. Where, having one island results in a larger discharge in the offtake then having two islands. Decreasing the length or width of the channel between the islands results in a maximum reduction of 0.3% in the offtake relative to the upstream discharge.

From the two-dimensional hydrodynamic simulations it was found that the discharge in the Canal del Dique reduces in the order of 0.2% relative to the upstream discharge (≈4% relative to the original discharge in the Canal del Dique) for the following cases:

- No small islands in between large islands
- Depth right side Isla la Loca 2x left side
- Depth right side Isla Becerra 4x left side
- Isla la Loca towards left river bank
- Isla la Loca located more towards or merged with Isla Becerra

When Isla la Loca is completely attached to the left river bank the largest reduction is found: 0.4% relative to the upstream discharge which is equivalent to 8% relative to the original discharge in the offtake.

When fine sediments are dominant, the reduction of discharge is equivalent to the reduction of sediments in the offtake. However, when taking into account coarse sediment no one-to-one relationship with the flow can be made and local factors play a role in the distribution of sediment. Therefore, the amount of *coarse* sediment in the offtake can be reduced by locating the island towards or attached to the left river bank, just upstream of the offtake. This causes a reduction of the amount of sediment in the offtake with a factor 2.5.

General conclusion on main research question:

What is the effect of size, position and shape of fluvial islands in the Río Magdalena on discharge and sediment transport into the Canal del Dique in Colombia?

Overall, it can be concluded that size and position of islands in the Río Magdalena have an appreciable effect on the discharge and sediment transport into the Canal del Dique and along the islands. Whereas, the shape of the islands do not impact the distribution of discharge and tends to evolve to the same equilibrium state of smooth bank-lines along smooth curved streamlines. Negative impacts of fine sediment in the Canal del Dique can be minimized by connecting the islands to the left bank with a reduction of 8%. Furthermore, this island configuration causes a reduction of the amount of coarse sediment entering the Canal with a factor 2.5.

7.2 Recommendations

How to use islands as measure for reducing sediment in the Canal del Dique

This study showed that islands can reduce the amount of water and fine sediment in the Canal del Dique with only 8% relative to the discharge in the Canal with the actual island configurations. This reduction is not large enough to reduce the negative impacts of sedimentation downstream in the Canal. Besides, navigation can be a problem when islands are located just in front of the offtake. Therefore, it is not feasible to use islands as a measure to reduce the amount of fine sediment in the Canal del Dique.

However, when reduction of coarse sediment is more important, using islands to reduce the amount of sediment entering the Canal can be a feasible measure. As the coarse sediment entering the Canal are reduced by a factor 2.5. However, in this case further research is necessary to investigate the uncertainties of morphological evolution of the islands, maintenance costs and other possible negative impacts. When a smaller reduction of coarse sediments is necessary, less extreme changes of island configurations are necessary and therefore, such a measure becomes more feasible.

Further research

In this study simulations have been carried out with a stationary flow corresponding to a relatively low discharge in the Río Magdalena. However with high discharges islands may be flooded and the banks

along the Río Magdalena may be overtopped causing inundation of the floodplains. This will impact the amount of discharge and sediment in the branches along the islands and in the Canal del Dique. Therefore, this should be investigated. Furthermore, when a non-stationary flow would be applied the morphologic dynamic character of the islands in the Río Magdalena could be better computed. For example a small island between Isla Becerra and Isla la Loca evolves and remains present, whereas from historical measurements it is seen that this island seems to appear and disappear. Furthermore, a slight favor of discharge to the left side of Isla Becerra results in siltation of the right branches as computed. However, this strong trend in siltation is less observed in reality.

Due to a lack of data of the *coarse* sediment transport rates and bed level changes in the Río Magdalena, the morphodynamic depth-averaged model could not be calibrated extensively. Therefore, more data on the coarse sediment are required and a more elaborate calibration should be carried out.

In this study simulations have been carried out on a one-dimensional and two-dimensional (depth-averaged) scale. Three dimensional simulations would result in a more detailed understanding of the processes occurring at the bifurcation. However, it is not to be expected that three-dimensional processes would result in large differences in discharge and sediment distribution as also found from a study of Edmond and Slingerland, 2008. Besides, this would allow the simulation of smaller scale turbulent motions and gain insight into the effect on the discharge and sediment distribution. Another option is to simulate turbulence with a HLES-turbulence model with combination of the two-dimensional model.

Finally, this research is only based on the Canal del Dique case, for which general conclusions on the effect of fluvial islands at a bifurcations are hard to obtain. To obtain general conclusions, more bifurcations with fluvial islands should be investigated.

REFERENCES

2015. Google earth. Google.

2015. Image: CALAMAR, Esri, Digital Globe, GeoEye, USGS, GIS User Community.

BERTOLDI, W., ZANONI, L., MIORI, S., REPETTO, R. & TUBINO, M. 2009. Interaction between migrating bars and bifurcations in gravel bed rivers. Water resources research, 45.

BOLLA PITTALUGA, M., REPETTO, R. & M.TUBINO 2003. Channel bifurcation in braided rivers: Equilibrium configurations and stability. Water resources research, 39.

BOSBOOM, J. & STIVE, M. J. F. 2013. Coastal Dynamics I, Lecture notes CIE4305, VSSD.

BULLE, H. 1926. Untersuchungen über die geschiebeableitung bei der spaltun. Forschungsarbeiten auf dem gebiete des ingenieurwesens.

CONSORCIO DIQUE 2013. Inception report watermanagement studies. Bogota.

CONSORCIO DIQUE 2014. Environmental restoration of the Canal del Dique - Development and calibration of numerical models.

CONSORCIO DIQUE 2014. Further Data Analysis Suspended Sediment Transport Canal del Dique. Royal HaskoningDHV.

CONSORCIO DIQUE 2014. Survey report campaign A - March 2014. Bogota.

CONSORCIO DIQUE 2014. Survey report campaign B - July 2014. Bogota.

CONSORCIO DIQUE 2015. Estudios y diseños definitivos para construcción de las obras del plan de manejo hidrosedimentológico y ambiental del sistema del Canal del Dique.

CONSORCIO DIQUE & FONDO ADAPTACIÓN 2015. Estudios y diseños definitivos para construcción de las obras del plan de manejo hidrosedimentológico y ambiental del sistema del Canal del Dique - Informe de dragados.

CORMAGDALENA & UNIVERSIDAD DEL NORTE 2013. Calamar comparativo de orillas 2009-2013. Image PLANO1

CORMAGDALENA & UNIVERSIDAD DEL NORTE 2013. Calamar velocidades octubre/2013 campaña IV.

CORMAGDALENA & UNIVERSIDAD DEL NORTE 2013. Canal del Dique levantamiento batimetrico K0+000 a K2+800 trampa de sedimentos.

DE VRIEND, H. J., HAVINGA, H., PROOIJEN, B. C. V., VISSER, P. J. & WANG, Z. B. 2011. CT4345 River Engineering, Delft University of Technology.

DELTARES 2012. Morphology and Sediment Transport - Technical Reference Manual. SOBEK RE 2.52.008 ed.

DELTARES 2012. Technical Reference Manual.

DELTARES 2012. User Manual SOBEK-RE.

DELTARES 2014. Delft3D-FLOW User Manual. 3D/2D modelling suite for integral water solutions. Delft: Deltares.

EINSTEIN, H. A. 1950. The bed-load function for sediment transportation in open channel flows. In: AGRICULTURE, D. O. (ed.) 1025 ed. Washington D.C.

ENGELUND, F. & HANSEN, E. 1967. A monograph on sediment transport in alluvial streams Copenhagen, Teknisk Forlag.

HARDY, R. J., LANE, S. N. & YU., D. 2011. Flow structures at an idealized bifurcation: a numerical experiment. Earth surface processes and landforms, 36, 2083-2096.

JANSEN, P. P., BENDEGOM, L. V., BERG, J. V. D., VRIES, M. D. & ZANEN, A. 1979. Principles of River Engineering, Londen, Pitman.

KARNSTEDT, A. 2010. Map of the Magdalena River watershed. 3 Arc Second. University of Maryland.

KLEINHANS, M. G. & BERG, J. H. V. D. 2010. River channel and bar patterns explained and predicted by an empricial and a physics-based method. Earth surface processes and landforms, 36.

KLEINHANS, M. G., FERGUSON, R. I., LANE, S. N. & HARDY, R. J. 2013. Splitting rivers at their seams: bifurcations and avulsion. Earth surface processes and landforms, 38, 47-61.

KLEINHANS, M. G., JAGERS, H., MOSSELMAN, E. & AL, E. 2008. Bifurcation dynamics and avulsion duration in meandering rivers by one-dimensional and three-dimensional models. Water resources research, 44.

MELMAN, F. C. R. 2011. Navigability at an unstable bifurcation - The Montaño-Murindó bifurcation of the Atrato river in Colombia. Master of Science Msc thesis, Delft University of Technology.

MEYER-PETER, E. & MÜLLER 1948. Formulas for bed-load transport.

MILLIMAN, J. D. & SYVITSKI, J. P. M. 1992. Geomorphic/tectonis control of sediment transport to the ocean: the importance of small mountainous rivers. The Journal of Geology, 100, 525-544.

MIORI, HARDY, R. J. & LANE, S. N. 2012. Topographic forcing of flow partition and flow structures at river bifurcations. Earth surface processes and landforms, 37, 666-679.

MOSSELMAN, E. 2013. Lecture notes - River Dynamics.

NANSON, G. C. & KNIGHTON, A. D. 1996. Anabranching rivers: their cause, character and classification. Earth surface processes and landforms, 21, 217-239.

NEDECO 1973. Río Magdalena and Canal del Dique survey project. The Hague.

ORTEGA, M. A., ESCOBAR, R. C., ROMERO, H. C., FLORES, J. C. M., CUERVO, G. V., MARTÍNEZ, G. C., HERAZO, H. A., REYES, J. C., FONSECA, A. E. D. & TIJERINO, G. R. 2008. Río Magdalena - Navegación marítima y fluvial (1986-2008), Barranquilla, Colombia, Ediciones Uninorte.

OSTERKAMP, W. R. 1998. Processes of fluvial island formation, with examples from Plum Creek, Colorado and Snake River, Idaho. Wetlands, 18, 530-545.

RESTREPO, J. D. & KJERFVE, B. 2000. Magdalena river: interannual variability (1975–1995) and revised water discharge and sediment load estimates. Journal of Hydrology, 137-149.

RIBBERINK, J. S. 1983. Introduction to a depth-integrated model for suspended transport. Delft: Delft University of Technology.

RIJN, L. V. 1984. Sediment Transport, Part I: Bed load transport. Journal of Hydraulic Engineering, 110, 1431-1456.

RIJN, L. V. 1984. Sediment Transport, Part II: Suspended Load Transport. Journal of Hydraulic Engineering, 110, 1613-1641.

SCHUURMAN, F. & KLEINHANS, M. G. 2013. 3D modelling of bar and bifurcation evolution. Book of abstracts.

SLINGERLAND, R. & SMITH, N. D. 1998. Necessary conditions for a meandering-river avulsion. Geology, 26, 435-438.

SLOFF, C. J. & MOSSELMAN, E. 2012. Bifurcation modelling in a meandering gravel-sand bed river. Earth surface processes and landforms, 37, 1556-1566.

UNIVERSIDAD NACIONAL DE COLOMBIA 2007. Estudios e investigaciones de las obras de restauración ambiental y de navegación del Canal del Dique.

WANG, Z. B., FOKKING, VRIES, H. J. D. & LANGERAK 1995. Stability of river bifurcations in 1D morphodynamic models. Journal de recherches hydrauliques, 33.

WYRICK, J. R. 2005. On the Formation of Fluvial Islands. Doctor of Philosophy, Oregon State University.

WYRICK, J. R. & KLINGEMAN, P. C. 2011. Proposed fluvial island classification scheme and its use for river restoration. River research and applications, 27, 814-825.

APPENDICES

Appendix A Data-analysis

A.1 Objective

In order to gain insight in the discharge and sediment distribution at the Río Magdalena and Canal del Dique near Calamar a data analysis is carried out based on measurements of Consorcio Dique, a consortium of Royal HaskoningDHV and Gomez Cajiao, from 2014 and historical data. This data analysis will help to obtain a better feeling on the specific system at Canal del Dique and the influence of the fluvial islands at this bifurcation. Besides, this data analysis will gain insight in the available data necessary for the study and possible extra data which need to be measured.

A.2 Climate Canal del Dique

The climate at the Canal del Dique and Rio Magdalena consists of a wet season around November-December and a dry season around February-March. Besides, a secondary wet peak occurs around June-July.

Besides, el Niño and la Niña occur approximately every three year. During el Niño extreme dries occur, whilst la Niña corresponds to extreme wets.

A.3 Sediment and discharge rates Rio Magdalena

The mean annual discharge of the Rio Magdalena at Calamar is 7.200 m^3/s with a mean low discharge of 4.068 m^3/s in March and a mean high discharge of 10.287 m^3/s in November (Restrepo and Kjerfve, 2000). The sediment load at Calamar has high values of $690x10^3$ t/day in November, a secondary peak of $443x10^3$ t/day in June-July and low values during Feb-March of $150x10^3$ t/day. The seasonal variability of discharge and sediment load is shown in Figure A.1.

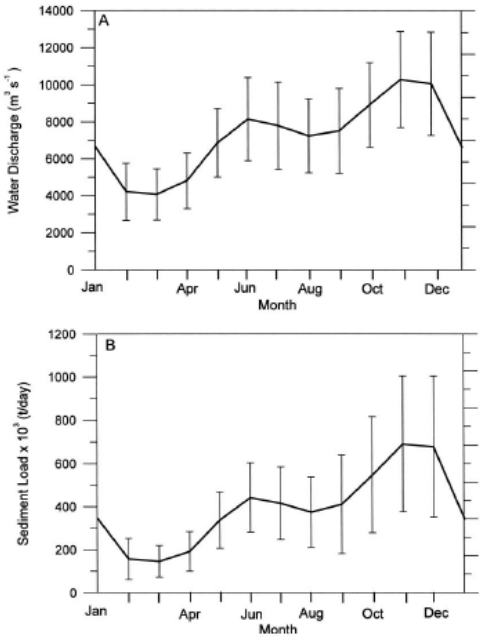

Figure A.1 - Monthly mean and standard deviation of water discharge and sediment load in the Rio Magdalena at Calamar from 1957-1995 (Restrepo and Kjerfve, 2000)

Besides, the seasonal variability the discharge and sediment load in the Rio Magdalena are highly influenced by the El Niño and La Niña which are related to respectively low and high river stages. Peak flows during La Niña exceed 12.000 m^3/s and low discharges of 2000-3000 m^3/s are observed during El Niño (Restrepo and Kjerfve 2000). Also, the sediment load varies interannually with La Niña and El Niño with daily mean sediment loads of 511 t/day and 256 t/day respectively. It appears that the effect of La Niña is larger than the impact of El Niño. Phase analysis between discharge and the Southern Oscillation Index (SOI), a measure of the large-scale fluctuations in air pressure occuring between the western and eastern tropical Pacific during El Niño and La Niña, shows that the discharge is in phase with the SOI anomalies at a period of 3 years (Restrepo and Kjerfve 2000). Meaning that extreme high and low discharges occur approximately every 3 years.

Measured sediment concentrations during high, intermediate and low discharge conditions during 1975-1995 indicate that in the Magdalena River the seasonal relation of sediment concentration and water discharge forms a clockwise loop, or hysteresis, as can be seen from Figure A.2. During rising stages sediment concentrations are higher than during falling water stages with equal discharges.

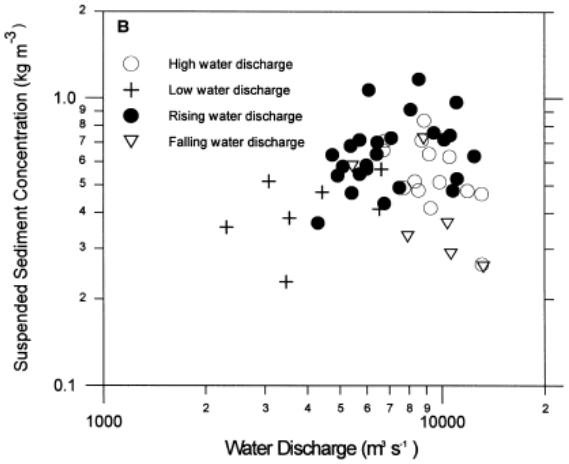

Figure A.2 - Water discharge and suspended sediment concentration based on 55 measurements during 1975-1995 (Restrepo and Kjerfve 2000)

From extensive study of Royal HaskoningDHV it follows that no one-to-one relation between sediment concentration and the discharge-water level distribution can be made at the bifurcation Canal del Dique – Rio Magdalena (Consorcio Dique, 2014). From Figure A.3 it can be seen that the same sediment concentration can occur at different river stages. Furthermore, Figure A.4 shows also that no clear relation between water level difference and sediment concentrations can be made.

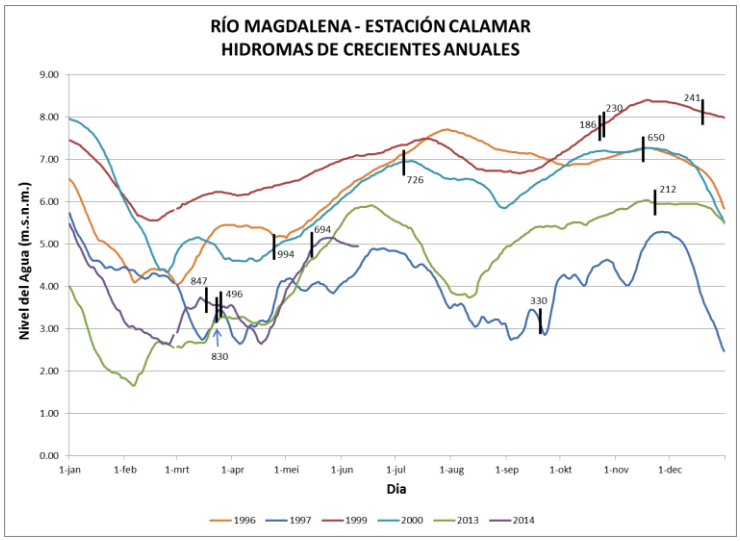

Figure A.3 – Variation in water level and sediment concentration in period 1996 to 2014 (Consorcio Dique, 2014)

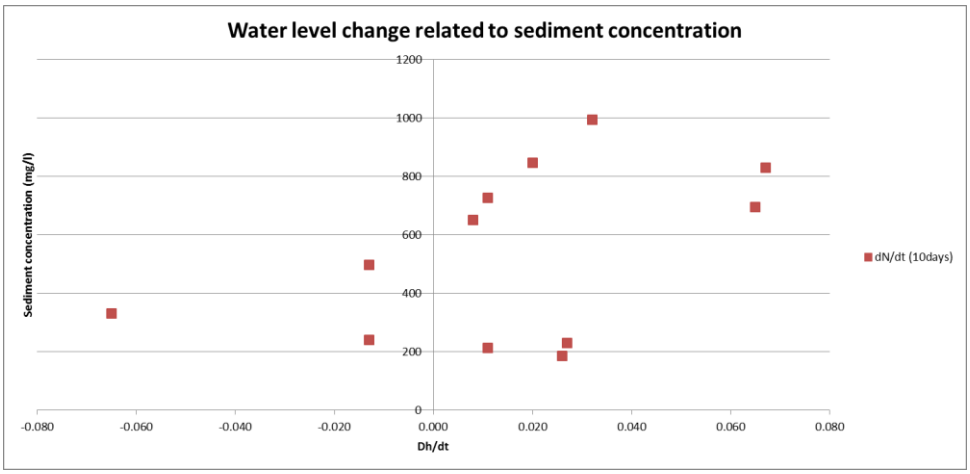

Figure A.4 - Sediment concentration vs water level difference (Consorcio Dique, 2014)

However, several observations are made (Consorcio Dique, 2014):

- "After a long period of high discharge, sediment concentrations seem to drop because of depletion of sediment in the river.
- Relatively low sediment concentrations are observed during decreasing water levels.
- Relatively high sediment concentrations are observed during increasing water levels.
- Also some low concentrations are observed during increasing water levels. It might be that the history of the water levels (time lag after last high water peak) has an impact on the sediment concentrations. This might be also related to the availability of sediment in the catchment area. It might be a threshold for these concentrations (sediment originated from the catchment area)."

Above observations reaffirm a hysteresis effect of suspended sediment concentration and water level variation, as also found from historical measurements (Restrepo and Kjerfve, 2000) mentioned before.

Although it is found that there is no one-to-one relationship between the water level-discharge distribution and sediment concentration, several correlation curves for the discharge and sediment transport are derived for the Rio Magdalena at Calamar and several locations in the Canal del Dique

(Universidad Nacional, 2007). Calibration curves are available for both *total* suspended sediment transport and transport of only fine or coarse grains. An example is given in Figure A.5, which shows the total suspended sediment transport for the Río Magdalena at Calamar.

Sediment transport consists of both suspended and bed load transport. In the Río Magdalena and Canal del Dique, suspended sediment transport is dominant. 90% of the grains consist of fine material (< 63 µm) which is more present in the water column than at the bed. Therefore, more information is available on suspended sediment than bed load transport.

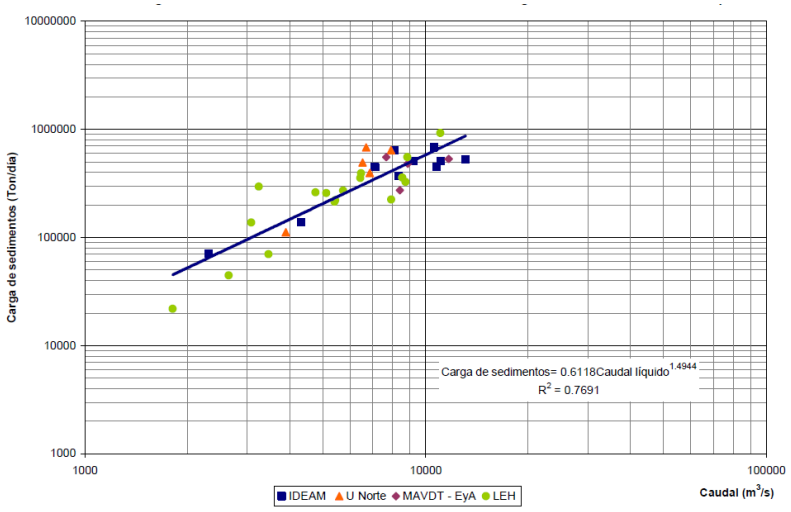

Figure A.5 - Q-Qs correlation curve for total suspended sediment transport in the Río Magdalena at Calamar (Universidad Nacional, 2007)

According to Milliman and Syvitski (1992), basin area and relief are the major controls for sediment concentrations and climate, geology and land-use are second-order influences. Besides, deforestation has led to severe soil erosion. In addition, high concentrations of suspended sediments have resulted from the rapid erosion of the lowlands, partly because of ongoing gold mining in the Cauca river basin which is located in the west of Colombia (Restrepo and Kjerfve, 2000).

A.3.1 Conclusion

Mean annual discharges in the Rio Magdalena at Calamar are approximately 7.200 m^3/s with low discharges around 4.000 m^3/s and high discharges of approximately 10.000 m^3/s. Discharges are varying seasonally with high discharges in November-December and low discharges in February-April. Besides, el Niño and la Niña occur in a 3 year cycle causing respectively extreme low and high discharges. Mean high sediment loads at Calamar are approximately $690x10^3$ t/day in November-December and low values during February-March of $150x10^3$ t/day occur.

A hysteresis correlation between water level variation and sediment concentration can be found for the Río Magdalena. Besides, sediment concentrations are highly influenced by deforestation and gold mining.

A.4 Discharge and sediment rates Canal del Dique

The Canal del Dique has a mean annual water discharge of 299 m^3/s and sediment load of $4.76x10^6$ t/yr. High discharge are around 800 m^3/s and high sediment loads around $600x10^3$ t/month occur

often during November (Restrepo and Kjerfve, 2000). Average sediment concentrations in the Canal del Dique as measured by Consorcio Dique in March 2014 are 930 mg/L in the Rio Magdalena and 947mg/L at the entrance of the canal. Sediment concentrations decrease downstream of the canal. Measured sediment concentrations at Calamar lie around 200-1100mg/L (Consorcio Dique, 2014)

Sediment concentration profiles are almost uniform along the depth in the Canal del Dique which indicates wash load. At Calamar, a more Rouse-profile can be seen (Figure A.6). Figure A.7 shows the particle size distribution as measured by Consorcio Dique in March 2014. This shows that the D50 is between 15-20 µm which is characteristic for wash load.

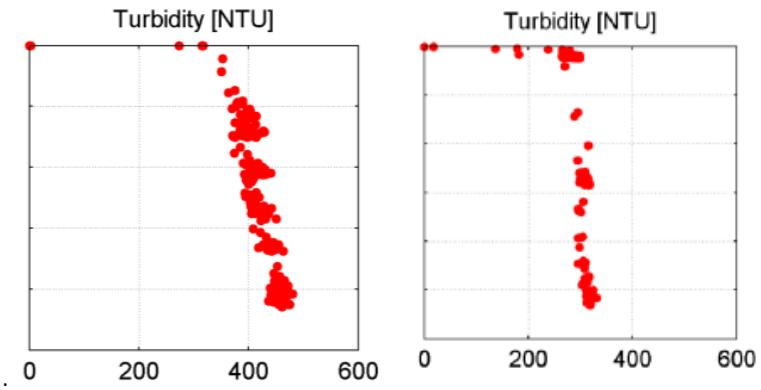

Figure A.6 - Turbidity profile measured with OBS at Calamar in March 2014 (left) and May 2014 (right) (Consorcio Dique, 2014)

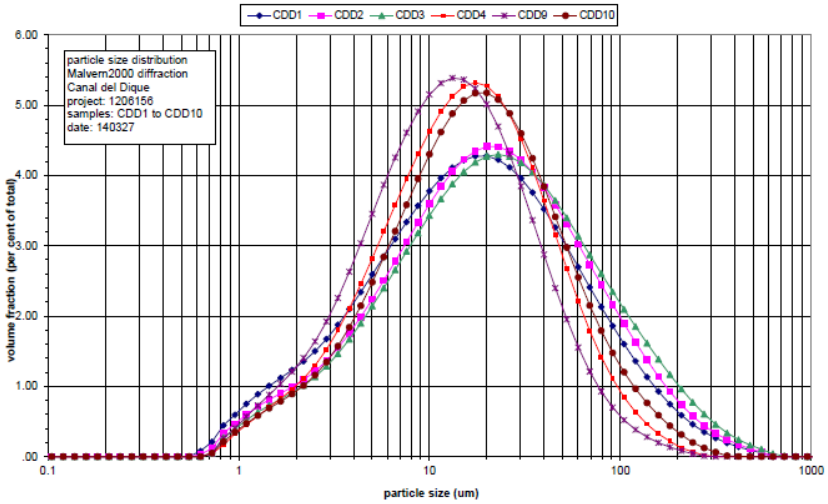

Figure A.7 - Particle size distribution of suspended sediment at different locations in Canal del Dique based on measurements of Consorcio Dique in March 2014 (Consorcio Dique, 2014)

The total annual suspended sediment transport in the Canal del Dique as measured by Universidad Nacional in 2007 is 135 t/yr, from which 34 t/yr is transport of coarse sediments and 101 t/yr is transport of fine sediments (Table A.1).

Table A.2 shows the total annual sediment load including bed load transport. The bed load transport at Calamar is 16 t/yr.

Table A.1 - Annual suspended sediment transport (Universidad Nacional, 2007)

Estación	Q_s Total (millones de Tons/año)	$Q_{sarenas}$ (arenas) (millones de Tons/año)	Q_{sfinos} (arcillas+limos) (millones de Tons/año)	% de arenas
Río Magdalena - Calamar	135	34	101	25%
Incora	8,6	3,2	5,4	37%
Gambote	8,7	2,0	6,7	23%
Santa Helena 1	6,0	1,2	4,8	20%
Caño Correa	0,9	0,1	0,8	15%
Santa Helena 2	4,5	1,0	3,5	23%
Caño Matunilla	1,2	0,4	0,8	36%
Caño Lequerica	0,7	0,1	0,6	16%
Pasacaballos	1,6	0,7	0,9	43%

Table A.2 - Total annual sediment load (including bed load) (Universidad Nacional, 2007)

Estación	Q_{stot} (millones de Tons/año)	Q_b (millones de Tons/año)	Q_{total} (millones de Tons/año)
Río Magdalena - Calamar	135	16	151
Incora	8,6	2,4	11
Gambote	8,7	2,0	6,7
Santa Helena 1	6,0	1,5	7,5
Caño Correa	0,9	0,5	1,4
Santa Helena 2	4,5	0,5	5
Caño Matunilla	1,2	0,5	1,7
Caño Lequerica	0,7	0,4	1,1
Pasacaballos	1,6	0,4	2

Just downstream of Calamar, at a distance of 100 m of the Rio Magdalena and with a depth of 5m, a sediment trap is located where yearly dredging activities take place. Besides, on two other locations in the Canal del Dique yearly dredging activities take place. These amounts of dredged volumes have to be taken into account when measuring the sediment concentrations downstream of the sediment trap. Figure A.8 shows the mean annual dredging volumes in the Canal del Dique as concluded from measurements since 2005 (Consorcio Dique, 2014) The mean annual dredged volume at Calamar is approximately 580.000 m^3. Besides, a correlation curve is derived for the occurring discharge and dredging volumes as shown in Figure A.9. This curve shows that the dredged volume decreases with decreasing discharge.

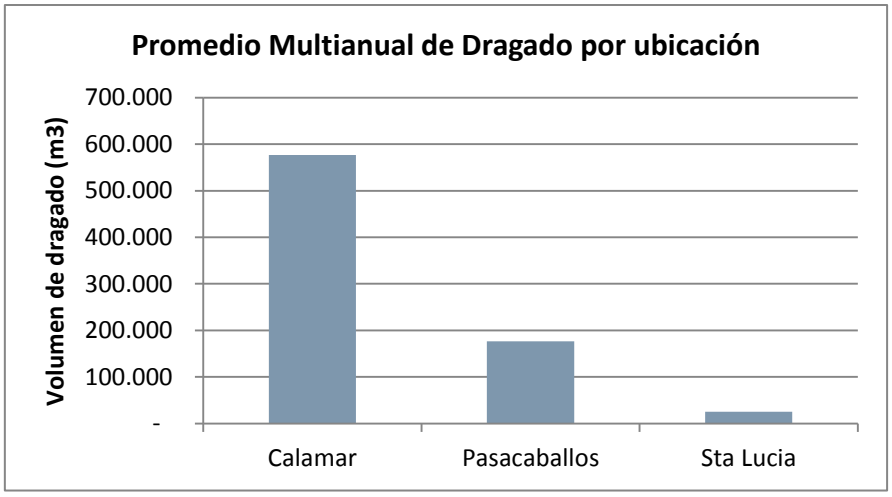

Figure A.8 - Yearly mean dredged volumes in the Canal del Dique (Consorcio Dique 2014)

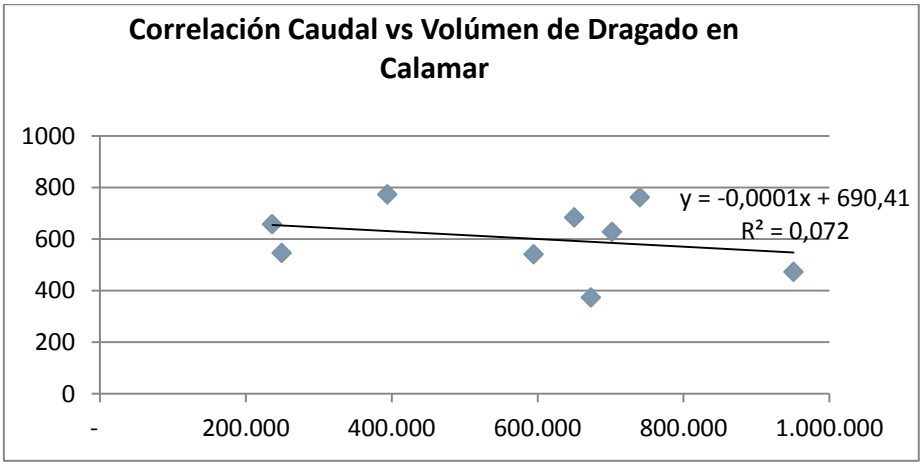

Figure A.9 - Correlation discharge and dredged volumes at Calamar (Consorcio Dique 2014)

From Universidad del Norte (2007) a rating curve is available at Incora, which is located 7 km downstream of Calamar in the Canal del Dique (Figure A.10).

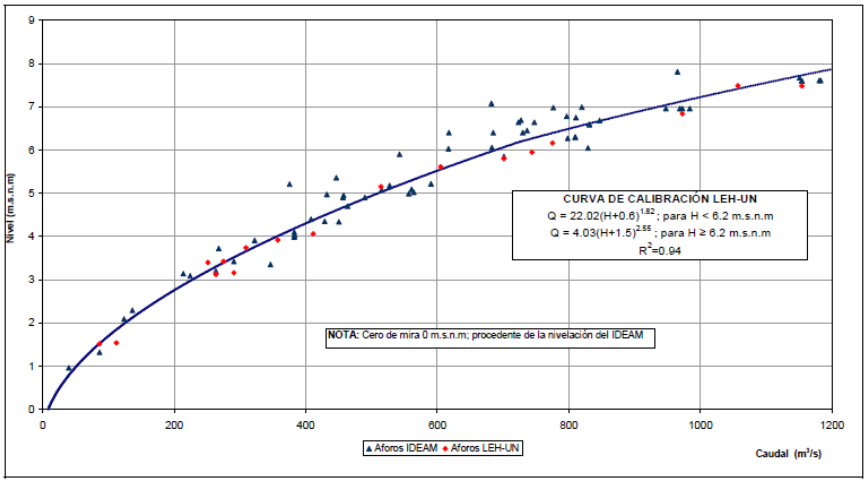

Figure A.10 - Rating curve at Incora, 7km downstream of Calamar in Canal del Dique (Universidad del Norte, 2007)

A.4.1 Conclusion

The Canal del Dique has a mean annual water discharge of 299 m^3/s, high discharges of around 800 m^3/s occur. The mean annual sediment load is around $4.76x10^6$ t/yr and high sediment loads around $600x10^3$ t/month which occur mostly during September. The mean sediment concentrations at Calamar are 930 mg/L and vary between 200-1100 mg/L during the year. Sediment concentrations have a Rouse-profile over depth and in the Canal del Dique a uniform profile can be distinguished indicating wash load. This is also confirmed by the measured mean grain size of 15-20 µm. Besides, a sediment trap is located just downstream of Calamar where a mean annual volume of 580.000 m^3 of sediment is dredged.

A.5 Discharge and water levels at Calamar

Consorcio Dique proposed a new rating curve for the Rio Magdalena at Calamar based on measurements from 'Instituto de Hidrología, Metereología y Estudios Ambientales' (IDEAM) throughout the years and other historical data. This new rating curve allows for extreme discharges as were measured in November- December 2010, see Figure A.11. From this curve, discharges corresponding to the occurring water level can be derived without the need to actually measure the discharge. Figure A.11 shows that the measurements of 2014 are in the 10% highest line. It has to be investigated if this is accidentally or can be explained by changed in morphology at the bifurcation.

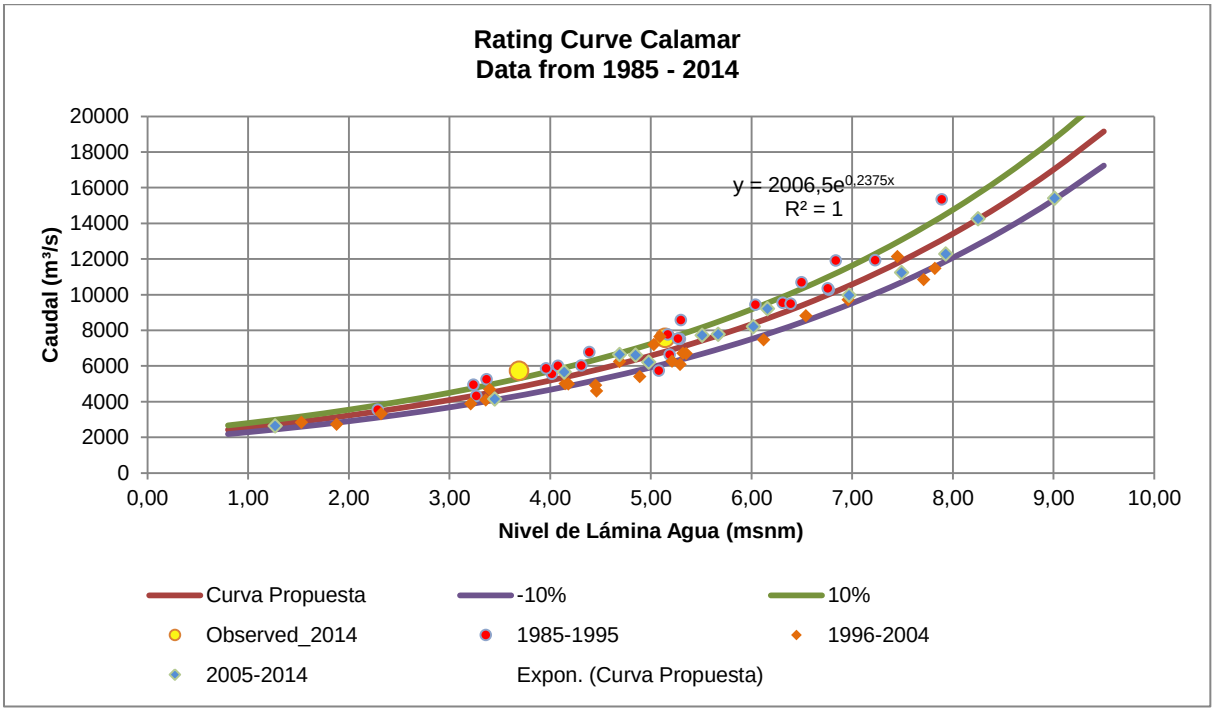

Figure A.11 – New rating curve Rio Magdalena at Calamar derived for higher discharges based on several measurements of IDEAM and Universidad del Norte (Consorcio Dique, 2014)

Several sources have measured discharges and (suspended) sediment transport rates along the fluvial islands in the Río Magdalena at Calamar. Figure A.12 shows for example the measurement locations of discharges by Cormagdalena and Universidad del Norte in the period from 2009-2013. Two islands can be seen which are located just upstream of the offtake from the Río Magdalena into the Canal del Dique. The upstream island is named 'Isla Becerra' and the downstream island 'Isla la Loca'. Table A.3

shows all the available historical measurements from the period of 1997-2015 along the islands and at the entrance of the Canal del Dique.

It can be seen that the discharge distribution along Isla Becerra from 1997-2011 was favourable along the right side with a percentage relative to the upstream discharge of approximately 65/30% (right/left side). From 2012-2015 the distribution is more equal (52/48%), where it is sometimes slight favourable along the right side and sometimes along the left side. The discharge distribution along Isla la Loca is much more favourable along the left side with a distribution of approximately 15/85% along the right and left side. Where a trend can be seen of more favourable left branches of Isla la Loca, but also along Isla Becerra (Figure A.13 and A.14)

It is investigated if the discharge distribution varies with the value of the upstream discharge as shown in Figure A.15 and Figure A.16) Although it can be seen that with higher upstream discharge the discharge distribution is often more favourable along the left side, also variations of this trend are seen. Therefore, no definite conclusion can be made on this.

More likely is that the morphological changes of the islands and bathymetrical changes of the branches along the islands influence the discharge distribution, which will be investigated in the next section.

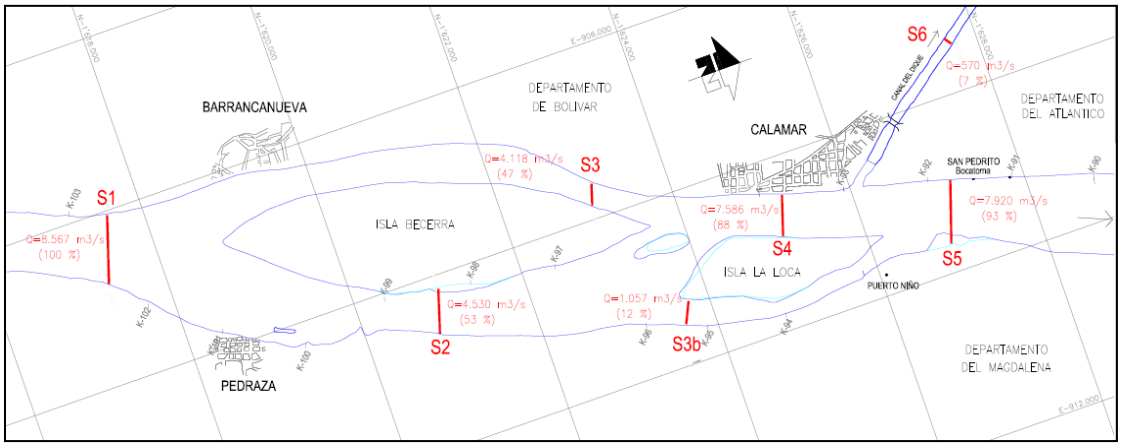

Figure A. 12 – Measurement locations at bifurcation Rió Magdalena and Canal del Dique (Cormagdalena and Universidad del Norte, 2013)

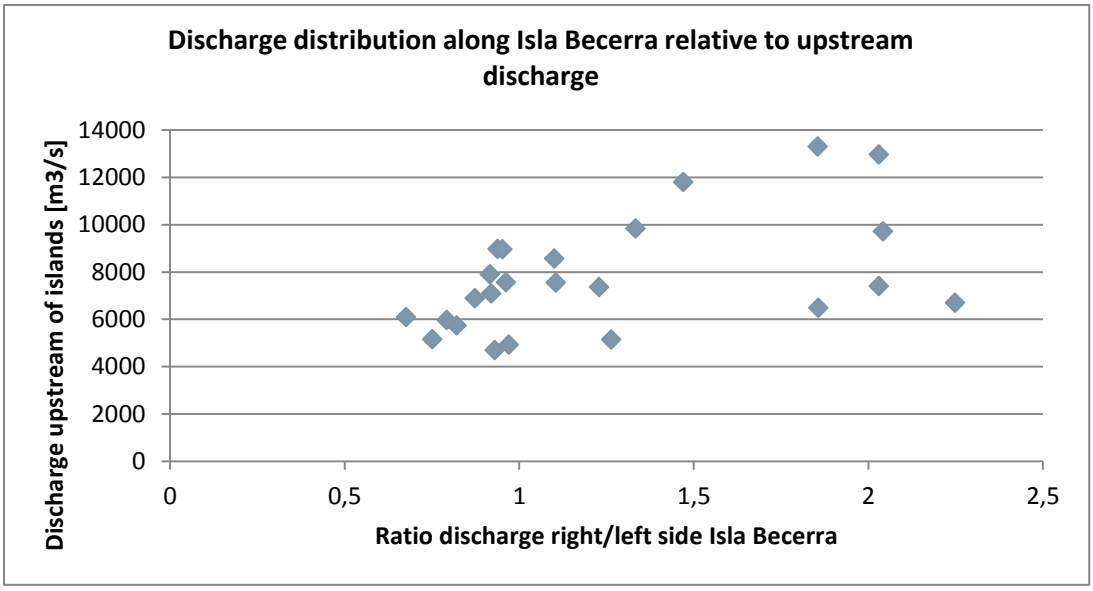

Figure A. 13 – Discharge distribution along Isla Becerra relative to upstream discharge based on historical measurements

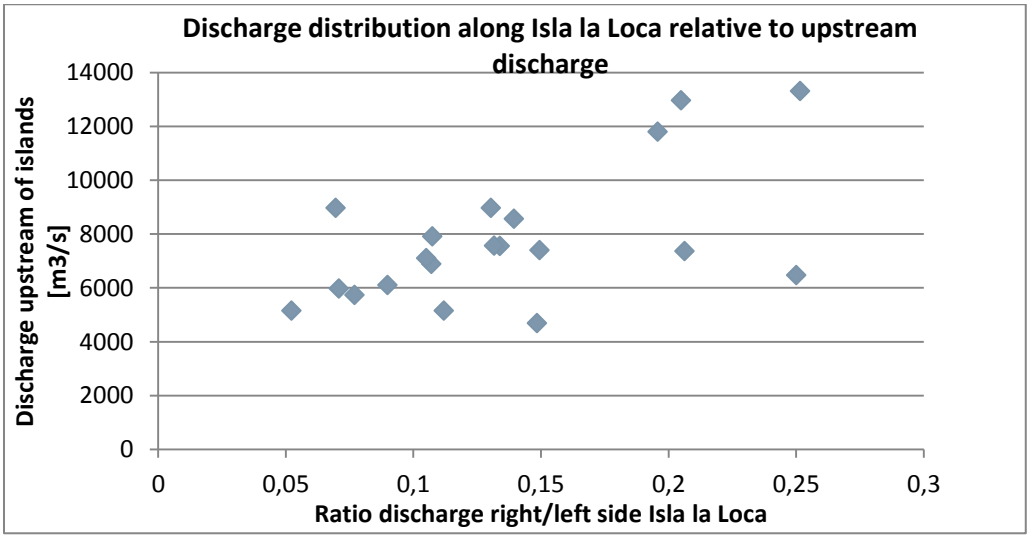

Figure A. 14 - Discharge distribution along Isla la Loca relative to upstream discharge based on historical measurements

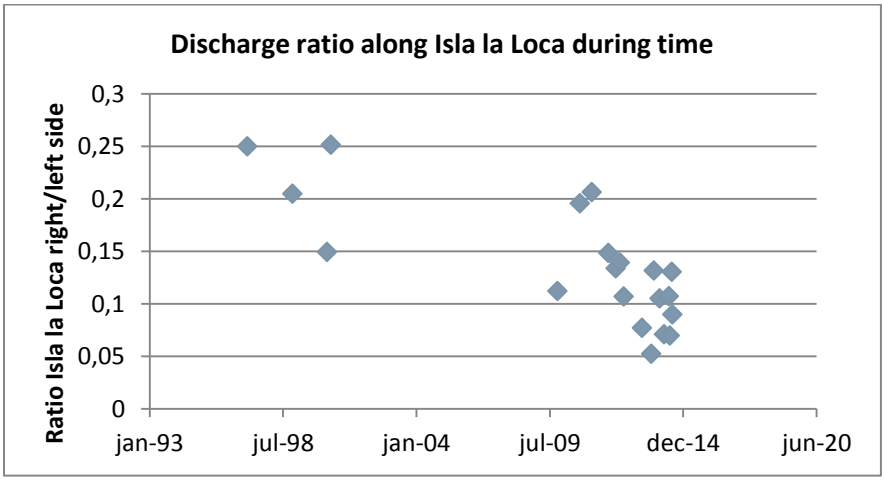

Figure A. 15 – Evolution discharge distribution Isla la Loca over time

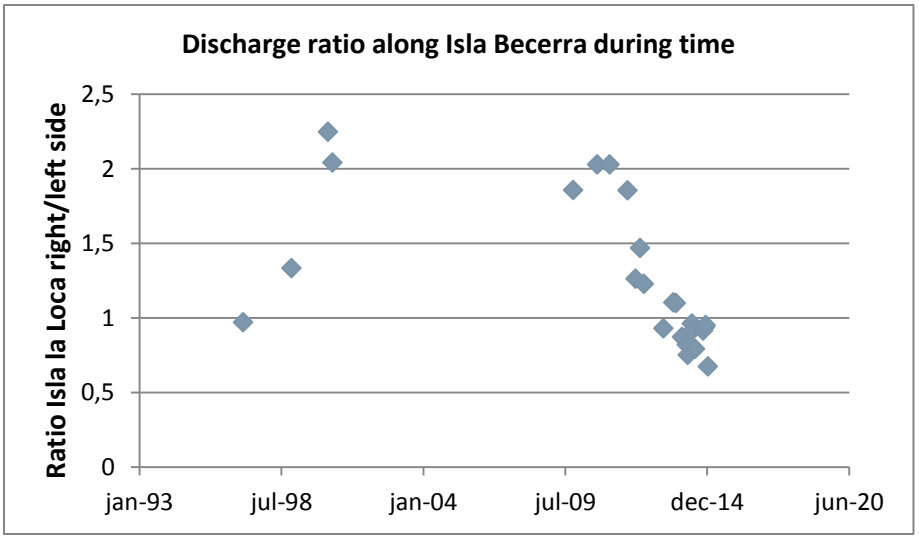

Figure A. 16 - Evolution discharge distribution Isla Becerra over time

It is found that the discharge entering the Canal del Dique at Calamar does increases with increasing discharge upstream of the islands at the Río Magdalena.

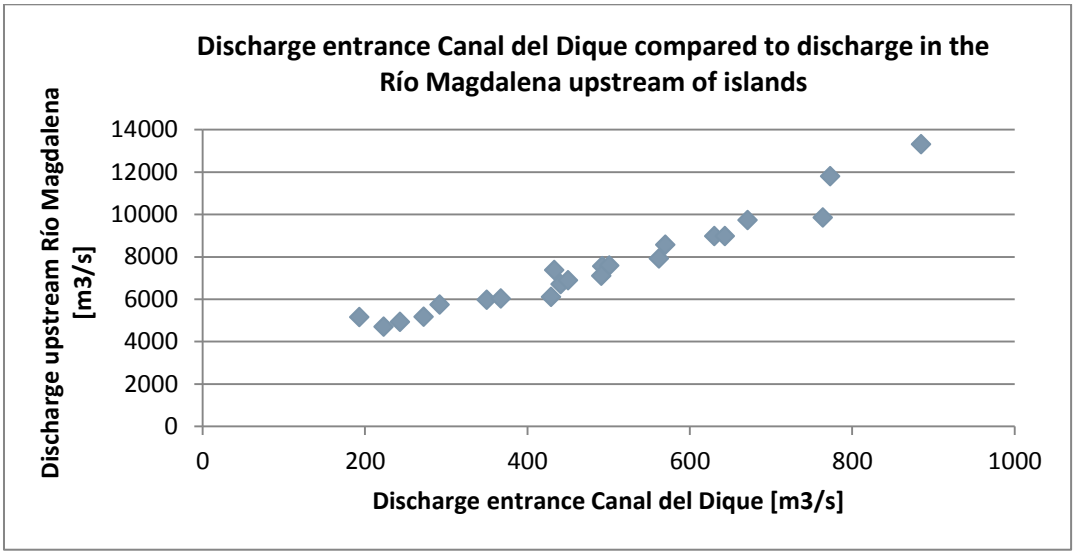

Figure A. 17 - Discharge entrance of the Canal del Dique for different upstream boundaries based on historical measurements

Table A. 3 - Historical discharge measurements along the fluvial islands and at the entrance of the Canal del Dique based on several sources

		Isla Becerra					Isla la Loca				Entrance Canal del Dique	
Date	Source	Discharge upstream islands [m^3/s]	Discharge left side [m^3/s]	Discharge left side [% from upstream discharge]	Discharge right side [m^3/s]	Discharge right side [% from upstream discharge]	Discharge left side [m^3/s]	Discharge left side [% from upstream discharge]	Discharge right side [m^3/s]	Discharge right side [% from upstream discharge]	Discharge [m^3/s]	Discharge [% from upstream discharge]
1-2-1997	IDEAM	4926	2516	51%	2441	50%					243	4,9%
13-12-1998	IDEAM	9843	4219	43%	5624	57%					764	7,8%
12-5-2000	IDEAM	6700	2063	31%	4639	69%					441	6,6%
10-7-2000	UniNorte	9723	3043	31%	6214	64%					671	6,9%
26-10-2009	Cormagdalena/UniNorte	6480		35%		65%		80%		20%		
27-09-2010	Cormagdalena/UniNorte	12970		33%		67%		83%		17%		
24-03-2011	Cormagdalena/UniNorte	7401		33%		67%		87%		13%		
1-12-2011	Cormagdalena/UniNorte	13308	4571	34%	8480	64%	10580	80%		20%	885	6,7%
21-03-2012	Cormagdalena/UniNorte	5150	2256	44%	2850	55%	4599	89%		10%	193	3,7%
23-05-2012	Cormagdalena/UniNorte	11799	4673	40%	6869	58%	9645	82%		16%	773	6,6%
18-07-2012	Cormagdalena/UniNorte	7367	3143	43%	3861	52%	6430	87%		18%	433	5,9%
19-04-2013	Cormagdalena/UniNorte	4696	2400	51%	2231	48%	4429	94%		14%	223	4,7%
4-09-2013	Cormagdalena/UniNorte	7552	3593	48%	3970	53%	6545	87%	876	12%	492	6,5%
13-10-2013	Cormagdalena/UniNorte	8567	4118	48%	4530	53%	7586	89%	1057	12%	570	6,7%
6-01-2014	Cormagdalena/UniNorte	6886	3685	54%	3216	47%	6440	94%	689	10%	450	6,5%
13-03-2014	Consorcio Dique	5737	3045	53%	2498	44%	5086	89%	391	7%	292	5,1%
26-03-2014	Cormagdalena/UniNorte	5156	2916	57%	2190	42%	4733	92%	247	3%	272	5,3%
23-05-2014	Consorcio Dique	7572	3837	51%	3692	49%	6590	87%	867	12%	501	6,6%
9-06-2014	Cormagdalena/ UniNorte	7100	3884	55%	3572	50%	6515	92%	684	10%	491	6,9%
8-07-2014	Cormagdalena/UniNorte	5970	3276	55%	2594	43%	5326	89%	377	9%	350	5,9%
15-07-2014	Consorcio Dique	6028								6%	367	6,1%
29-10-2014	Cormagdalena/UniNorte	7914	4177	53%	3827	48%	7229	91%	776	9%	562	7,1%
27-11-2014	Consorcio Dique	8973	4593	51%	4308	48%	5462	61%	380	12%	630	7,0%
4-12-2014	Cormagdalena/UniNorte	8967	4690	52%	4465	50%	7937	89%	1035	11%	643	7,2%
6-01-2015	Cormagdalena/UniNorte	6100	3695	61%	2496	41%	5755	94%	517	6%	429	7,0%

A.6 Flow velocity at Calamar

Measurements of flow velocity at the bifurcation have been carried out with the use of ADCP's in March 2014 by Consorcio Dique. The flow velocity at the entrance of the Canal del Dique is shown in Figure A. 18. Flow velocities at the entrance are around 1 m/s. Also 3-dimensional flow data around the bifurcation and islands are available.

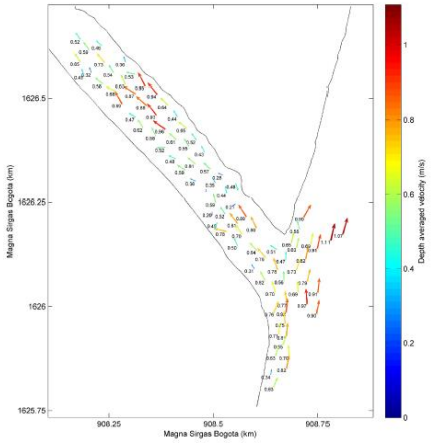

Figure A. 18 - Flow velocity measurement campaign Consorcio Dique, March 2014 (Consorcio Dique, 2014)

A.7 Sediment distribution at Calamar

Measurements of sediment fluxes at the bifurcation and around the islands have been carried out by Consorcio Dique in March, May and November 2014. The sediment distribution around Isla Becerra in 2014 was approximately 50/50 and the sediment distribution along Isla la Loca was around 90/10 (left side/right side) Table A.4 shows a comparison of the sediment and discharge distribution around the islands as measured in March, May and November 2014. From this table, it can be seen that the sediment distribution is almost equal to the discharge distribution. This confirms the presence of fine sediment, which follows the distribution of discharge. However, the amount of sediment at the entrance of the Canal del Dique is slightly lower than the amount of water entering the Canal. However, as this is based on only three measurements no hard conclusions should be made from this analysis.

Table A. 4 - – Discharge and sediment distribution around the islands at the bifurcation Canal del Dique – Rio Magdalena as function of total upstream discharge as measured in March, May and November 2014 (Consorcio Dique, 2014)

Date	Total discharge [m^3/s]	Isla Becerra		Isla la Loca		Canal del Dique	Total sediment flux [kg/s]	Isla Becerra		Isla la Loca		Canal del Dique
		Left	Right	Left	Right			Left	Right	Left	Right	
March 2014	5.737	53%	44%	89%	7%	5%	5560	53%	47%	93%	7%	4.5%
May 2014	7.572	53%	49%	87%	12%	7%	6382	50%	50%	88%	12%	5%
November 2014	8.973	51%	48%	84%	12%	7%	3219	54%	57%	94%	14%	5%

A.8 Morphology at Calamar

Several data is available on the morphology of the bifurcation Rio Magdalena – Canal del Dique. From a selection of data from 1973-2014, contours of the islands are shown in Figure A.19. This figure shows the formation of islands and their disappearance. The shape of Isla Becerra remains almost equal since 1996, with a slight accretion on the downstream part of the island. Isla la Loca is more dynamic and migrates downstream and to the right river bank.

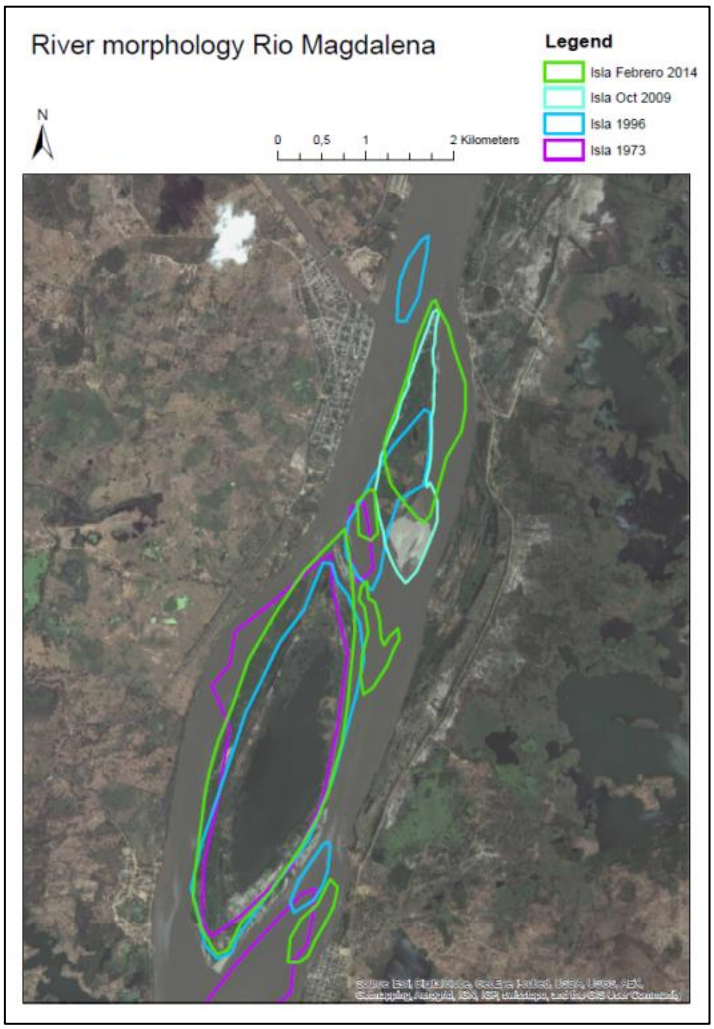

Figure A.19 - Morphologic activity islands (Consorcio Dique, 2014)

Besides the island morphology, also the bathymetry changes during time are known, as shown in Figure A.20 and Figure A.21. These figures show the deepening of the Rio Magdalena at the entrance of the Canal del Dique. Also, a small decrease in depth of the right channel next to Isla Becerra is shown. These changes in morphology (width and depth) can explain the increase in discharge in the left channel of Isla Becerra and the left channel of Isla la Loca as observed in the previous sections.

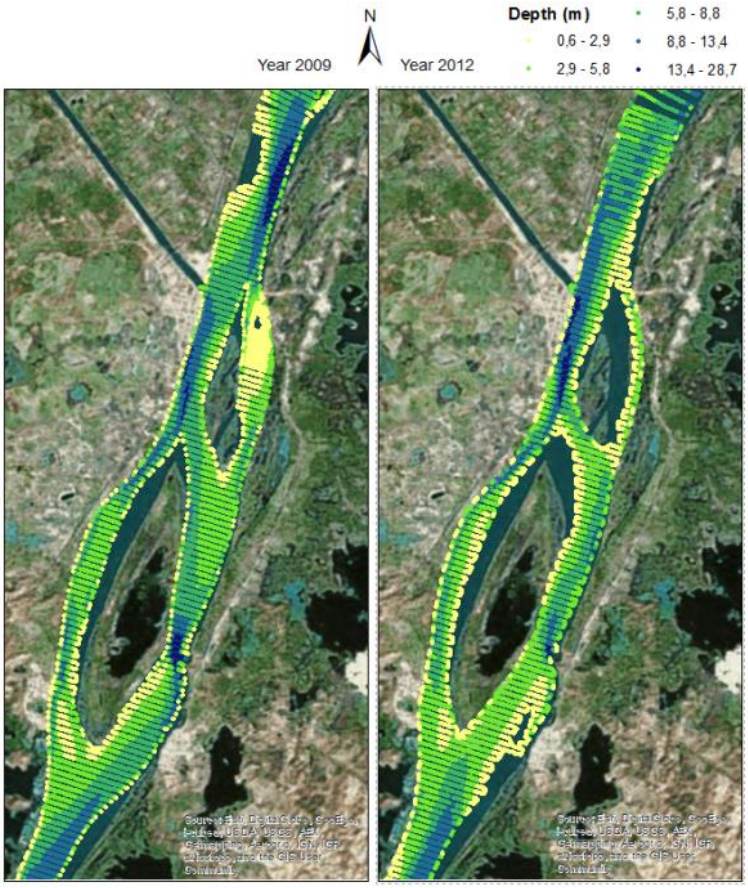

Figure A.20 - Comparison bathymetry 2009 and 2012 (Consorcio Dique, 2014)

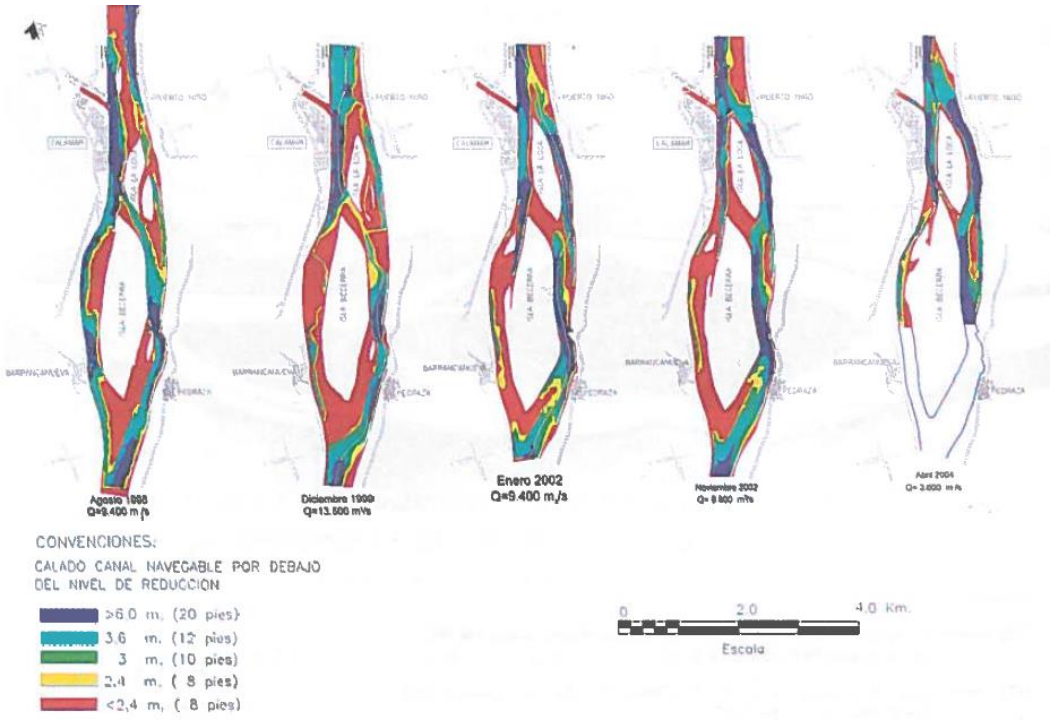

Figure A.21 - Bathymetry from 1998-2004 (Ortega et al., 2008)

A.9 Navigation in Canal del Dique and Rio Magdalena

The average draught of the ships sailing on the Canal del Dique and the Rio Magdalena at Calamar is 8 feet (approximately 2,44 m) (Ortega et al., 2008). The average yearly ship load on the Rio Magdalena is 2.5 million ton/year. The total amount of ships as measured from 1999-2002 (Ortega et al., 2008) is 3371 ships. Currently, the design ship of the Canal del Dique is a tugboat with a maximum length of 223 meter and width of 32 meter as shown in Figure A.22.

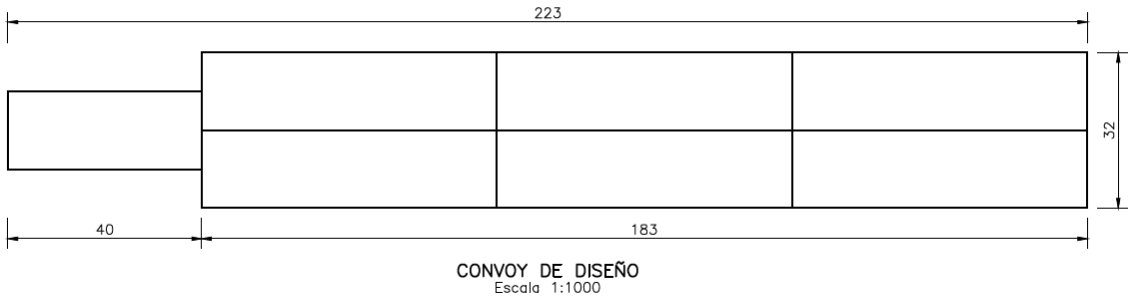

Figure A.22 - Design ship Canal del Dique (Consorcio Dique, 2015)

A.10 Alternatives previous studies

During the past 10 years several studies have been carried out to find alternatives in the Canal del Dique against the sedimentation in the bay of Cartagena. Although there have been several studies to find alternatives in the bay of Cartagena, none of them take into account all the aspects of sedimentation in the bay, navigation and environmental and social aspects. Besides, no study seems to have feasible and effective measures against sedimentation in the bay. Therefore, a new study has to be carried out taking into account all the import aspects and providing new validated model studies for the Canal del Dique, the bifurcation at Rio Magdalena and the bay of Cartagena.

Appendix B – Manual calculations

B.1 Theory

At a bifurcation the discharge distribution is such that the water levels match at the bifurcation. This holds for one-dimensional calculations. The discharges and water levels can be calculated from the continuity and momentum equation.

The continuity equation and momentum equation in one-dimensional horizontal direction are:

Continuity: $$\frac{\delta h}{\delta t} + h\frac{\delta u}{\delta x} + u\frac{\delta h}{\delta x} = 0 \qquad \text{(B.1)}$$

Momentum: $$\frac{\delta u}{\delta t} + u\frac{\delta u}{\delta x} - gi_b + g\frac{\delta h}{\delta x} + \frac{gu^2}{C^2 h} = 0 \qquad \text{(B.2)}$$

Where:

h= depth
u= velocity in horizontal direction
x= longitudinal co-ordinate
t= time
i_b= slope of the river bed
g= gravitational acceleration
C= Chézy-coefficient

For a steady water flow the first terms in the momentum and continuity equation can be neglected. For a straight canal with a shallow, rectangular cross-section the canal can be described per unit width, as if the canal has an infinite width. The mean flow over the depth of the canal can now be described by:

Continuity: $$\frac{d(uh)}{dx} = 0 \qquad \text{(B.3)}$$

Momentum: $$u\frac{\delta u}{\delta x} - gi_b + g\frac{\delta h}{\delta x} + \frac{gu^2}{C^2 h} = 0 \qquad \text{(B.4)}$$

When the discharge is given per unit width the continuity equation can be written as: $u = \frac{q}{h}$

Substituting this in the momentum equation gives:

$$\left[g - \frac{q^2}{h^3}\right]\frac{dh}{dx} = gi_b - \frac{g}{C^2}\frac{q^2}{h^3} \qquad \text{(B.5)}$$

The critical depth (when Fr=1) is: $h_c = \frac{u^2}{g} = \left(\frac{q^2}{g}\right)^{\frac{1}{3}}$

The equilibrium or normal depth is: $h_e = \frac{u^2}{C^2 i_b} = \left(\frac{q^2}{C^2 i_b}\right)^{\frac{1}{3}}$

Substituting the critical depth and the equilibrium depth in the momentum equation gives:

$$\frac{dh}{dx} = i_b \frac{h^3 - h_e^3}{h^3 - h_c^3} \qquad \text{(B.6)}$$

This is equation of Bélanger, which provides the basis for calculations of the surface profiles (backwater curves) in case of a steady and straight-lined flow.

Using the approximation of Bresse, the water depth along the canal can be determined:

$$h = h_e + (h_0 - h_e)\left(\frac{1}{2}\right)^{\frac{(x-x_0)}{L_{1/2}}} \qquad \text{(B.7)}$$

where,

$L_{1/2} = \frac{0.24 h_e}{i_b}\left(\frac{h_0}{h_e}\right)^{\frac{4}{3}}$: the length over which half of the water level is reached from the downstream water level to the equilibrium depth.

To find the discharge distribution at a bifurcation the above equations have to be iterated such that the water levels at the bifurcation match.

Besides, to avoid backwater effects in the area of interest, meaning the area where the relation between discharge and water level is not uniquely defined, the downstream boundary should be located outside the backwater adaptation length. This is the length over which the effect of backwater is damped with 63%.

The backwater adaptation length can be calculated with:

$$\lambda_{bw} = \frac{1}{3}\frac{h_e}{ib}$$

Manual calculations become complex, as there are several confluences and bifurcations. Therefore, the use of one-dimensional models is recommended. In order to have an idea of the order of discharge distribution, the bifurcation is simplified as shown in Figure B.1. When using this simple case with one bifurcation, the discharge distribution becomes 4346 m^3/s for branch 12 and 654 m^3/s for branch 13 with an upstream discharge of 5000 m^3/s in branch 1 using the equations as given in section B.1. So, the discharge in the offtake (branch 13) is 13% of the upstream discharge in this case. The half lengths of branch 12 and 13 in this case are respectively 6422 m and 6417.5 m which means that the equilibrium depth is reached at approximately 15km upstream of the downstream boundaries. The length of the downstream branches (branch 12 and 13) are 20 km, so the equilibrium depth is reached in these branches. The equilibrium depths in the branches are respectively 4.2275 m and 4.2365m. The water level at the bifurcation is 4.09 m.

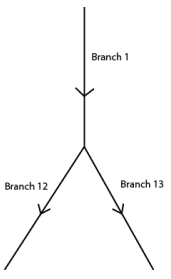

Figure B.1 – Schematisation bifurcation

Appendix C – Sobek model description and results

C.1 Model description

SOBEK-RE is not the most recent version of the software package. However, at the start of this research the possibility wanted to be maintained to make morphodynamic calculations which do not seem to be predicted accurately with more up-to-date version. However, due to the limited time of the research morphodynamic calculations were not carried out. Besides, the distribution of sediment at a bifurcation on a one-dimensional scale is calculated with a nodal point relation (described in 2.3.2). As these functions are poorly known and unique for every bifurcation, the choice is made to only make hydrodynamic simulations with the one-dimensional model.

C.1.1 Theory

The one-dimensional flow is described by two equations: the momentum- and continuity equation. The used formulas in SOBEK-RE are described in the following (Deltares, 2012).

The continuity equation reads:

$$\frac{\delta A_t}{\delta t} + \frac{\delta Q}{\delta x} = q_{lat} \qquad \text{(C.1)}$$

in which
A_t= total cross-sectional area [m^2]
q_{lat}= lateral discharge per unit length [m^2/s]
Q= discharge [m^3/s]
t= time [s]
x= distance in flow direction [m]

The momentum equation reads:

$$\frac{\delta Q}{\delta t} + \frac{\delta}{\delta x}\left(\alpha_B \frac{Q^2}{A_f}\right) + gA_f \frac{\delta h}{\delta x} + \frac{gQ|Q|}{C^2 R A_f} - W_f \frac{\tau_{wi}}{\rho_w} + gA_f(\eta + \xi Q|Q|) + \frac{g}{\rho_w}\frac{\delta \rho}{\delta x} A_{lm} = 0 \qquad \text{(C.2)}$$

1 2 3 4 5 6 7

in which
1= the acceleration term
2= the convection term
3= the water level gradient
4= the bottom friction term
5= the wind friction term
6= the extra head loss term
7= the density term
and
Q= discharge [m^3/s]
t= time [s]
x= distance [m]
α_B= Boussinesq constant [-]
A_f= cross-section flow area [m^2]
g= gravity acceleration [m/s^2]
h= water level (with respect to the reference level) [m]

C= Chézy coefficient [$m^{1/2}/s$]
R= hydraulic radius [m]
W_f= flow width [m]
τ_{wi}= wind shear stress [N/m^2]
ρ_w= water density [kg/m^3]
η= first additional resistance coefficient [-]
ξ= second additional resistance coefficient [-]
A_{lm}= first order moment cross-section [N/m^2]

In the water level gradient the slope of the river bed is neglected. For this reason this approximation is not suited for steep bottom gradients. (Deltares, 2012).

C.2 Schematisation

The Canal del Dique case is schematised one-dimensionally as shown in Figure C.1. It can be seen that the system is complex with several confluences and bifurcations. Node 2, 5 and 8 represent bifurcations. Node 10 and 6 are confluences. At the confluences the discharges are easily determined by adding the upstream discharges (e.g. $Q_{branch10}+Q_{branch11}=Q_{branch12}$). At the bifurcations the same water balance applies, however the distribution of discharges is unknown now (e.g. $Q_{branch1}=Q_{branch2}+Q_{branch3}$ = ??). The discharge distribution can be determined such that the water levels match at the bifurcation.

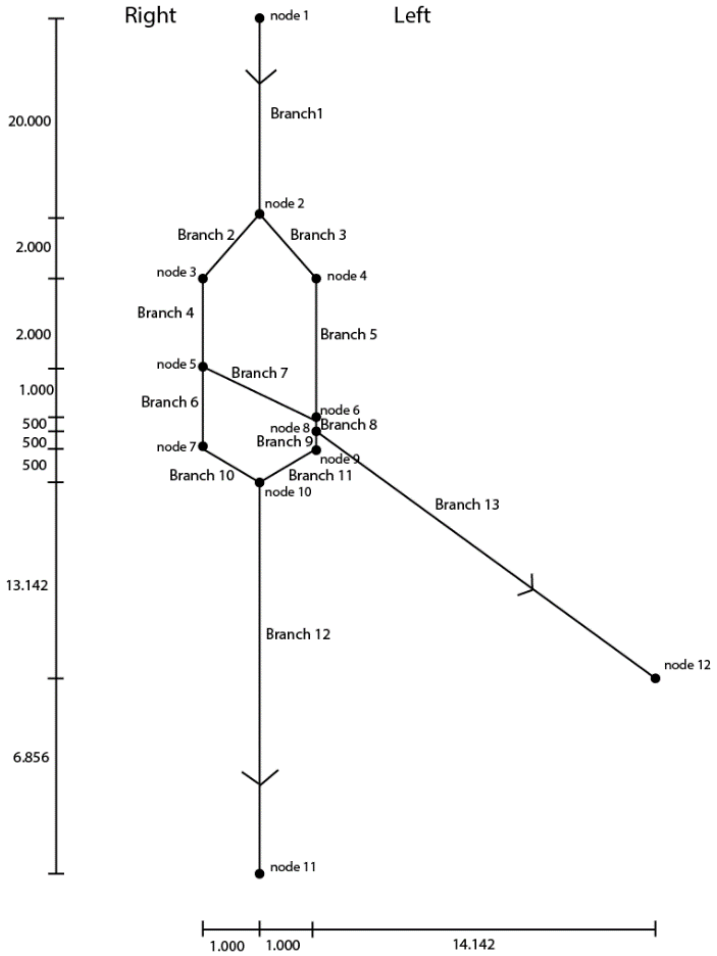

Figure C 1– Schematisation Sobek (length in meters)

The following parameters are used in the reference case:

Parameter	Value	Unit
Width offtake (Branch 13)	150	m
Depth offtake (Branch 13)	3	m
Width main channel (Branch 1 and Branch 12)	2000	m
Depth in all the branches	3	m
Width mid channel (Branch 7)	1000	m
Depth midchannel (Branch 7)	10	m
Width right channels (Branch 2, 4, 6, 10)	500	m
Width left channels (Branch 3, 5, 8, 9, 11)	500	m
Bed friction (Chézy)	50	$m^{1/2}/s$
Bed slope in the branches	0.0001	-
Discharge boundary x=0	5000	m^3/s
Waterlevel boundary offtake	3	m
Waterlevel boundary mainchannel	3	m

When the calculation is made for the more complex system as shown in Figure C. the calculation is made with the use of the one-dimensional hydrodynamic model Sobek. From this calculation it follows that the discharge in the offtake (branch 13) is 653.4 m^3/s and the discharge in the downstream main channel (branch 12) is 4346.6 m^3/s. So, again 13% of the upstream discharge is entering branch 13. These values correspond to the values with one bifurcation. The water depth at the beginning of branch 12 is 4.06 meter and the water depth at the beginning of branch 13 is 4.1062 meter. With the discharge and water levels following from Sobek, the equilibrium depth and half lengths of the branches can be calculated manually as shown in Table.1. Branches that are connected to each other and do not have offtakes are taken together (e.g. branch 2+4, branch 3+5, branch 6+10, branch 9+11).

Table C. 1 - Length, discharge, water levels and equilibrium depths of branches for the reference case

Branch	Length [m]	Discharge in branch [m^3/s]	Water level at downstream point branch [m]	Bed level	Water depth [m]	Equilibrium depth branch [m]	Half-length branch [m]
1	10000	5000	7.0228	2.7354098	4.2874	4.6416	1002.1
2+4	4236.07	2603.9	6.3757	2.311803	4.0639	4.7693	9246.6
3+5	5236.07	2369.1	6.3716	2.211803	4.1598	4.4781	9741.1
7	2236.07	564	6.3716	2.211803	4.1598	1.0836	1563.2
8	500	2960	6.2679	2.1618	4.1061	5.1948	9111.6
6+10	3118.03	2039.8	6.0610	2	4.0610	4.0529	9752.9
9+11	1618.03	2306.8	6.0610	2	4.0610	4.3993	9489.9
12	20000	4346.6	3	0	3	4.2279	6421.9
13	20000	653.4	3	0	3	4.2339	6418.9

From Table C.1 it can be seen that the equilibrium depth is reached in branch 12, 13 and 1 as twice the half-length is smaller than the length of the branch. In the branches around the islands, the equilibrium depth is not reached by far, so it has to be bared in mind that backwater-effects might occur here.

It is tested if the distribution of the discharges relative to the upstream discharge varies with different values of the upstream discharge boundary. Figure C. 1 shows that this is not the case. It is also tested if the relative discharge varies with different water level boundaries. Figure C. 2shows that there is no or no large variation in relative discharge. As we are interested in the discharge *distributions* it does not matter which upstream discharge and downstream water level is used. In this case an upstream boundary of 5000 m^3/s is chosen and downstream water level boundary of 3 meter. Nevertheless, it has to be bared in mind that changing the upstream discharge and downstream water level will change the equilibrium water level thus the water level and absolute discharges in the branches. However, in order to decrease the amount of simulations, the same boundary conditions are used in all the simulations. Besides, prismatic cross-sections are used to start with simplified cross-sections.

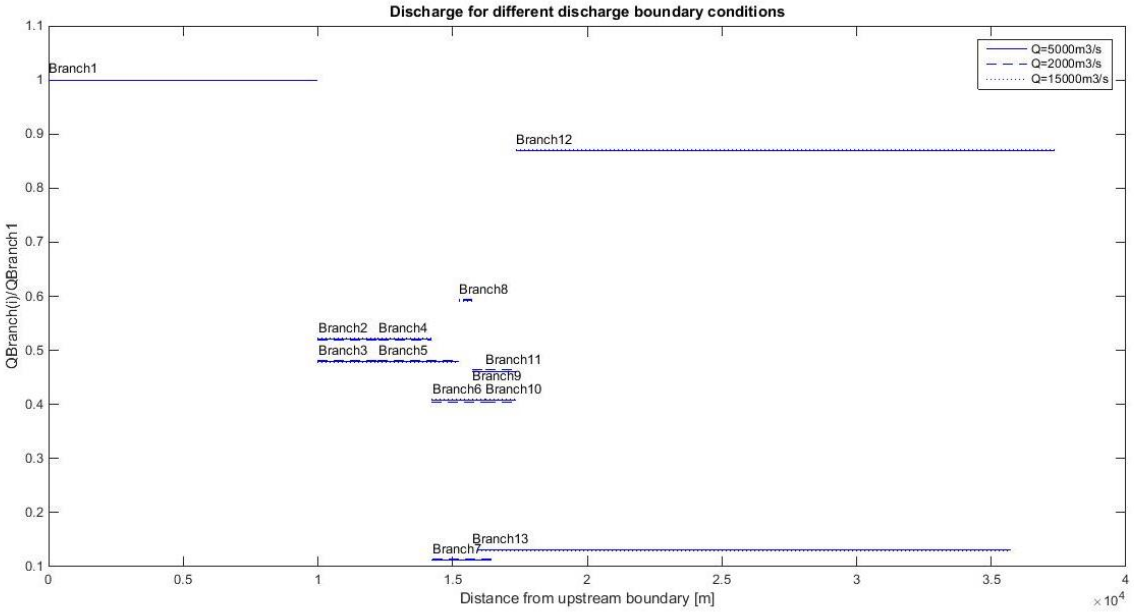

Figure C. 1 - Relative discharge along branches for different upstream discharge boundaries

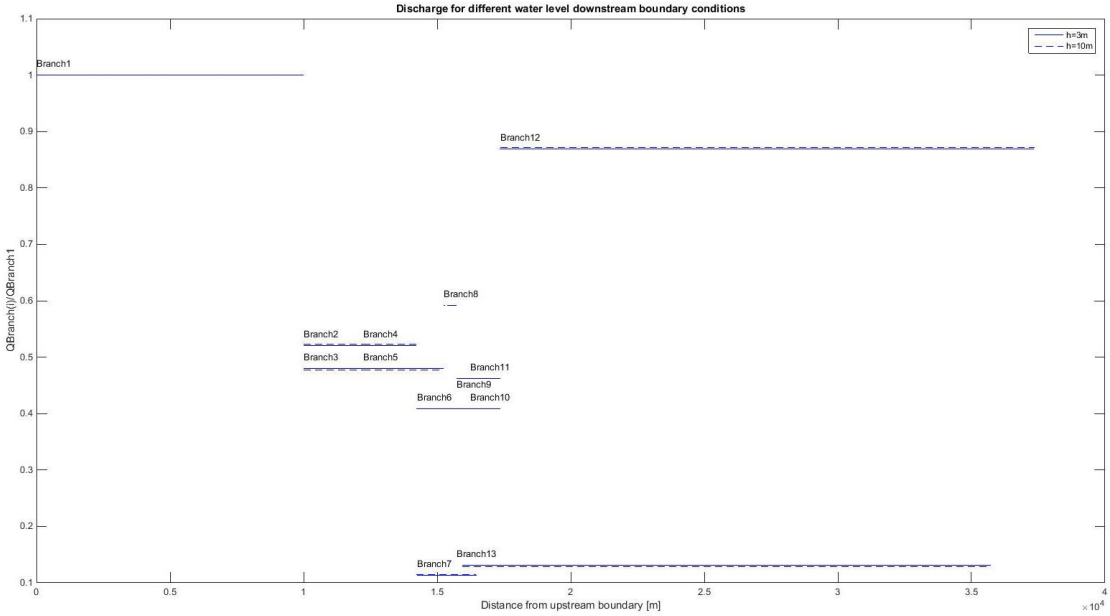

Figure C. 2- Relative discharge along branches as function of different downstream water level boundaries

C.1 Results

C.1.1 Sensitivity of the length of the mid channel (branch 7)

The sensitivity of the length of the mid channel between the two fluvial islands (branch 7) to the discharges and water levels is tested, as schematised in Figure C.3. Figure C.4 shows the relative discharges in all the branches. The discharges in the branches are taken relative to the upstream boundary condition (Q= 5000 m^3/s). To obtain the different lengths, the begin- and end position of branch 7 are varied as shown in Table C.1 The discharge for the case when the length of branch 4 is smaller than length of branch 5 is shown in Figure C.5.

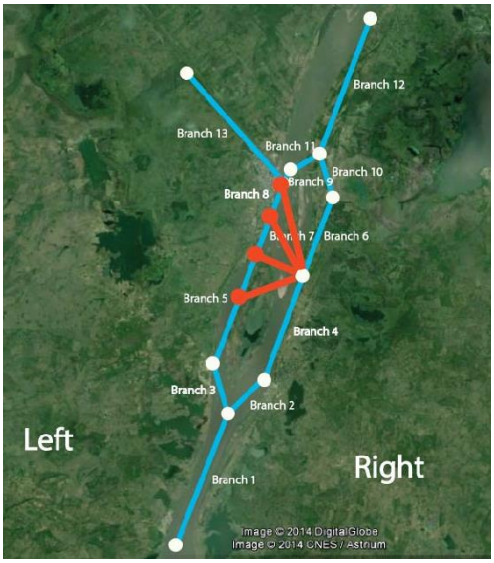

Figure C. 3 - Schematisation bifurcation with length of mid channel variation marked in red

Table C. 2– Length of branch 7 (mid channel) with begin and end position

Position node 5 (begin branch 7) [m]	Position node 6 (end branch 7) [m]	Length branch 7 [m]
14000	15500 (node 6 = node 8)	2500
14000	15000	2236.07
14000	14000	2000
14000	13000	2236.07

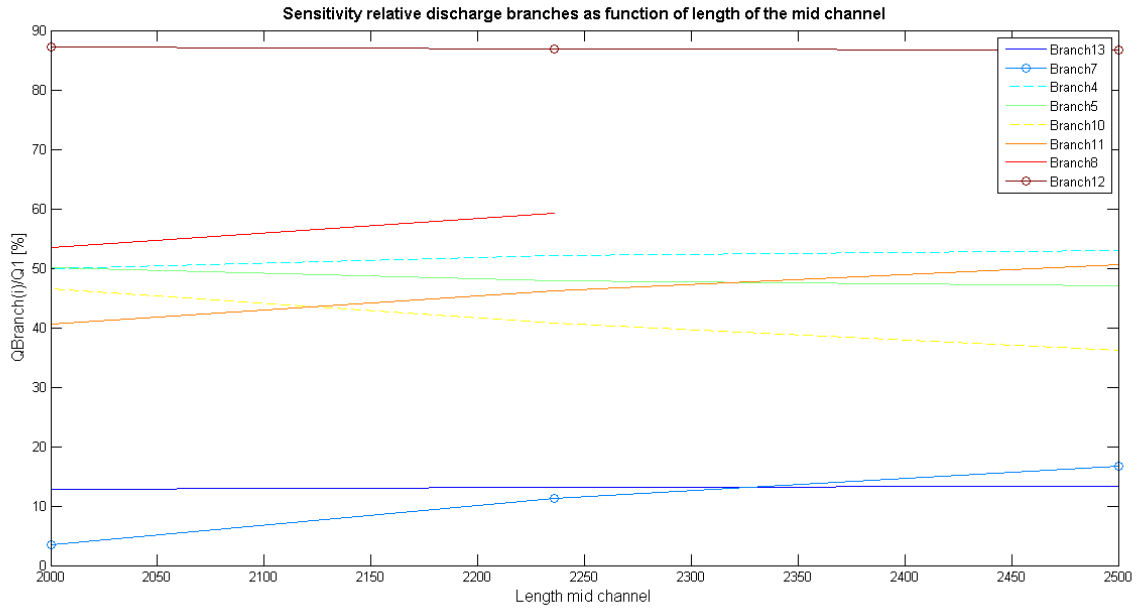

Figure C. 4– Discharge in the branches for different length of the mid channel

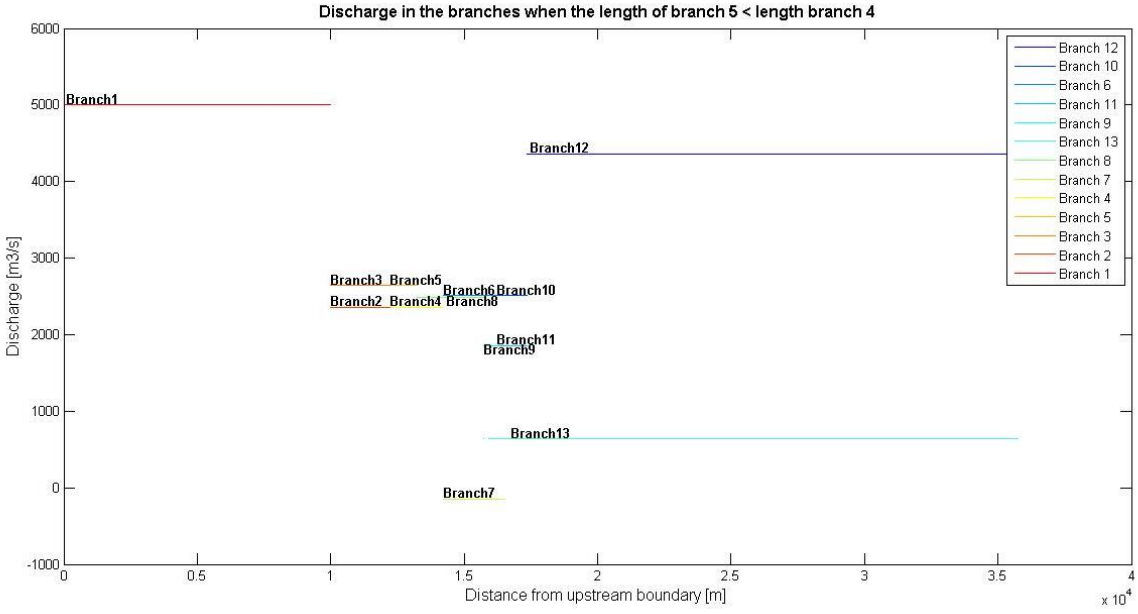

Figure C. 5 – Discharge in the branches for length branch 5 is smaller than length branch 4

C.1.2 Sensitivity of the offtake position

The sensitivity of the position of the offtake 'branch 13' (see Figure C.6) to the discharges and water levels is tested. The discharges in the branches are taken relative to the upstream boundary condition (Q= 5000 m^3/s). The positions of the start of the offtake are taken relative to the upstream boundary and shown in Table C.2. The length of branch 13 is kept the same. At a distance of 15 km of the upstream boundary, the offtake is directly connected to the mid channel. Figure C.7 shows the relative discharges in all the branches. Figure C.8 shows the water level along the branches for different position of the offtake.

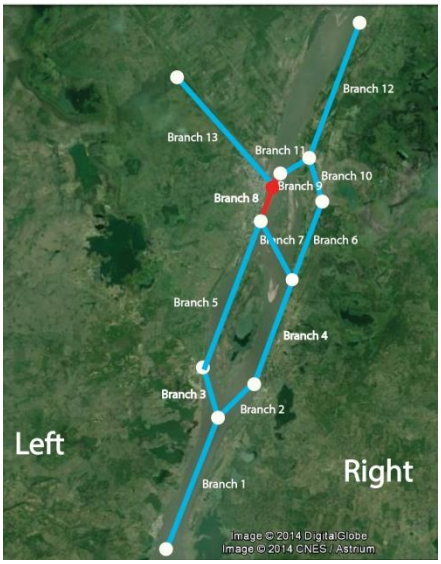

Figure C. 6- Schematisation bifurcation with changed position of the offtake (marked red)

Table C. 3– Values for position of the offtake

Cases	Offtake position [km]
1	15
2 (reference case)	15.02
3	15.1
4	15.25
5	15.5
6	15.75
7	15.9

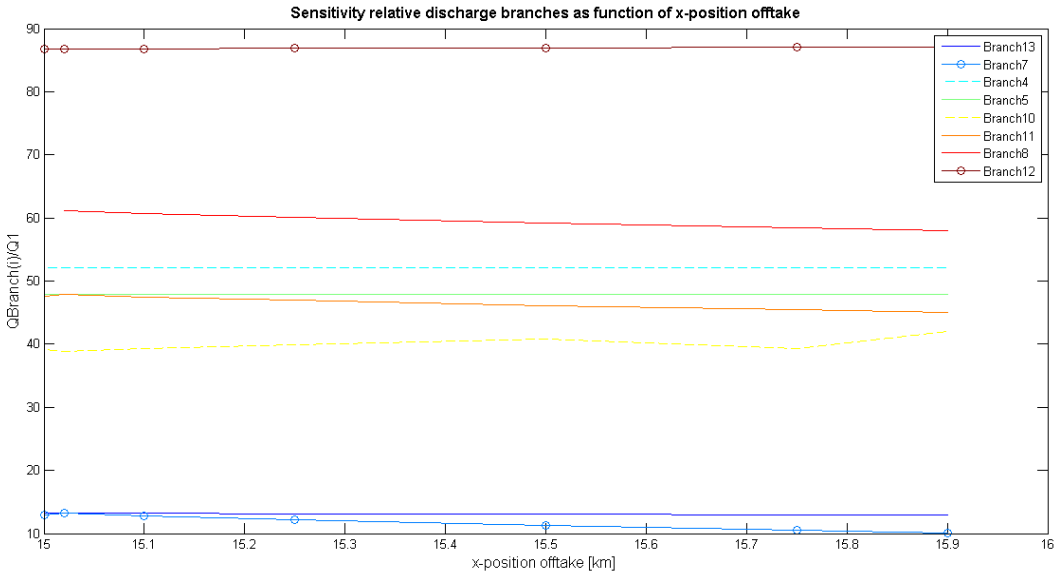

Figure C. 7 - Relative discharge branches as function of x-position offtake (downstream of node 1)

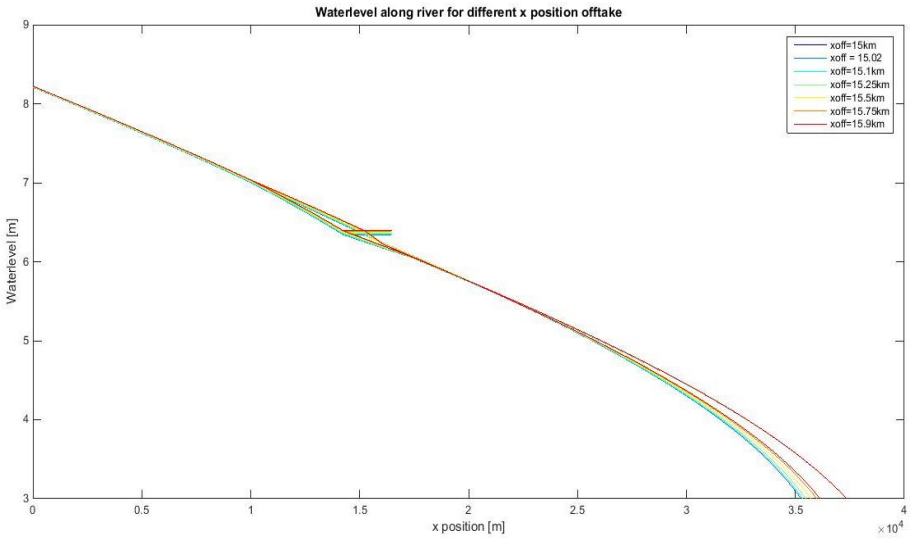

Figure C. 8 - Water level for different position of the offtake (branch 13)

C.1.3 Sensitivity of the ratio of the depth right and left branches

The sensitivity of the ratio of the depth of the right (branch 2, 4, 6, 10) and left branches (branch 3, 5, 8, 9), marked in red in Figure C. 9, to the discharges and water levels is tested. The discharges in the branches are taken relative to the upstream boundary condition (Q= 5000 m^3/s). Table C. 4 shows the used ratios. Ratios lower than 0.2 or larger than 2 are not possible. Figure C. 10 shows the relative discharges in all the branches.

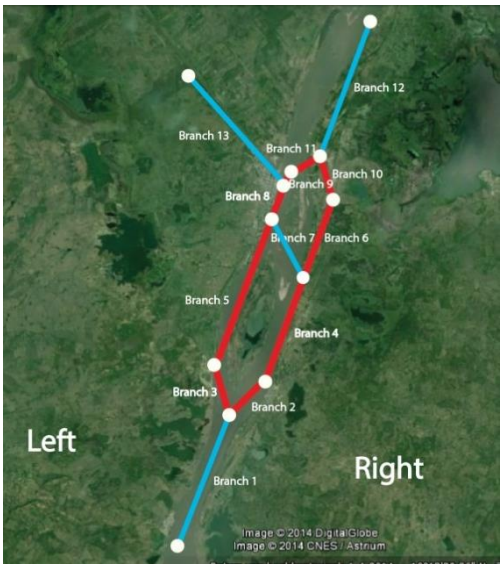

Figure C. 9– Schematisation bifurcation with changed depth of the branches marked in red

Table C. 4 Used ratio depth right/left branches

Cases	Ratio depth right / left branches [-]	Depth right branches [m]	Depth left branches [m]
1	0.3	0.9	3
2	0.5	1.5	3
3 (reference case)	1	3	3
4	1.5	4.5	3
5	2	6	3

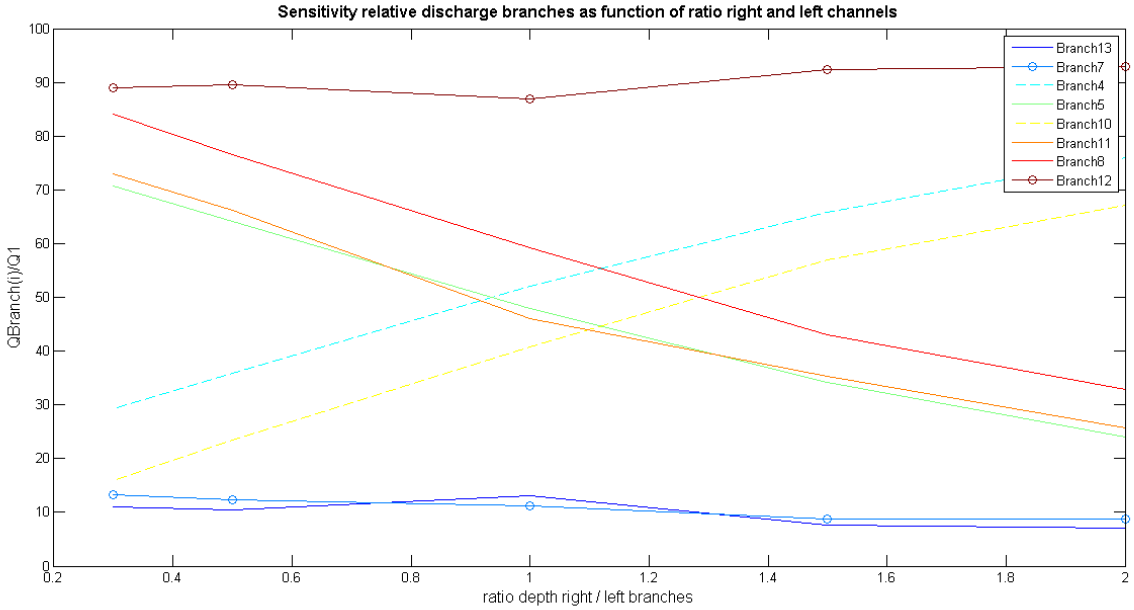

Figure C. 10- Relative discharge branches as function of ratio depth right and left branches

C.1.4 Sensitivity of the ratio of the width right and left branches

The sensitivity of the ratio of the width of right and left branches (marked in red in Figure C.11), to the discharges and water levels is tested. The discharges in the branches are taken relative to the upstream boundary condition (Q= 5000 m^3/s). Table C. 5 shows the used ratios for the calculations. Figure C. 12 shows the relative discharges in all the branches.

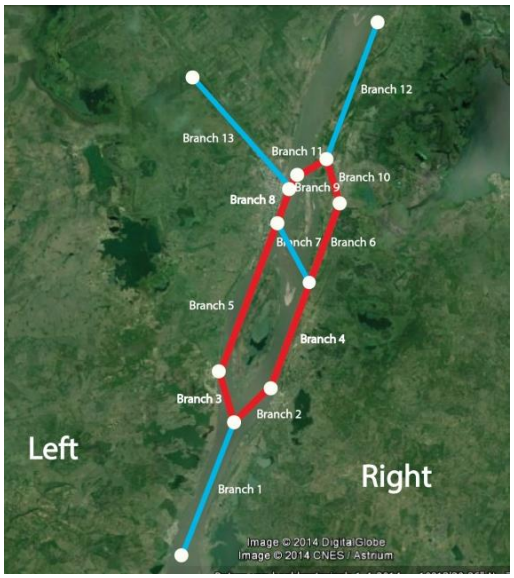

Figure C. 11 - Schematisation bifurcation with changed width of the branches marked in red

Table C. 5 Used ratio width right/left branches

Cases	Ratio width left / right branches [-]	Width right branches [m]	Width left branches [m]
1	0.1	100	1000
2	0.5	500	1000
3 (reference case)	1	500	500
4	2	800	400
5	5	1000	200
6	10	1000	100

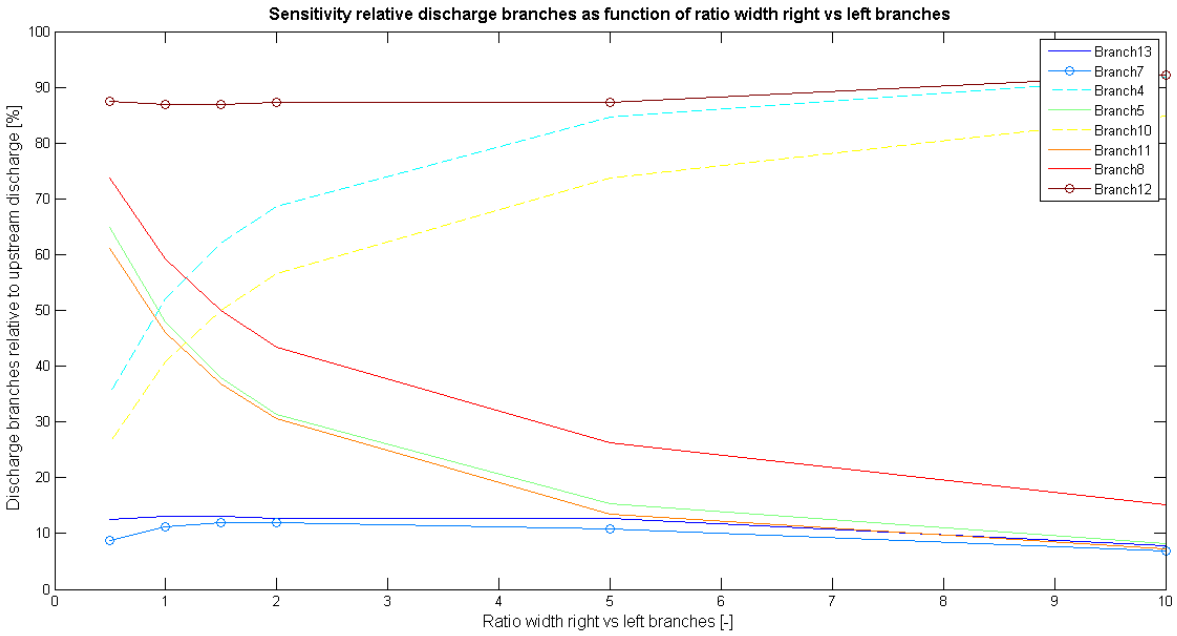

Figure C. 12 - Discharges as function of ratio width right and left branches

C.1.5 Sensitivity of the length of branch 9

The sensitivity of the length of branch 9 (marked in red in Figure C. 13) to the discharge and water level is tested. The length of branch 10 and 11 and 12 is kept equal with increasing length of branch 9. Therefore branch 10, 11 and 12 are located more downstream with increasing length of branch 9. The used lengths of branch 9 are shown in Table C. 6. The discharges in the branches are taken relative to the upstream boundary condition (Q= 5000 m^3/s).Figure C. 14 shows the relative discharges in all the branches and Figure C. 15 shows the relative discharge of the offtake (branch 13). Figure C. 16 shows the water level along the branches for different length of branch 9.

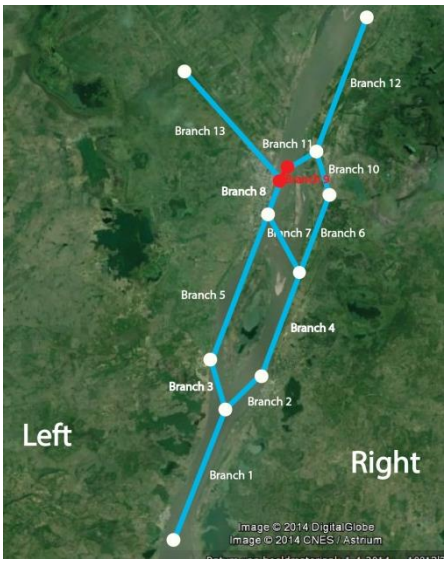

Figure C. 13 - Schematisation bifurcation with branch 9 marked in red

Table C. 6 Used length of branch 9

Cases	Length branch 9 [m]
1	100
2	200
3 (reference case)	500
4	1000
5	1500

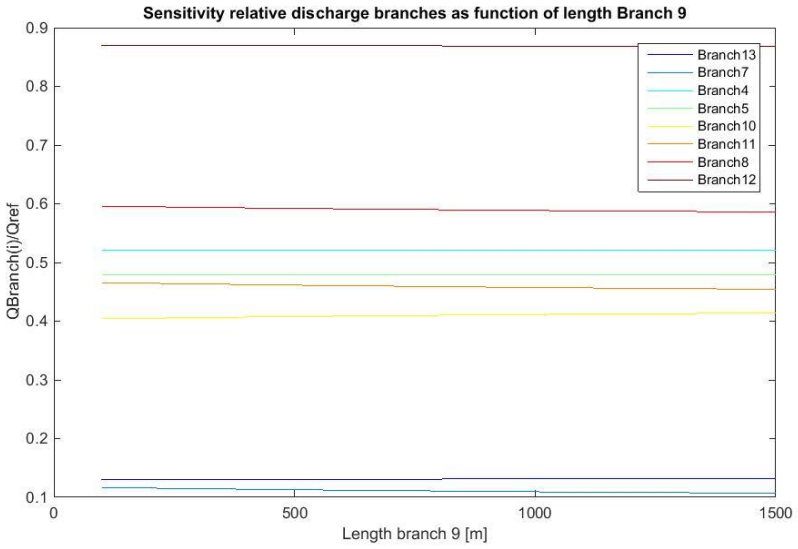

Figure C. 14 - Relative discharge branches as function of length branch 9

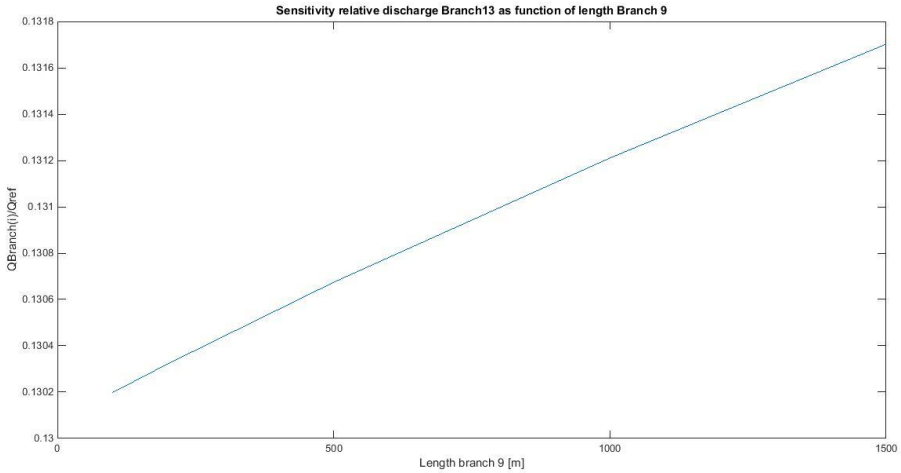

Figure C. 15 - Relative discharge offtake (Branch13) as function of length branch 9

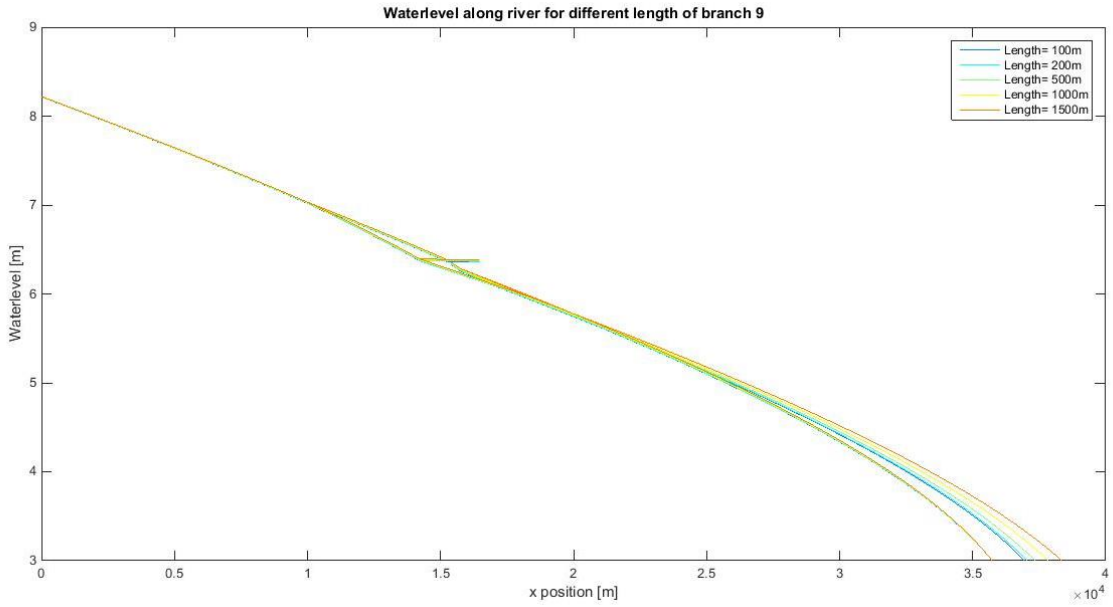

Figure C. 16 - Water level for different length branch 9

C.1.6 Sensitivity width of the mid channel (branch 7)

The sensitivity of the width of the mid channel (Figure C. 17) to the discharge and water level is tested. The discharges in the branches are taken relative to the upstream boundary condition (Q= 5000 m^3/s). The used widths of the mid channel (branch 7) are shown in Table C. 7. Figure C. 18 shows the relative discharges in all the branches.

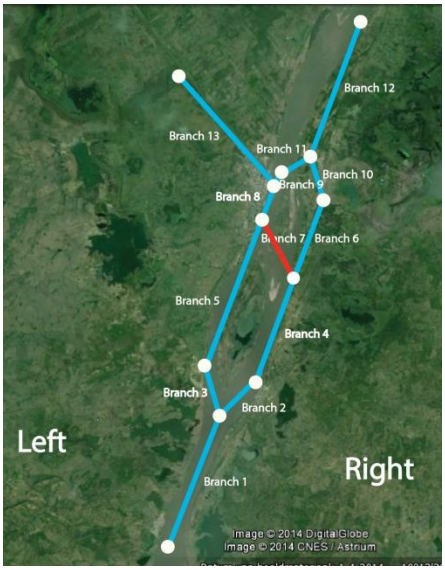

Figure C. 17- Schematisation bifurcation width mid channel (Branch 7) marked in red

Table C. 7 - Used width of the mid channel (branch 7)

Cases	Width branch 7 [m]
1	0
2	100
3	200
4	500
5 (reference case)	1000
6	2000
7	5000

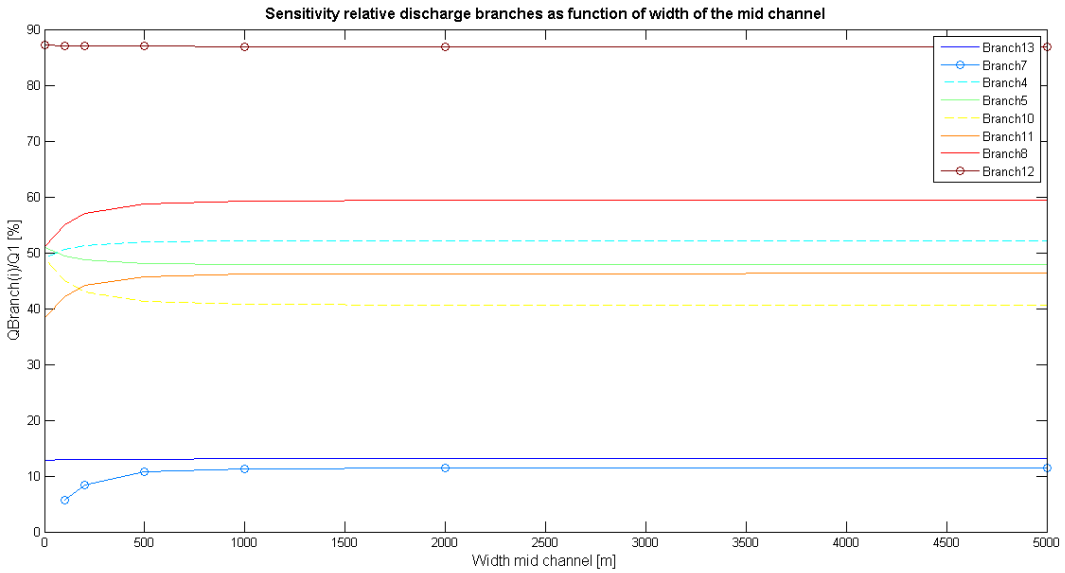

Figure C. 18 - Relative discharge branches as function of width mid channel

C.1.7 Sensitivity of the width of branch 8 and 9

The sensitivity of the width of branch 8 and 9 (marked in red in Figure C. 19) to the discharge and water level is tested. The discharges in the branches are taken relative to the upstream boundary condition (Q= 5000 m^3/s). Table C. 8 shows the used width of branch 8 and 9. Figure C. 20 the relative discharges in all the branches and Figure C. 21 shows the relative discharge of the offtake (branch 13).

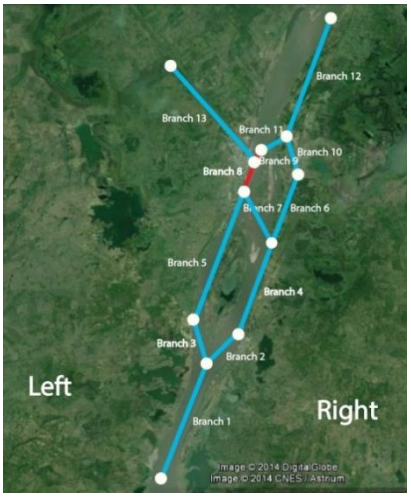

Figure C. 19 - Schematisation bifurcation width branch 8 and 9 marked in red

Table C. 8– Used values for width in branch 8 and 9

Cases	Width branch 8 and 9 [m]
1	200
2 (reference case)	500
3	1000
4	2000
5	5000

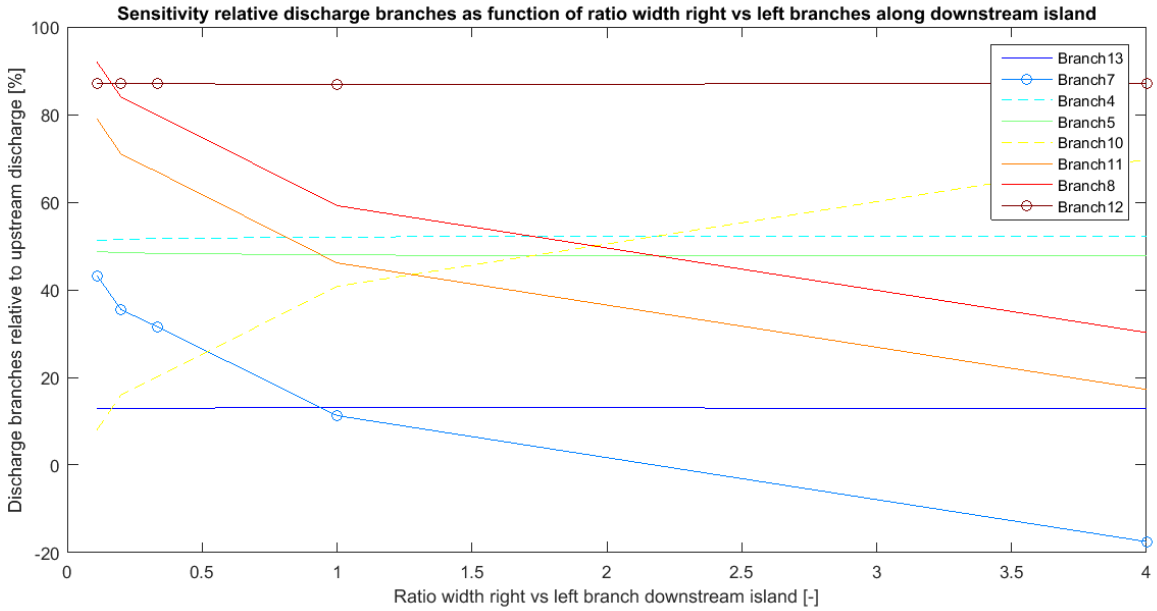

Figure C. 20 - Relative discharge branches for different width of branch 8 and 9

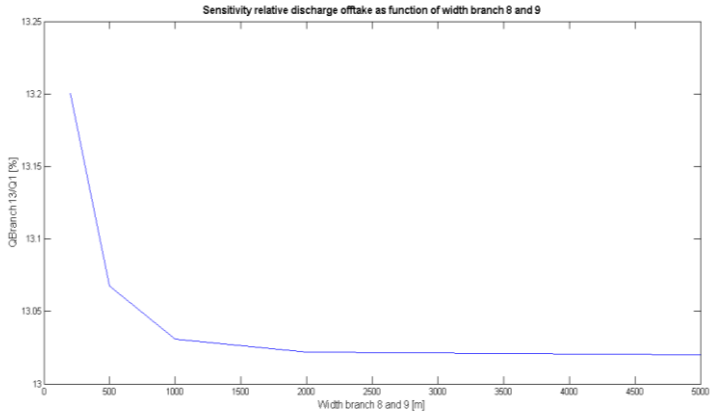

Figure C. 21 - Relative discharge branch 13 for different width of branch 8 and 9

C.1.8 Sensitivity of the width of the offtake

The sensitivity of the width of the offtake 'branch 13' (Figure C. 22) to the discharges and water levels is tested. The discharges in the branches are taken relative to the upstream boundary condition (Q= 5000 m^3/s). The chosen widths for the calculations are shown in Table C. 8. It has to be bared in mind that a width of 10 km will probably not occur, but it is taken into account to test the sensitivity to the system. Figure C. 23 shows the relative discharges in all the branches and Figure C. 24 shows the relative discharge of the offtake (branch 13). It has to be bared in mind that the scale of the axis of these figures are not equal.

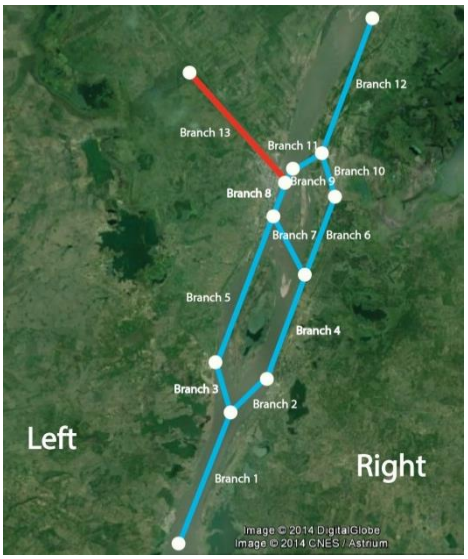

Figure C. 22 - Schematisation bifurcation with parameter changed in the offtake (marked in red)

Table B. 1 - Used width of the offtake

Cases	Width offtake [m]
1	20
2	50
3	100
4 (reference case)	150
5	200
6	500
7	1000
8	2500
9	5000
10	10000

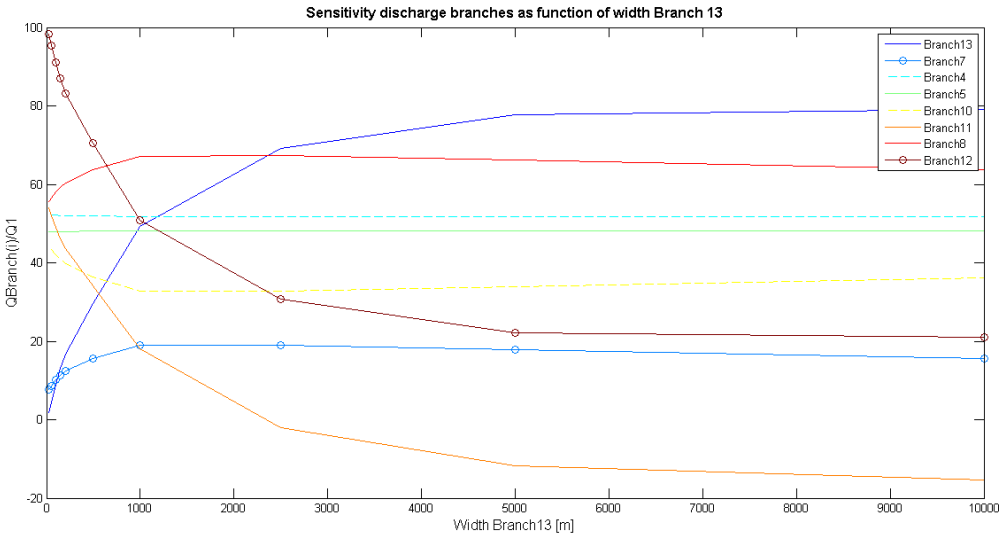

Figure C. 23- Relative discharges in the branches as function of width in the offtake (branch 13)

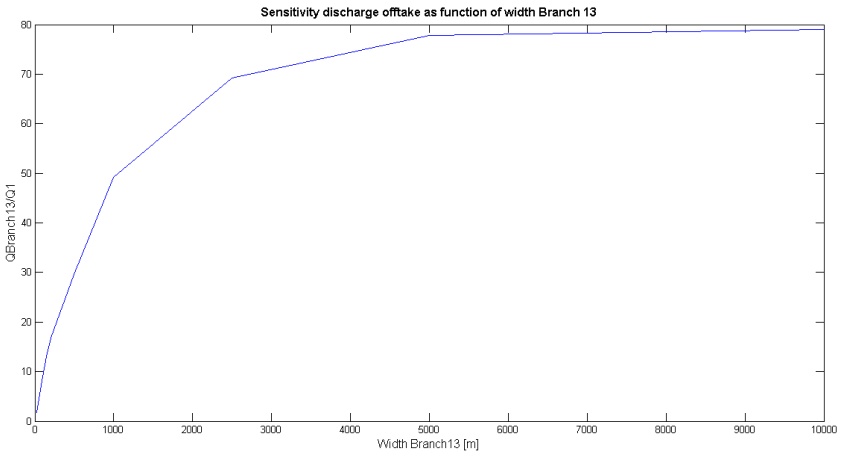

Figure C. 24 - Relative discharge in the offtake (branch 13) as function of width in the offtake

C.1.9 Sensitivity of the depth of the offtake

The sensitivity of the depth of the offtake 'branch 13' (Figure C. 22) to the discharges and water levels is tested. The discharges in the branches are taken relative to the upstream boundary condition (Q= 5000 m^3/s). The chosen of the offtake are shown in Table C. 8. Figure C. 25 shows the relative discharges in all the branches and Figure C. 26 shows the relative discharge of the offtake (branch 13). Figure C. 27 shows the water level along the branches for different depth of the offtake.

Table B. 2 - Used depth of the offtake

Cases	Depth offtake [m]
1	2
2 (reference case)	3
3	5
4	9
5	10
6	15
7	20
8	25
9	28

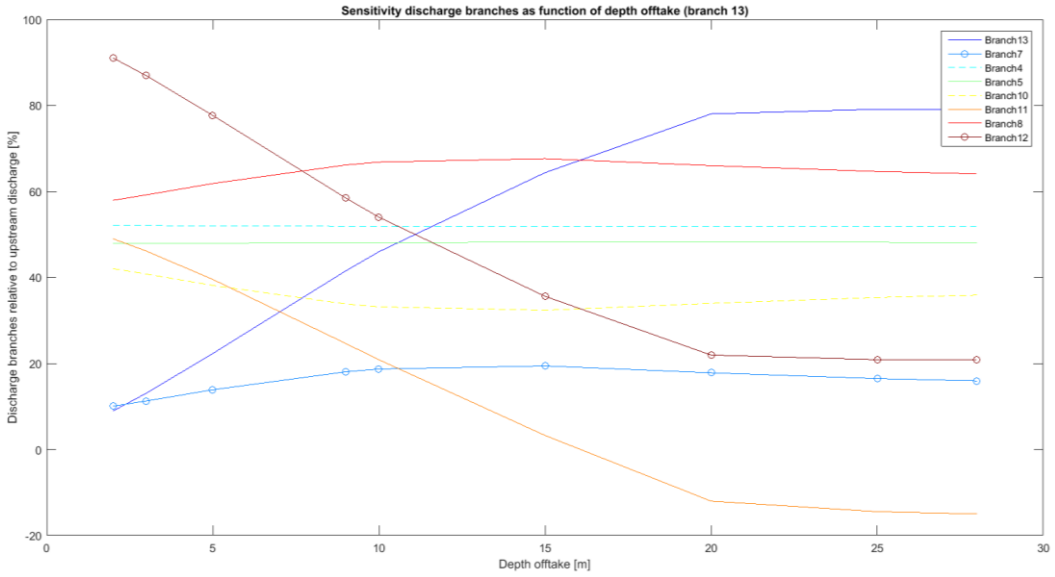

Figure C. 25 - Relative discharges in the branches as function of depth in the offtake (Branch13)

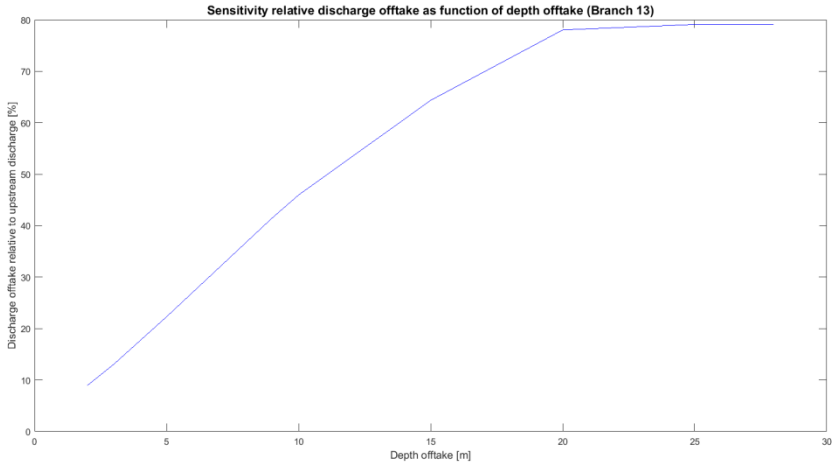

Figure C. 26 - Relative discharge in the offtake (Branch13) as function of depth in the offtake

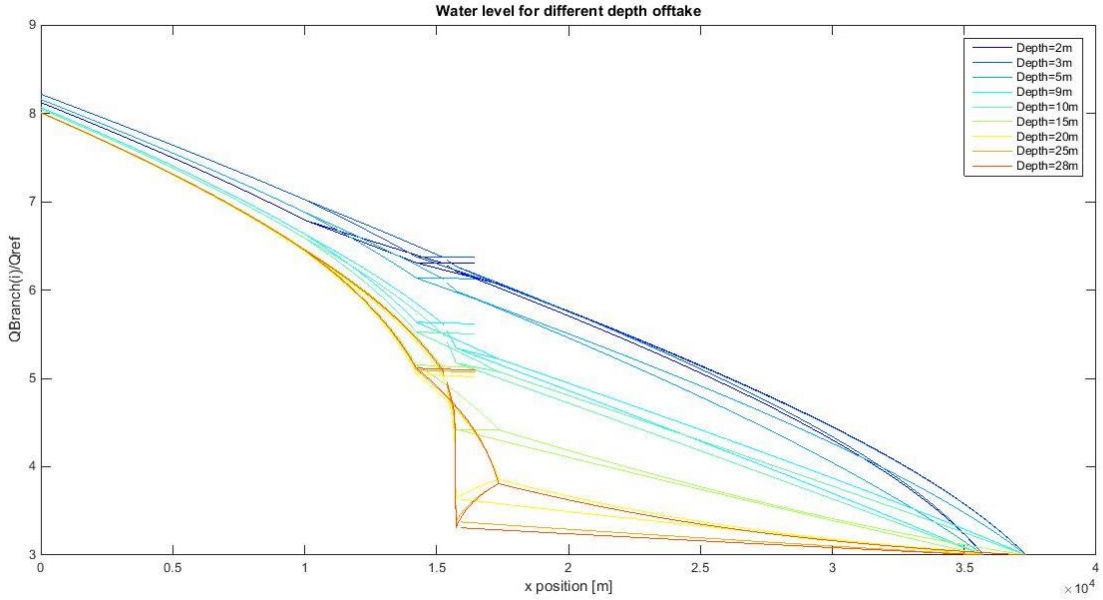

Figure C. 27- Water surface profiles as function of depth offtake (Branch13)

C.1.10 Sensitivity of the bed-friction of the offtake

The sensitivity of the bed friction of the offtake 'branch 13' (see Figure C. 22), to the discharges and water levels is tested. The discharges in the branches are taken relative to the upstream boundary condition (Q= 5000 m^3/s). The used bed-frictions of the offtake are shown in Table B.3. Larger bed-frictions than 300 $m^{1/2}/s$ cannot occur. Figure C. 28 shows the relative discharges in all the branches and Figure C. 29shows the relative discharge of the offtake (branch 13). Figure C. 30 shows the water level along the branches for different bed friction of the offtake.

Table B. 3 - Used bed-friction of the offtake

Cases	Chézy-coefficient [$m^{1/2}/s$]
1	10
2	20
3 (reference case)	50
4	100
5	200
6	300

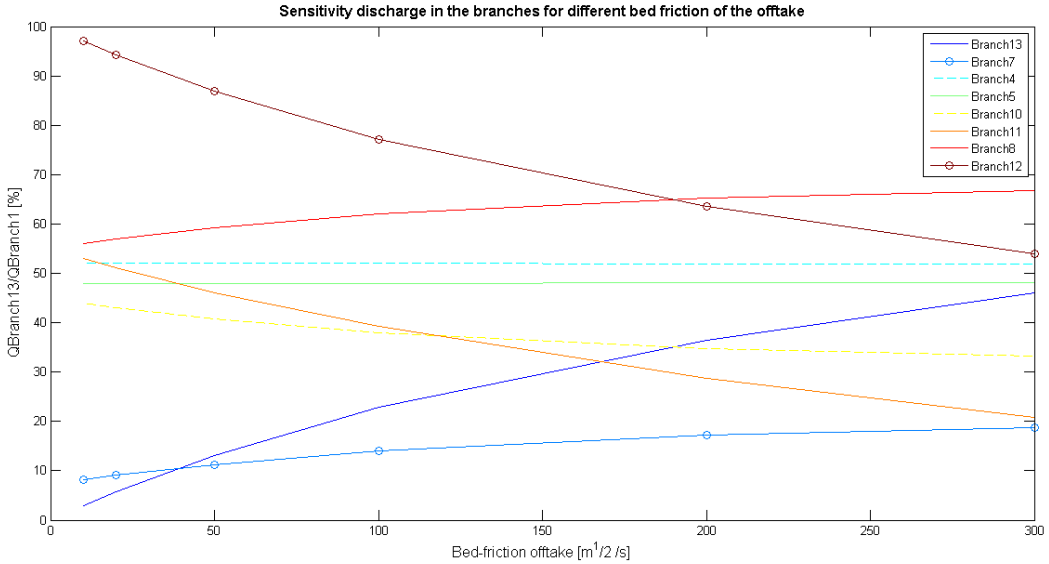

Figure C. 28 - Relative discharge branches as function of bed-friction offtake

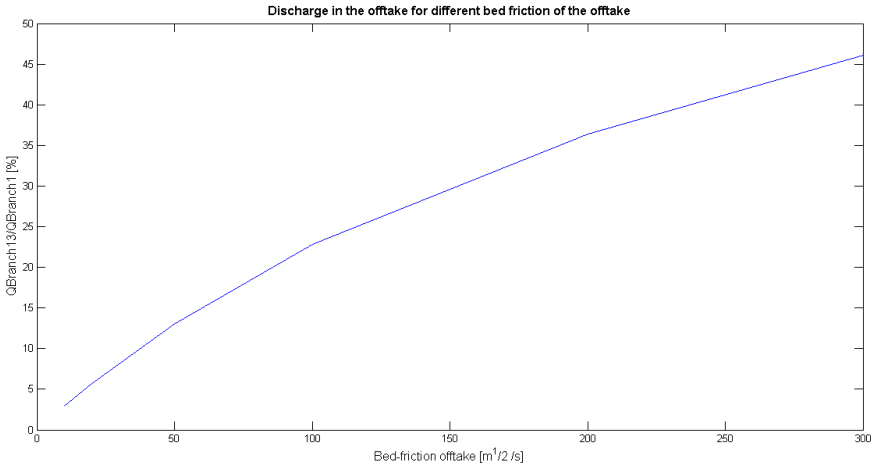

Figure C. 29 - Relative discharge offtake (branch 13) as function of bed friction offtake

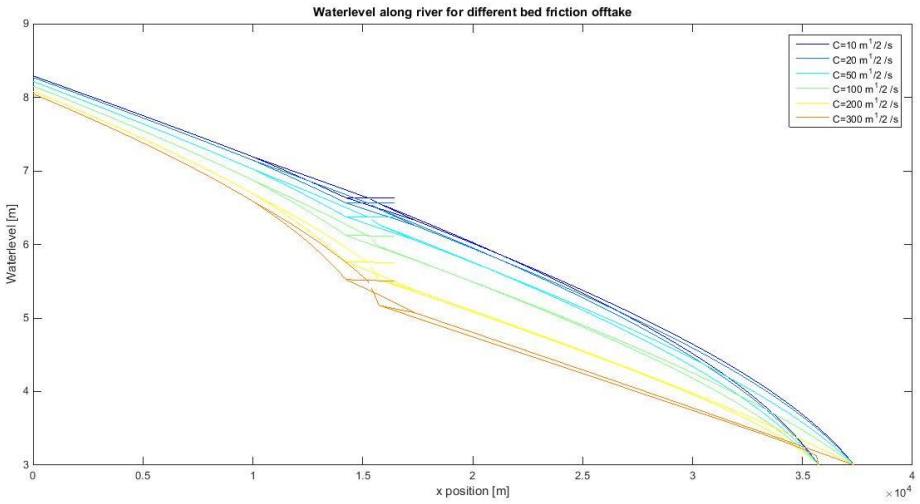

Figure C. 30 - Water level as function of bed friction offtake

C.1.11 Sensitivity of the bed slope of the offtake

The sensitivity of the bed slope of the offtake 'branch 13' to the discharges and water levels is tested. The discharges in the branches are taken relative to the upstream boundary condition (Q= 5000 m^3/s). Figure C. 32shows the relative discharges in all the branches and Figure C. 32 shows the relative discharge of the offtake (branch 13). Figure C. 33 shows the water level along the branches for different bed slope of the offtake. Table C.8 shows the used bed slopes of the offtake. Larger bed slopes than 1e-3 cannot be modelled.

Table C. 9- Values for different bed slope of the offtake.

Cases	Bed slope offtake [-]
1	1e-5
2	5e-5
3 (reference case)	1e-4
4	3e-4
5	5e-4
6	7e-4
7	1e-3

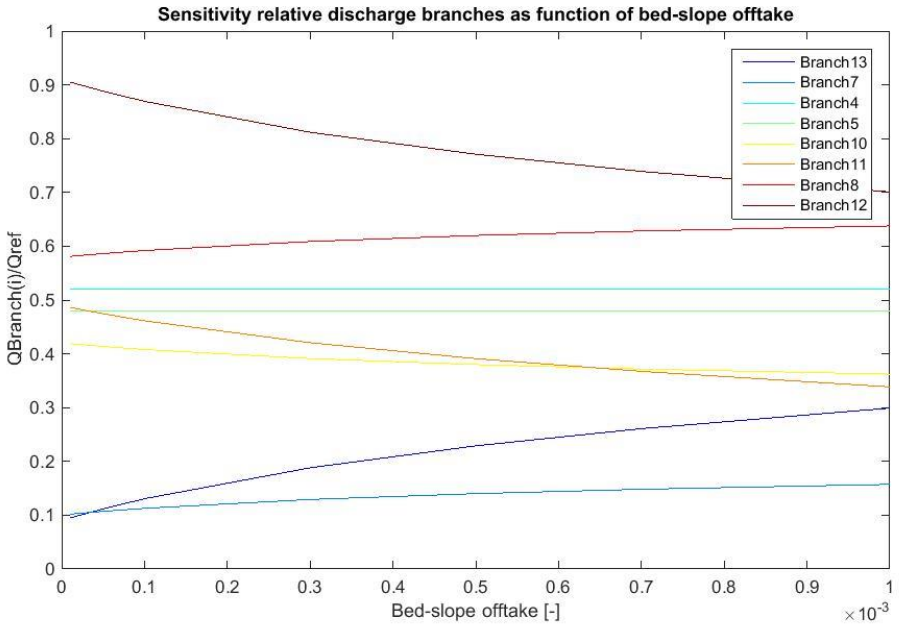

Figure C. 31 - Relative discharge branches as function of bed slope offtake

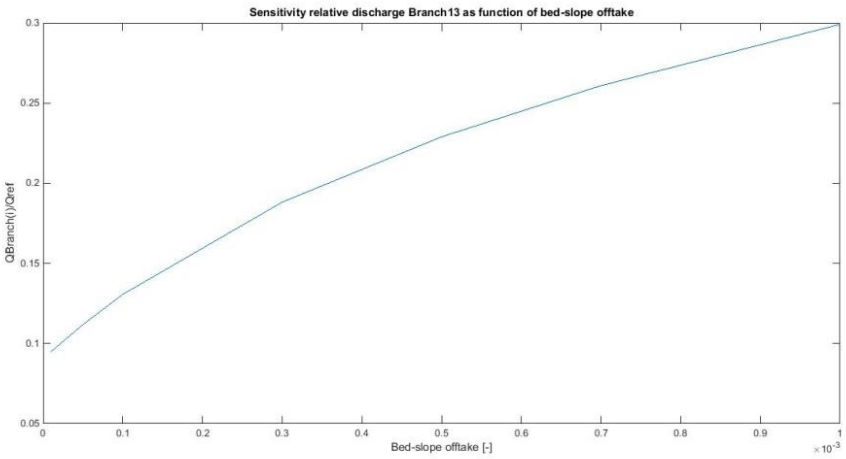

Figure C. 32 - Relative discharge as function of bed slope offtake

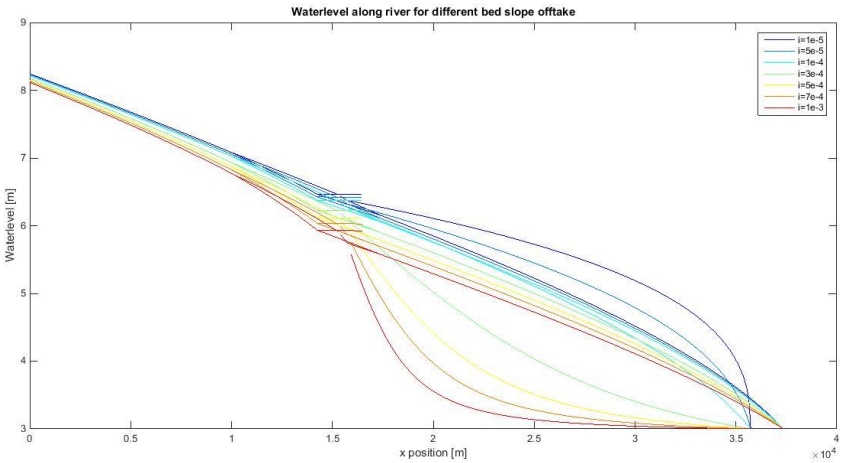

Figure C. 33 - Water level for different bed slope offtake

Appendix D Delft3D 2DH-hydrodynamics

D.1 Model description

Delft3D is a model which is able to calculate hydrodynamic and morphodynamic flows in a two- and three- dimensional mode. It is a widely accepted and used program created by Deltares. Besides, it is open-source which makes it widely accessible. Currently, a new version of Delft3D is under construction 'Delft3D-FLOW Flexible Mesh' which uses a flexible mesh instead of a rectangular or curvilinear grid. This makes it easy to make grids for difficult geometries. However, at the moment Delft3D-FLOW FM is only reliable for calculation of hydrodynamic flows. As in this study we are also interested in sediment distribution and morphological variations Delft3D-FLOW is preferred above Delft3D-FLOW FM.

D.1.1 Theory

Delft3D-FLOW solves the unsteady shallow water equations in two (depth-averaged) or three dimensions. The system of equations consists of the horizontal equations of motion, the continuity equation, and the transport equations for conservative constituents (Deltares, 2014).

The shallow water equations used in Delft3D are derived from the three dimensional Navier-Stokes equations. Several assumptions are made for which an overview can be find in the Delft-3D FLOW user manual (Deltares, 2014).The most relevant assumptions for this study are:

- The flow is assumed to be incompressible. Therefore a constant density can be applied.
- The horizontal length scale and time scales are assumed to be much larger than the vertical scales. The vertical accelerations other than the gravitational acceleration are assumed to be very small and are therefore neglected. Therefore, the shallow water equations and hydrostatic pressure equation can be applied.
- The process of drying and flooding is determined by the water depth. When the water depth is below a user-specified threshold depth, the point is set dry. When the water level reaches the threshold depth, the grid cell is set wet again. The grid points which become dry are removed from the active flow domain and are added again when they become wet. The process of drying and flooding may generate small oscillations in water levels and velocities.

With these assumptions the shallow water equations are reduced to:

Continuity equation:

3D- continuity equation: $\frac{\partial U}{\partial x} + \frac{\partial V}{\partial y} + \frac{\partial W}{\partial z} = 0$

Integrating over the depth and substitution of the kinematic boundary condition gives the 2D-depth integrated continuity equation:

$$\frac{\partial \zeta}{\partial t} + \frac{\partial (HU)}{\partial x} + \frac{\partial (HV)}{\partial y} = 0.$$

Where,
H = water depth.

Depth-averaged momentum equation in x- and y-direction:

$$\frac{\partial U}{\partial t} + U\frac{\partial U}{\partial x} + V\frac{\partial U}{\partial y} - fV + g\frac{\partial \zeta}{\partial x} + \nu_h\left(\frac{\partial^2 U}{\partial x^2} + \frac{\partial^2 U}{\partial y^2}\right) + \frac{gU\sqrt{U^2+V^2}}{HC^2} = 0$$

$$\frac{\partial V}{\partial t} + U\frac{\partial V}{\partial x} + V\frac{\partial V}{\partial y} + fU + g\frac{\partial \zeta}{\partial x} + \nu_h\left(\frac{\partial^2 V}{\partial x^2} + \frac{\partial^2 V}{\partial y^2}\right) + \frac{gV\sqrt{U^2+V^2}}{HC^2} = 0$$

where:

f= Coriolis parameter [1/s];
C = Chézy-coefficient [$m^{1/2}/s$]
v_H=horizontal eddy viscosity [m^2/s]

The first term is the local flow acceleration, the second and the third term correspond to the advection terms in x- and y-direction. The fourth term is the Coriolis force and the fifth term represents the acceleration due to pressure gradients. The sixth and the seventh term are the turbulent Reynold stresses. The last term is the friction term.

The bottom friction terms are described as:
$\tau_{bx} = \frac{g}{C^2}U\sqrt{U^2+V^2}$ and $\tau_{by} = \frac{g}{C^2}V\sqrt{U^2+V^2}$

In Delft3D-FLOW not all quantities, such as water level, depth, velocity or concentration of substances, are defined at the same location of the numerical grid. Instead, a staggered grid is used as given in Figure D. 1. Signs in the numerical grid show the locations where different constituents are calculated. One of the main advantages of a staggered grid is that different types of boundary conditions can easily be implemented.

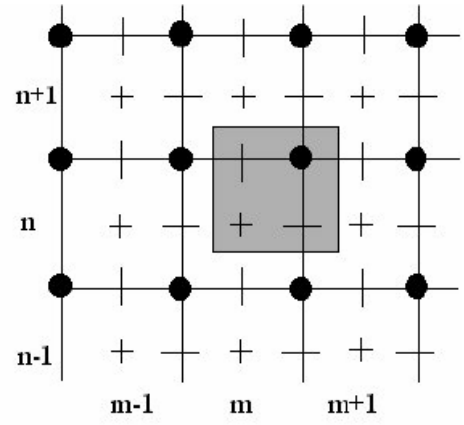

Figure D. 1 - Staggered grid Delft3D-FLOW (Deltares, 2014)

+ water level, concentration of constituents, salinity, temperature
- horizontal velocity component in ξ- direction (also called *u* and *m*-direction)
| horizontal velocity component in η- direction (also called *v* and *n*-direction)
• depth below mean water level (reference level)

Numerical stability of the grid can be checked with the Courant number. The CFL-condition can help calculate the maximum time step for which the numerical solution is still stable. The default scheme in Delft3D, also called the 'cyclic scheme', is implicit and unconditionally stable. However, for large time

steps the solution becomes less accurate. For explicit schemes, the CFL-condition should be used which holds:

$$CFL = \frac{\Delta t}{\Delta x, \Delta y}(u + \sqrt{gh}) \leq 1 \quad \text{(D.1)}$$

where,
CFL = Courant number
Δt = timestep
Δx, Δy = grid spacing in x-and y- direction
g= gravitational acceleration
h= local water depth
u= horizontal velocity

D.2 Model set-up

D.2.1 Bathymetry

The most recent bathymetry of the Río Magdalena and Canal del Dique is used as a starting point for the bathymetry. For the Canal del Dique, measurements have been carried out by Consorcio Dique in 2014. This data is available as cross-sections with a spatial resolution of 250 m as shown in Figure D. 2 and Figure D. 3. For the Río Magdalena a combination of Lidar-data measured by Consorcio Dique in 2014 and bathymetric measurements of 2013 from Cormagdalena is used with a resolution of 5x5m as shown in Figure D. 4. Also, historical bathymetric data is available from various sources since 2002 which can be used for validation of the different cases. For more information on the available data, see data-analysis Appendix C.

Figure D. 2 - Cross-sectional locations as measured by Consorcio Dique in 2014

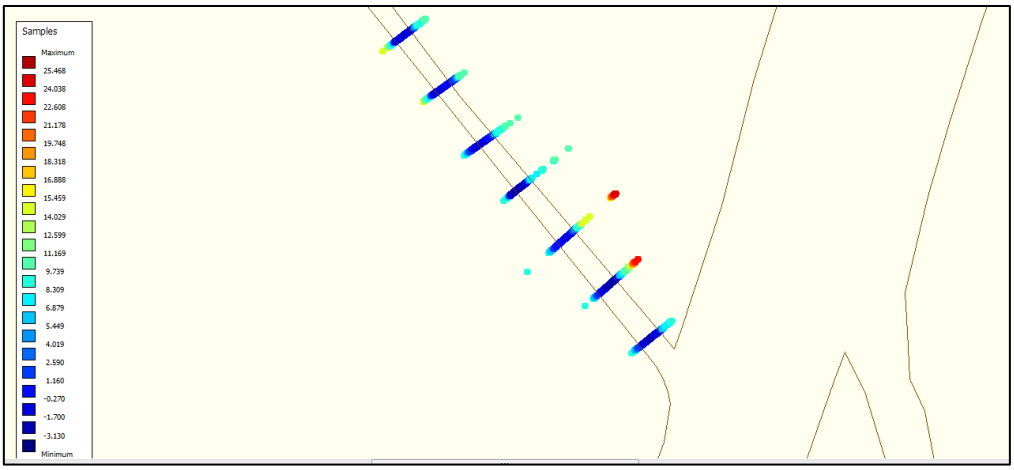

Figure D. 3 - Cross-sectional profiles Canal del Dique as shown in QUICKIN (toolbox Delft3D)

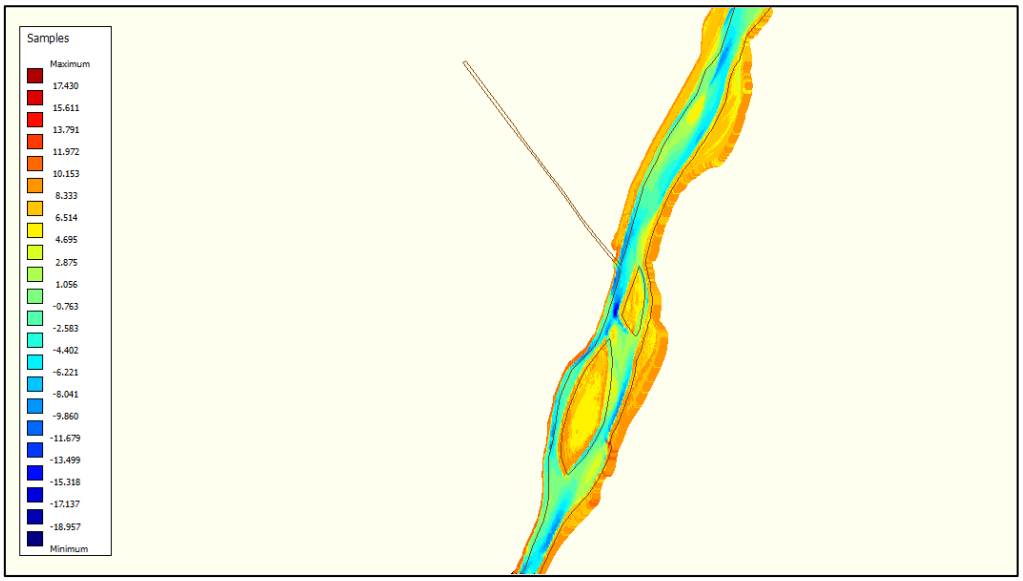

Figure D. 4 - Bathymetry Río Magdalena as shown in QUICKIN

D.2.2 Grid

A curvilinear grid is constructed for the area from 10km upstream of the bifurcation at Calamar, until 10 km downstream of Calamar both on the Río Magdalena and Canal del Dique ('the offtake') as shown in Figure D. 5. With these dimensions of the model it is expected that boundary effects will not impact the results in the area of interest and no backwater effects will occur (see Appendix A). The mesh is generated using the toolbox RGFgrid, which is part of the modeling software of Delft3D. The grid has been constructed such that it fits within the following requirements as stated in the Delft3D-Flow user manual (Deltares,2014):

- Orthogonality of the grid is less than 0.02 in the area of interest. Orthogonality is the cosine of the angle between the grid lines. Near closed boundaries larger values can be tolerated.
- The smoothness of the grid is less than 1.2. In order to avoid inaccurate results the ratio between adjacent grid cell lengths should not be too large in the area of interest. (Ratio of neighbouring grid cell dimensions.)

- Aspect ratio is between 1 and 2. Aspect ratio is the ratio of grid cell dimension in ξ- and η-direction.

In this study, two kinds of computational grids are developed: a grid that follows the main stream (along the Río Magdalena) and a grid that follows the offtake the best. Tests will identify the most appropriate grid.

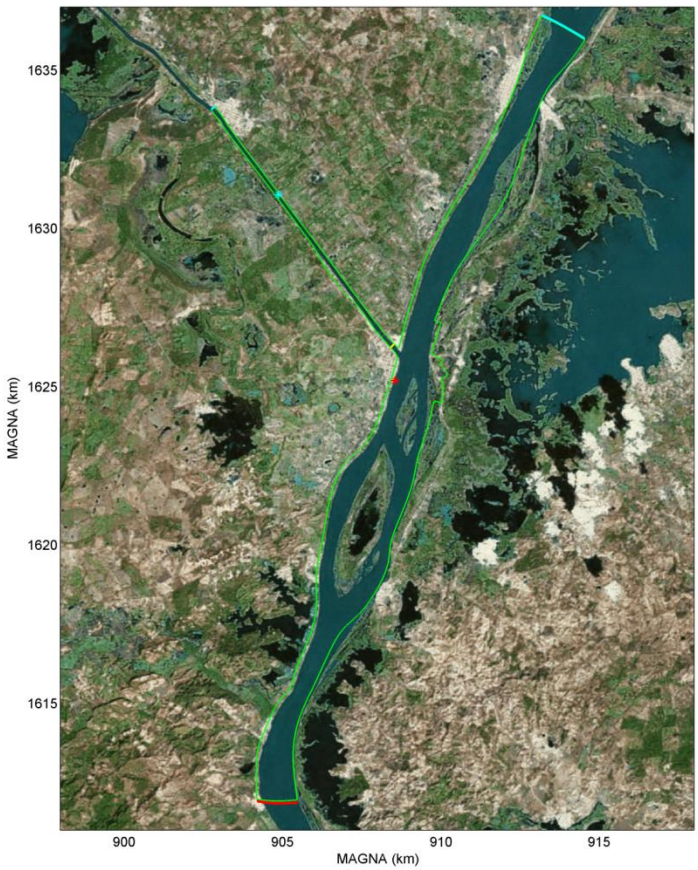

Figure D. 5 - Model extent and location of model boundaries. The upstream model boundary is shown in red, the downstream boundaries in cyan. The water level station Calamar is shown by the red symbol.

D.2.2.1 Grid following the main stream

The largest stream is the Río Magdalena. From a hydrodynamic view, a grid which follows this stream is obvious. However, the angles between the grid cells around the bifurcation are larger and it is harder to maintain the required orthogonality of the grid in the area at the entrance of the offtake. Figure D. 6 shows the total grid following the main stream and Figure D. 7shows a detail of the grid at the bifurcation. From Figure D. 8 it can be seen that the required orthogonality is obtained in the entire grid. However, when looking more closely at the entrance of the offtake (Figure D. 9) it can be seen that some grid-cells in the corner do not meet the required orthogonality. However, these grid cells lie outside of the land boundary, which is assumed to stay dry, so the flow will not be influenced by this.

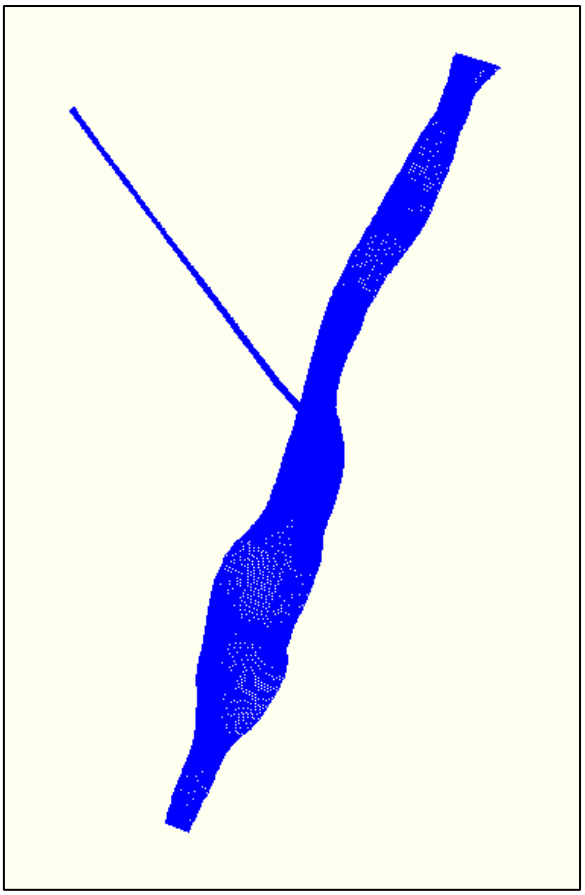

Figure D. 6 - Grid following the main stream

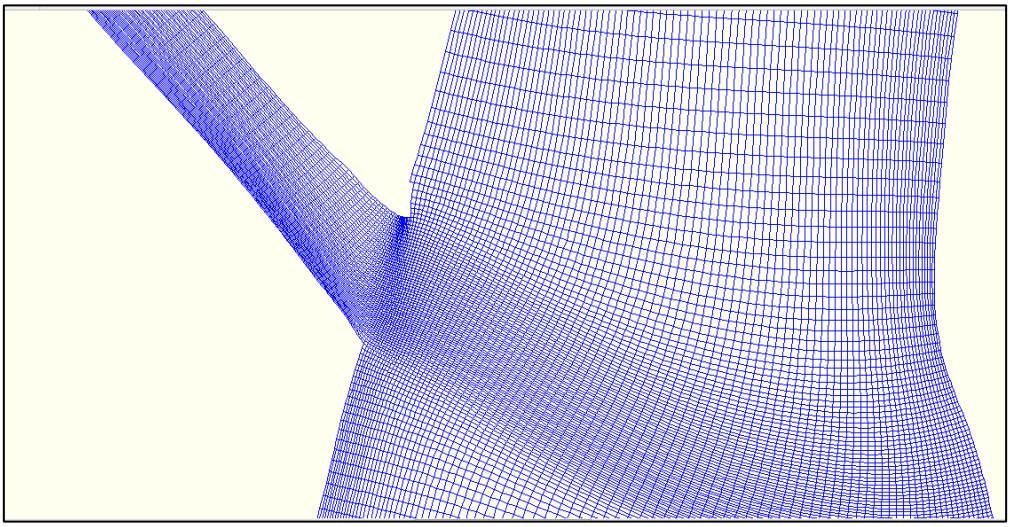

Figure D. 7 - Detail grid following the main stream

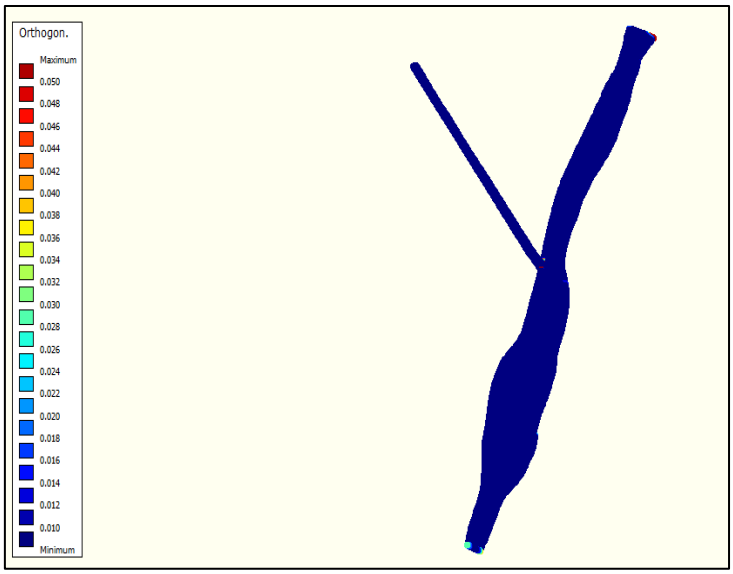

Figure D. 8 - Orthogonality grid

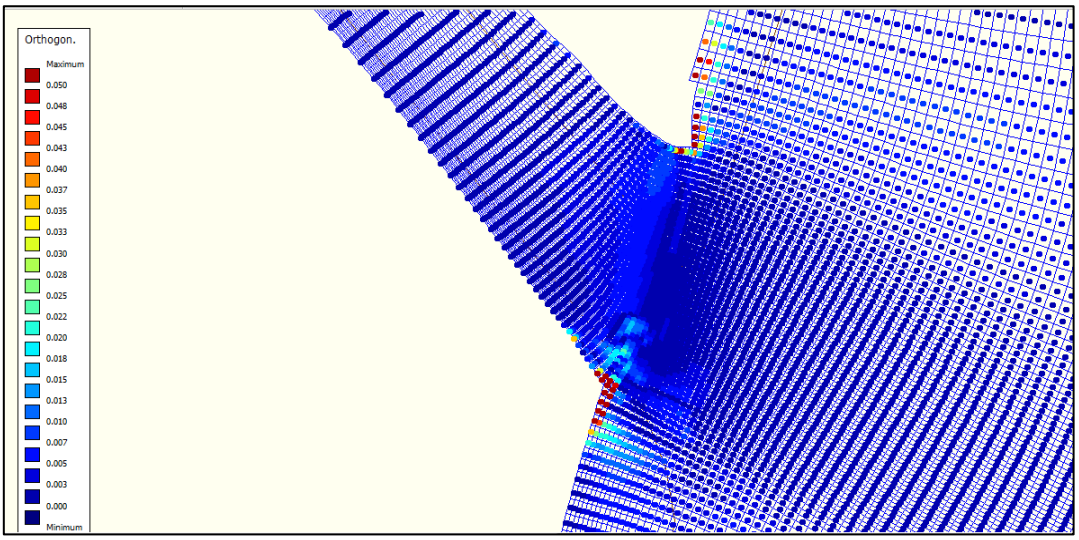

Figure D. 9 - Orthogonality of detail of grid

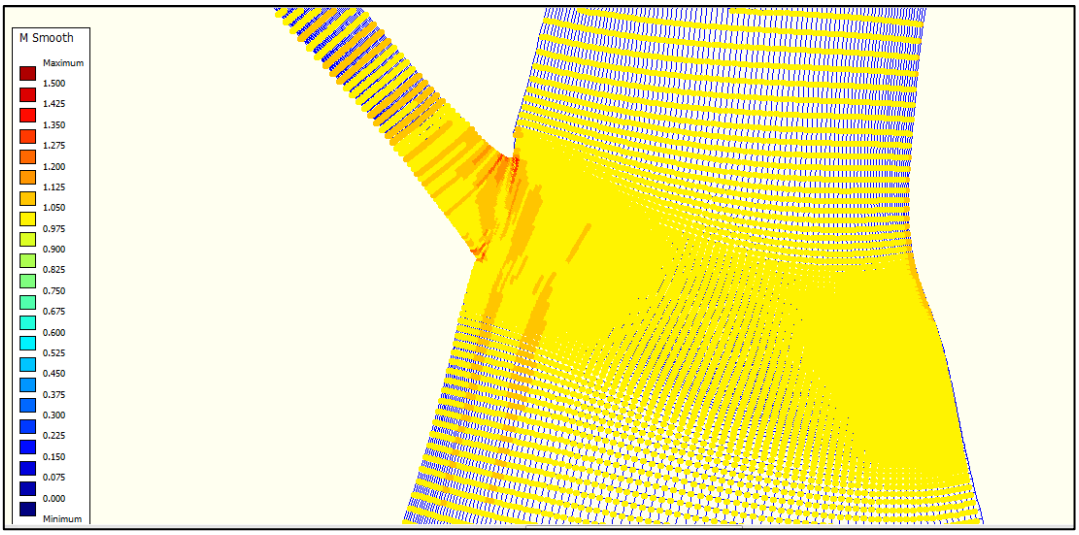

Figure D. 10 - Smoothness grid in m-direction

D.2.2.2 Grid following the offtake

Within this study we are interested in representing the currents and sediment transport in the offtake accurately, as the main aim of this study is to decrease the discharge and sediment transport in the offtake. The contour lines are chosen to create a stream from the Río Magdalena to the Canal del Dique as shown in Figure D. 11 and detailed in Figure D.12. The orthogonality of the grid is given in Figure D.13 and detailed in Figure D.14. Finally, the smoothness in m-direction is shown in Figure D.15.

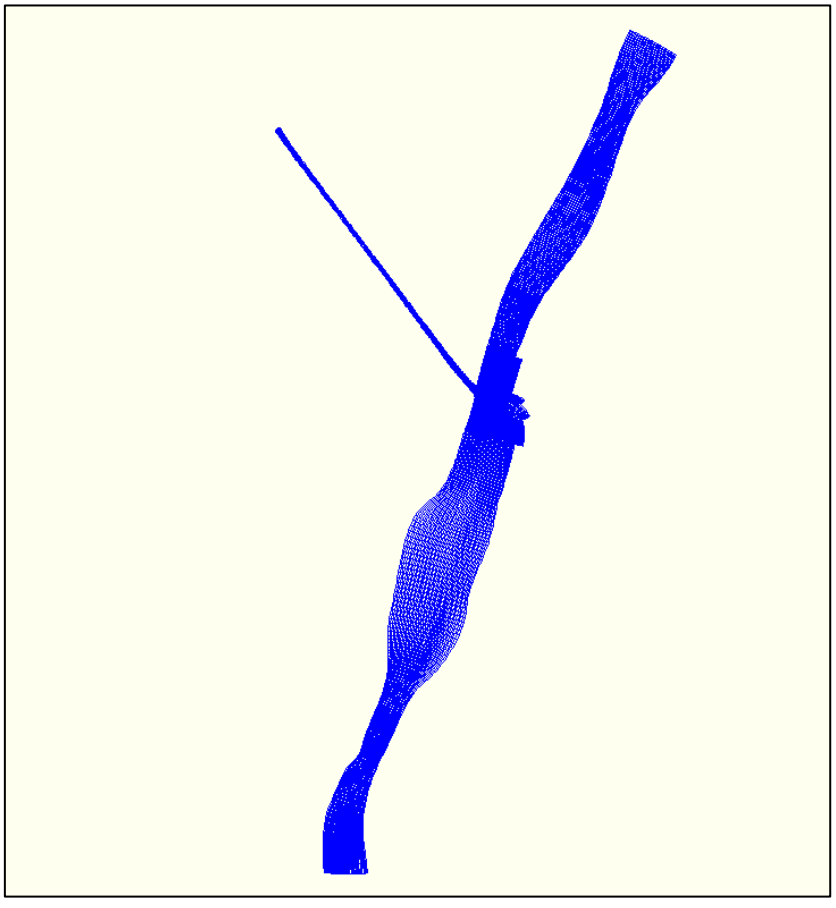

Figure D. 11 - Grid following offtake

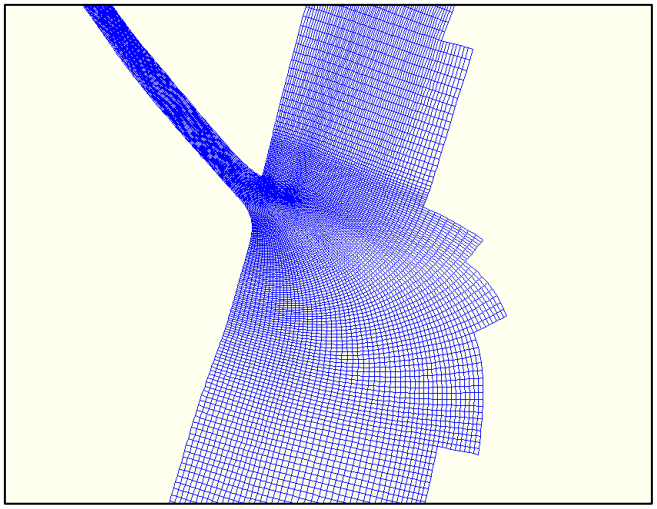

Figure D.12 - Detail of grid following the offtake

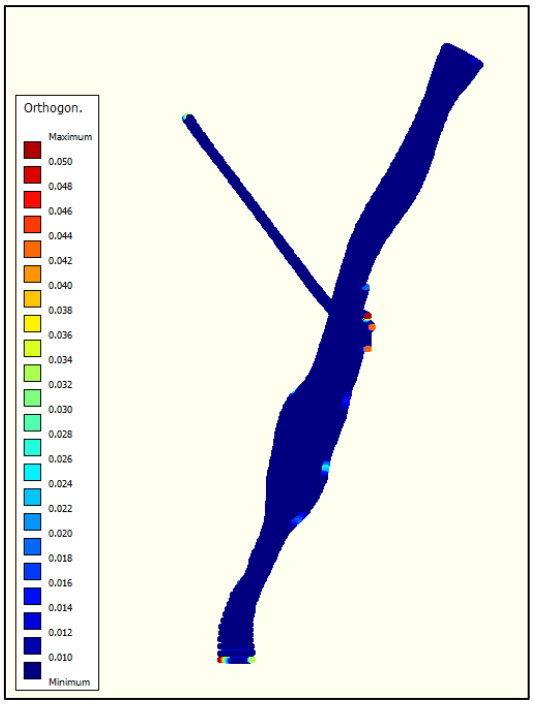

Figure D.13 - Orthogonality grid following offtake

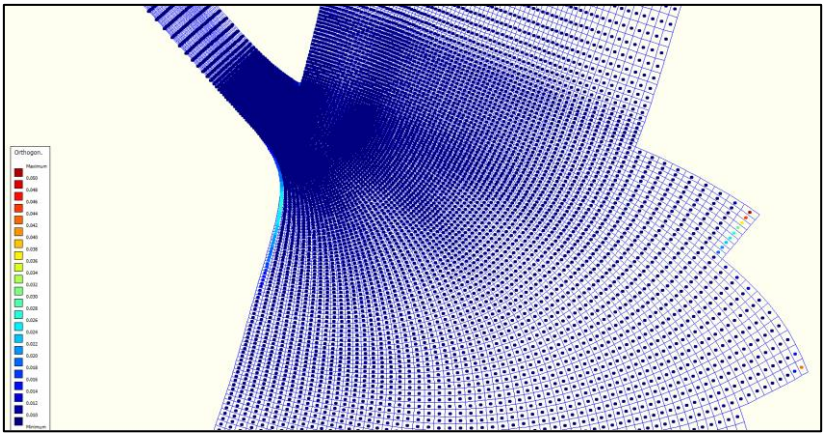

Figure D.14 – Orthogonality detail grid following offtake

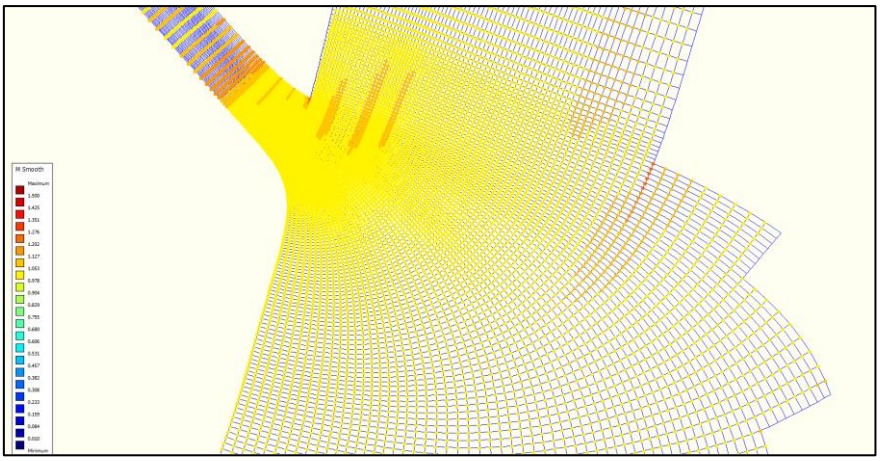

Figure D.15 – Smoothness grid in m-direction

D.2.2.3 Resolution grid

The resolution of the grid, the square root of the grid cell area, is for both generated grids around 4 meter in the area of interest. It is to be expected that this resolution is small enough to compute accurate results, but large enough to avoid long computation times. However, it has to be checked if difference in flow simulation can be seen when applying a smaller grid resolution.

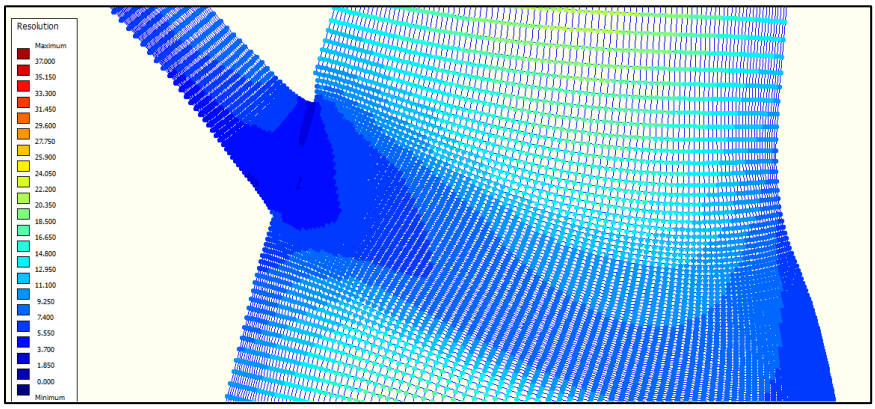

Figure D. 16 - Resolution grid for grid following main stream

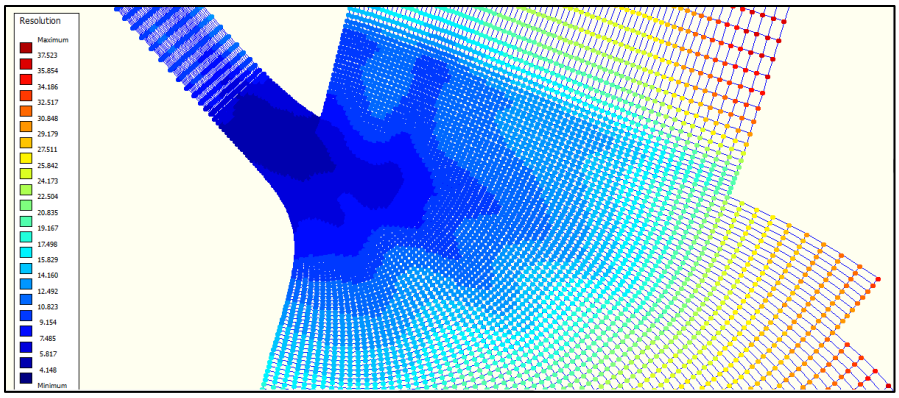

Figure D. 17 - Resolution grid for grid following offtake

D.2.2.4 Conclusion

From Figure D. 9 and Figure D.14 it can be seen that the orthogonality of both grids are met between the land boundaries. However, the orthogonality of the grid following the main stream is harder maintained in the left corner at the entrance of the offtake. On the other hand, the smoothness of the grid following the main stream is higher than the smoothness of the grid following the offtake. Therefore, a simulation with both grids should be made to find possible differences.

Figure D. 20 to Figure D. 22show the depth averaged velocities for the grid following the offtake in comparison to the grid following the main stream. It is visible that the velocities are slight different. For example the velocity is higher along the left branch of the upstream island and along the right branch of the downstream island for the grid following the main stream However, differences in velocity are mostly caused by different grid domain (the upstream boundary of the grid following the offtake lies more downstream) and difference in depth. Figure D. 18 and Figure D. 19 show the differences in depth of both grids. These differences in depth occur as the bathymetry is made using the grids.

However, the differences in velocity between both grids are minimal and mostly caused by differences in depth. As the smoothness and orthogonality of the grid is better obtained with the grid following the offtake and our interest lies in the discharge in the offtake, this grid is chosen for the simulations.

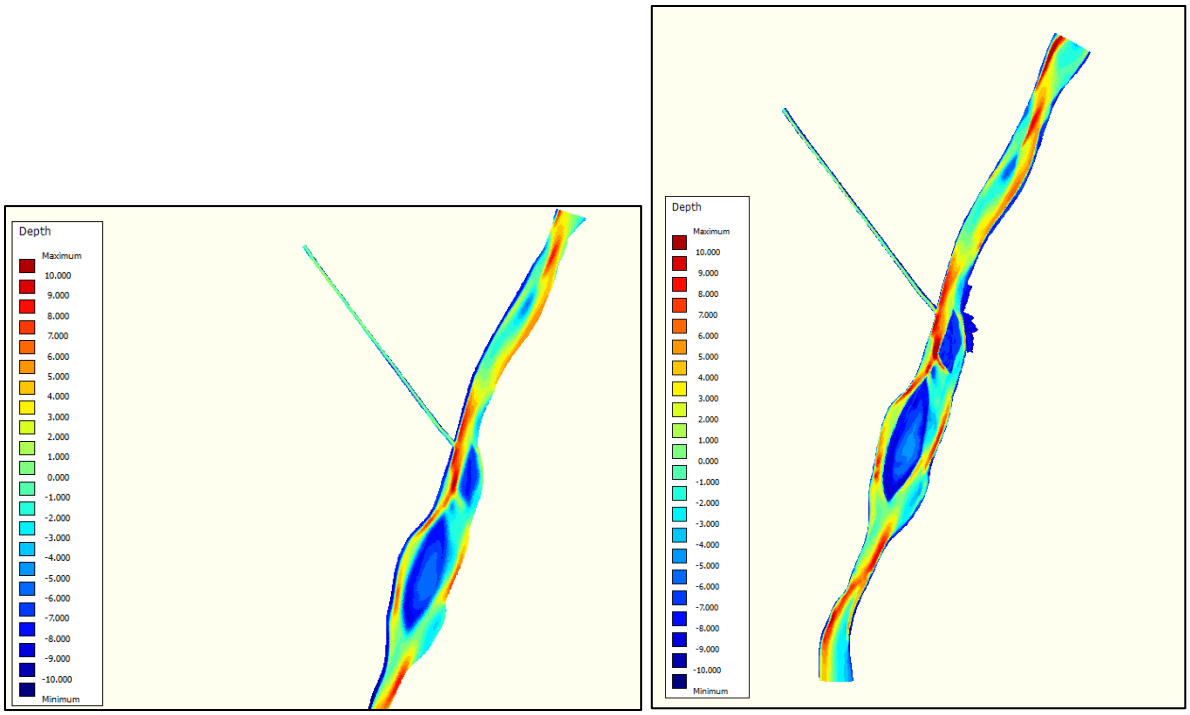

Figure D. 18 - Depth for grid following main stream (left) and grid following offtake (right)

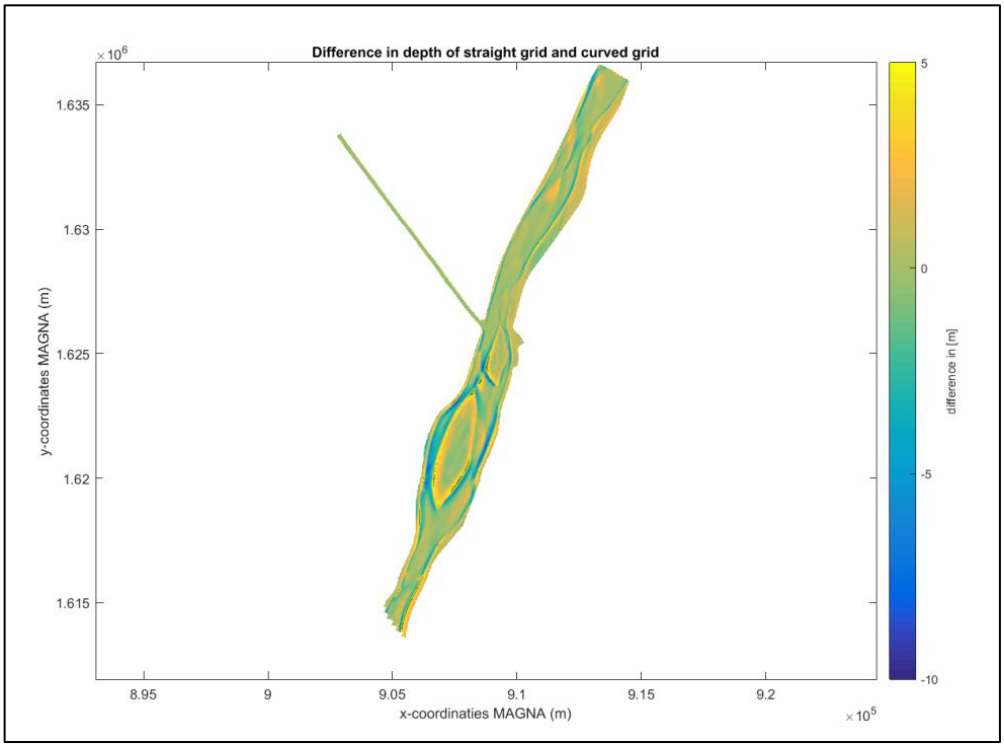

Figure D. 19 - Difference in depth of grid following main stream and grid following offtake.

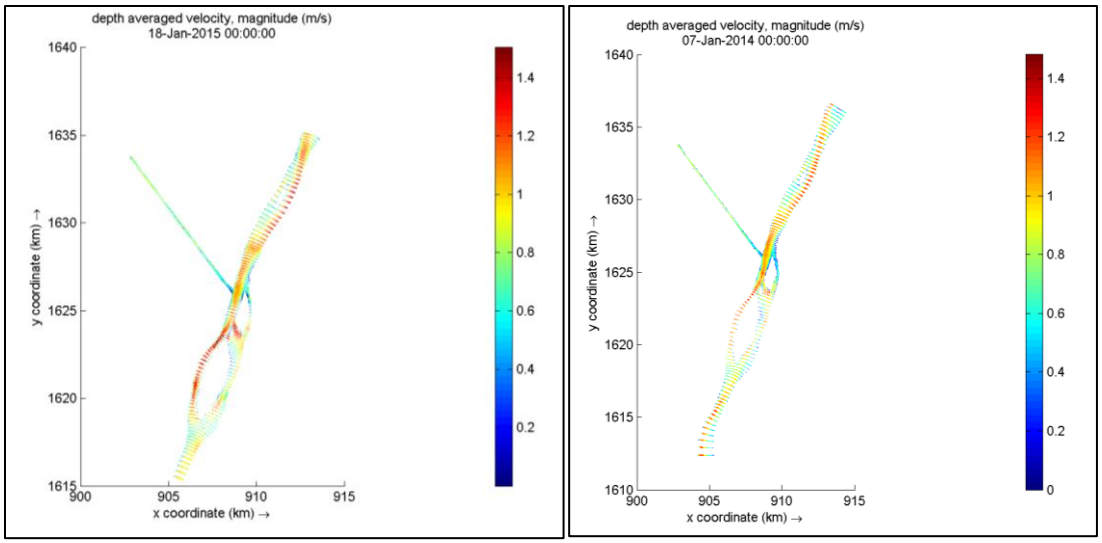

Figure D. 20 - Depth averaged velocity for grid following main stream (left) and grid following offtake (right)

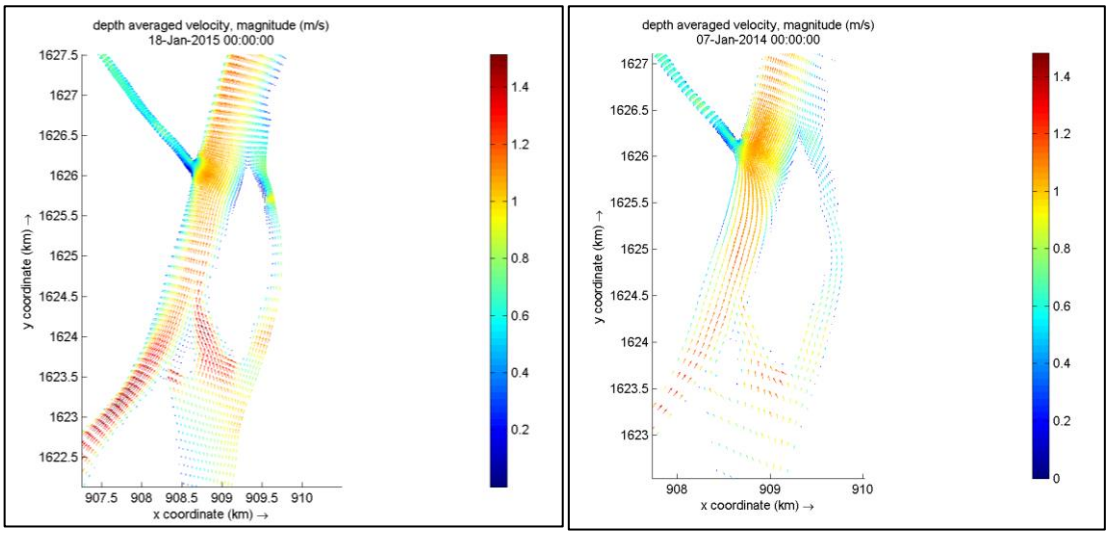

Figure D. 21 – Depth averaged velocity for grid following main stream (left) and grid following offtake (right)

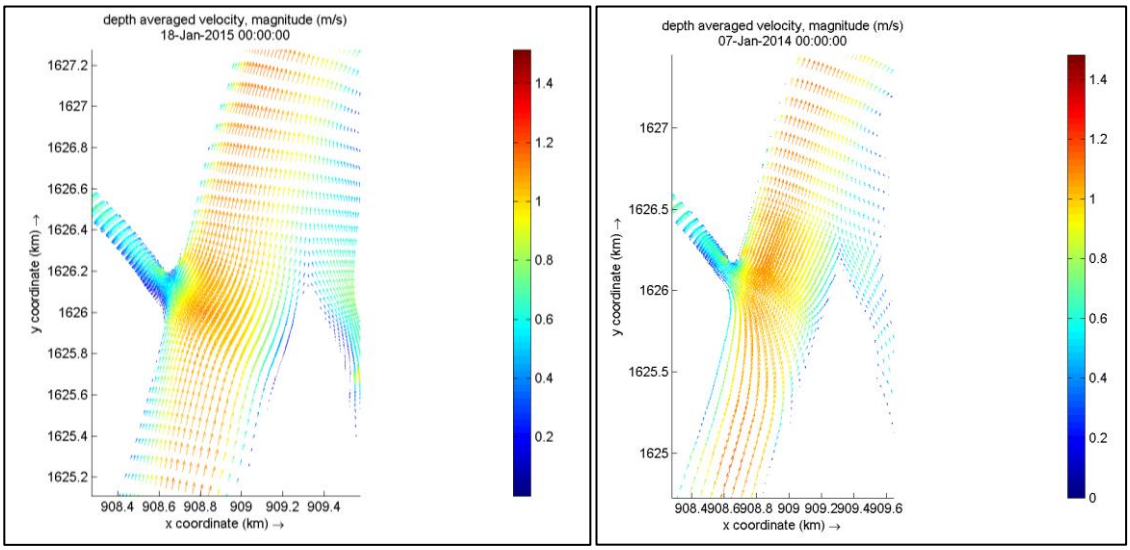

Figure D. 22 - Depth averaged velocity for grid following main stream (left) and grid following offtake (right)

D.2.3 Boundary conditions

In this study, a combination of discharge at the upstream boundary and water level at both downstream boundaries is used. As we are interested in changes in the discharge of the offtake a downstream water level boundary is preferred above a fixed discharge boundary. However, when it is desired to obtain a fixed discharge in one of the branches a discharge boundary can be imposed downstream. The influence of this boundary condition will be investigated in the calibration phase.

However, it has to be bared in mind that using a discharge boundary upstream *and* downstream can cause unstable results. As when the downstream imposed discharge does not correspond to the equilibrium volume, excess or shortage of water cannot leave the area resulting in inaccurate results. Therefore, small errors are easily occurred. An example is shown in Figure D. 23, from which it can be seen that the equilibrium water depth is not reached and the water level downstream is too high resulting in high flow velocities downstream. Other combinations as two water levels, two velocity boundaries or a water level upstream and a discharge downstream gives inaccurate results as not enough information is available to solve the back-water equations.

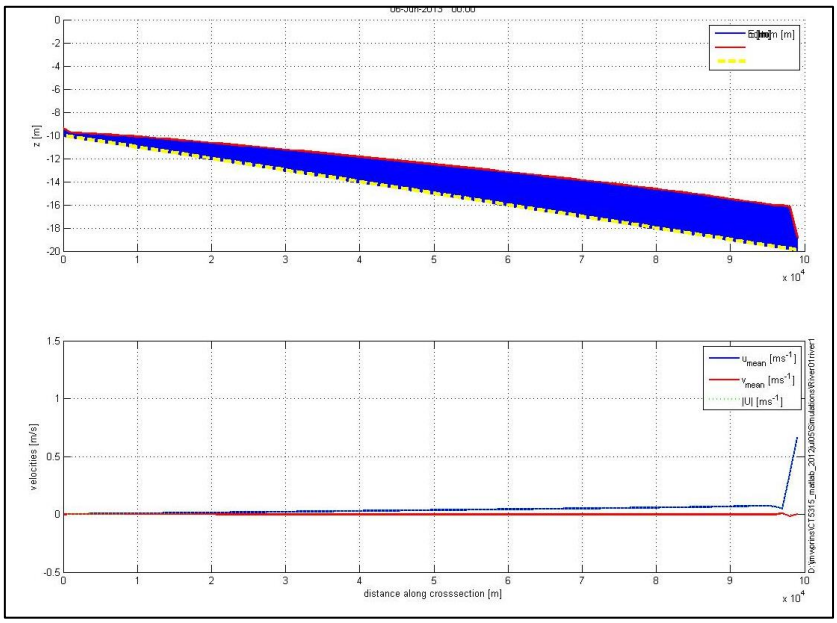

Figure D. 23 - Example of a combination of imposed discharge upstream and downstream on a river stretch

In this study, three different boundary combinations are used corresponding to seasonally low, mean and high discharge of the Río Magdalena and Canal del Dique. The discharge at the upstream boundary is obtained from three measurement campaigns of Consorcio Dique during March, May and November 2014 for respectively low, medium and high discharge. These measurements are assumed to be reliable and will therefore be used.

Nevertheless, water level measurements at the exact location of the boundaries of our model are not available. Therefore, water level data at the location of the boundaries is obtained from the Sobek model of Consorcio Dique (2015) which is assumed to be reliable. The Sobek model covers the whole Canal del Dique and the Río Magdalena from Barrancavieja, approximately 10km upstream of the Canal del Dique, to the sea at Barranquilla. The model uses historical water level and discharge data from January 1985 to October 2014 and is calibrated to the mean rating curve (red line in Figure D. 24) obtained from these historical measurements.

It appears that the measurements of 2014 lie 10% above this mean rating curve. Therefore, the discharges from the Sobek model at the measurement dates are computed lower than the measured values. To avoid these differences in computed discharges the measured discharges are used in combination with the water levels at the downstream boundary locations as computed with the Sobek model at the same date. The used boundary conditions for low, medium and high discharge are shown in Table D. 1.

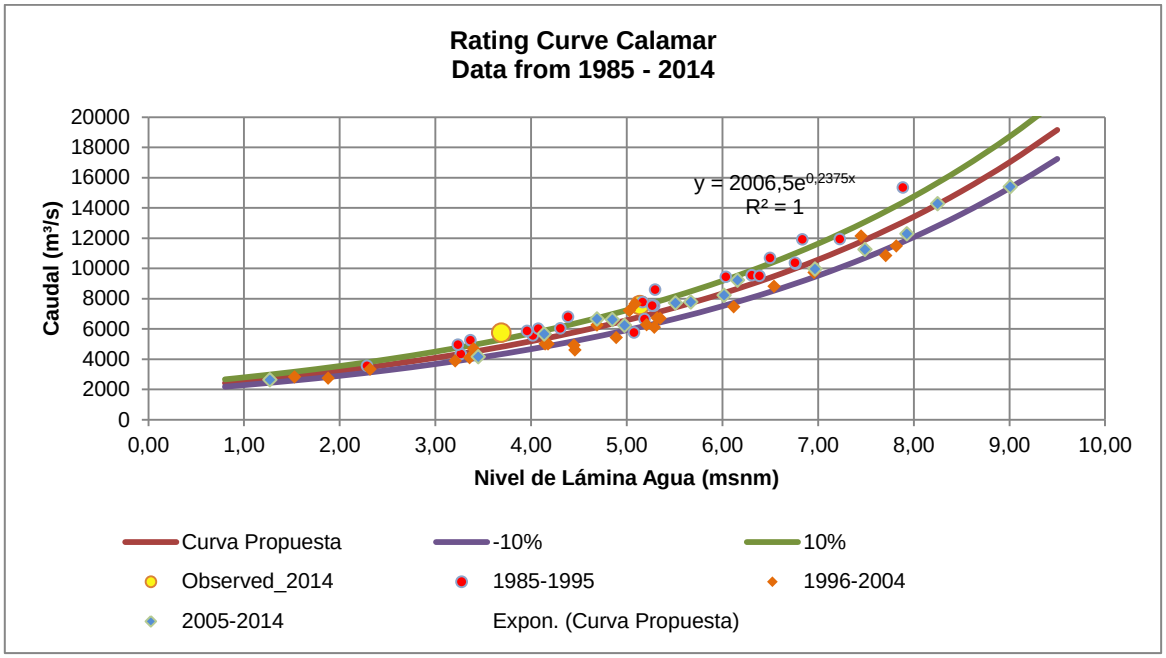

Figure D. 24 - Rating curve for Calamar at Río Magdalena (Consorcio Dique, 2015)

Table D. 1 - Boundary conditions used for this study

Measurement date	Discharge at upstream boundary [m^3/s]	Water level at downstream boundary Canal del Dique [m]	Water level at downstream boundary Río Magdalena [m]
March 13, 2014	Q low = 5737 m^3/s	3.28	3.03
May 23, 2014	Q mean = 7572 m^3/s	4.54	4.32
November 29, 2014	Q high = 8973 m^3/s	5.5	5.29

D.2.4 Model settings

In Delft3D-FLOW several settings can be used concerning the applied numerical scheme and the calculated flow of the grid sized. As a starting point the default settings are used:

- Bathymetry: values specified at corners and cell centre values computed using maximum value.
- Grid:
  - Latitude: 10 [dec. deg]
  - Orientation: 0 [dec. deg]
  - Number of layers: 1 (depth-averaged)
- Numerical parameters:
  - Depth at grid cell faces: mean
  - Advection scheme for momentum: cyclic (implicit scheme, unconditionally stable)

D.3 Calibration

D.3.1 Hydrodynamics

For calibration of the hydrodynamics the bed roughness and viscosity are varied in order to find the best fit in modelled and measured water level and discharge. Besides, the influence of the time step is investigated to obtain the optimal time step in order to reduce simulation time and to obtain accurate results. Also, the sensitivity of changes in boundary conditions and the grid resolution is tested.

Minimum and maximum values for bed roughness, viscosity and Courant number (time step restriction) are obtained from the Delft3D-FLOW user manual (Deltares,2014). The values between which the model has been calibrated and the values used in the reference case are shown in Table D. 2.

Table D. 2 – Calibration values of bed roughness, viscosity and time step

Parameter	Variation	Reference case
Bed roughness (Manning-coefficient [$s/m^{1/3}$])	[0:0.04]	Río Magdalena: 0.03; Canal del Dique: 0.025
Viscosity [m^2/s]	[1:10] (for grid sizes < 10m)	1
Courant number	[1:10]	Time step 1 min

The offtake-model will be calibrated on the discharge in the Canal del Dique, the water level at Calamar and Incora and the discharge distribution along the islands at the Río Magdalena. Besides, the water level gradient at the Canal del Dique and Río Magdalena will be checked to avoid backwater effects. Also, the velocity profiles at the cross-section locations are checked. An overview of the cross-sections and water level measurement locations is shown in Figure D. 25.

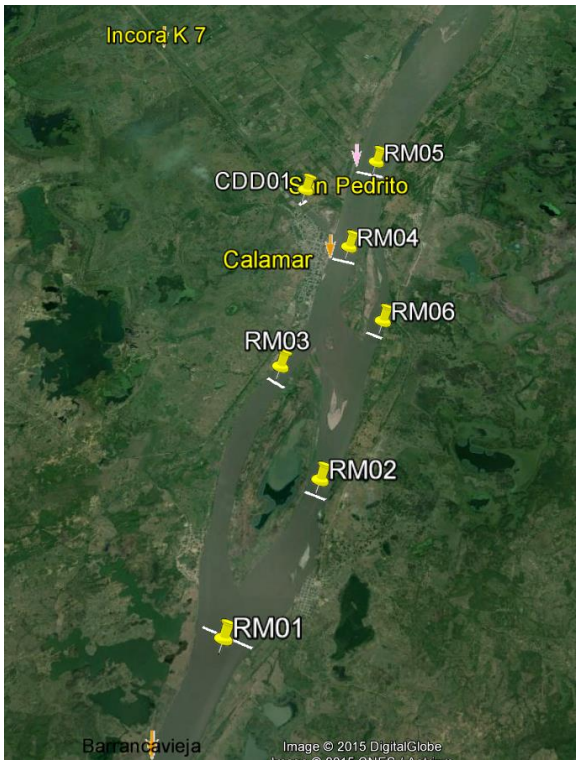

Figure D. 25 - Overview measurement locations

D.3.1.1 Time step

First of all, it is investigated what the preferred time step and simulation time should be in order to obtain accurate results and minimise simulation time. Therefore a time step of 1, 0.1 and 10 minutes will be applied to assess the differences. From Figure D. 26 it can be seen that the solution converges after half a day for all of the simulation times. However, when applying a time step of 10 minutes the solution shows wiggles. Therefore, it can be concluded that this time step is too large to give accurate results. On the other hand, when applying a time step of 0.1 minute, the simulation increases largely compared to a time step of 1 min. Besides, it can be seen that the result of water level and discharge are almost equal for a time step of 1 and 0.1 min.

From this investigation it can be concluded that a time step of 1 min with a simulation time of 1 day gives accurate results and the shortest simulation time. However, the accuracy of the model should be checked every simulation. When the time step of 1 minute becomes too large a smaller time step should be applied.

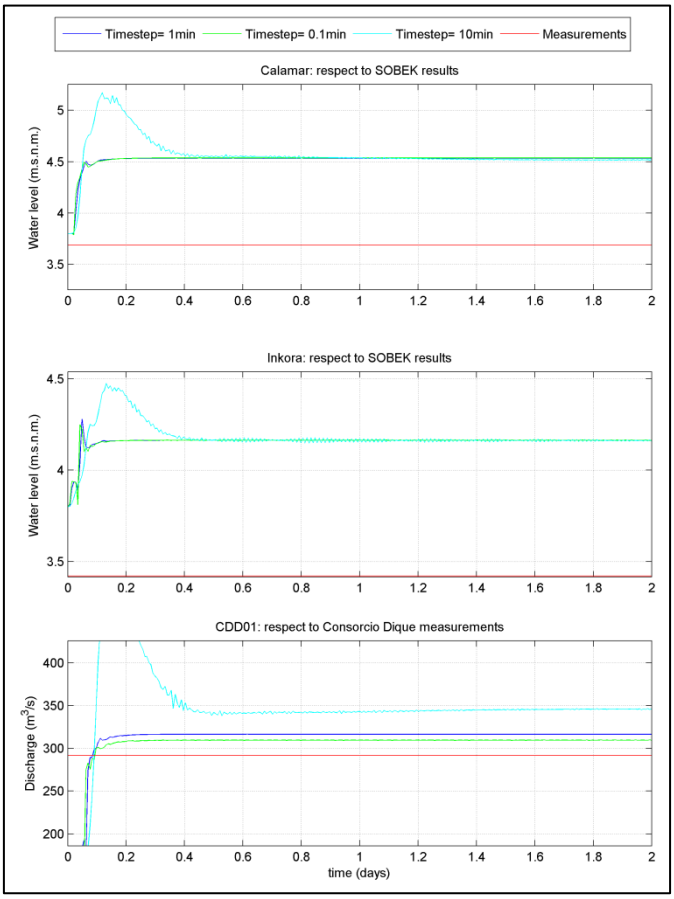

Figure D. 26 – Water level and discharge calibration for different time step

D.3.1.2 Boundary-condition

The sensitivity of the downstream boundary-condition is investigated. First of all, the downstream water level at the Canal del Dique is lowered with a few centimetres for which the result is shown in Figure D. 27. It can be seen that therefore also at Inkora, located 7km downstream of the Canal del Dique, the water level is lower. The water level at Calamar, located at the Río Magdalena just

upstream of the bifurcation, remains equal. Therefore the water level gradient in the Canal del Dique becomes larger causing a higher discharge.

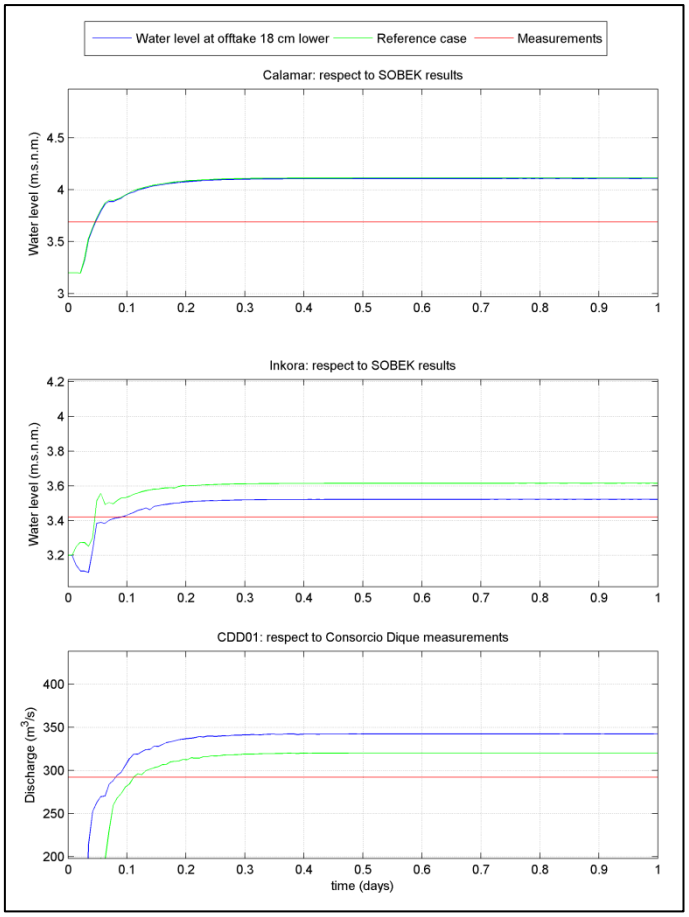

Figure D. 27 - Discharge and water level for reference case (green), downstream water level at Canal del Dique lowered with 18cm (blue) and the measured value (red)

Furthermore, a fixed discharge at the downstream boundary of the Canal del Dique is imposed. Imposing a discharge downstream can be preferred when the discharge in the offtake is regulated to a fixed discharge in the offtake. The difference between a water level boundary at the offtake and discharge is shown in Figure D. 28. From which it is seen that (of course) the discharge in the offtake fits perfectly, however the water level at Inkora is overestimated compared to the measurements.

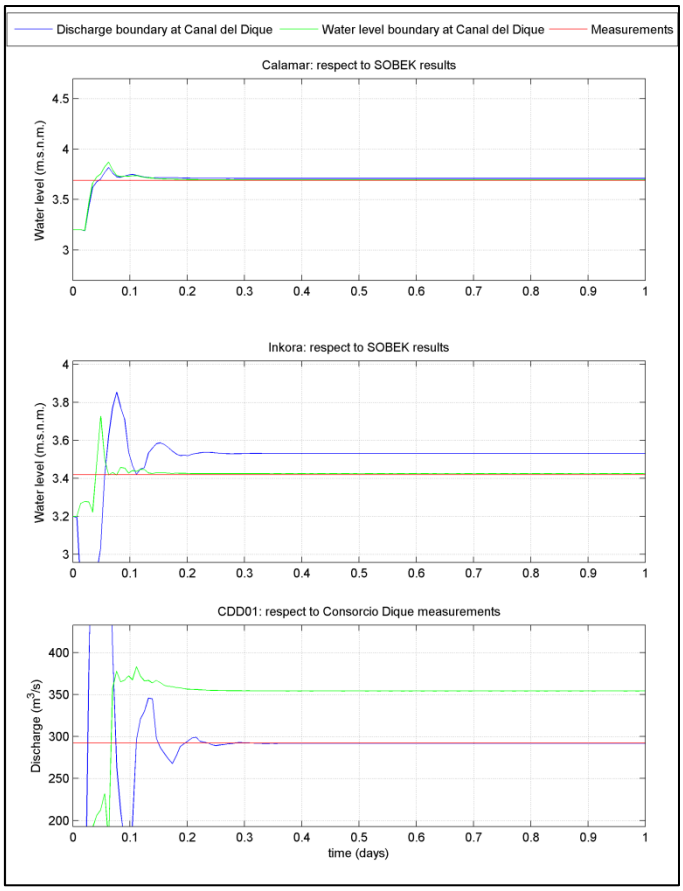

Figure D. 28 - Calibration boundary condition with fixed boundary offtake (blue), water level boundary (green) and measurement

Finally, it is evaluated whether the values for the three measurement campaigns with a low, medium and high discharge give different results regarding the discharge distribution along the islands and the bifurcation. The results are shown in Figure D. 29, where the discharges are taken relative to the corresponding upstream discharge. It can be seen that discharge increases in the offtake ('CDD01') and the right branches ('RM02' and 'RM06') and slightly decreases in the left branches ('RM03' and 'RM04') for the medium and high discharge. This is due to the fact that the islands are partly flooded during medium and high discharge (Figure D. 30) causing a lower water level along the right branches and respectively higher discharge.

In this study, the low discharge boundary will be used for calibration and simulation of several cases as this corresponds best to the upstream discharge boundary as used in the one-dimensional model. However, as it is seen that for high discharges the islands can be partially flooded, also checks should be made for medium and high discharge.

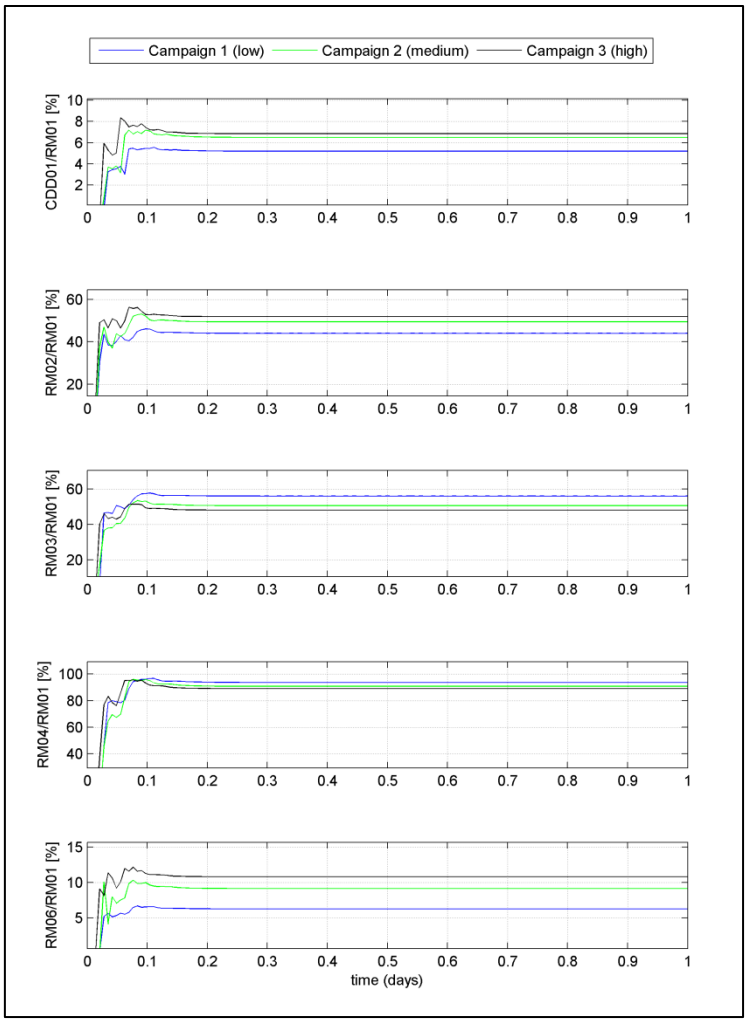

Figure D. 29 - Relative discharge distribution to upstream boundary condition for low (blue), middle (green) and high (red) discharge

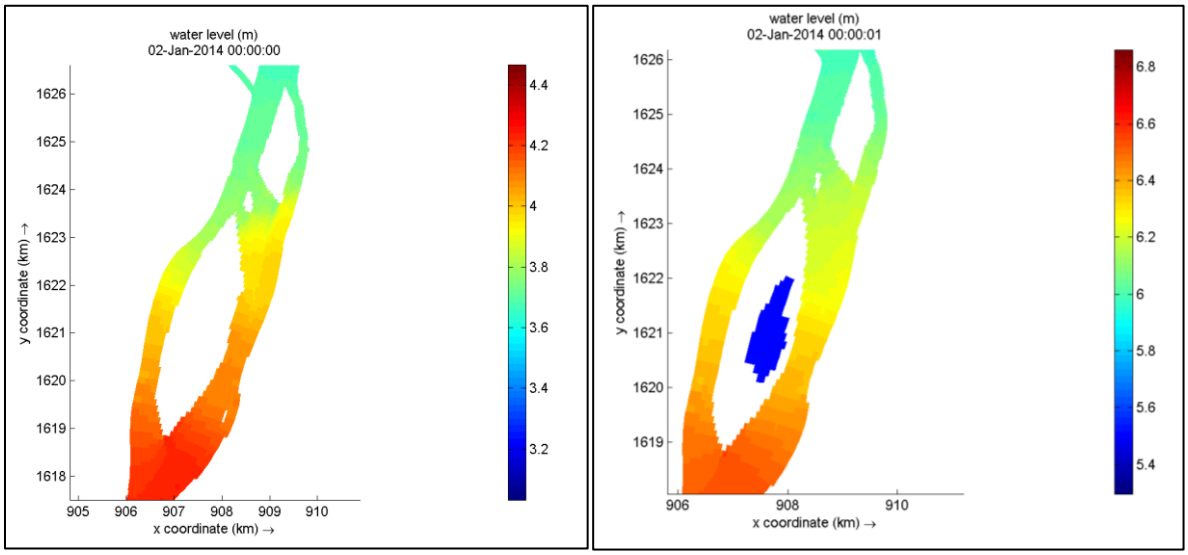

Figure D. 30 – Water level for low discharge (left) and high discharge (right)

D.3.1.3 Grid resolution

The resolution of the grid should be small enough to capture most of the import flow structures, like (large) turbulent eddies, but large enough to decrease computation time. Therefore, a grid with a resolution of approximately 4x4 metre in the area of interest at the bifurcation is used (Figure D. 31). Secondly, this grid is refined in m- and n-direction with a factor 2 resulting in a resolution of 1x1 metre in the area of interest (Figure D. 32).

It is tested if using a finer grid will impact the discharge distribution along the branches and the flow pattern. From Figure D. 33 it can be seen that the discharge distribution remains equal for both grids. Also, the flow pattern for both grid sizes is the same as visible from Figure D. 34.

However, the computation time for the fine grid increases largely. Hence, it is preferred to use the grid with a resolution of 4x4 metre to be able to compute a lot of simulations in a smaller amount of time. Though, it has to be bared in mind that in the case of complex geometries where small scale turbulent patterns can play a role it might be necessary to use a finer grid.

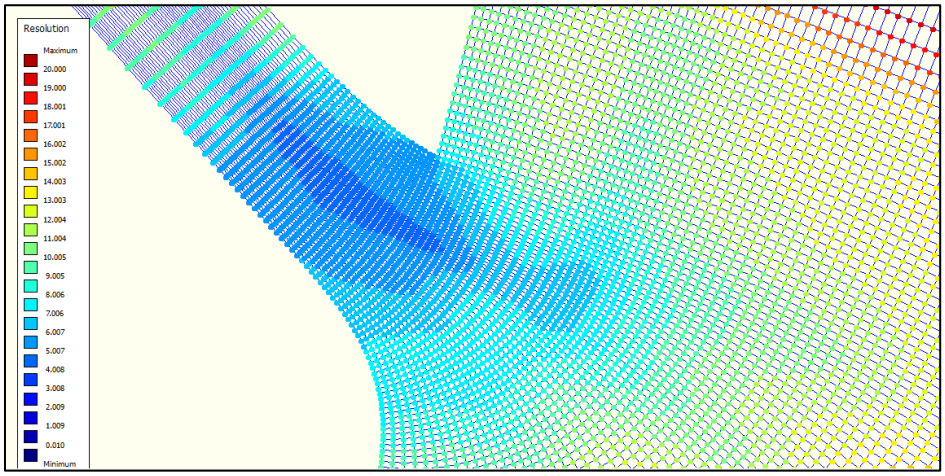

Figure D. 31 — Resolution grid with finest grid size of 4x4 metre

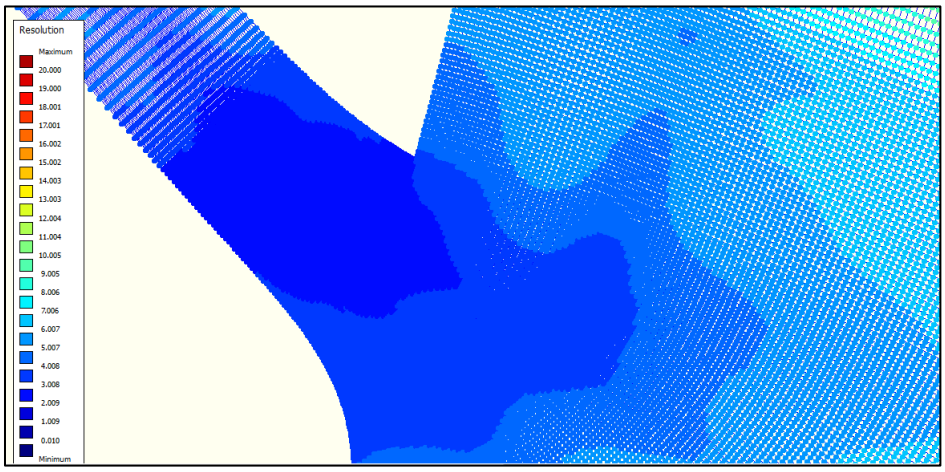

Figure D. 32 - Resolution grid with finest grid size of 1x1m

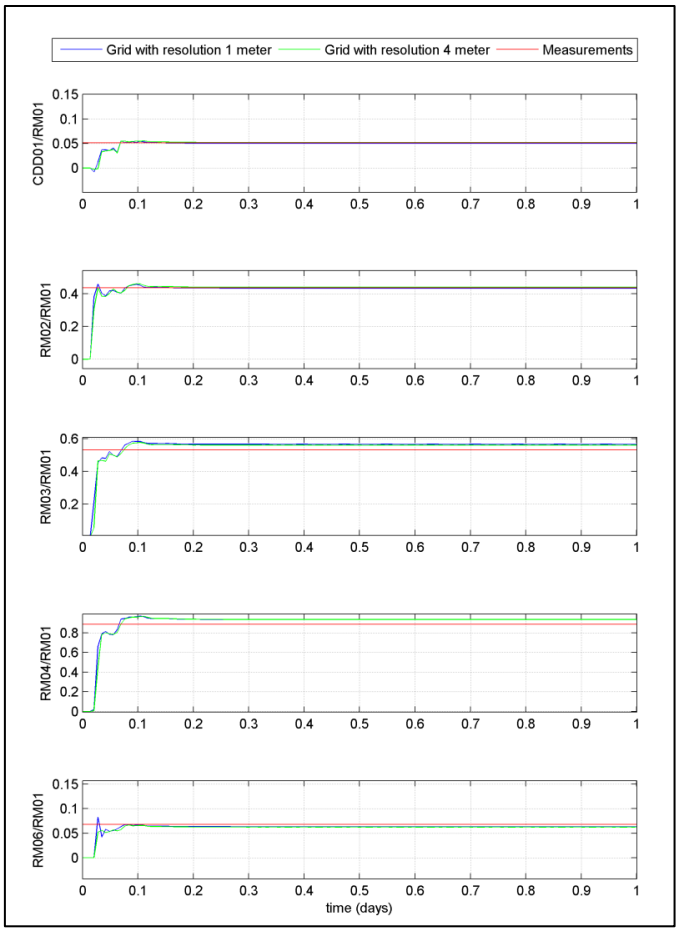

Figure D. 33 - Discharge distribution grid size with resolution 1 meter and 4 meter

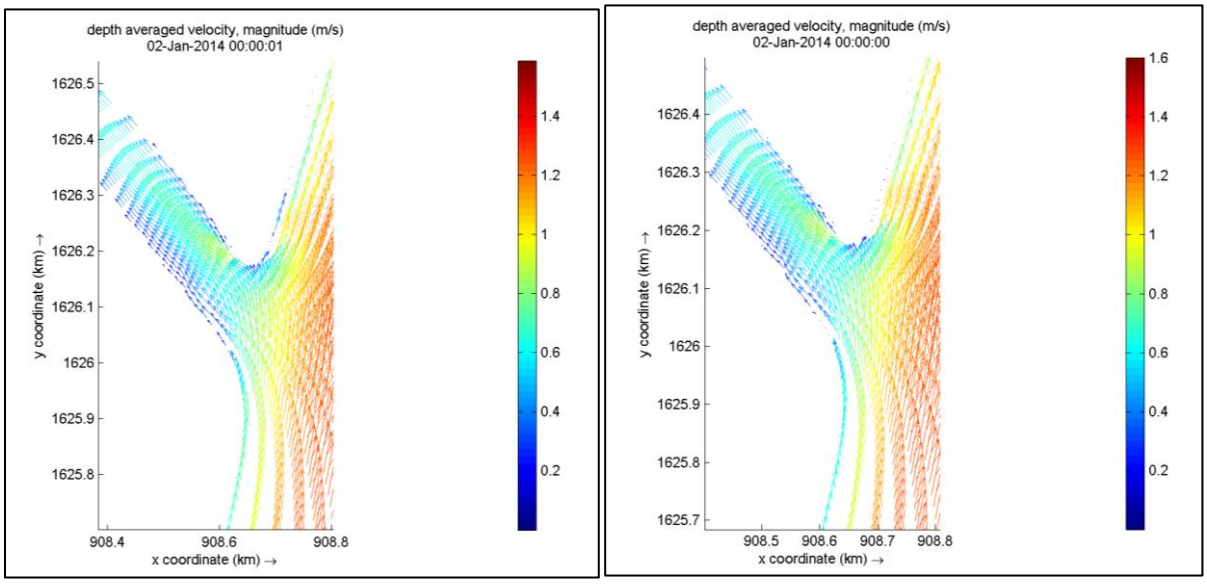

Figure D. 34 - Left: flow for grid with resolution 1 meter; right: velocity for grid with resolution 4 meter

D.3.1.4 Viscosity

The horizontal eddy viscosity (ν_H) in the depth-averaged mode of Delft3D represents the horizontal turbulent motions and forcing that are not resolved by the horizontal grid, so called 'sub-grid scale turbulence', or the Reynolds-averaged shallow water equations. The horizontal eddy viscosity is user

defined or can be calculated through the Horizontal Larger Scale Eddy Simulation (HLES). For this case, the horizontal eddy is taken uniform over the grid and will be determined by calibration. For grid sizes of 10 meter or smaller a viscosity between 1 and 10 m^2/s is typically applied where a viscosity of 1 m^2/s is used as default in Delft3D-FLOW (Deltares 2014). The vertical eddy viscosity is not calculated in depth average calculations and is generally much smaller than the horizontal eddy viscosity.

Computing different viscosity values gives different results for water level and discharge as shown in Figure D.35. It can be seen that the water level at Calamar and Inkora, however smaller, increases with higher viscosity. For low viscosity values the discharge in the offtake increases and fits the measured discharge less. This is also seen when the discharge distribution for different viscosity values is computed as shown in Figure D. 36. Due to the lower viscosity, smaller scale turbulent motions are computed as shown in Figure D. 37. Due to these turbulent motions, higher shear stresses occur which cause higher flow velocities in the offtake. Besides, the eddies in the corners of the offtake cause the main streamlines to become more contracted which also explain the higher velocity in the offtake. Furthermore, due to the higher shear stresses more dissipation of energy occurs causing lower water levels. Finally,Figure D. 38 shows that the same holds for different upstream discharges.

So, using a lower viscosity gives smaller turbulent motions which might represent reality better. However, low viscosity values also causes more unstable results. Therefore, higher viscosity values are used to numerically supress the non-physical spurious oscillations, or so called 'wiggles', resulting in a more stable solution. This is for example shown in Figure D. 39, where the water level at Incora shows wiggles at a viscosity of 0.5m^2/s and not for a viscosity of 5 m^2/s.

As it is seen from Figure D. 35 that the discharge in the offtake is best represented with a horizontal eddy viscosity of 1m^2/s, which is also the default value in Delft3D, this value will be used in this study.

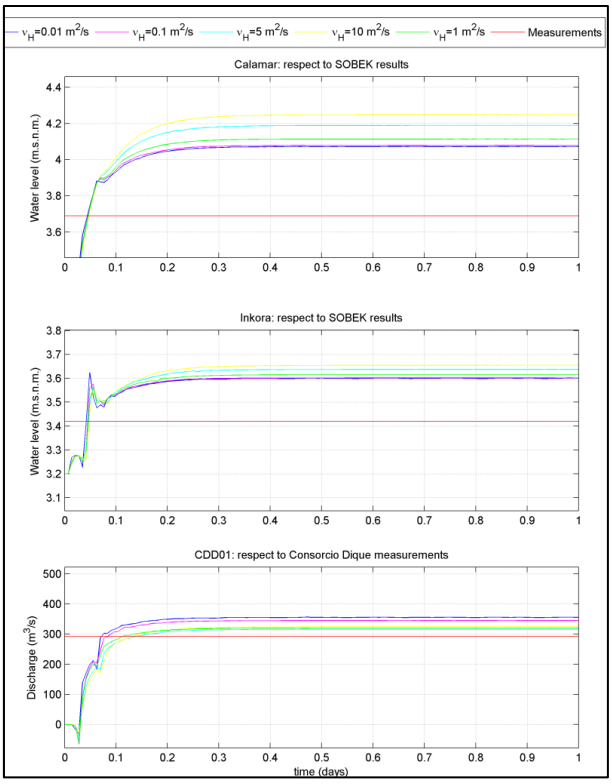

Figure D. 35 - for different horizontal eddy viscosity, campaign 1: Q=5737 m^3/s

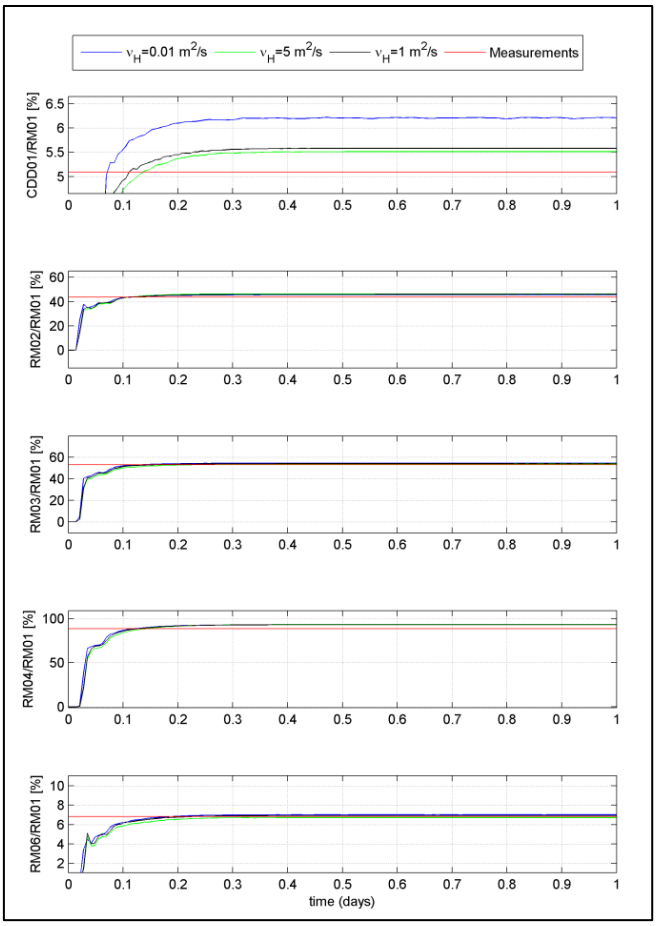

Figure D. 36 – Discharge distribution relative to upstream discharge for different viscosity values

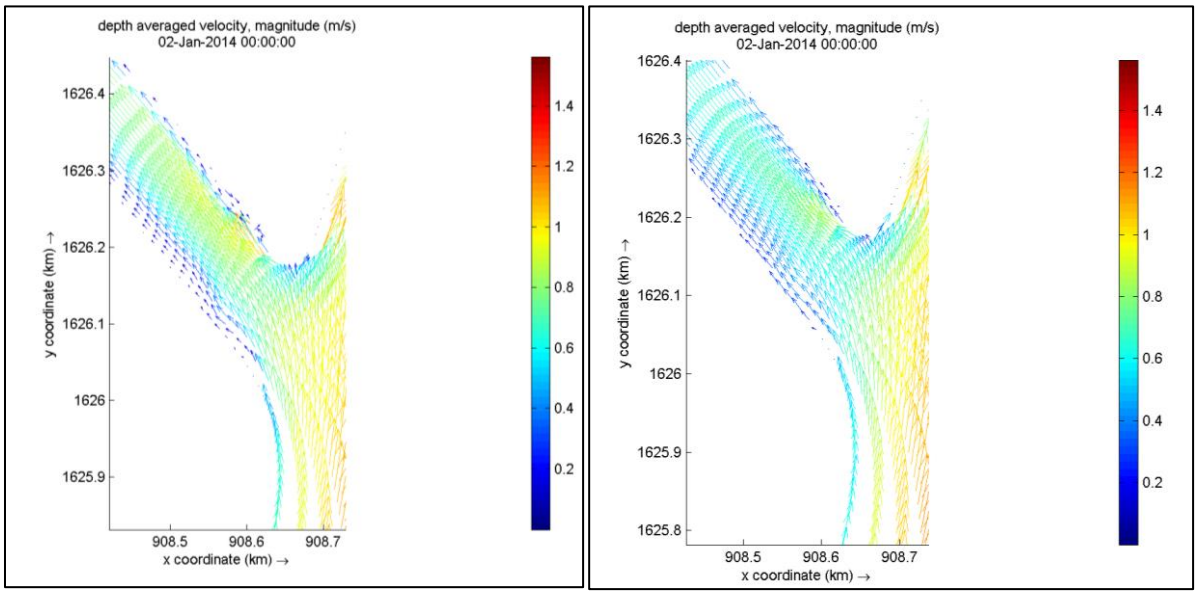

Figure D. 37 - Left: velocity for viscosity of 0.01 m^2/s; right: velocity for viscosity of 1 m^2/s

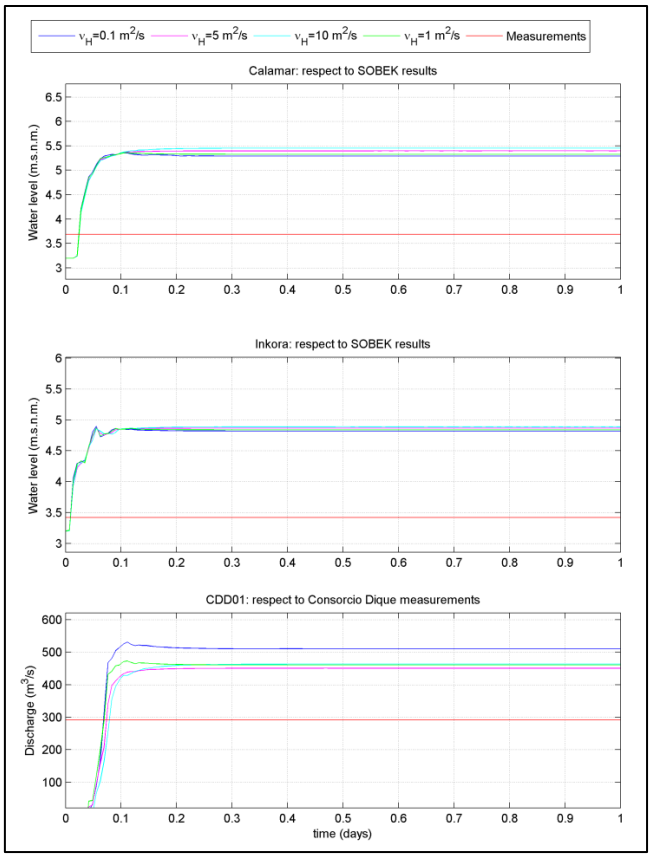

Figure D. 38 – Calibration for different horizontal eddy viscosity, campaign 2: Q= 7572 m^3/s

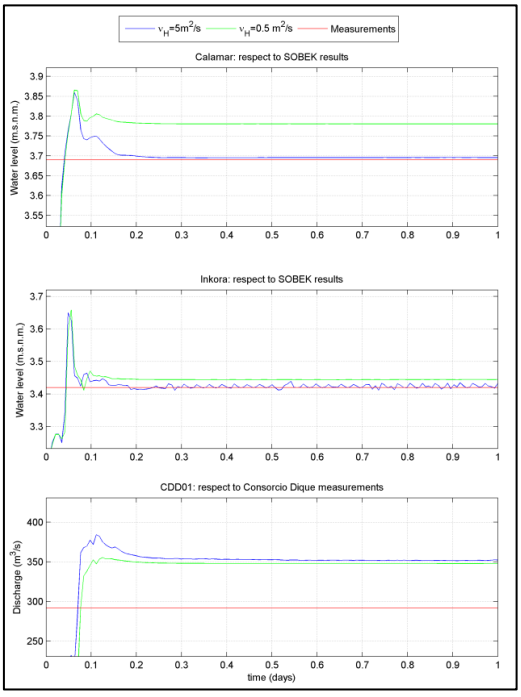

Figure D. 39- Calibration water level and discharge for a horizontal eddy viscosity of 5 m^2/s and 0.5 m^2/s

D.3.1.5 Bed-friction

The bed-roughness can be implemented in Delft3D using different roughness formula. In this study, the formula according to Manning is used, where the Manning coefficient n [s/m$^{1/3}$] must be specified. The corresponding Chézy friction coefficient is calculated from:

$$C = \frac{H^{1/6}}{n}$$

where, H is the water depth.

The calibration process showed that not one value for the bed-friction of the Río Magdalena can be found for which the water level and discharge in the Canal del Dique fits with the measured values for both low, medium and high discharges. This can be caused due to the formation of bed forms during high discharges, which increases bottom roughness. The bed-friction in the canal is however constant for all calibration cases. Overall, calibration using bottom roughness as calibration parameter shows good results. Water levels are predicted within a few centimetres accuracy and discharges within a few percent as shown in Table D. 4. The exact roughness values which gave the best fit for the three discharges (low, medium and high) are shown in Table D. 3.

Table D. 3 - Calibration results for the three measurement campaigns

		Case 1	Case 2	Case 3
Q CDD01 (m^3/s)	Observed	292	501	630
	Delft3D	298	492	615
H Calamar (m.s.n.m.)	SOBEK	3.69	5.01	6.01
	Delft3D	3.72	5.07	6.03
H Incora (m.s.n.m.)	SOBEK	3.42	4.70	5.67
	Delft3D	3.44	4.73	5.67

Table D. 4 - Manning's n values for which the best results were obtained

	Case 1	Case 2	Case 3
Río Magdalena	0.022	0.025	0.027
Canal del Dique	0.016	0.016	0.016

The best fit for low discharge occurs for a bed roughness of 0.016 (Manning n) at the Canal del Dique and at the Río Magdalena of 0.022 (Figure D. 40).

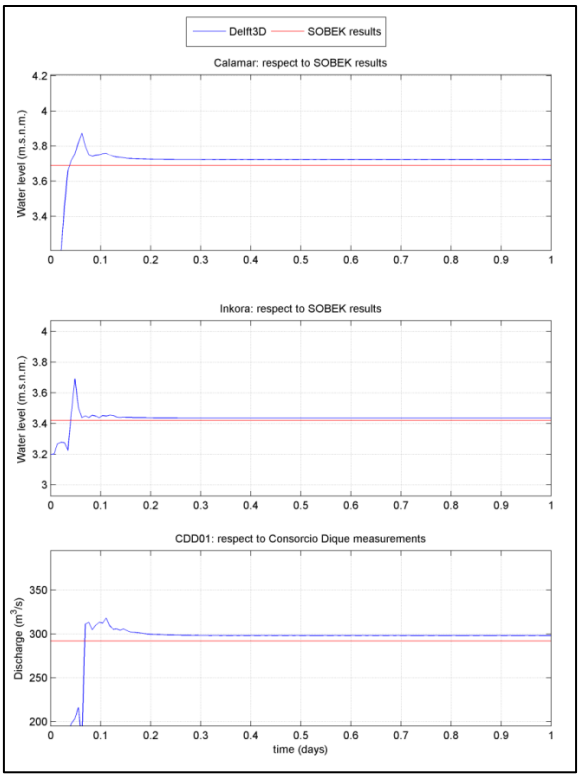

Figure D. 40 – Calibration result for low discharge (case 1)

The best fit for the medium discharge of 7572 m^3/s occurs for a bed roughness of 0.016 at the Canal del Dique and at the Río Magdalena of 0.025 (Figure D. 41).

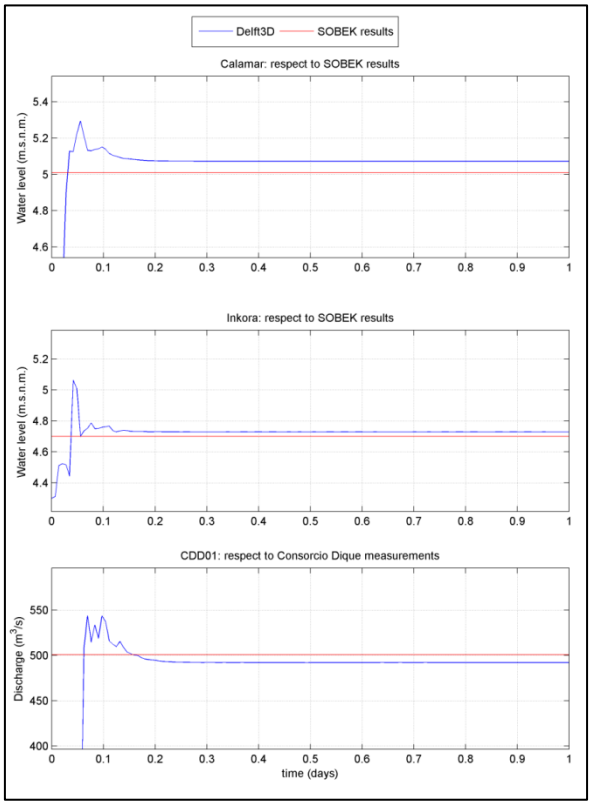

Figure D. 41 - Calibration result for medium discharge (case 2)

Finally, for the high discharge, with a discharge of 8973 m^3/s, the best fit occurs for a bed roughness of 0.016 at the Canal del Dique and at the Río Magdalena of 0.027 (Figure D. 42).

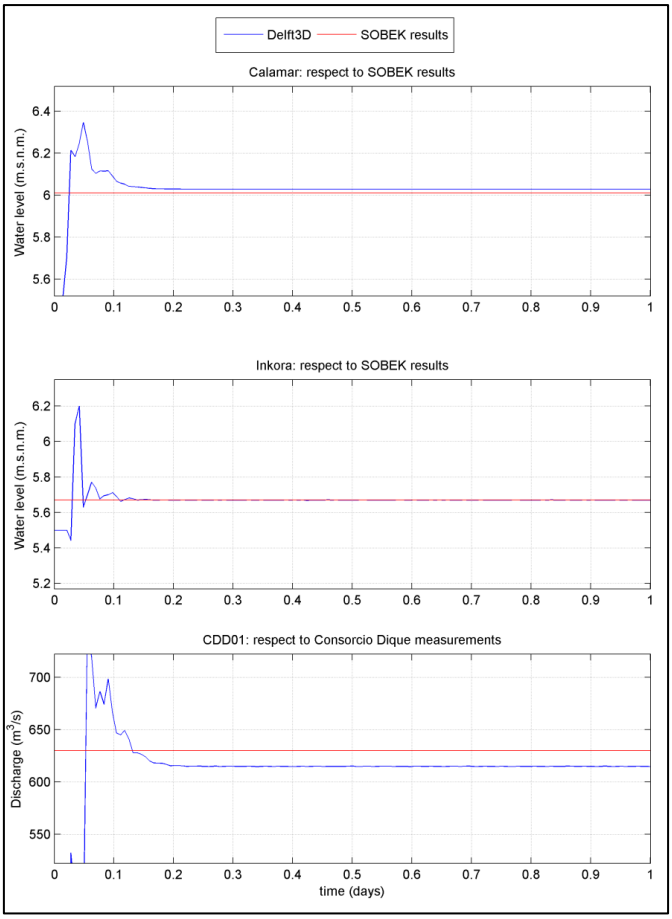

Figure D. 42- Calibration case for high discharge (case 3)

It can be concluded that a relation exists between the bed roughness and the discharge at the Río Magdalena. While, the bed roughness at the Canal del Dique is calibrated at a Manning value of 0.016 (viscosity= 1 m^2/s). The relationship between the Manning value and discharge from the three measurement campaigns is shown in Figure D. 43. It is expected that for high discharges the Manning value will smoothen as there is a maximum in dune forming. Therefore, the sensitivity of the bed friction for high discharges has to be investigated. However, in the range of the measurement campaign and for lower discharges, a linear relationship can be applied.

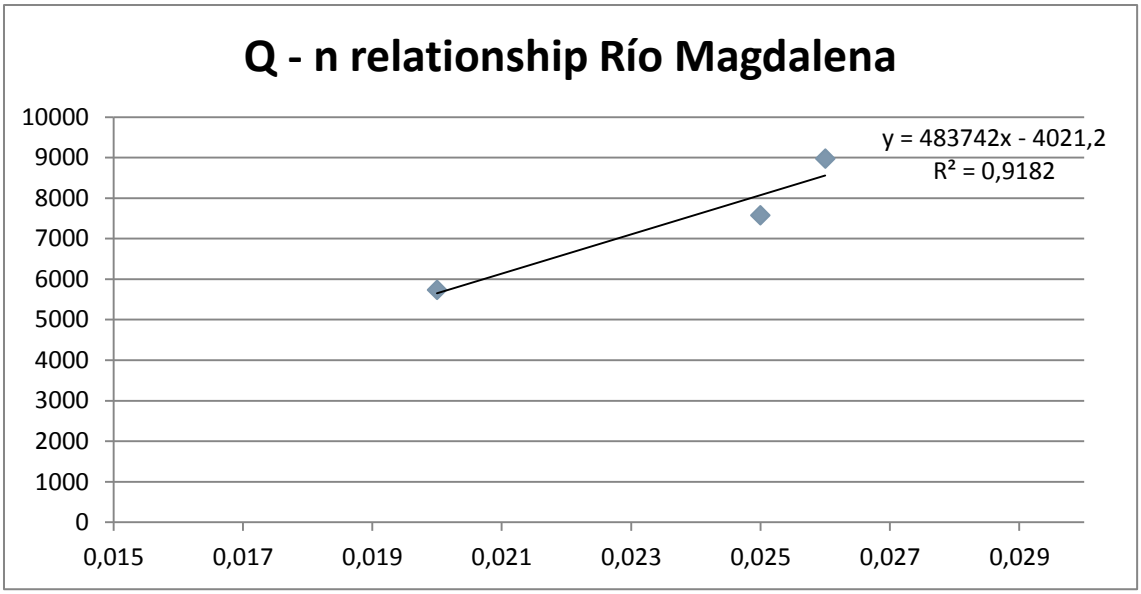

Figure D. 43 - Relationship Manning roughness and discharge at the Río Magdalena

D.3.1.6 Bathymetry

Finally, as sometimes a bed level step is present at the entrance of the Canal del Dique. The effect of including a bed level step in the bathymetry on the water levels and discharge in the offtake is assessed. The computed bathymetries with and without bed level step are shown in Figure D. 44. From Figure D. 45 it can be seen that no differences in water level and discharge occur when applying a bed level step or with the original bathymetry. Therefore, the original bathymetry will be used in the computations.

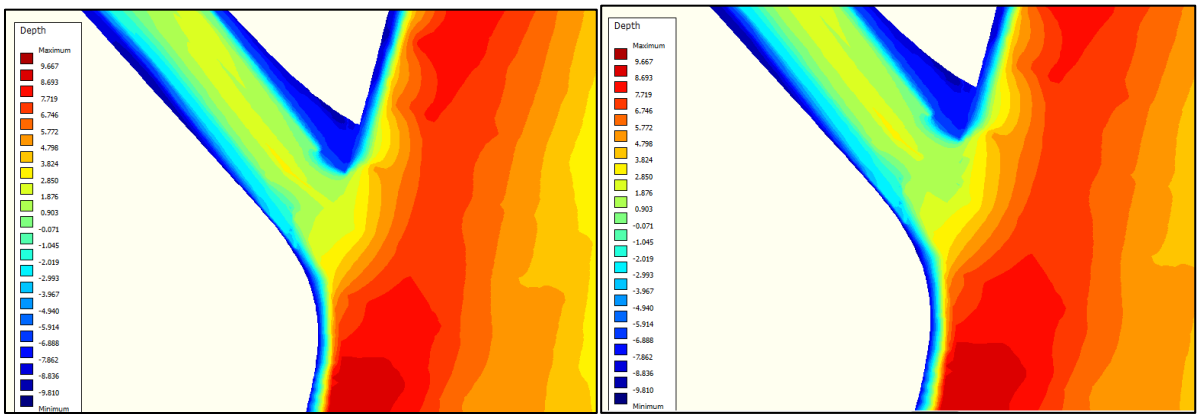

Figure D. 44 – Bathymetry without bed level step (left) and with bed level step (right)

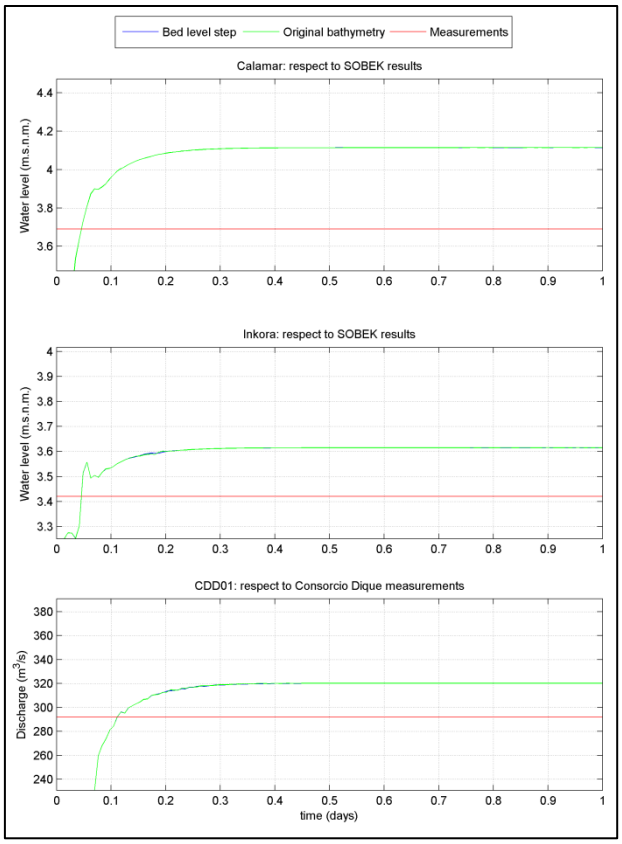

Figure D. 45 - Calibration for bed level step at the entrance of the Canal del Dique: without bed level step (green) and with bed level step (blue)

D.3.2 Check on discharge distributions

Final checks are made on the calibrated cases with the best fits to the discharge distribution along the islands and the offtake. The result for low, medium and high discharge is shown in respectively Figure D. 46 to Figure D. 48. It can be seen that the discharge distribution fits quite well with only a few percent of deviation in the computed and measured discharge distributions.

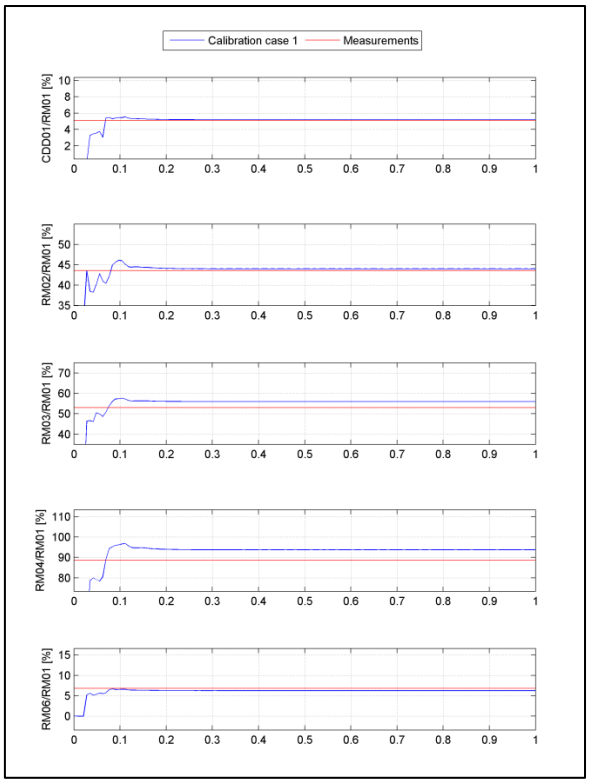

Figure D. 46 – Discharge distribution along islands and offtake for a discharge of 5737 m^3/s

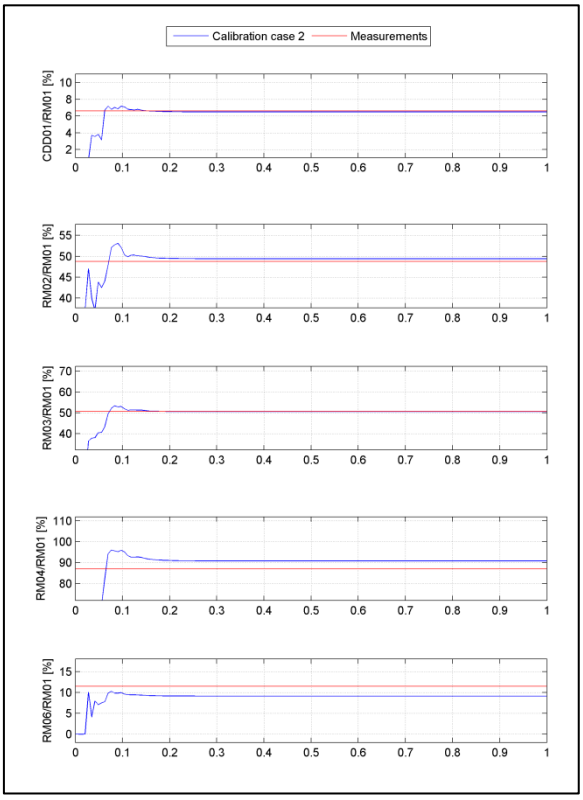

Figure D. 47- Discharge distribution along islands and offtake for a discharge of 7572 m^3/s

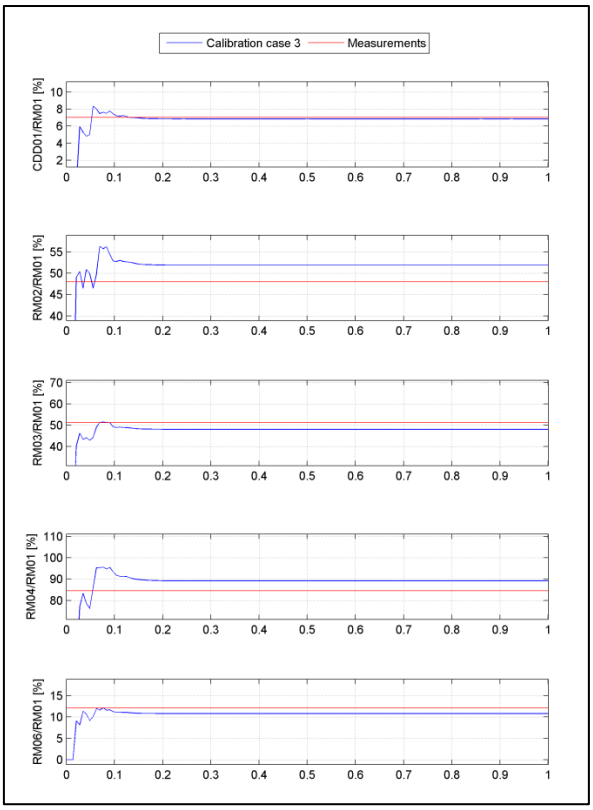

Figure D. 48- Discharge distribution along islands and offtake for a discharge of 8973 m^3/s

D.3.3 Check on velocities

It is also checked if the modelled velocities at the cross-sections match with the measured velocities. Figure D. 49until Figure D. 55 show the measured and modelled velocities at several cross-sections around the bifurcation for the case of high discharge with the best calibrated model. It has to be bared in mind that the modelled velocity is depth-averaged and the measured velocity is three-dimensional. However, a qualitative comparison on the modelled flow velocities can be made. It can be seen that the magnitude of the measured velocities are almost equal to the modelled velocities. Therefore it can be stated that the model predicts the velocities accurately.

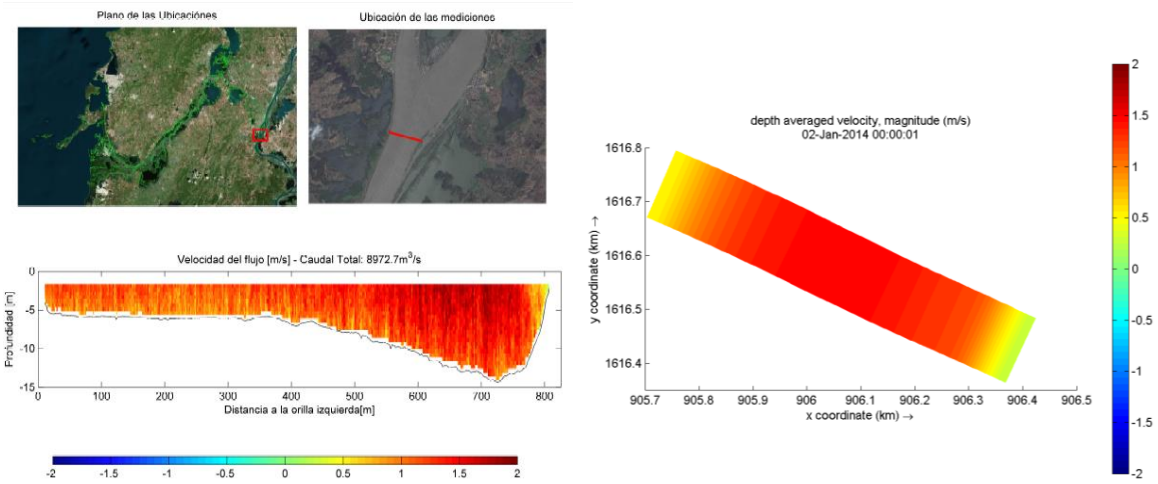

Figure D. 49 – Left: measured velocity at RM01 for high discharge (campaign 3), right: modelled velocity

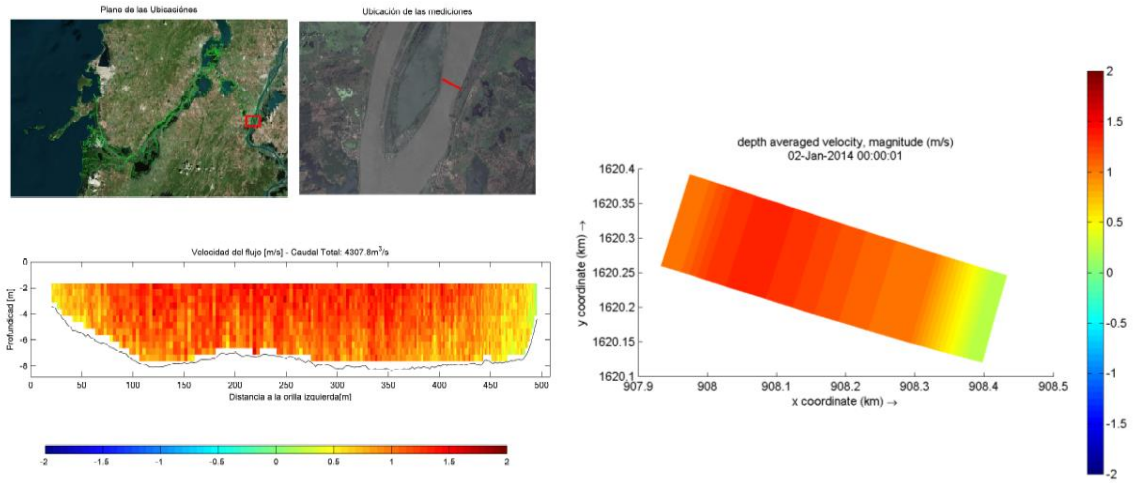

Figure D. 50 - Left: measured velocity at RM02 for campaign 3 (high discharge), right: modelled velocity

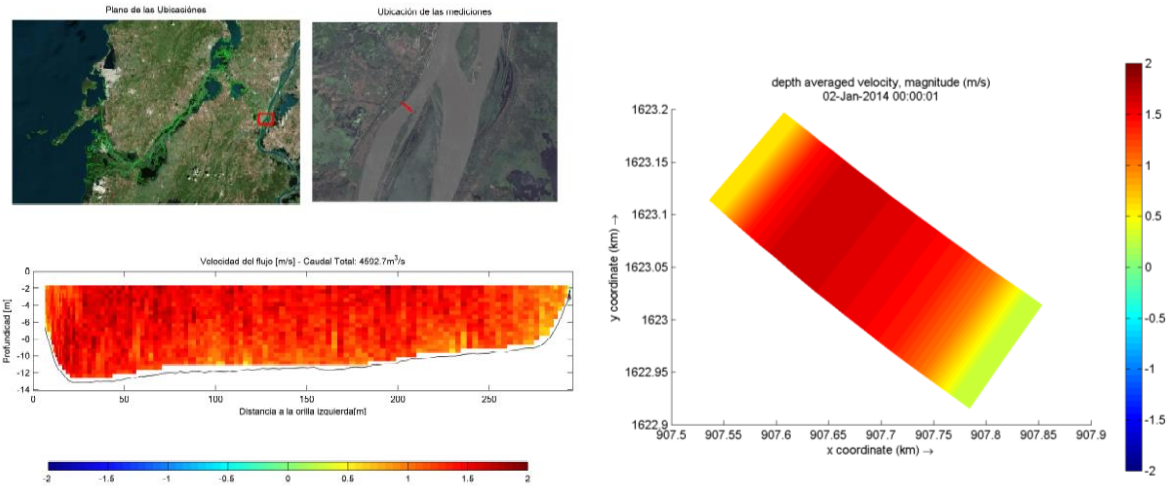

Figure D. 51– Left: measured velocity at RM03 for campaign 3 (high discharge), right: modelled velocity

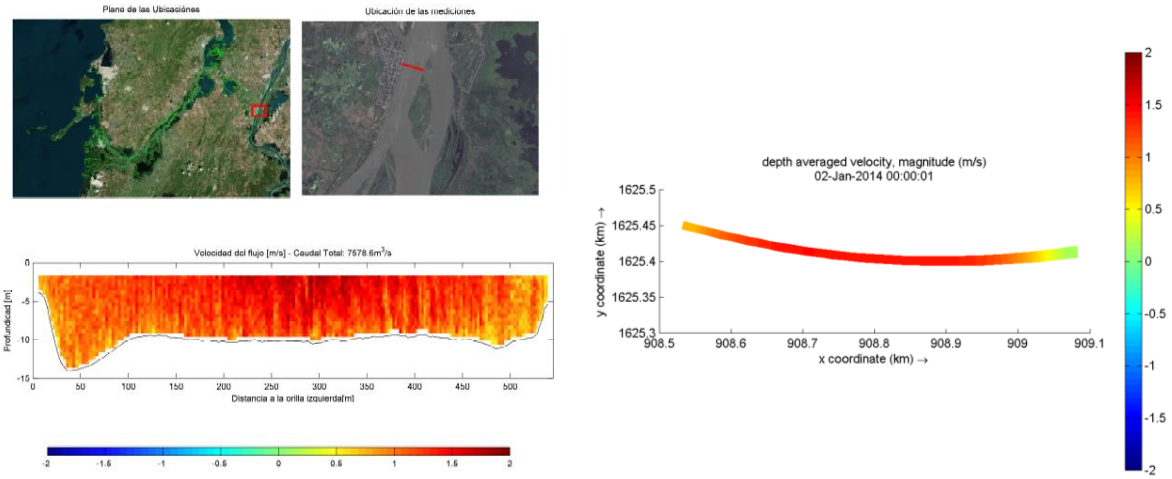

Figure D. 52 – Left: measured velocity at RM04 for campaign 3 (high discharge), right: modelled velocity

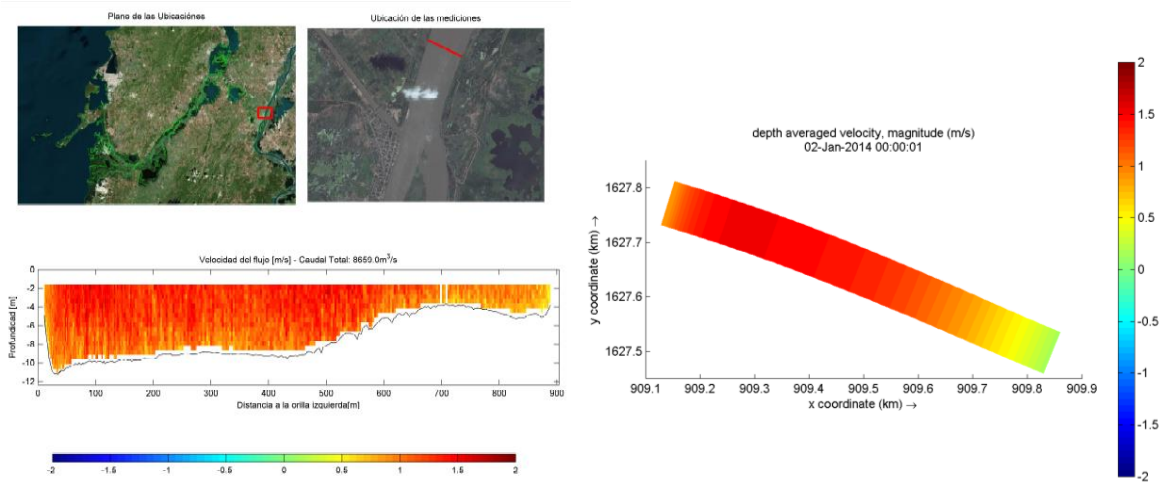

Figure D. 53– Left: measured velocity at RM05 for campaign 3 (high discharge), right: modelled velocity

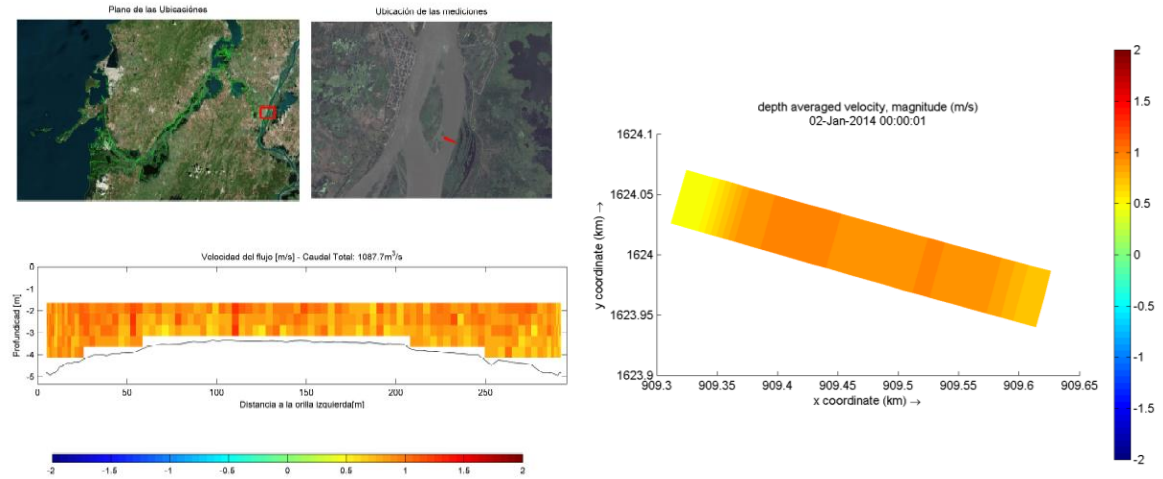

Figure D. 54 – Left: measured velocity at RM06 for campaign 3 (high discharge), right: modelled velocity

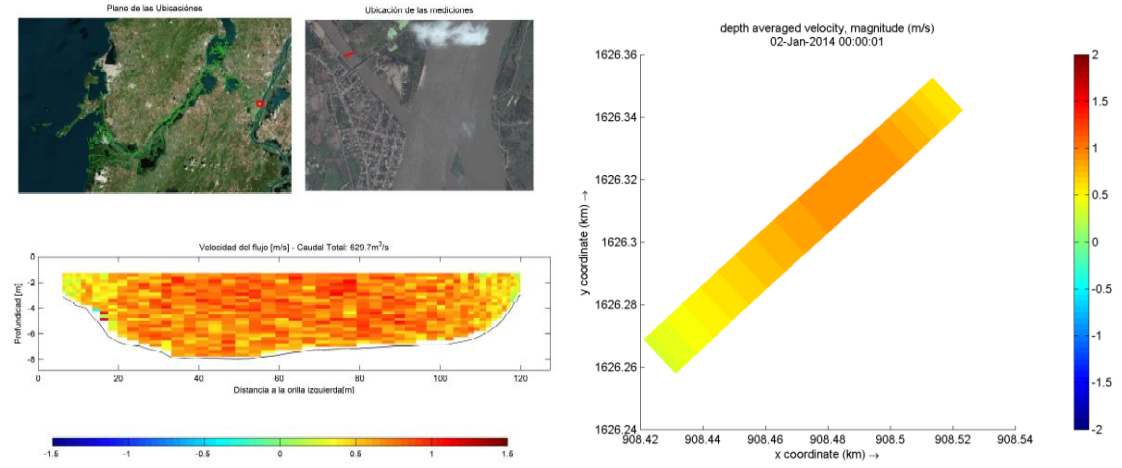

Figure D. 55 – Left: measured velocity at RM06 for campaign 3 (high discharge), right: modelled velocity

D.3.4 Water level gradient check

In order to check if no backwater effects occur in the Canal del Dique and Río Magdalena, the water level gradients are checked. Figure D. 56 shows the water level at the Canal del Dique along one grid-line for the calibrated measurement case 1 (low discharge). Figure D. 57 shows the water level at the Río Magdalena along one grid line for the same model. These figures show that no backwater effects occur in the area of the bifurcation. Therefore, it can be stated that the discharges in the area of interest are uniquely defined by the water levels and velocity in the branches.

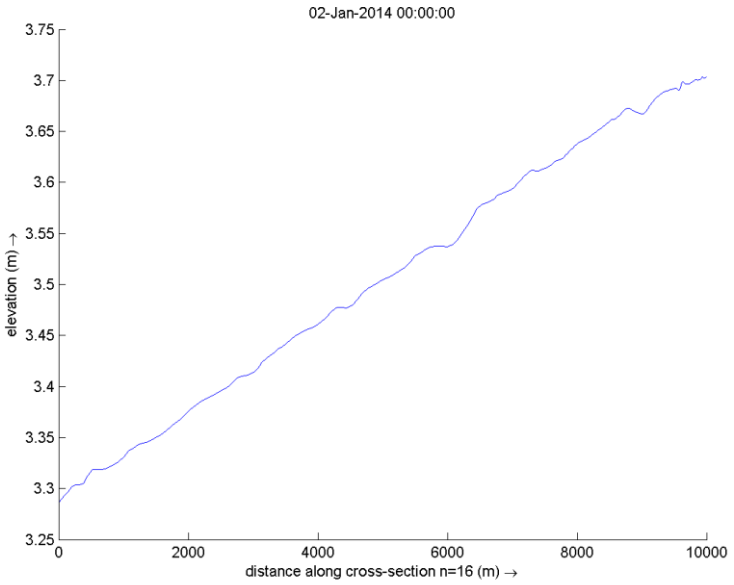

Figure D. 56 – Water level along grid line n=16 in Canal del Dique until Calamar

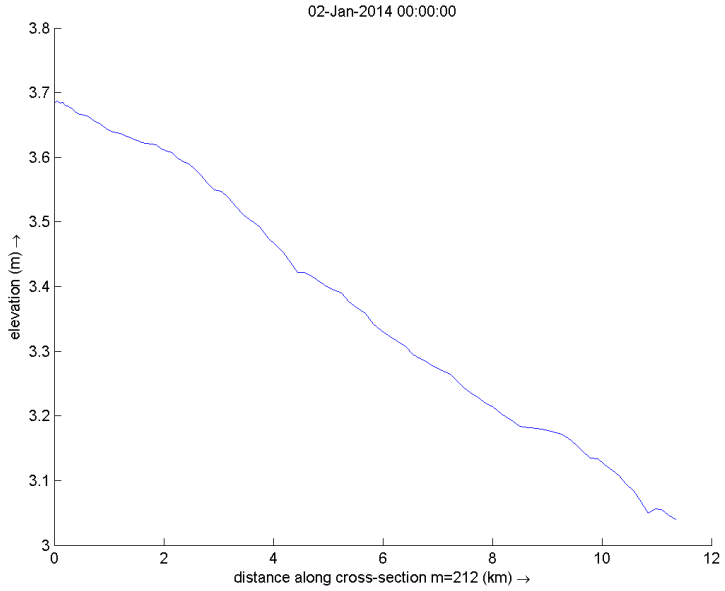

Figure D. 57 – Water level along grid line m=212 in Río Magdalena until just downstream of the offtake

D.4 Results

D.4.1 Bathymetric changes along both islands

The depth along both islands is changed and the effect of these bathymetric changes is investigated. When first deepening the right side of 'Isla Becerra', while keeping the depth along the right branch of Isla la Loca four times larger than the right side, causes changes in discharge distribution along the islands but only a very small change in the offtake (Figure D. 58). It can be seen that the discharge in the right branches (RM02 and RM06) increases due to the larger flow area, while the discharge in the left branches decreases (RM03 and RM04). The discharge in the offtake *decreases* when comparing this to a depth ratio of 2.

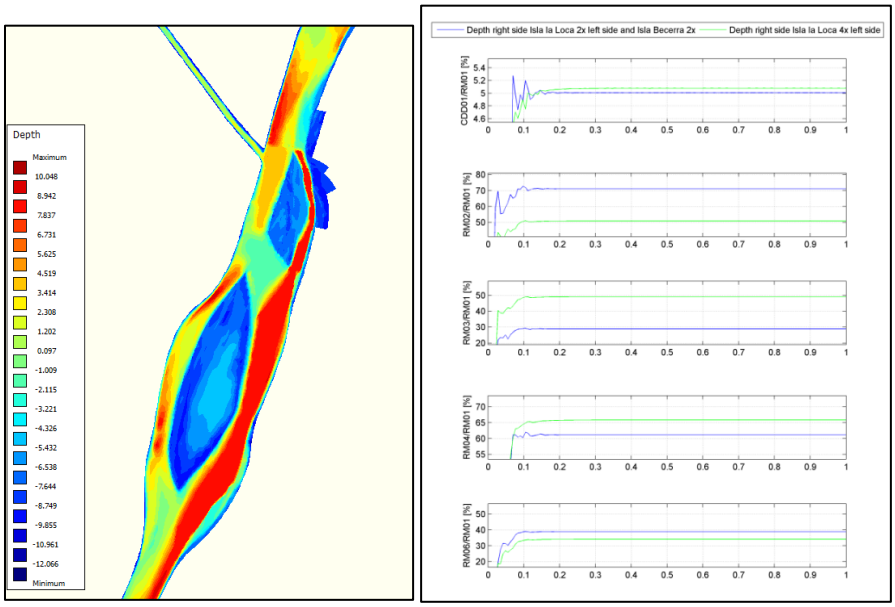

Figure D. 58 – Left: bathymetry with deep right branches and shallow branch at left side Isla la Loca; right: relative discharge distribution for this bathymetry (blue) compared to only change in depth along Isla la Loca (green)

D.4.2 Bathymetric changes along Isla la Loca only

First of all, the depth at the left side of the most downstream located island 'Isla la Loca' is decreased compared to the original case (Figure D. 59). However, it should be noted that the depth along the left side is still two times larger than the right side. From Figure D. 60 it is visible that this change in depth has small effects on the discharge distribution. It causes a decrease of discharge in the left branch along Isla la Loca (RM04), due to the smaller flow area. Therefore, also the discharge in the offtake decreases slightly with approximately 0.2%. Also, the discharge in the left upstream branch (RM03) decreases. In contrary, the discharge in the right branches increase. So, for a decrease in flow area of the left downstream branch, the discharge decreases in *both* branches along the left side of the islands and, by continuity, increases in the right branches.

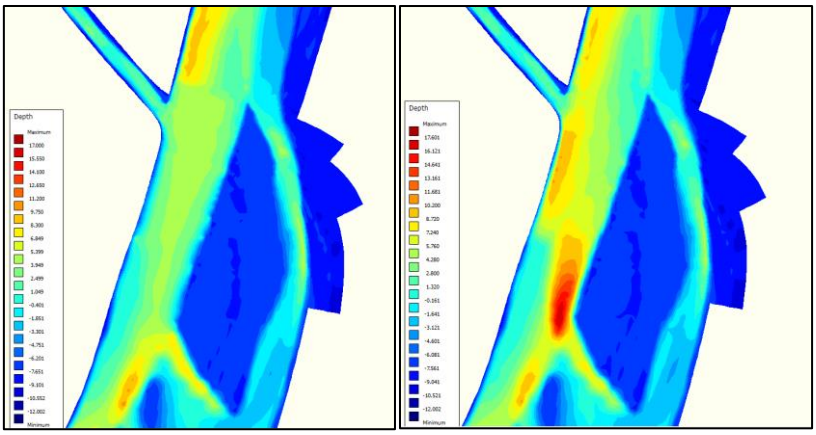

Figure D. 59– Left: shallow depth at the left side of Isla la Loca; right: original bathymetry

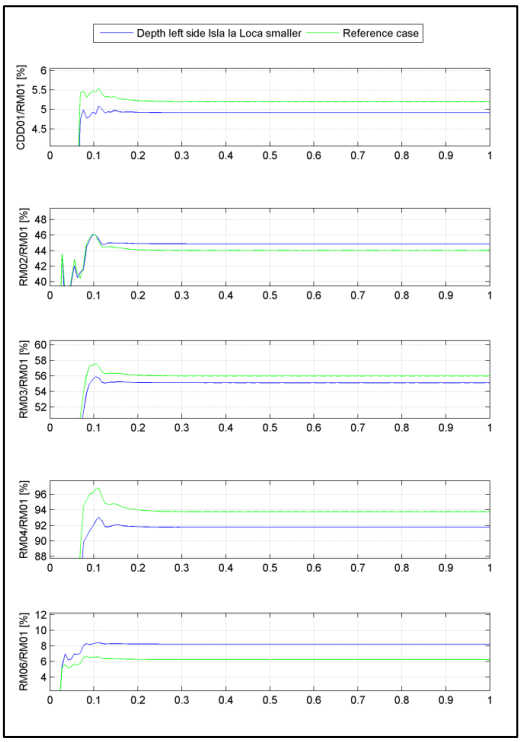

Figure D. 60– Discharge distribution for shallow depth at left side along Isla la Loca (blue) and original bathymetry (green)

D.4.3 Position Isla la Loca

D.4.3.1 Isla la Loca attached to left

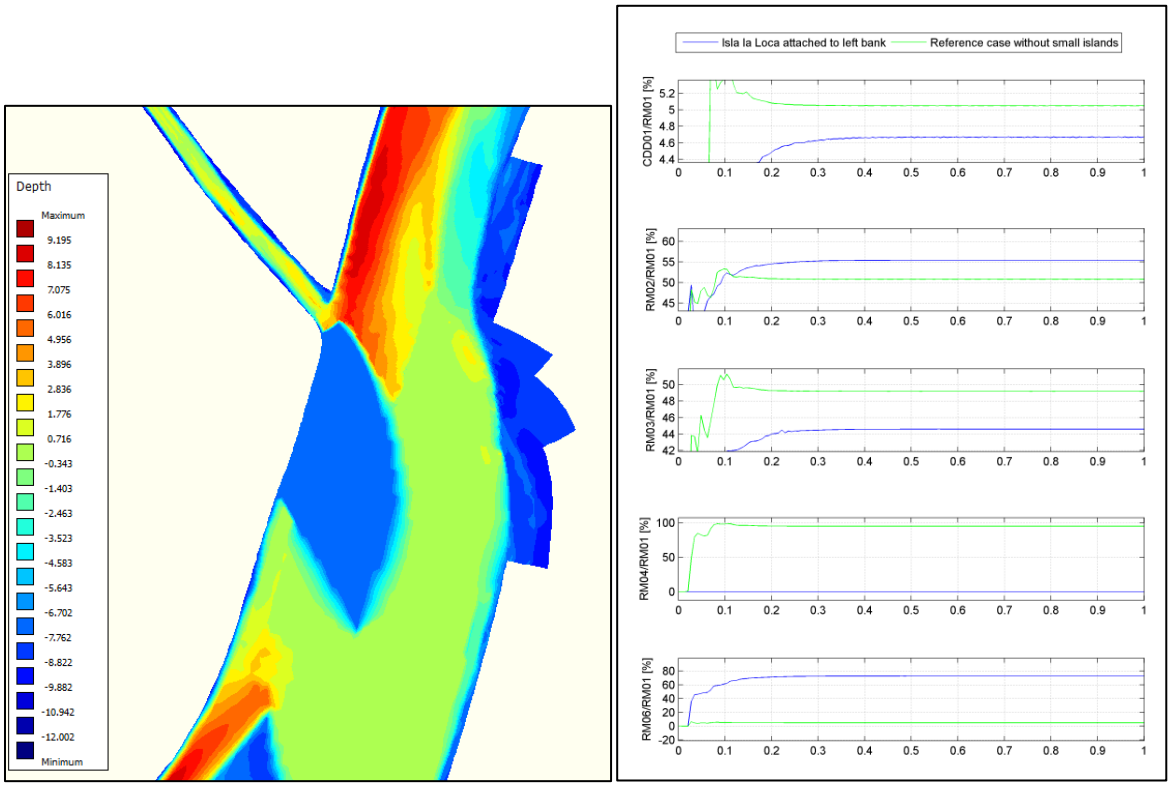

Figure D. 61 – Left: bathymetry with Isla la Loca attached to left bank; right: Discharge distribution relative to upstream discharge for island attached to left bank and reference case without the small islands

D.4.3.2 Combined bathymetry and position change Isla la Loca

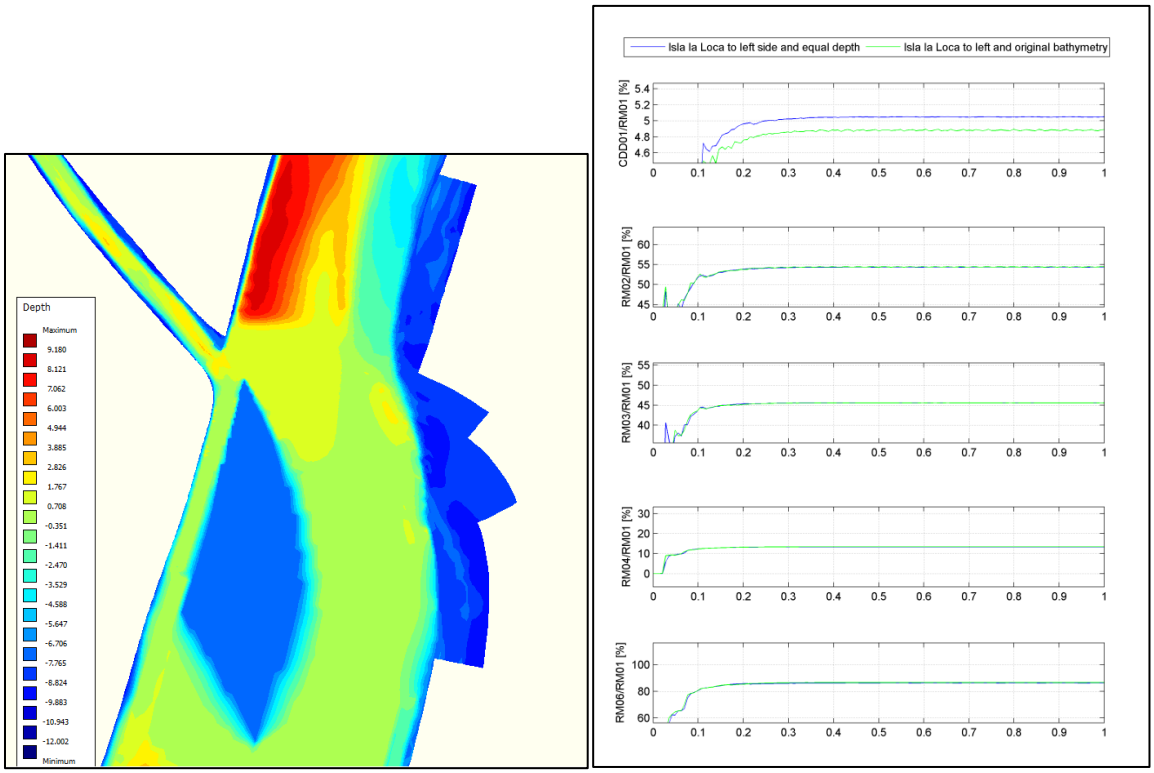

Figure D. 62 - Right: bathymetry with Isla la Loca positioned in front of bifurcation with equal depth around bifurcation; left: relative discharge distribution with position Isla la Loca in front of bifurcation and equal depth around bifurcation (blue) or depth Canal del Dique smaller than Río Magdalena (green)

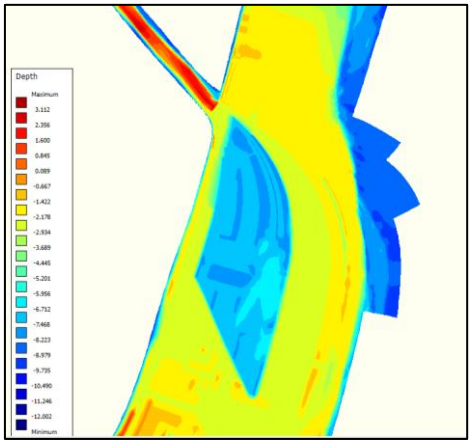

Figure D. 63 - Bathymetry at bifurcation with Isla la Loca located in front of bifurcation

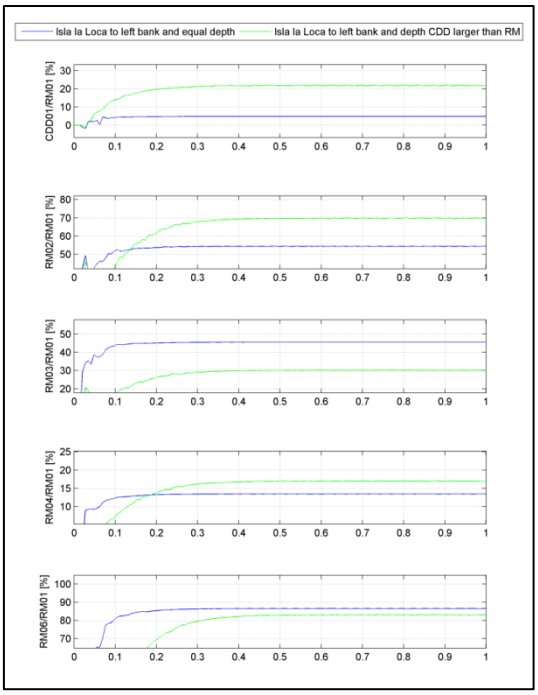

Figure D. 64 – Discharge distribution for island placed just in front of offtake with depth of the offtake larger than at the Río Magdalena just downstream of the bifurcation (green) and depth larger at the Río Magdalena than at the offtake (blue)

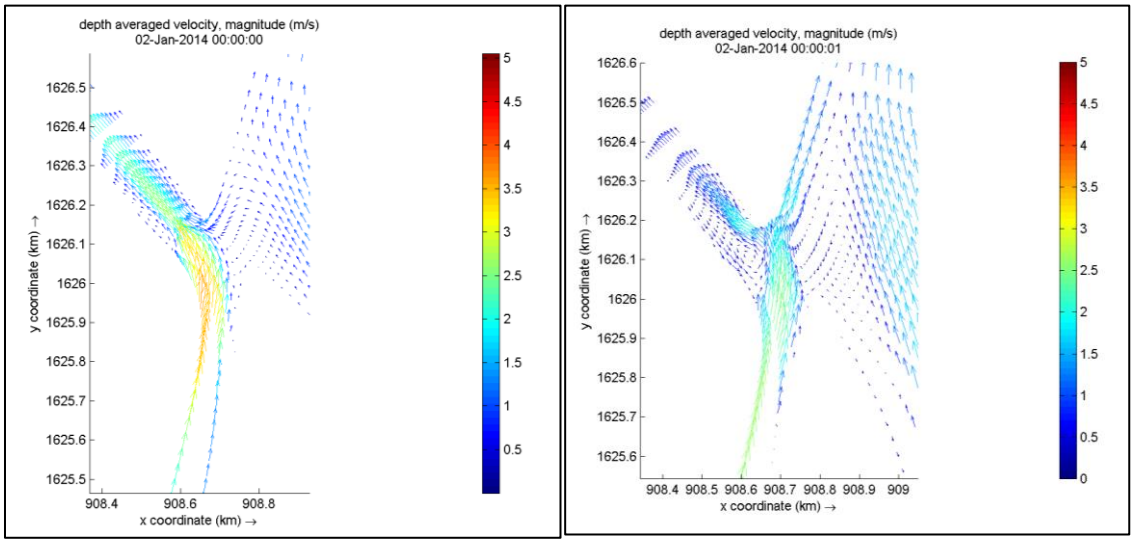

Figure D. 65 - Left: velocity at entrance offtake for depth offtake larger than depth Río Magdalena; right: velocity at entrance offtake for depth offtake equal to depth Río Magdalena

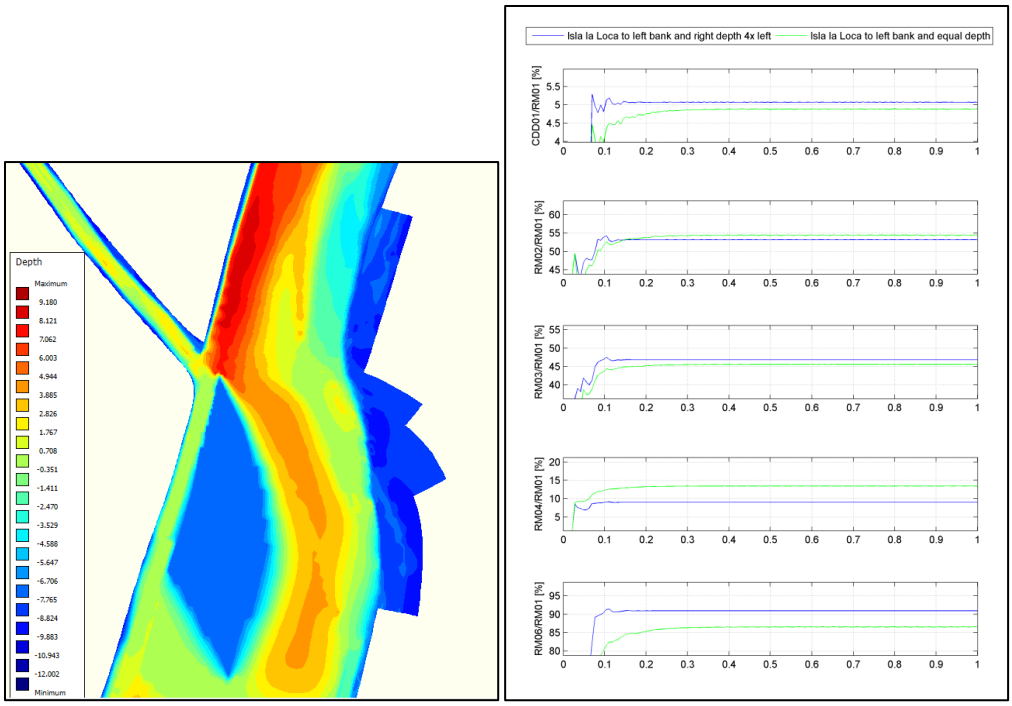

Figure D. 66– Left: bathymetry with island located in front of offtake and bed level step at entrance offtake; right: Relative discharge distribution for island in front of bifurcation with larger depth at right side than left side (blue) and equal depth (green)

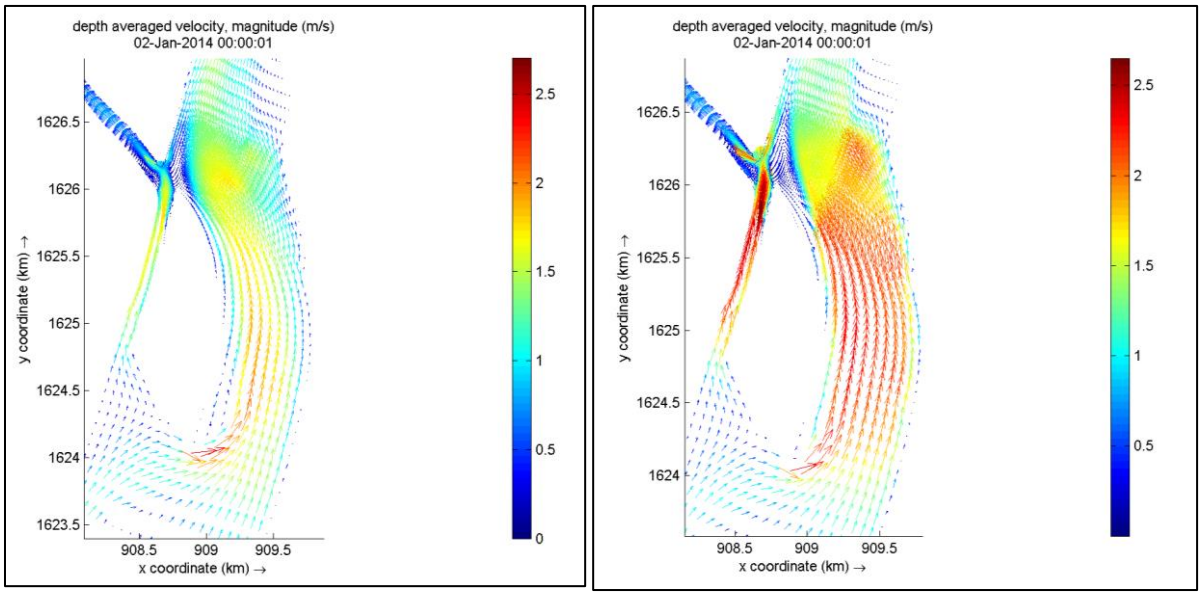

Figure D. 67 - Left: velocity with Isla la Loca at left bank and depth right side four times larger than left side; right: velocity with Isla la Loca at left bank and depth right side equal to left side

D.4.4 Impact of the shape of the islands

The island is located at the left river bank, which resulted in less discharge in the offtake as found from the previous sections. In the Canal del Dique case we are interested in further reducing the discharge in the offtake therefore it is investigated if the shape of the island can improve this. When the shape of the island is changed the discharge in the offtake remains almost equal as shown in Figure D. 68. Also, in the other branches, the discharge does not change significantly. However, from Figure D. 69 it

can be seen that the flow pattern along the right branch of Isla la Loca increases due to the less smooth shape of the island which causes an increase in discharge and flow separation downstream.

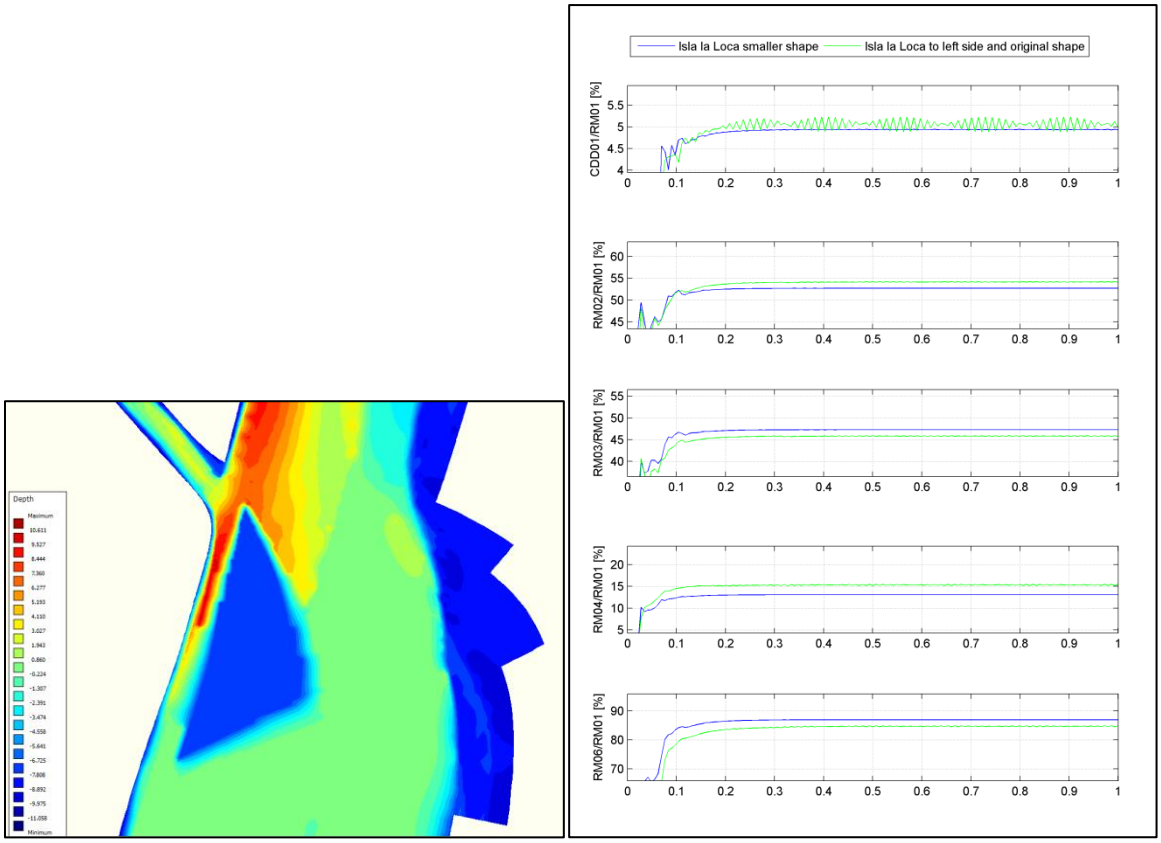

Figure D. 68 – Left: bathymetry with different shape Isla la Loca; right: Relative discharge distribution for different shape Isla la Loca (blue) and original shape (green) while located at left river bank

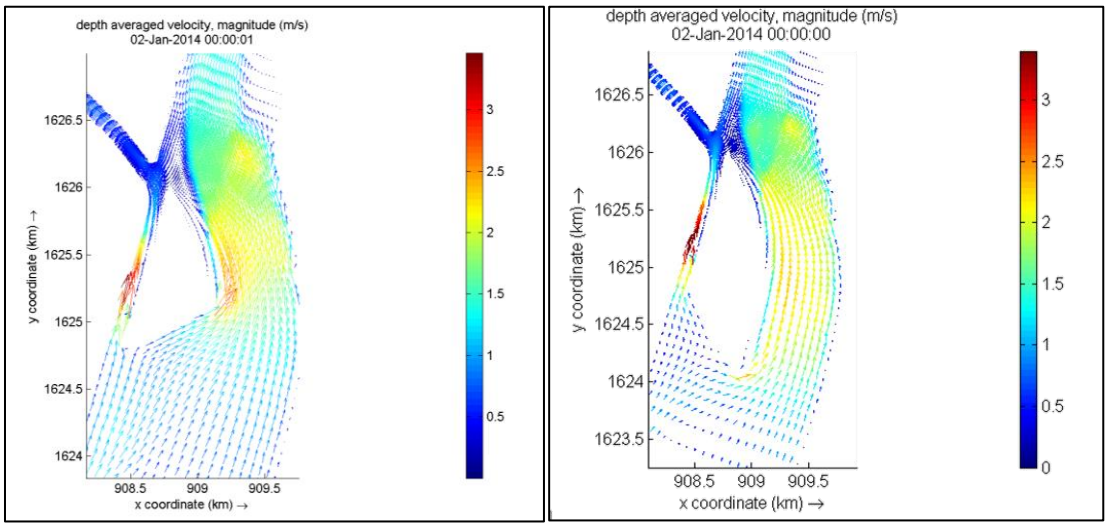

Figure D. 69- Velocity for different shape Isla la Loca and located at left river bank

When on the other hand the shape of the island is made larger than the reference case when the island is located to the left bank (Figure D. 70), the discharge in the offtake becomes lower but unstable due to the occurrence of a lot of eddies at the area of the bifurcation as shown in Figure D. 71. Furthermore, the discharge in the right branch along Isla la Loca (RM06) decreases due to the

decreased with of the branch. By continuity, the discharge in the left branch (RM04) increases. The discharge in the other branches remains almost equal.

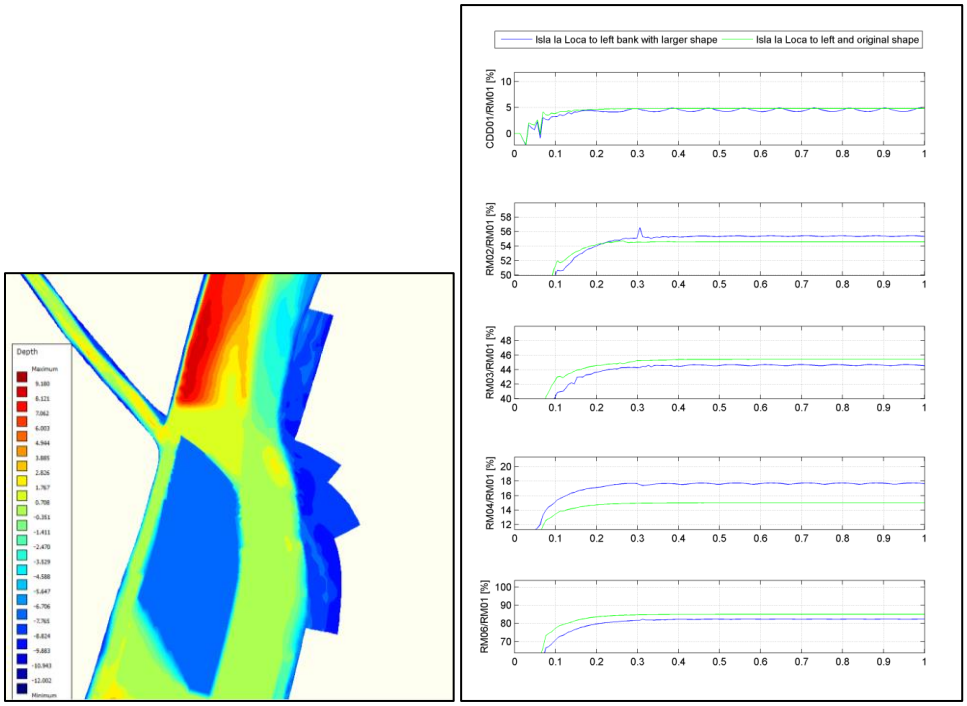

Figure D. 70 - Left: bathymetry for larger shape island; right: Relative discharge distribution for island located completely in front of bifurcation (blue) and not completely (green)

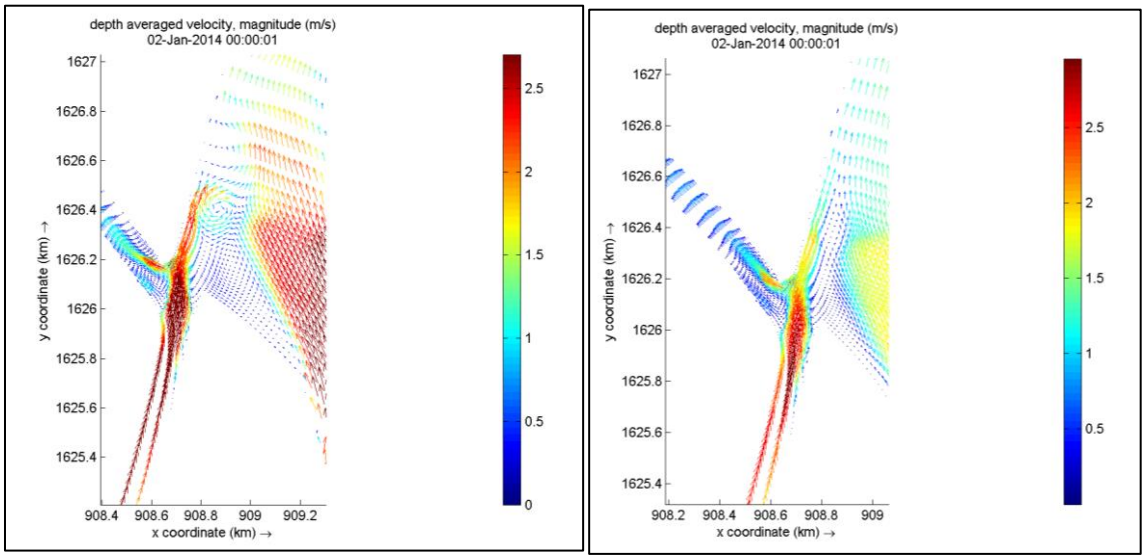

Figure D. 71 – Left: velocity for larger shape Isla la Loca and placed to left river bank; Right velocity for Isla la Loca at left river bank and original shape

D.4.5 Offtake angle

The effect of changes of the offtake angle could not be investigated in Sobek as this is a one-dimensional model which does not take into account effect of different approach angles and consequently separation of flow. Therefore, the effect of changing the angle of the offtake to 90 degrees instead of the 'original' angle of around 45 degrees is investigated. The result is shown in Figure D. 72 It can be seen that when the angle of the offtake is 90 degrees, the discharge in the

offtake increases very slightly with approximately 0.02%. This fits with the theory of Bulle where the sediment and discharge distribution for different angle of the offtake is shown in Figure 2.8. Furthermore, it can be seen from Figure D. 73 that with an angle of 90 degrees a wide narrow eddy occurs at the entrance of the offtake which does not occur at an angle of 45 degrees. The slight increase of discharge in the offtake can be explained by more curved streamlines causing a higher velocity at the entrance of the offtake for which the discharge in the offtake increases. Finally, it can be seen that the discharge distribution along the islands is not influenced by the offtake angle. So, the angle of the offtake impacts only the discharge in the offtake but does not have influence on discharges upstream.

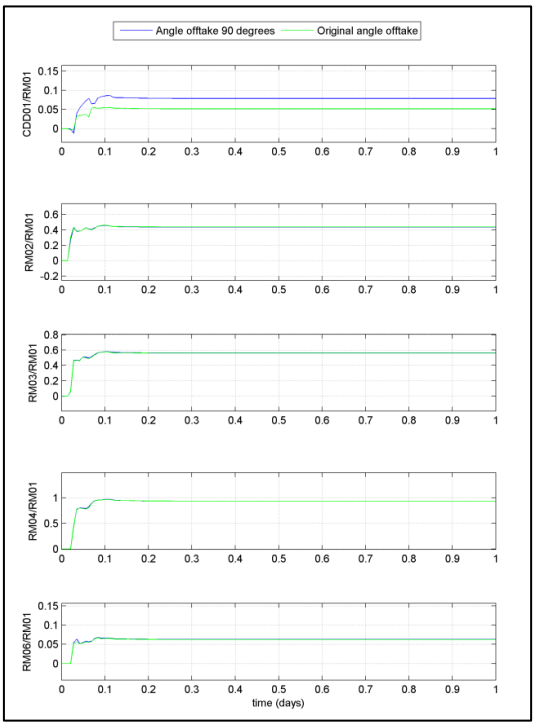

Figure D. 72 - – Discharge distribution for offtake angle of 90 degrees (blue) and offtake angle of 45 degrees (green)

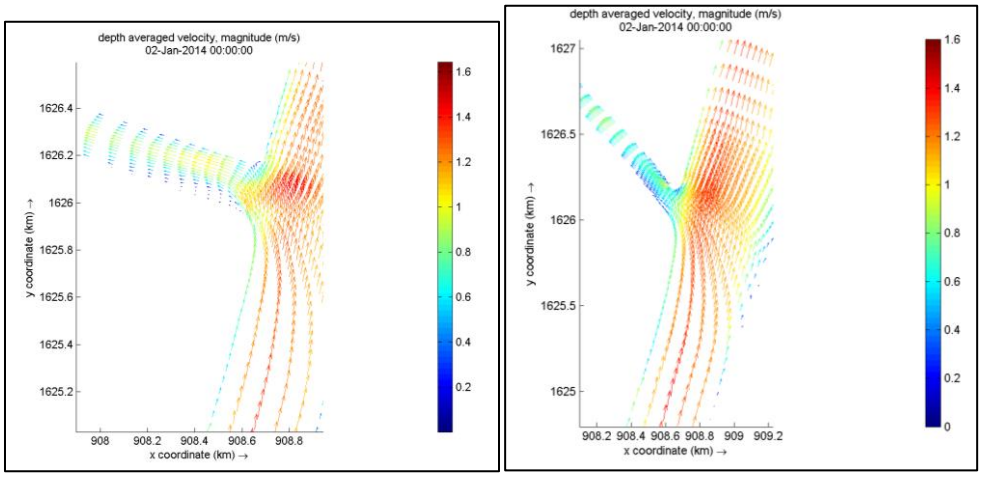

Figure D. 73 – Left: velocity at the entrance of the offtake for an angle of the offtake of 90 degrees; right: velocity for angle offtake 45 degrees (right)

D.4.6 Impact of a bed level step at the entrance of the offtake

The effect of imposing a bed level step at the entrance of the offtake is investigated as sometimes a bed level step is apparent in the Canal del Dique case. Besides, it is to be expected that imposing a bed level step will decrease the discharge in the offtake. However, Figure D. 74 shows that imposing a bed level step does not influence the discharge in the offtake and along the islands. Calculations show a decrease of discharge in the offtake with bed level step of 0.02%, which is negligible. However, Figure D. 75 shows that the flow velocities at the location of the bed level step increase slightly for which it is to be expected that the bed level step will wash away in time. Also, the water level decreases slightly, approximately 1 cm, at the location of the bed level step as can be seen from Figure D.76. Apparently, the water level decrease is large enough to compensate for the increase in velocity and causing a slight decrease in discharge in the offtake

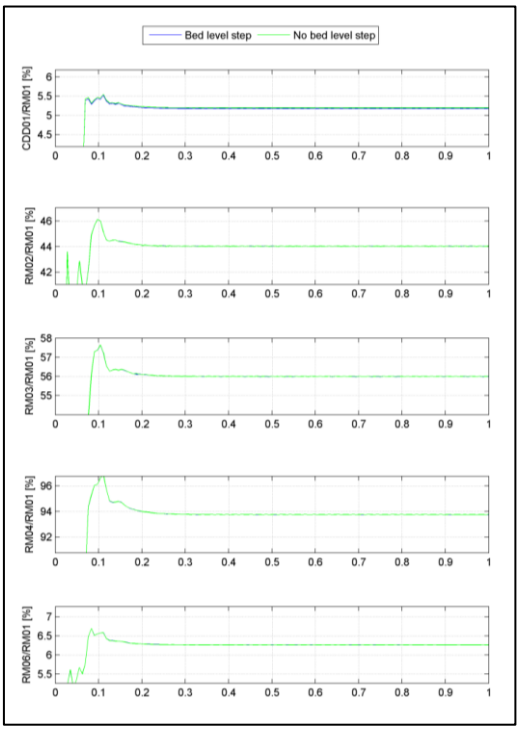

Figure D. 74– Discharge distribution relative to upstream discharge (RM01) along islands and offtake with a bed level step at the entrance of the offtake (blue) and without bed level step (green)

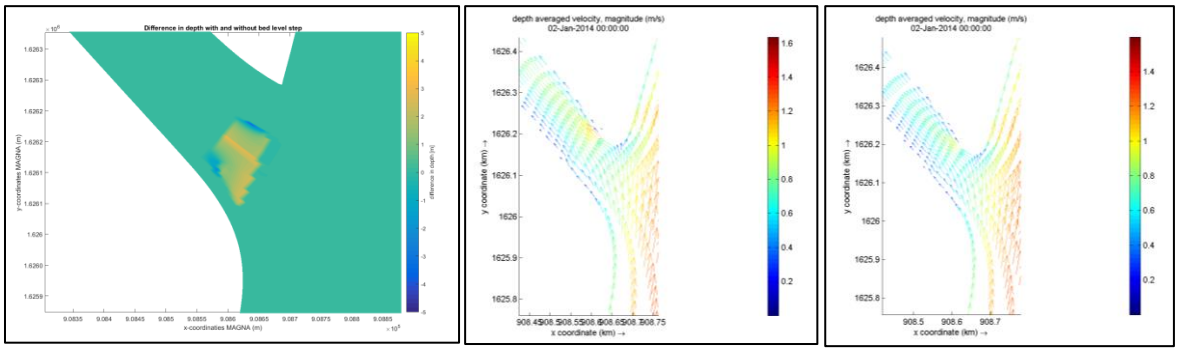

Figure D. 75 – Left: bed level step; middle: velocity with bed level step (left); right: velocity without bed level step (right) at the entrance of the offtake

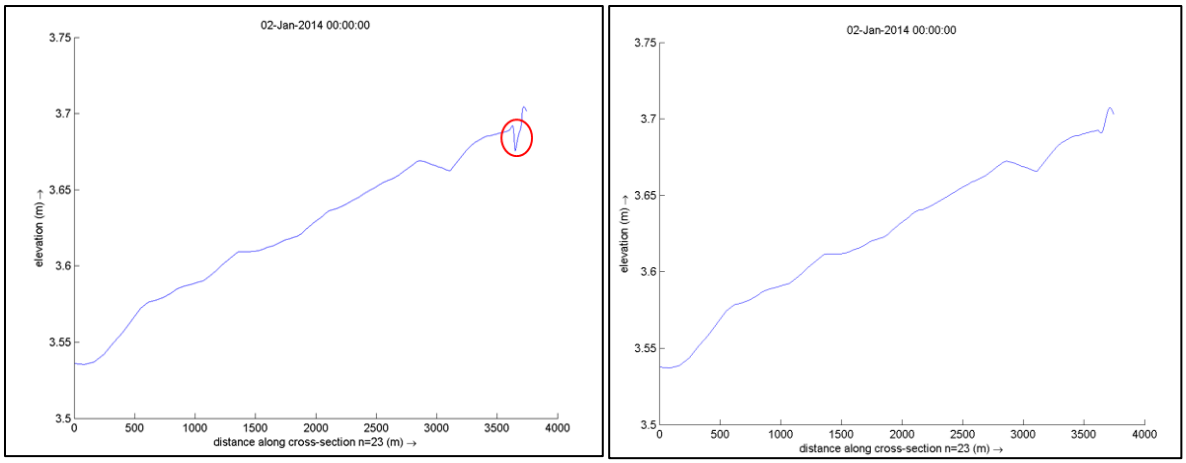

Figure D. 76 – Waterlevel gradient in the offtake near the bifurcation. Left: with bed level step; right: without bed level step

D.4.7 One island

When only the downstream island, Isla la Loca, is deleted the discharge distribution changes very slightly along the upstream island (RM02 and RM03) causing a totally equal distribution as visible from Figure D. 77. The discharge in the offtake increases slightly with 0.2%.

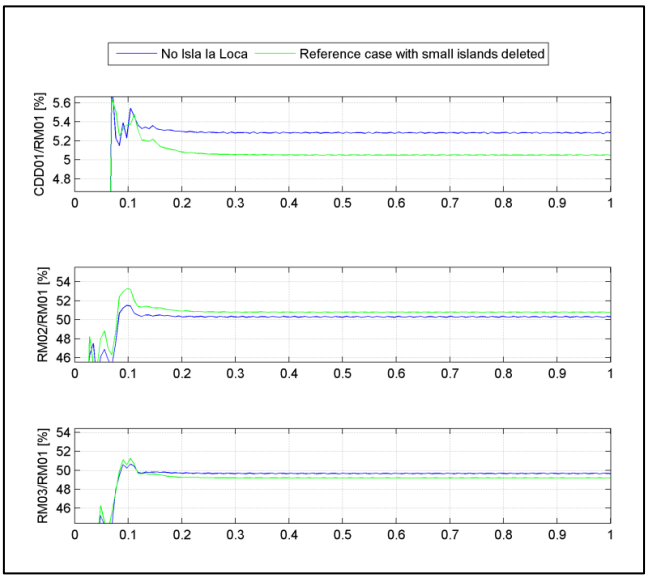

Figure D. 77–Discharge distribution relative to upstream discharge without Isla la Loca compared to reference case

Appendix E - Morphodynamics

E.1 Model input

As stated before, the hydrodynamic model is used as a basis for this study. Therefore, the hydrodynamic input will not be discussed here again. Data from the Río Magdalena and Canal del Dique will be used as a basis in order to validate the results. As in this study the focus is on the coarser fractions, only non-cohesive sediment will be taken into account. The parameters regarding the morphodynamics that need to be specified are:

- Median sediment diameter (D50)
- Density of the sediment fractions
- Sediment transport formula
- Boundary conditions

Besides, secondary flow should be switched on as in the areas where secondary flow occur sedimentation and erosion takes place. Also, morphological updating is switched on causing dynamically updating of the bed at each computation time step. In this way the hydrodynamic flow calculations are carried out using the correct bathymetry at every time step (Deltares 2014).

D50

A grain size distribution of the bed material in the Río Magdalena is obtained from measurements of Universidad Nacional in 2007 as shown in Figure E. 1. This shows a median grain diameter of approximately 200 µm. However, the sensitivity of this parameter should be investigated. Besides, from measurements of Consorcio Dique in 2014 it is found that the suspended sediment material in the Canal del Dique consists for 15% of coarse sediment with a medium grain diameter (D50) of approximately 90 µm (Figure E. 2). Therefore, also the influence of this smaller fraction should be investigated.

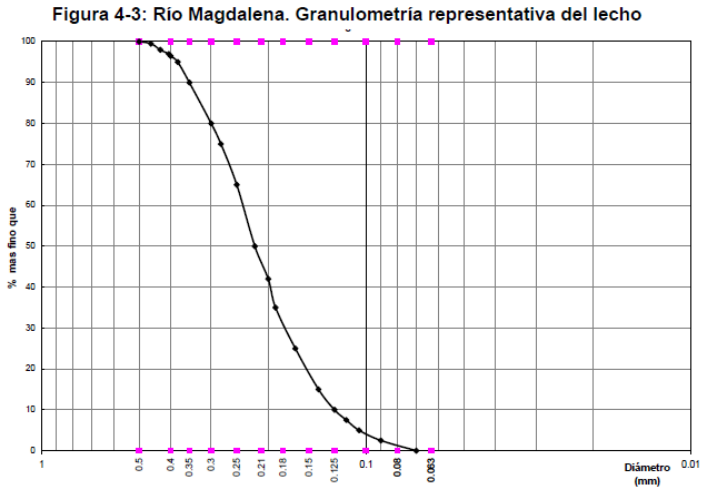

Figure E. 1- Grainsize distribution of bed material in the Río Magdalena (Universidad Nacional de Colombia 2007)

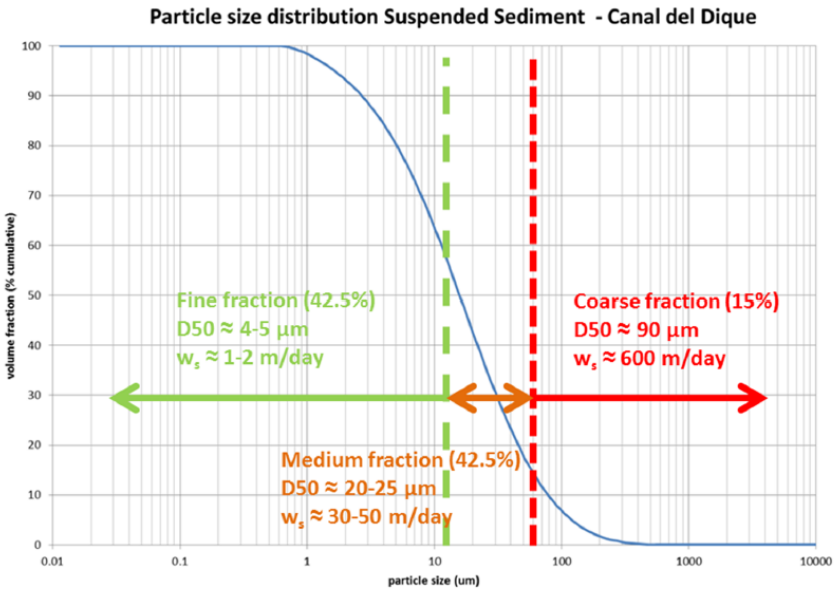

Figure E. 2– Grain size distribution Canal del Dique (Consorcio Dique 2015)

Density

A specific density of 2650 kg/m^3 is applied which is a general value for sand particles and used as default value in Delft3D. A dry bed density of 550 kg/m^3 is applied as used in the 1D model of the Canal del Dique of Consorcio Dique (2015) based on expert judgements. This corresponds to a bed porosity of 0.792.

Sediment transport formula

Several sediment transport formula exists. For non-cohesive sediment the following transport formulas can be specified in Delft3D (Deltares 2014):

- Van Rijn (1993): bed load + suspended load. Sediment transport is divided into suspended transport above the specified reference height and bed load transport below the reference height. The application area of this transport formula is large as an explicit distinction is made between bed load and suspended transport.
- Engelund-Hansen (1967): total load (both bed load and suspended load but no wash load). The formula was originally derived for bed load, but proves especially applicable for the total load of relatively fine material in which the suspended load plays a vital role (de Vriend, Havinga et al. 2011). It is a semi-empirical formula which is applicable for median grain sizes (D50) between 0.93 and 0.19 mm and $\frac{w_s}{u_*} < 1$ indicating fine material.
- Meyer-Peter-Müller (1948): bed load transport. This transport formula is applicable for median grain sizes (D50) larger than 0.4 mm and $\frac{w_s}{u_*} > 1$.
- Bijker (1971): bed load + suspended. This formula is mostly used in coastal areas as it appears to calculate sediment transport correctly under combination of both current and waves.
- Van Rijn (1984): bed load + suspended. This formula is commonly used for fine sediments without waves.
- Soulsby/Van Rijn: bed load + suspended
- Soulsby: total transport

- Ashida-Michiue (1974): Bed load due to currents
- Wilcock-Crowe (2003): bed load transport of mixed sand and gravel sediment
- Gaeuman et al. (2009): bed load

For non-cohesive sediment the transport formula of Van Rijn (1993) is used as default in Delft3D (Deltares 2014). Another formula of the above list can be implemented manually. The sensitivity of applying several sediment transport formula should be investigated. In this study the default formula Van Rijn (1993) is used and a sensitivity analysis is carried out with Engelund-Hansen as both formulas seem to meet the required conditions.

Boundary conditions

At the boundaries the equilibrium sediment concentration should be applied. In this way, the incoming sediment load always equals the sediment transport capacity of the downstream reach. Hence, no excess or shortage of sediment at the upstream boundary occurs which can cause disturbances travelling in downstream direction. Delft3D has a feature which calculates the equilibrium sediment concentration at the inflow boundary and is applied in this study.

Table E. 1 summarizes the input parameters as used in the reference case before calibration.

Table E. 1 - Input parameters reference case

Parameters	Value	Unit
Grain size (D50)	200	µm
Specific density	2650	kg/m^3
Dry bed density	550	kg/m^3
Reference density for hindered settling	1600	kg/m^3
Initial sediment layer thickness at bed	50	m
Morphological scale factor	12	-
Sediment concentration at boundaries	Equilibrium sediment concentration	kg/m^3
Sediment transport formula	Van Rijn 1993	-
Hydrodynamic upstream boundary condition	7572	m^3/s

E.2 Calibration

As mentioned before, no recent measurements are available of sediment transport rates of the bed material. However, calibration curves of the bed load transport of coarse fractions are available from a study of Universidad Nacional de Colombia in 2007. The bed load transport was calculated with the Einstein method (Einstein 1950), based on discharge and suspended sediment measurements from 1996 to 2003. Besides, based on the annual dredged volumes in the sediment trap at the entrance of the Canal del Dique, annual transport rates entering the canal can be deducted, assuming the coarse material only settles in the sediment trap. Because the available data is not very precise, it is hard to calibrate the model. However, a rough estimate can be made giving an idea of the order of magnitude of the sediment transport rates.

In general, calibration parameters for sediments are:

- Sediment transport parameters including grain size and sediment characteristics.
- Sediment transport formula

Calibration curves for the bed load transport of coarse sediment as a function of the discharge are available for the Río Magdalena at Calamar and the Canal del Dique as obtained from a study of Universidad Nacional de Colombia in 2007 (Figure E. 3 and Figure E. 4). It can be seen that a stationary discharge of approximately 7500 m^3/s, as used in the reference cases, corresponds to a bed load transport (Q_{bb}) of approximately 8000 t/day in the Río Magdalena at Calamar and 700 t/day in the Canal del Dique. With a specific density of the grains of 2650 kg/m^3 this results in a bed load transport of $3.5*10^{-2}$ m^3/s in the Río Magdalena and $3*10^{-3}$ m^3/s in the Canal del Dique.

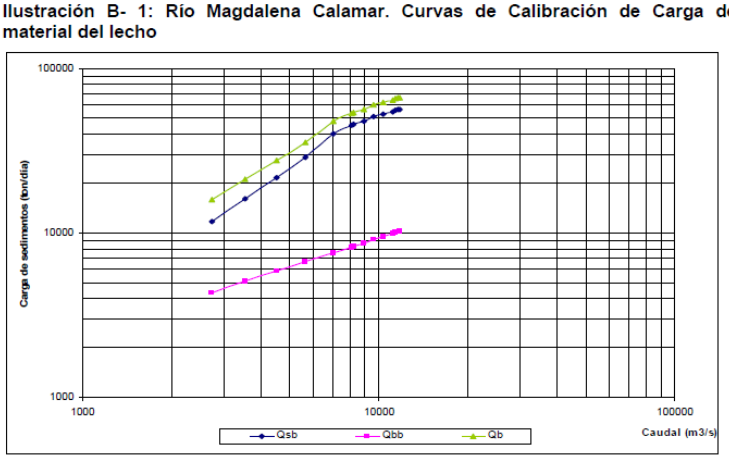

Figure E. 3– Calibration curve for bed load transport of coarse sediment in the Río Magdalena at Calamar (Universidad Nacional de Colombia 2007), where Qbb= bed load transport, Qsb = suspended load transport (excluding wash load) and Qb = Qbb + Qsb = total transport

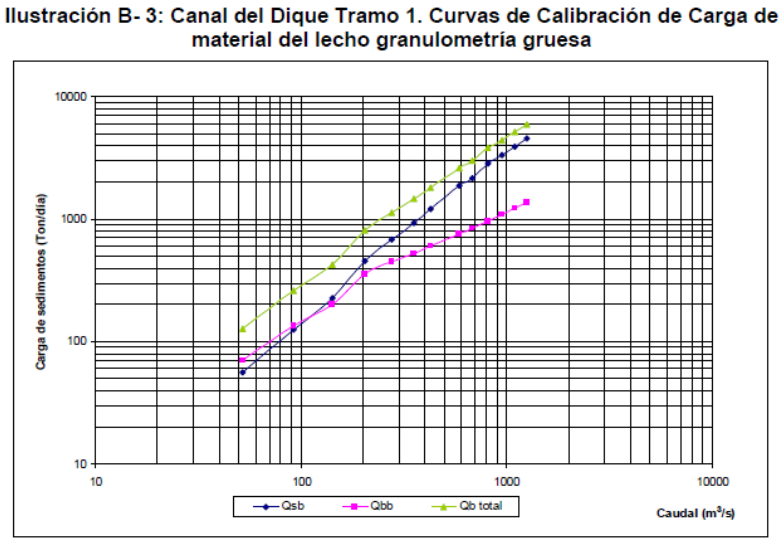

Figure E. 4 - – Calibration curve for bed load transport of coarse sediment in the entrance of the Canal del Dique (Universidad Nacional de Colombia 2007). Qbb= bed load transport, Qsb = suspended load transport (excluding wash load) and Qb = Qbb + Qsb = total transport

Furthermore, annually dredged volumes of the sediment trap at the entrance of the Canal del Dique are available. However, it appears that the dredged volumes vary largely per year in a range of 385.000 m^3 to 1.164.000 m^3 based on measurements of the last decade (Consorcio Dique and Fondo Adaptación 2015). This variation can be ascribed by variations in discharges as a correlation was found between the mean annual discharge of the previous year to the dredged volume of the present year (Figure E. 5).The sediment trap has a length of approximately 600 meter and width of 65 meter (Cormagdalena and Universidad del Norte 2013). With a mean annual dredged volume of approximately 775.000 m^3 the mean annual sedimentation height in the sediment trap is 20 meter. Moreover, with a mean flow of 7572 m3/s corresponding to a discharge in the Canal del Dique of 501 m3/s (Consorcio Dique 2014) results in a mean annual dredged volume of approximately 400.00 m^3 as can be deducted from Figure E.5. This corresponds to a mean annual sediment transport of $1.3*10^{-2}$ m^3/s in the Canal del Dique and sedimentation height of 10 meter during the year. It can be assumed that mostly the large sediment fractions settle in the sediment trap, while the fine sediments remain in the water column. In comparison to the calibration curve for coarse sediment in the Canal del Dique the total transport (Qb,total) for a discharge of 7500 m^3/s is $1.5 *10^{-2}$ m^3/s which is almost equal to the value obtained from the mean annual dredged volumes.

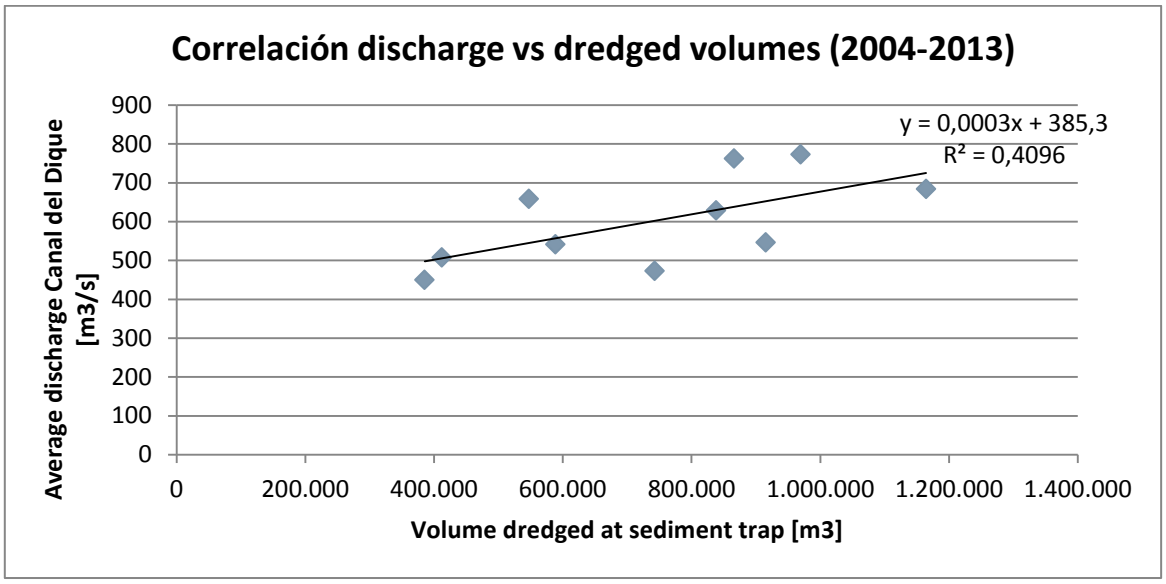

Figure E. 5 - Correlation between mean annual discharge of the previous year to the dredged volume in the present year (Consorcio Dique and Fondo Adaptación 2015)

As mentioned before, calibration can be carried out by adjusting grain size and the sediment transport formula. Target is to obtain a *computed* bed load transport at the Río Magdalena at Calamar and entrance of the Canal del Dique in the same order as the value obtained from the calibration curves.

Grain size

The grain size is varied to a larger grain size of 500 and 250 µm as well as application of two sediment fractions and 100 µm compared to the reference grain size of one sediment fraction of 200 µm. In all the cases the sediment transport formula of Van Rijn (1993) is used as in the reference case.

From Figure E.6 it can be seen that the bed load transport increases for increasing grain size. However, the increase is not very large (twice as large bed load transport for D50= 500 µm compared to D50=

200 µm). Besides, it can be seen that all of the computed bed load transports are an order of 3 smaller compared to the calibration value. Figure E. 6 shows the bed load transport when applying two sediment fractions compared to one. It can be seen that applying two sediment fractions causes a lower bed load transport, fitting the calibration value less. The lower bed load transport can be explained by the grains being more packed with two sediment fractions, hence it is more difficult to bring the grains of the bed into motion.

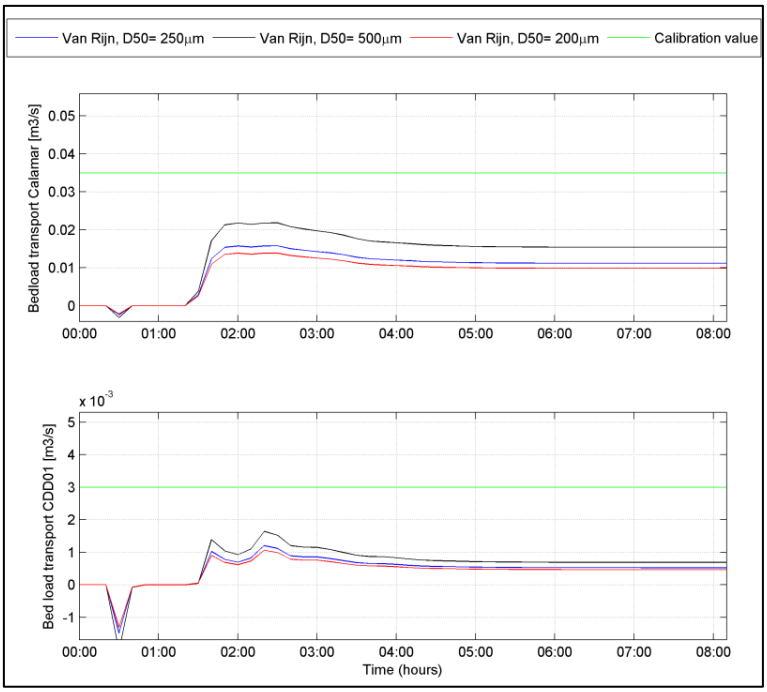

Figure E. 6 – Bed load transport at Calamar and the entrance of the Canal del Dique for different sediment fractions

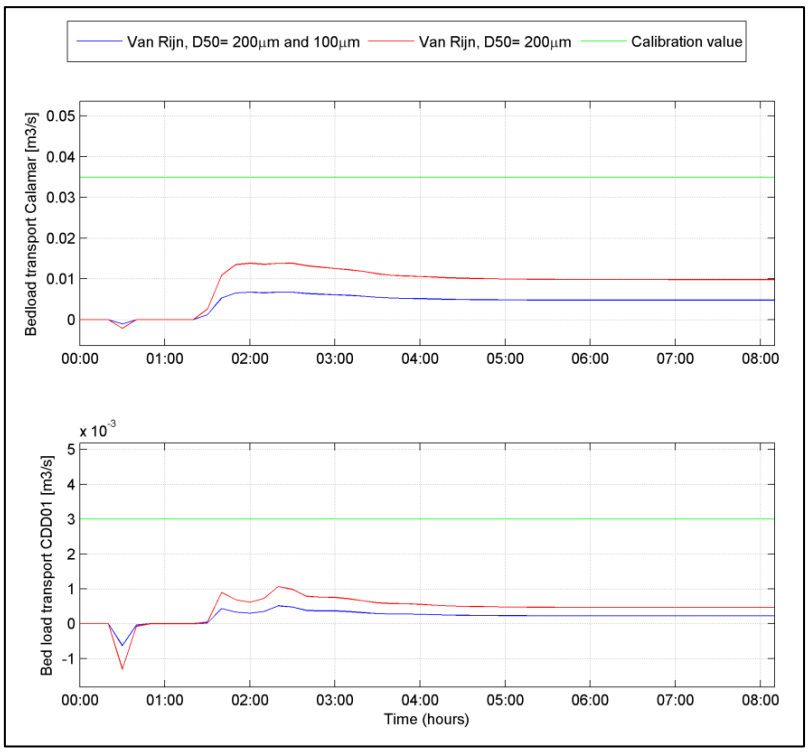

Figure 0.1 – Bed load transport at Calamar and the Canal del Dique for two sediment fractions and one

Sediment transport formula

A lot of sediment transport formulas are available, as explained in the previous section. Therefore, the sensitivity of applying different sediment transport formula should be tested. In this case the default formula of Van Rijn (1993) and Engelund-Hansen is used as these formulas are applicable for the used grain size and calculate both suspended and bed load transport. Figure E. 7 shows that the bed load transport is larger when applying Engelund-Hansen compared to van Rijn. Where, the bed load transport at the entrance of the Canal del Dique fits the calibration value better with Engelund-Hansen but overestimates the calibration value at Calamar.

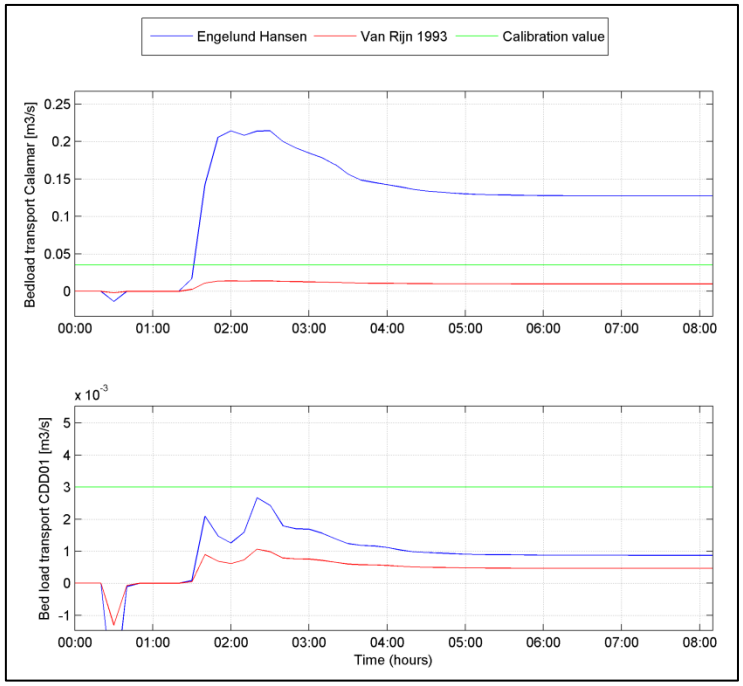

Figure E. 7- Bed load transport at Calamar and entrance of the Canal del Dique for Engelund-Hansen and Van Rijn (1993) sediment transport formula

E.2.1 Conclusion

Applying different grain sizes results in slight difference bed load transports. Where, the bed load transport increases for larger grain sizes with the sediment transport formula of Van Rijn (1993). Applying the sediment transport formula of Engelund-Hansen results in larger differences between bed load transports (factor 8 at Calamar), where the computed bed load transport with Engelund-Hansen is larger than Van Rijn (1993). Therefore, further investigation is necessary to define the preferable formula.

E.3 Sensitivity analysis

In this study we are not only interested in sediment transport distributions, but also in sedimentation and erosion patterns. Therefore, a sensitivity analysis is carried out using several sediment transport characteristics and different flow input in order to investigate the most reliable transport formula and grain size. Besides, calibration shows relatively large differences between Engelund-Hansen and van Rijn (1993). Due to lack of time, this analysis will also be used to find the most assumable transport formula predicting the correct sedimentation and erosion patterns.

The sensitivity of the following parameters is tested:

- Grain size
- Sediment transport formula
- Peak discharge vs. stationary discharge

Grain size

Applying larger grain sizes results in less erosion in the channels along the islands and more gradual transverse bed slopes (Figure E.8). As it is more difficult to bring coarser grains into motion, less erosion in the channels occurs. On the other hand, smaller grain sizes can be transported more easily for which morphological developments will occur faster. This is for example shown in Figure E.9 presenting the bed level evolution at the entrance of the offtake. This shows that the equilibrium bed level is reached faster with smaller grain size.

Furthermore, in the Canal del Dique also coarse sediment grains of around 100 µm are available. Therefore, it is investigated what the effect is of applying two different sediment fractions. Figure E.10 shows that when a gradation of two sediment fractions is applied the channels along the islands experience more and wider erosion. Due to the different sediment fractions hindered settling occurs, hence less sedimentation. On the other hand, areas of low flow velocities as for example at the lee side of the small island, more sedimentation can be seen. As the different fractions cause the sediments to be more packed a higher flow velocity is necessary to bring the sediment particles into motion.

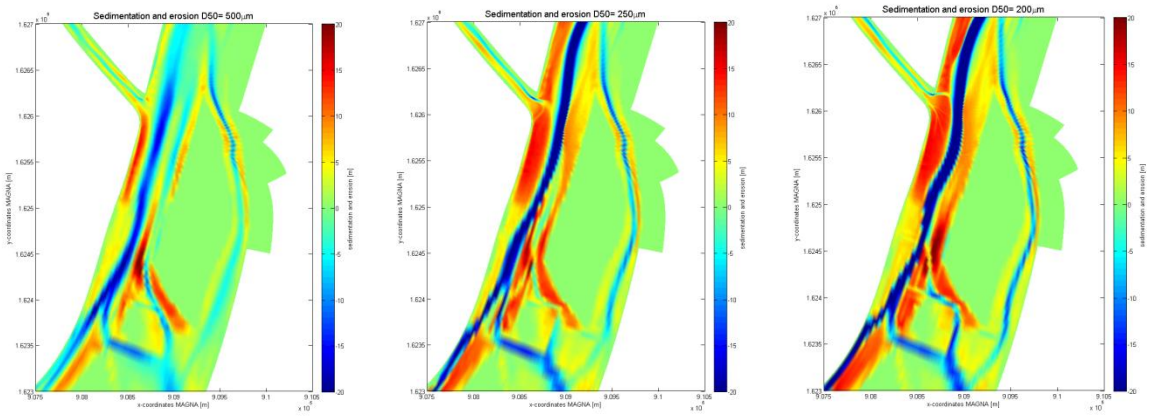

Figure E. 8 – Sedimentation and erosion after one year compared to initial sediment thickness for applying a median grain size of 500, 250 and 200 µm (from left to right).

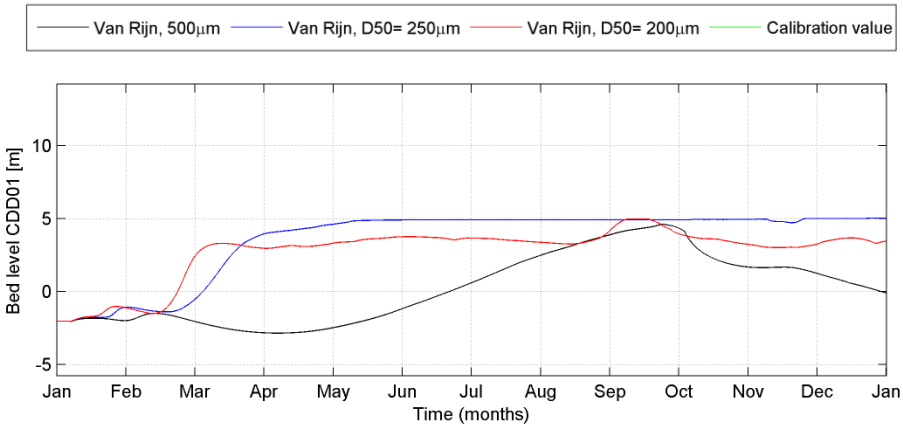

Figure E. 9 – Bed level evolution at the entrance of the offtake for different grain sizes

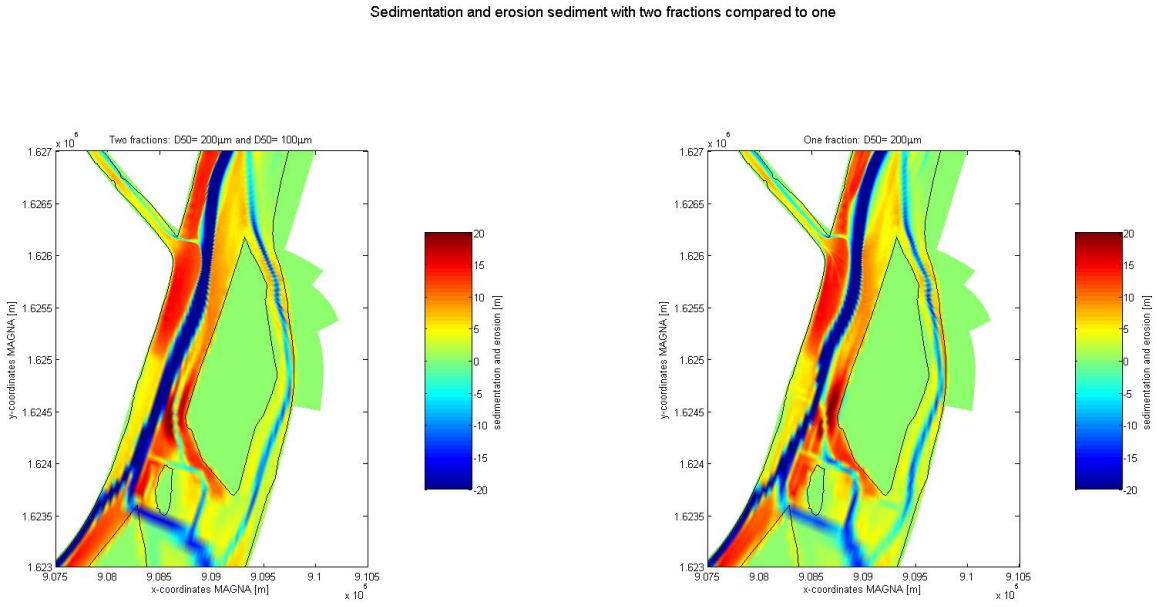

Figure E. 10- Sedimentation and erosion after one year compared to initial sediment thickness when applying two sediment fractions (left) of 200 µm and 100 µm compared to one fraction of 200 µm (right)

Sediment transport formula

The sensitivity of applying different sediment transport formula is tested. In this case the difference between Engelund-Hansen and van Rijn 1993 is investigated as shown in Figure E. 11 and Figure E. 12. It can be seen that the resulting sedimentation and erosion pattern varies largely between both formulas. In the case of van Rijn the channels around the islands erode largely, while the sedimentation and erosion pattern with Engelund-Hansen is more gradual. However, both transport formulas show sedimentation around the entrance of the offtake and at the left tip of the downstream located island, where flow velocities are low.

In historical bathymetries highly erodible channels are not seen. Besides, measurements carried out in the Río Magdalena and tributaries by NEDECO in 1973 show that the Engelund-Hansen formula fits

fairly well with field data (Figure E. 13). Therefore, it is preferred to use the transport formula of Engelund-Hansen is above van Rijn 1993.

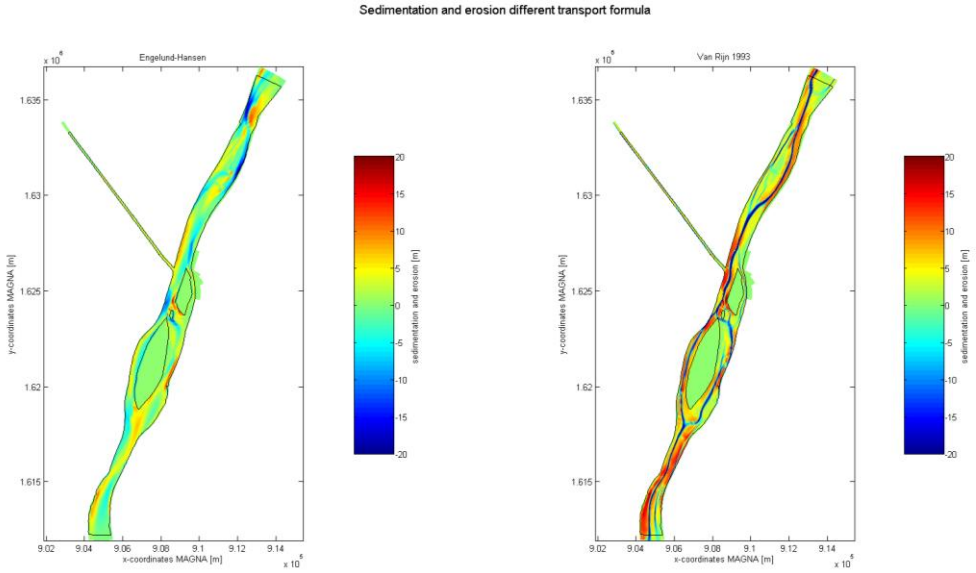

Figure E. 11- Sedimentation and erosion pattern for sediment transport formula Engelund-Hansen and Van Rijn 1993

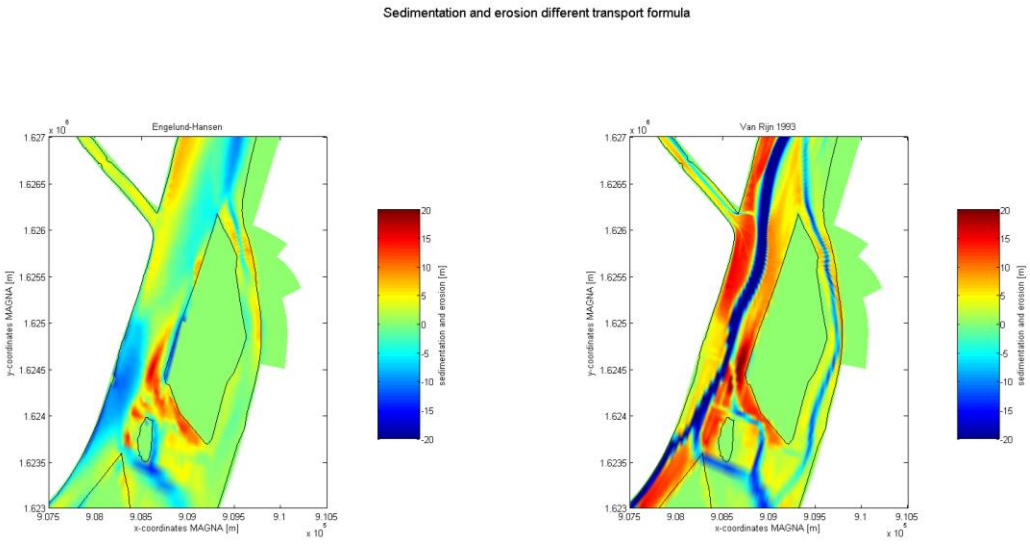

Figure E. 12–Sedimentation and erosion pattern in the area of the bifurcation after simulation of one year with sediment transport formula Engelund-Hansen and Van Rijn 1993

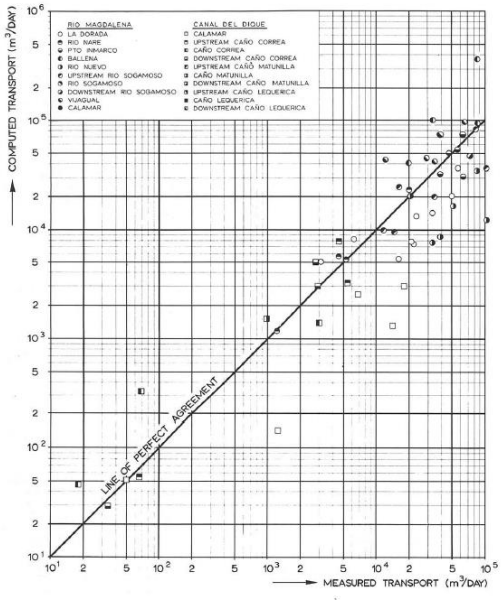

Figure E. 13 – Measured transport rates compared to computed rates with the Engelund-Hansen formula in the Río Magdalena and Canal del Dique (NEDECO 1973)

Flow input

The effect of peak discharges compared to a stationary flow is investigated. First of all, a peak discharge is applied during two months of the one year simulation period. Thereafter, a simulation is carried out with a hydrograph following the annual mean hydrograph of the Río Magdalena.

Figure E. 14 and Figure E. 15 show the resulting sedimentation and erosion pattern when applying a peak discharge of two months compared to a stationary flow. It can be seen that the sedimentation and erosion pattern is smoother when applying a peak flow. Besides, more sedimentation occurs at the entrance of the bifurcation. Furthermore, Figure E. 16 shows a sudden drop in bed load transport at the beginning of the peak discharge (in June), causing a sedimentation bump at the entrance of the offtake. Shortly, after the peak flow the morphological response counteracts the sedimentation bump causing a decrease of bed level and increase of bed load transport. At the end of the peak discharge the flow suddenly decreases causing a decrease in bed load transport and increase in bed level.

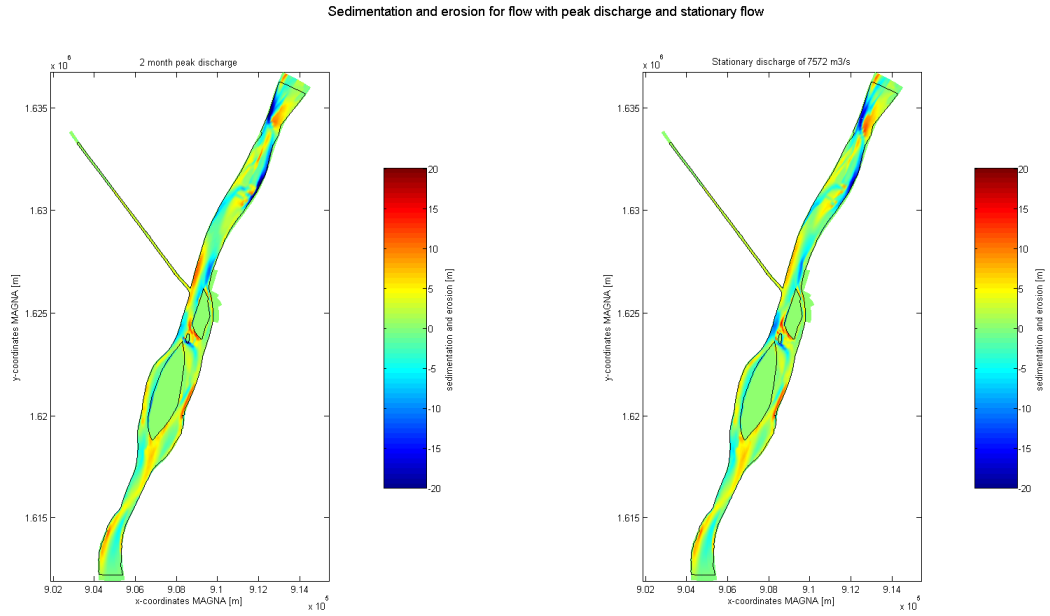

Figure E. 14 – Sedimentation and erosion pattern after one year for applying a peak discharge during two months of the year (left) and stationary flow (right)

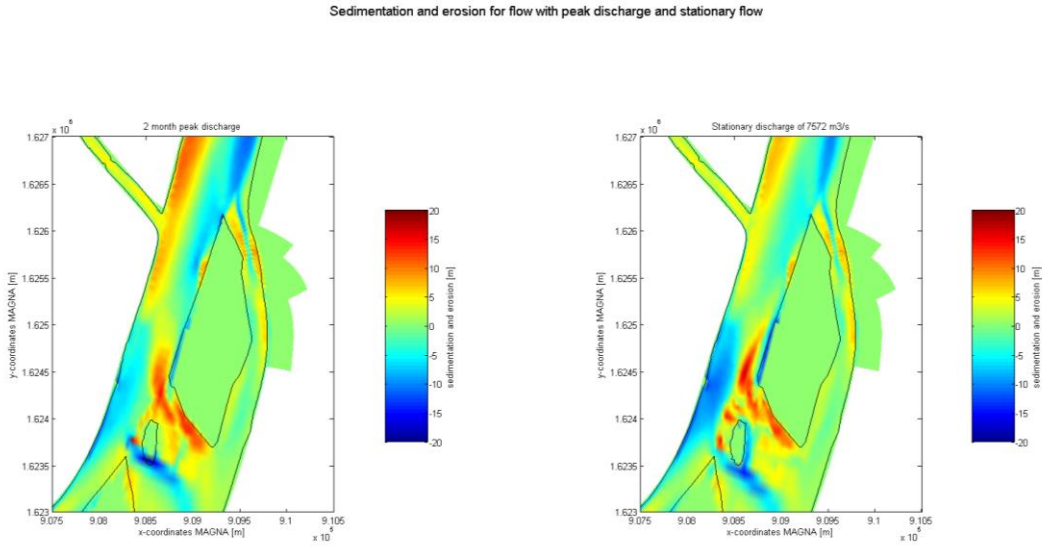

Figure E. 15 - Sedimentation and erosion in the area of the bifurcation after one year for applying a peak discharge during two months of the year (left) and stationary flow (right)

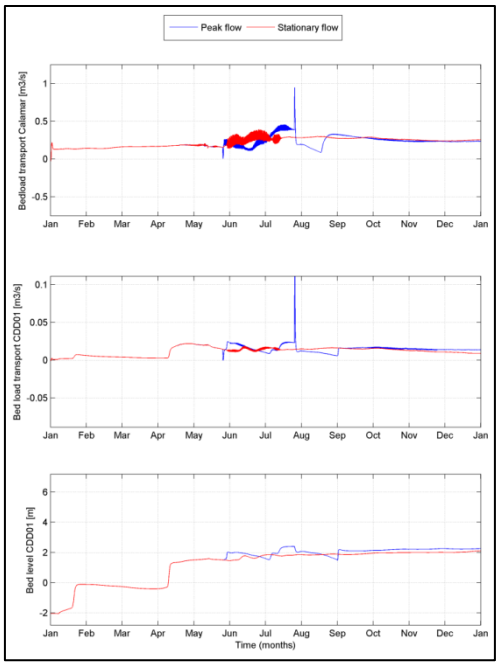

Figure E. 16 – Bed load transport at the Canal del Dique and Río Magdalena at Calamar and bed level evolution at the entrance of the Canal del Dique for peak flow and stationary flow

Furthermore a hydrograph is computed following the mean annual hydrograph of the Río Magdalena (Figure E. 17). The hydrograph is simplified into monthly stationary flows Figure E. 18 resulting in a quasi-stationary computation.

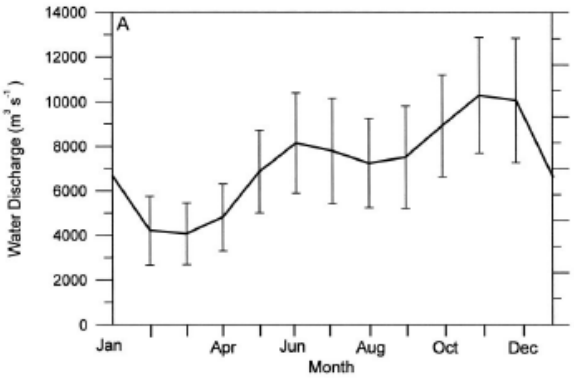

Figure E. 17 - Monthly mean and standard deviation of water discharge in the Río Magdalena at Calamar based on measurements from 1975-1995 (Restrepo and Kjerfve 2000)

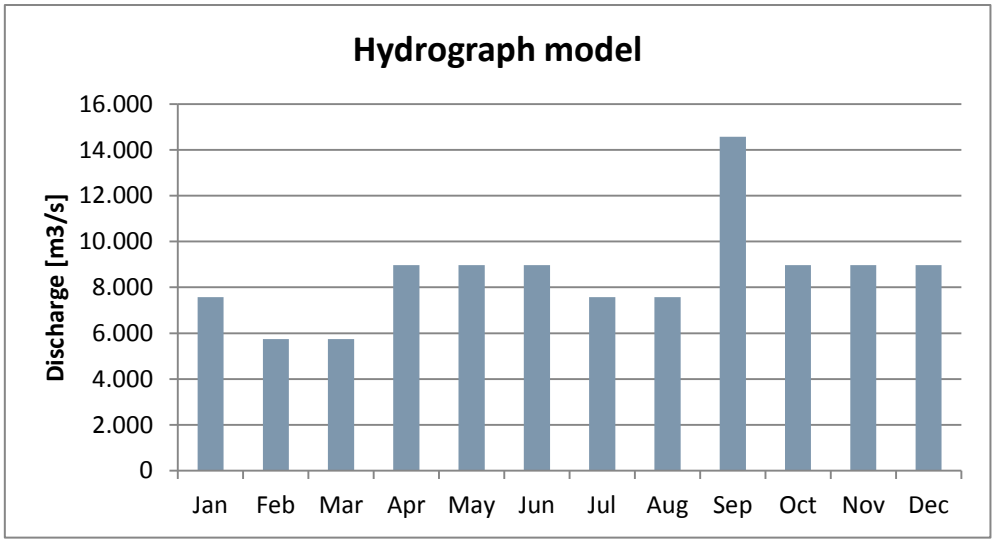

Figure E. 18 – Monthly discharge as applied in model

Figure E. 19 and Figure E. 20 show the sedimentation and erosion pattern after one year when applying the hydrograph compared to a stationary flow. It can be seen that the sedimentation and erosion pattern is smoother in the case of the hydrograph resulting in a bed level which matches better with the measured bathymetry. Again, a very large sedimentation bump can be seen at the entrance of the Canal del Dique which occurs right after the start of the high peak flow of September. However, an increase in bed level of 40 meter is not assumable in reality. This large increase is caused by the sudden changes in discharge, which would be smoother in reality. Furthermore from Figure E. 22 it can be seen that the bed load transport both in the Río Magdalena and Canal del Dique reaches almost the same equilibrium state when applying a hydrograph compared to a stationary flow. However, when applying a hydrograph more sedimentation occurs in the offtake due to the large sediment bumps caused by the peak discharges.

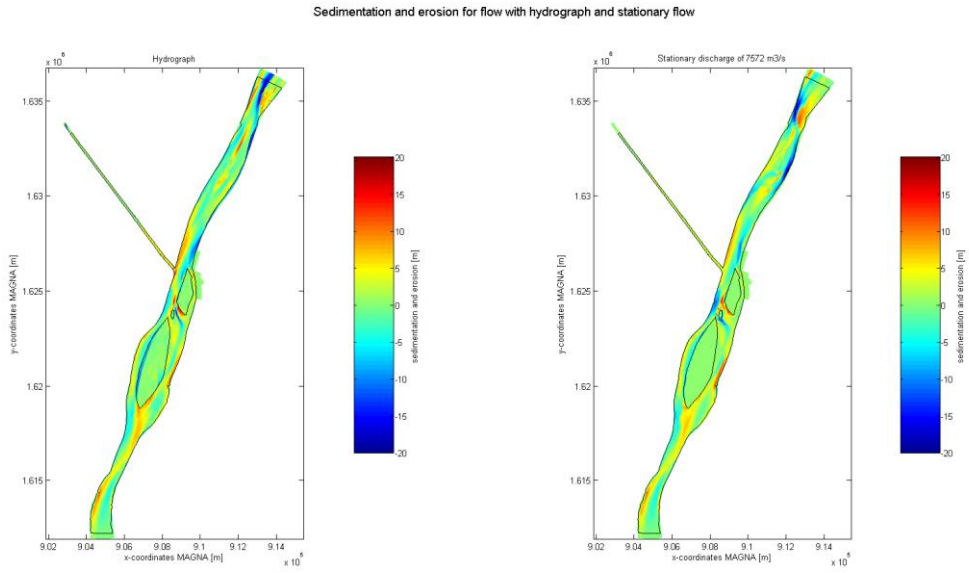

Figure E. 19 – Sedimentation and erosion with hydrograph compared to stationary flow

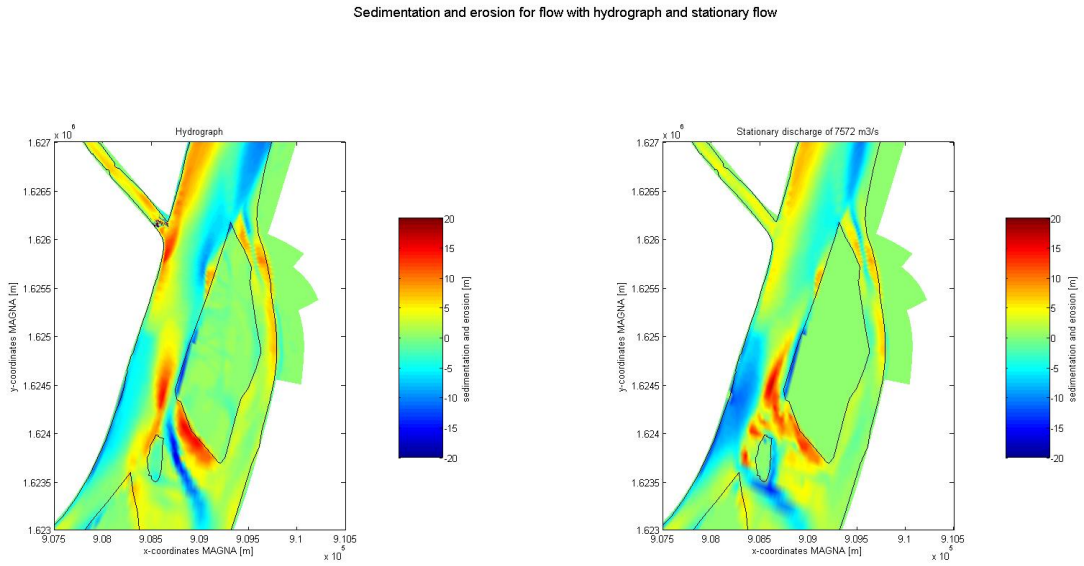

Figure E. 20 - Sedimentation and erosion with hydrograph (left) compared to stationary flow (right) zoomed in to the area of the bifurcation

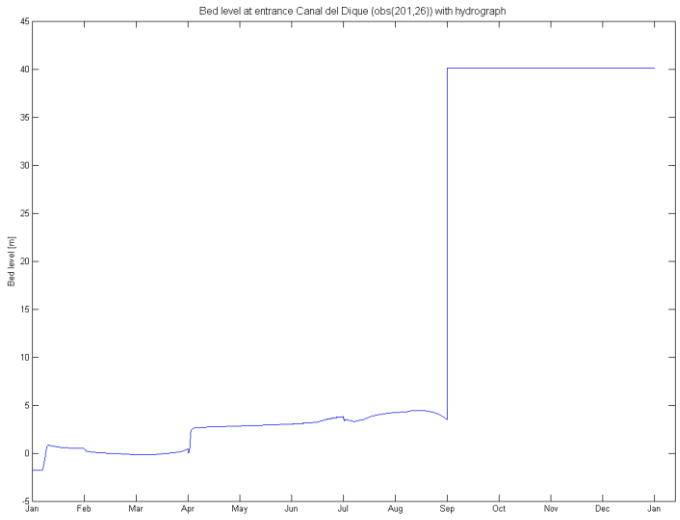

Figure E. 21 – Bed level evolution at entrance Canal del Dique for hydrograph

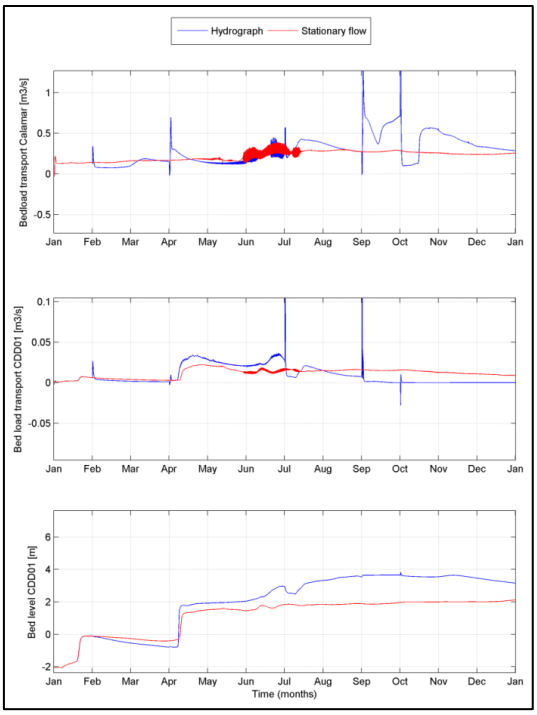

Figure E. 22 – Bed load transport at the Canal del Dique and Río Magdalena at Calamar and bed level evolution at the entrance of the Canal del Dique for hydrograph and stationary flow